The Role of Capsular Polysaccharide in *Acinetobacter baumannii* Virulence

By

Jennifer Singh
BMSc Honours

Thesis
Submitted to Flinders University
for the degree of Doctor of Philosophy

College of Science and Engineering
10 May 2022

Table of Contents

Summary

The Gram-negative opportunistic bacterium *Acinetobacter baumannii* is a significant cause of hospital-borne infections worldwide. Alarmingly, the rapid development of antimicrobial resistance coupled with remarkable ability of isolates to persist on surfaces for extended periods of time has led to infiltration of *A. baumannii* into our healthcare environments. Treatment options for *A. baumannii* infections are becoming increasingly limited, and the urgency to develop effective infection control strategies and therapies to combat infections is apparent.

Capsular polysaccharide is comprised of tightly packed repeating oligosaccharide units and forms a barrier around the bacterial cell providing protection from environmental stressors found in the nosocomial environment as well as host immune responses during infection. Additionally, capsule has been shown to contribute resistance to a range of clinically relevant antimicrobial compounds. An increased understanding of the contribution of capsule to the pathobiology of *A. baumannii* is required to determine its feasibility as a target for new strategies to combat drug resistant infections.

Phenomenal diversity exists between capsule structures (K types) identified for various *A. baumannii* strains, with over 150 distinct capsule biosynthesis gene clusters have been identified to date. In this study, capsule related phenotypes of twelve *A. baumannii* strains, representing nine distinct capsule types were assessed to identify correlations between capsule structure and phenotype. Cell surface hydrophobicity, acid stress tolerance, lysozyme resistance and serum resistance were compared between the twelve strains. A correlation was found between capsule charge and cell surface hydrophobicity, but no relationships were identified between K type and any other phenotype assessed.

Manipulation of the *A. baumannii* genome is essential for investigating the role capsule plays in persistence, resistance, and host immune evasion. Genetic manipulation of *A. baumannii* has historically been difficult, though recent advances in cloning methodologies have led to improvements. For some bacterial strains, such as *Streptococcus pneumoniae*, K type is highly correlated to disease potential. The gold standard for studying the role of K type on disease potential is assessing ‘capsule

swapped' isogenic strains expressing heterologous K types. For most *A. baumannii* strains, the K loci, which encodes genes specific to capsule production, is located between two highly conserved genes, *lldp* and *fkpA* Several attempts were made to make capsule swapped variants of *A. baumannii* strains ATCC 17978 and 04117201 but ultimately proved unsuccessful.

The contribution of capsule to *A. baumannii* environmental persistence and host immune evasion was assessed by generating acapsular mutants with one or more gene/s required for capsule production removed. Three acapsular mutants, removing the initial transferase (Δ*itrA2*), variable region genes (Δ*cps*), and capsule polymerase (Δ*wzy*), were generated in the *A. baumannii* strain ATCC 17978. The elimination of capsule production altered the response of *A. baumannii* to various stressors including growth in acidic pH, the osmotic stress response, resistance to human complement and lysozyme killing, macrophage phagocytosis, growth under iron limitation, and resistance to antimicrobial compounds. This study has defined a role for capsule in *A. baumannii* survival in adverse environments and highlights the importance of capsule in evasion of the host immune system and resistance to antimicrobial compounds. Notably, the response of acapsular mutants to some stressors varied considerably depending on what gene/s were removed, demonstrating that abrogation of capsule production at different stages of synthesis can differentially affect stress responses.

Declaration

I certify that this thesis does not incorporate without acknowledgment any material previously submitted for a degree or diploma in any university; and that to the best of my knowledge and belief it does not contain any material previously published or written by another person except where due reference is made in the text.

Jennifer K. Singh

Acknowledgements

Firstly, I would like to express my sincere gratitude to my supervisor Prof. Melissa Brown for her supervision, advice, support and patience during my Ph. D study. I would also like to thank Associate Professor Jill Carr and Associate Professor Sophie Leterme for their supervision, support and assistance.

I would also like to thank all the members of the Brown lab, particularly Sarah, Mohsen, Abol and Syliva for the banter, laughs and enthusiasm I needed daily.

A special thanks to my favourite lab buddy Felise. You have been there for me since the beginning, through the ups and the downs, the good and the bad, and I can truly say you are my best friend. I will love you forever Pookie.

A big thanks to Sam and Yasna for being my emotional supports during this time.

A huge thankyou to my Mum and Dad, who have supported me through all my life endeavours and have always encouraged me to pursue my passions no matter what they are.

Last but not least, thank-you to my dog Percy for all the cuddles and kisses when I needed them the most.

Contributions

Generation of acapsular mutants using the recombineering system were performed in parallel with Dr. Felise Adams (Flinders University, Adelaide, Australia). Isolation of monocytes was performed with the assistance of Dr. Jill Carr (Flinders University, Adelaide, Australia). The genome sequence of the *Acinetobacter baumannii* strain 04117201 was provided by Ruth Hall (University of Sydney, Sydney, Australia). *Saccharomyces cereviciae* and *Escherichia coli* strains, as well as cloning vectors for the operon assembly protocol were provided by Michael Liu (University of Sydney, Sydney, Australia) and Johanna Kenyon (Queensland University of Technology, Brisbane, Australia).

1 INTRODUCTION

1.1 *Acinetobacter baumannii*: A troublesome pathogen

1.1.1 Classification and characteristics of Acinetobacter baumannii

Acinetobacter baumannii is an opportunistic pathogen and a significant cause of hospital-borne infections worldwide. The genus *Acinetobacter* are comprised of non-fermentative, strictly aerobic, Gram-negative coccobacilli which are ubiquitously found in nature (Giamarellou et al., 2008). These bacteria grow happily on routinely used media at 37^{o}C, forming smooth creamy white colonies 1.5-2 mm in diameter. More than 50 distinct species of *Acinetobacter* have been identified, most of which are non-pathogenic environmental isolates (Nemec et al., 2011, Wong et al., 2017, Al Atrouni et al., 2016). *A. baumannii* is the most common *Acinetobacter* species to cause disease, though infections with other species including *Acinetobacter calacoaceticus*, *Acinetobacter lwoffii*, *Acinetobacter pittii*, and *Acinetobacter nosocomialis* are occasionally reported (Fitzpatrick et al., 2016, Dexter et al., 2015, Dijkshoorn and van der Toorn, 1992).

Traditionally, epidemic *A. baumannii* fall into three distinct lineages, international clones (IC) I, II and III; yet at least eight additional lineages and numerous novel isolates have been identified world-wide (Higgins et al., 2010, Higgins et al., 2017, Fitzpatrick et al., 2016). *A. baumannii* have also been categorised based on pulse field gel electrophoresis into sequence type or ST groups (Higgins et al., 2010, Tomaschek et al., 2016). Determining the meaningfulness of these typing schemes is difficult due to the immense strain diversity and frequent identification of unique isolates which do not fall into already established groupings. The core genome of *A. baumannii* has been established by the comparison of over 1500 whole genome sequences (WGS), providing a basis for a superior typing scheme for tracking *A. baumannii* evolution and outbreaks (Higgins et al., 2017). With the advent of cost-effective and efficient sequencing methods this new scheme based on WGS may soon replace the traditional ST and IC typing schemes currently used (Fitzpatrick et al., 2016, Higgins et al., 2017).

1.1.2 Epidemiology

Although some *Acinetobacter* such as *A. lwoffii* and *A. johnsonii* commonly contribute to the normal flora of humans, it is uncommon for the most pathogenic species, *A. baumannii*, to colonise healthy individuals (Peleg et al., 2008, Berlau et al., 1999). Isolates of *A. baumannii* have been found in a variety of environmental samples and urban environments but with no real consistency, as such the primary reservoir for this bacterium remains unconfirmed (Peleg et al., 2008, Davis et al., 2014). Nonetheless, many potential reservoirs for *A. baumannii* have been identified; including soil, food, and hospital environments, but there is no clear consensus in the literature on the contribution to outbreaks each of these reservoirs may make (Peleg et al., 2012).

Our understanding of the global epidemiology of *A. baumannii* outbreaks is limited due to this difficulty to identify outbreak causing reservoirs, diagnostic tests are often unreliable (Higgins et al., 2010, Fournier et al., 2006), and it is hard to determine sporadic cases from outbreaks in hospitals. Outbreaks of *A. baumannii* have been reported in most regions of the world; and are becoming increasingly frequent in China and India (Gogou et al., 2011, Dijkshoorn et al., 2007, Runnegar et al., 2010, Zhou et al., 2018, He et al., 2011, Gupta et al., 2006, Shah et al., 2015, Wieland et al., 2018). Additionally, combat wound infections with *A. baumannii* were a major cause of morbidity and mortality in United States military personnel returning from Iraq and Afghanistan (Scott et al., 2007), and *A. baumannii* are the most commonly identified Gram-negative bacteria causing infections in the Middle East (Lob et al., 2016). In Australia nosocomial outbreaks of *A. baumannii* have been reported in most major cities including Perth, Brisbane, Sydney and Melbourne (Peleg et al., 2006, Lin et al., 1998, Valenzuela et al., 2007). Furthermore, the spread of *A. baumannii* isolates from South East Asia to Australia has been reported after disastrous events such as the 2002 Bali bombings and the 2004 tsunami (Heath et al., 2003, Uckay et al., 2008).

The vast majority of reported *A. baumannii* outbreaks are hospital acquired infections in immune compromised patients, especially within the intensive setting (Fournier et al., 2006, Martín-Aspas et al., 2018). Although *A. baumannii* is primarily a nosocomial pathogen there are many reports of community acquired infections, predominantly in tropical regions including the Asia Pacific region and tropical Northern Australia

(Dexter et al., 2015, Leung et al., 2006, Meumann et al., 2019). Not surprisingly, *A. baumannii* strains isolated from hospital borne infections show much higher rates of antibiotic resistance than those isolated from the community (Martín-Aspas et al., 2018).

1.1.3 Clinical impact

Common manifestations of *A. baumannii* infections include pneumonia, bloodstream infections, wound infections, urinary tract infections and meningitis, especially in health care settings (Peleg et al., 2008, Lee et al., 2017a). Treatment of *A. baumannii* infections is becoming increasingly difficult as most outbreak strains have developed a multidrug resistance (MDR) phenotype. Additionally, elimination of infection reservoirs is challenging as *A. baumannii* is exceptionally adept at surviving in hospital environments (Blanco et al., 2018, Isler et al., 2019). Transmission within the hospital setting may occur via transient colonisation of the hands of health care workers, long term colonisation of hospital surfaces and equipment, and the inhalation of contaminated aerosols (Takoi et al., 2019, Spellberg and Bonomo, 2013, McDonald et al., 1999).

Several factors are associated with an increased risk of developing an *A. baumannii* infection within the hospital environment. These include mechanical ventilation, invasive procedures, prolonged hospital admissions, previous antibiotic treatment and underlying pulmonary conditions (Martín-Aspas et al., 2018, Blanco et al., 2018, Howard et al., 2012, Garnacho-Montero et al., 2005, Shete et al., 2010, Subramaniyan et al., 2017, Fournier et al., 2006). The most frequent site of infection with *A. baumannii* is the respiratory tract, especially in ventilated patients (Garnacho-Montero and Amaya-Villar, 2010, Garnacho-Montero et al., 2005). In the community setting, infections manifest predominantly as pneumonia and risk factors include alcohol consumption, diabetes mellitus, smoking, and chronic lung disease (Dexter et al., 2015).

The disruption of anatomical barriers is a major risk factor for developing *A. baumannii* infections. Urinary tract infections and meningitis caused by *A. baumannii* can often be attributed to the insertion of urinary catheters and external ventricular drains, respectively (Peleg et al., 2008). Although rare, the mortality rate for *A. baumannii* meningitis can be as high as 70% (Metan et al., 2007). Furthermore, *A. baumannii* skin

infections, including burns and combat wounds, are often associated with high mortality (Sebeny et al., 2008, Trottier et al., 2007). Bloodstream infections with *A. baumannii* are typically secondary to underlying pneumonia, urinary tract, central line or wound infections (Peleg et al., 2008, Hidron et al., 2008, Chusri et al., 2019, Papathanakos et al., 2020).

1.2 Virulence factors in *A. baumannii*

The success of this tenacious pathogen is facilitated by its ability to survive on hospital surfaces compounded by its rapid ability to acquire MDR. Additionally, once inside the human host, *A. baumannii* is highly capable of evading rapid clearance by the immune system. The possession of a multitude of virulence factors aids the success of *A. baumannii* as a human pathogen. Factors contributing to increased *A. baumannii* virulence include the production of biofilm, survival on dry surfaces, adhesion and invasion of epithelial cells, the ability to evade host immune defences and the possession of antibiotic resistance determinants (Loehfelm et al., 2008, Wendt et al., 1997, Lee et al., 2008, Gordon and Wareham, 2010). Capsule is a distinct layer of polysaccharide which surrounds the bacterial cell wall and influences survival on dry surfaces, the ability to evade host defences and confers antibiotic resistance to a number of compounds (Tipton et al., 2018, Geisinger and Isberg, 2015). In this thesis environmental persistence/survival will refer to any environment where *A. baumannii* is not interacting with a host cell or product secreted/ produced by the host. Interactions between *A. baumannii* and host cells or cell products or mimics of cell products will represent host microbe interactions. Many virulence traits of *A. baumannii* serve multiple functions and a great deal of overlap can be seen between determinants of environmental persistence and host immune modulation. As such, the role of many disease associated traits are complex and multifaceted, and /or interrelated. It is therefore not possible to easily categorise traits and the aim of these sections are to give an overview of important phenotypes which play a role in the infection process; namely, the maintenance of reservoirs, transmission, and disease progression. The following sections describe survival related factors in *A. baumannii* including; mechanisms of environmental persistence, antimicrobial resistance, and the modulation of host immune defences. Finally, specific attention will be paid to the role of surface polysaccharides in *A. baumannii*.

1.2.1 Micronutrient acquisition systems

The transition metals iron, zinc and manganese are essential for life due to their ability to readily accept and donate electrons (Kehl-Fie and Skaar, 2010, Skaar, 2010). These micronutrients play important roles as co-factors for enzymes essential for energy generation, DNA replication, protection from oxidative stress, and oxygen transport (Skaar, 2010). As these molecules have a highly reactive nature, hosts have developed sophisticated mechanisms for tight regulation of metal acquisition and storage. For example, in the human host iron is primarily found complexed with iron binding molecules such as heme, lactoferrin, and transferrin (Dorsey et al., 2003, Parrow et al., 2013, Skaar, 2010). Sequestering of metals by the host not only prevents intoxication but provides a form of nutritional immunity by limiting bioavailability of metals to invading organisms (Parrow et al., 2013, Nwugo et al., 2011). Additionally, during infection changes in iron and zinc metabolism occur within the host which further limits availability to pathogens (Parrow et al., 2013). For example, during infection with bacteria including, *A. baumannii*, the host releases hepcidin and calprotectin, which reduces accessibility of iron and zinc, respectively (Parrow et al., 2013, Hood et al., 2012, Vignesh and Deepe Jr, 2016).

In *A. baumannii* specifically, acquiring iron and zinc from the host is important for survival and thus many mechanisms for the acquisition of these metals have evolved (Mortensen and Skaar, 2013). Most strains of *A. baumannii* are capable of survival under iron limiting conditions, mimicking conditions found in the host, though the capacity for survival differs between strains (Zimbler et al., 2009, Actis et al., 1993). *A. baumannii* has evolved numerous mechanisms to acquire iron from host environments including iron uptake systems and production of high affinity iron scavenging siderophores (Dorsey et al., 2003, Wu et al., 2014, Parrow et al., 2013, Actis et al., 1993).

The production of siderophores is the primary mechanism of iron acquisition in *A. baumannii*. Siderophores are released into the environment and remove iron bound to host proteins, receptors on the bacterial cell then recognise the iron bound siderophore and it is transferred to the cytoplasm (Zimbler et al., 2009, Mihara et al., 2004). The transport of iron bound siderophores into the cytosol is an energy dependant, multistep

process involving a TonB associated siderophore complex receptor for transfer across the outer membrane (OM) and an ATP-binding cassette (ABC) transporter to transfer the siderophore into the cytosol (Moeck and Coulton, 1998, Wilson et al., 2016). Several siderophores have been identified in *A. baumannii*, though the most studied is acinetobactin (Eijkelkamp et al., 2011a, Gaddy et al., 2012). The production of acinetobactin is essential for invasion of lung epithelial cells and pathogenesis in a wax moth larvae and mouse sepsis models using *A. baumannii* strain ATCC 19606 (Gaddy et al., 2012). *A. baumannii* also possesses a high affinity zinc acquisition system (Hood et al., 2012). Two zinc transporters, ZnuD1 and ZnuD2, transport zinc through the OM in conjunction with a TonB energy transduction system (Mortensen et al., 2014). The inner membrane transporter complex ZnuABC then transfers zinc into the cytoplasm (Mortensen et al., 2014).

Iron and zinc acquisition is tightly regulated to maintain homeostasis during infection. Additionally, regulation of transition metals is needed to prevent intoxication, which leads to the impairment of oxidative stress mechanisms, disruption of carbon metabolism, and disruption of membrane biology in *A. baumannii* (Hassan et al., 2017). In *A. baumannii*, control of iron acquisition is regulated by the ferric uptake regulator (Fur) protein (Eijkelkamp et al., 2011a, Mihara et al., 2004). Under iron limiting conditions, Fur is de-repressed, resulting in the upregulation of iron uptake systems and siderophores (Eijkelkamp et al., 2011a). Similar to the action of Fur, the zinc uptake regulator (Zur) regulates the response to fluctuating levels of zinc (Mortensen et al., 2014). Both Fur and Zur recognise and bind to conserved genetic motifs upstream of regulated genes, leading to transcriptional repression (Mortensen et al., 2014, Eijkelkamp et al., 2011a). Besides regulating metal acquisition, both Fur and Zur act as global regulators of pathogenesis, as low levels of available iron and zinc are a signal to *A. baumannii* that they are within a host environment (Nwugo et al., 2011, Eijkelkamp et al., 2011a, Skaar, 2010).

1.2.2 Biofilm production

A key factor in the remarkable ability of *A. baumannii* to persist within the hospital environment is the production of a biofilm. A biofilm is a highly organised community in which bacteria attach to a surface, form micro-colony aggregates, and produce a

protective extracellular matrix of polysaccharide (Tomaras et al., 2003). The ability of bacterial communities to form a biofilm aids in survival by providing a barrier from environmental stressors and antimicrobial compounds (Høiby et al., 2011). *A. baumannii* can form biofilm on a range of different surfaces including glass, polypropylene and polycarbonate (Pour et al., 2011), as well as at the air-liquid interface, where it is known as a pellicle (McQueary and Actis, 2011, Giles et al., 2015).

Although most *A. baumannii* isolates are generally capable of producing robust biofilms, many studies show a wide distribution of biofilm forming capabilities exist between strains (Badave and Kulkarni, 2015, Rodríguez-Baño et al., 2008, Eijkelkamp et al., 2011b, McQueary and Actis, 2011, De Breij et al., 2010). In addition, variations in the process of biofilm production and biofilm architecture between *A. baumannii* strains has been reported (Dahdouh et al., 2016). The location and severity of *A. baumannii* infections may be associated with the ability to produce biofilm. For example, *A. baumannii* strains isolated from infections associated with indwelling devices such as urinary catheters, venous catheters, and endotracheal tubes of ventilated patients, showed higher biofilm forming capabilities (Gil-Perotin et al., 2012, Pour et al., 2011, Rodríguez-Baño et al., 2008). Furthermore, increased biofilm forming capabilities may be linked with an increased severity of infections (McQueary and Actis, 2011, Colquhoun and Rather, 2020).

Production of biofilm is a multifactorial process which directly involves a number of bacterial features including the production of pili (Wood et al., 2018, Tomaras et al., 2003, Pakharukova et al., 2018, Colquhoun and Rather, 2020), production and secretion of poly-N-acetyl glucosamine (PNAG) (Choi et al., 2009), and bacterial adhesins including the Biofilm Associated Protein (BAP) (Loehfelm et al., 2008) and BAP-like proteins (Eijkelkamp et al., 2014). The presence of other factors such as an O-linked protein glycosylation systems (Iwashkiw et al., 2012), outer membrane protein (OMP) A (Gaddy et al., 2009), and the histone-like nucleoid structuring protein (H-NS) (Eijkelkamp et al., 2013), greatly enhance biofilm production. Correlations between biofilm production and several other virulence factors have been made including; the ability to resist human serum complement (King et al., 2009), survival on dry surfaces (Espinal et al., 2012), adherence to epithelial cells (Lee et al., 2008) and both positive and negative correlations with antimicrobial resistance (Lee et al., 2008, Yoon et al.,

2015, Qi et al., 2016).

Levels of biofilm production are influenced by a number of environmental cues including temperature, light (Wood et al., 2018), cell density (Tomaras et al., 2003), iron availability, and the presence of quorum sensing molecules (Bhargava et al., 2014). Regulatory systems, including the BfmRS two component system (TCS) and the H-NS global transcriptional repressor have been shown to play a role in modulating biofilm production (Gaddy and Actis, 2009, Eijkelkamp et al., 2013).

1.2.3 Desiccation tolerance

Water is important for the survival of all life, though many microorganisms have adapted to survival in low water environments, such as innate surfaces (Lebre et al., 2017, Zeidler and Müller, 2019a). Clinical *A. baumannii* isolates have a remarkable tolerance to desiccation and can survive on inanimate hospital surfaces such as bed rails and tables for months at a time (Jawad et al., 1998). Desiccation tolerance is an important virulence factor and increases transmission of infection between patients and facilitates environmental persistence (Selasi et al., 2016, Han et al., 2016). Furthermore, desiccation tolerance allows for the maintenance of infection reservoirs, a common source of outbreaks in the hospital setting (Jawad et al., 1998, Wendt et al., 1997, Zenati et al., 2016). Factors involved in the survival of bacteria in dry conditions include growth phase (Farrow III et al., 2018), the presence of compatible solutes (Zeidler and Müller, 2019b), lipid and DNA metabolism pathways (Li et al., 2012, Mandal and Kwon, 2017), heat-shock proteins (Katoh et al., 2004) sigma factors (Hu et al., 2017), and capsule production (Tipton et al., 2018).

Studies have shown that a subset of an *A. baumannii* population are capable of existing in a dormant state during desiccation stress, then resume growth upon favourable environmental conditions (Gayoso et al., 2013, Bravo et al., 2016). Not only is *A. baumannii* highly resistant to desiccation stress, but after stress recovered isolates retain full virulence potential (Chapartegui-González et al., 2018). Studies suggest *A. baumannii* are more resistant to desiccation during the stationary phase of growth and regulated by the BfmRS TCS (Zeidler and Müller, 2019b, Farrow III et al., 2018). Additionally, in one study the non-pathogenic SDF *A. baumannii* strain was found to be significantly less tolerant of desiccation than clinical *A. baumannii* isolates (Antunes et

al., 2011). Opaque variants of a phase variable *A. baumannii* strain AB5075 showed enhanced capsule production and higher desiccation tolerance compared to translucent counterparts (Chin et al., 2018). This observation led to a subsequent study which showed acapsular mutants of AB5075 were much less tolerant to desiccation stress than the wild-type (WT) parental strain (Tipton et al., 2018).

1.2.4 Cell surface hydrophobicity

The hydrophobicity of bacterial cell surfaces contributes to the ability of bacteria to adhere to a range of surfaces including plastics used for medical equipment and indwelling medical devices such as catheters and tracheal tubing (Pour et al., 2011, Costa et al., 2006, Boujaafar et al., 1990, McQueary and Actis, 2011). Furthermore, high levels of cell surface hydrophobicity may dampen electrostatic interactions between the *A. baumannii* OM and cationic antimicrobial compounds such as polymyxins (Powers and Trent, 2018). It has also been shown that high cell surface hydrophobicity may increase the uptake of *A. baumannii* cells by phagocytic host immune cells during infection (Arakawa, 1994). Cell surface hydrophobicity has previously been shown to vary substantially between *A. baumannii* strains and may be higher in virulent isolates (Giles et al., 2015, Boujaafar et al., 1990). For example, a study comparing the hydrophobicity of 88 *A. baumannii* isolates found an increase in hydrophobicity in clinical isolates (92%) compared to control strains (5%) (Boujaafar et al., 1990). Clonal lineage has also been correlated with hydrophobicity profiles of *A. baumannii*. A study investigating surface related features of clinical *A. baumannii* isolates found those belonging to clonal lineage I to be hydrophobic whereas those isolate belonging to clonal lineage II showed varying degrees of hydrophobicity (Skerniškytė et al., 2018). Cell surface hydrophobicity in *A. baumannii* has been associated with a number of surface structures including lipooligosaccharide (LOS), CsuE pili, OM receptors and BAP (Pakharukova et al., 2018, Brossard and Campagnari, 2012, Soon et al., 2012, Lee et al., 2006, Abdollahi et al., 2018). Furthermore, structural modifications to Type IV pili have also recently been associated with changes in cell surface hydrophobicity in *A. baumannii* (May et al., 2019).

1.2.5 Antimicrobial resistance mechanisms

Effective antimicrobial treatment is critical for the treatment of severe *A. baumannii*

infections. Furthermore, adequate environmental disinfection during outbreaks significantly reduces patient to patient transmission. However, due to the high frequency of antimicrobial resistance in this organism, this is a difficult task. As rates of antimicrobial resistance in clinical *A. baumannii* isolates are remarkably high, the World Health Organisation (WHO) identified combating resistance in *A. baumannii* as a task of critical priority (WHO, 2017). Carbapenems, such as imipenem and meropenem, are typically used as a first line treatment of susceptible *A. baumannii* infections. Alarmingly, infections with carbapenem resistant *A. baumannii* (CRAB) are becoming increasingly common (Piperaki et al., 2019, Ng et al., 2018). Alternative agents to treat CRAB include polymyxin B and polymyxin C (colistin), though the latter is a drug of last resort as it is highly nephrotoxic and neurotoxic; furthermore resistance to these compounds is emerging (Qureshi et al., 2015, Isler et al., 2019). Tigecycline is an alternative drug used to treat resistant *A. baumannii*, but with inferior patient outcomes compared to other antimicrobial treatments (Isler et al., 2019). Frequently, combinations of the aforementioned drugs are employed as this has been proven effective and reduces the risk of resistance development (Piperaki et al., 2019).

A. baumannii possess a diverse repertoire of antimicrobial resistance mechanisms (Ayoub Moubareck and Hammoudi Halat, 2020). Intrinsic antimicrobial resistance mechanisms of *A. baumannii* include low OM permeability, biofilm formation and LOS (Geisinger et al., 2019, Geisinger and Isberg, 2015, Badave and Kulkarni, 2015, Carretero-Ledesma et al., 2018, Moffatt et al., 2010). Capsule provides indirect resistance to antimicrobial compounds by forming a barrier around the bacterial cell (Geisinger et al., 2019, Geisinger and Isberg, 2015). In addition to these intrinsic factors, the plasticity of the *A. baumannii* genome facilitates the acquisition of new resistance mechanisms from the environment and modification of existing mechanisms in response to antimicrobial challenge (Fernández-Cuenca et al., 2015).

Efflux pumps are membrane proteins which expel antimicrobials from the bacterial cell and are a major contributor to antimicrobial resistance in *A. baumannii* (Li et al., 2016a). Efflux pumps, such as the Ade Resistance-Nodulation-Cell Division Type (RND) efflux pumps, AdeABC and AdeIJK, extrude multiple classes of antimicrobials (Yoon et al., 2015, Leus et al., 2018). Other efflux pumps convey resistance to a single antimicrobial or can be limited to a class of antimicrobials. For example, EmrAB is

associated with colistin resistance (Lin et al., 2017), TetA and TetB convey resistance to tetracycline and minocycline (Ribera et al., 2003, Vilacoba et al., 2013), and CraA resistance to chloramphenicol (Roca et al., 2009). Additionally, overproduction of certain efflux pumps, for example mutations in promoter regions which lead to overexpression, is common and contributes to the MDR phenotype of many *A. baumannii* strains (Yoon et al., 2015, Kornelsen and Kumar, 2021).

Antibiotic target modifying enzymes such as β-lactamases, aminoglycoside modifying enzymes, and penicillin binding proteins are common in *A. baumannii* (Vila et al., 1993, Shi et al., 2005). For example, β-lactamases have been identified which contribute to resistance to ampicillin, imipenem, and carbapenem (Poirel and Nordmann, 2006, Bou and Martínez-Beltrán, 2000, Rumbo et al., 2013). Furthermore, resistance to fluoroquinolones is commonly acquired in *A. baumannii* via mutations in the intended drug targets, DNA gyrase and topoisomerase (Kakuta et al., 2020). New therapeutic treatments, improved infection control measures, and enhanced antimicrobial stewardship are sorely needed to combat MDR *A. baumannii*.

1.3 Host immune response to *A. baumannii* infection

A characteristic of many virulent *A. baumannii* strains is the ability to dampen the immune response. This promotes bacterial proliferation, which increases the severity of infection and the risk of disseminated illness (De Breij et al., 2012). Factors involved in modulation of the host immune response are complex and vary greatly between *A. baumannii* isolates (De Breij et al., 2012, García-Patiño et al., 2017, King et al., 2009). Numerous virulence factors contribute to successful colonisation and infection by *A. baumannii* including iron acquisition systems (Eijkelkamp et al., 2011a), OM proteins (Choi et al., 2008), TCSs (Liou et al., 2014), superoxide dismutase (Bhargava et al., 2014), LOS (Moffatt et al., 2013, García-Quintanilla et al., 2014), type VI secretion systems (Repizo et al., 2015), outer membrane vesicles (Li et al., 2015), RecA (Aranda et al., 2011), and capsule (Russo et al., 2010, Geisinger and Isberg, 2015, Tipton et al., 2018, Wong et al., 2017).

Host defence mechanisms against *A. baumannii* are vital for the resolution of *A. baumannii* infections, yet host derived factors remain largely understudied (García-Patiño et al., 2017). *A. baumannii* is capable of infecting multiple cell lines and animal

models to varying degrees and host innate immune defences have been implicated in clearance of *A. baumannii*. Early clearance of *A. baumannii* infection by interaction with host innate defence mechanisms is the primary factor in determining disease outcomes (Bruhn et al., 2015). A primary driver of *A. baumannii* bacteraemia is to escape from host innate effectors, thus allowing for proliferation in blood and dissemination of infection (Bruhn et al., 2015). Several reviews have been published on the immune response to *A. baumannii* infections, see Garcia-Patiño *et al* (García-Patiño et al., 2017) Chen (Chen, 2020), and Pires and Parker (Pires and Parker, 2019) for a more comprehensive information. This section outlines the major players in the host innate immune response to *A. baumannii* infection.

1.3.1 Cellular innate immune response to *A. baumannii* infection

The innate cellular immune response to *A. baumannii* infection involves macrophages (Qiu et al., 2012), neutrophils (Qiu et al., 2009), dendritic cells (Lee et al., 2007), natural killer (NK) cells (Tsuchiya et al., 2012), and epithelial cells (Choi et al., 2008). Of these, macrophages, neutrophils, and epithelial cells are considered the primary players in providing a robust innate response to *A. baumannii* infection. Although not a traditional intracellular pathogen, *A. baumannii* is capable of invading host epithelial cells, which may assist this bacterium in evading host defences and facilitating dissemination of infection (Choi et al., 2008, Sycz et al., 2021).

1.3.2 Macrophages

Alveolar macrophages (AMs) are the first line of defence against pulmonary *A. baumannii* infections (Gordon and Read, 2002, Qiu et al., 2012). Additionally, macrophages which circulate in the blood are vital for combating *A. baumannii* bacteraemia and dissemination of infection (Bruhn et al., 2015). Macrophages have phagocytic, antigen processing, and immunoregulatory functions in response to *A. baumannii* infection. During infection, interactions between specific *A. baumannii* pathogen associated molecular patterns (PAMPs), such as lipid A or peptidoglycan, and cognate pattern recognition receptors (PRRs) located on the macrophage cell surface, trigger the internalisation of the bacterial cell within a phagosome (Gordon and Read, 2002). The phagosome then fuses with a lysosome, a vacuole containing lysozyme and reactive oxygen species (ROS), forming a phagolysosome where the bacterial cell is

degraded (Gordon and Read, 2002). Antigens can then be processed and displayed on the macrophage surface to signal subsequent immune responses. In response to internalisation of *A. baumannii*, or *A. baumannii* PAMPs, macrophages produce a range of proinflammatory cytokines and chemokines including tumour necrosis factor (TNF)-α, interleukin (IL)-1β, IL-6, and IL-10, macrophage inflammatory protein (MIP)-2, and the antimicrobial nitric oxide (NO) (Qiu et al., 2012). Furthermore, opsonisation of *A. baumannii* by host complement proteins (Section 1.3.3) increases phagocytosis and immune modulator production by macrophages (Bruhn et al., 2015).

The role of AMs in defence against pulmonary *A. baumannii* infections has been assessed experimentally using *in vitro* macrophage culture as well as *in vivo* murine intranasal challenge (Qiu et al., 2009). One study showed intracellular killing of phagocytised *A. baumannii* by J774 macrophages was over 80% and 99% killing after 24 and 48 hours, respectively (Qiu et al., 2012). Infection induced the coordinated production of cytokines/chemokines by the macrophages in a time dependent manner (Qiu et al., 2012). For example, the induction of TNF-α and IL-6 occurred as early as 4 hours post infection whereas levels of IL-10 and NO were undetectable at 4 hours but peaked at 24-48 hours post incubation. *In vivo* studies were also carried out by inoculating C57BL/6 mice, which showed a robust innate immune response to infection with the *A. baumannii* strain ATCC 17961 (Qiu et al., 2009, Qiu et al., 2012). In a subsequent study, intranasal infection resulted in macrophage uptake of *A. baumannii* as early as 4 hours post infection, and a significant recruitment of macrophages to the infection site was seen at 24 hours post infection (Qiu et al., 2012).

In addition to responding to pulmonary infection, macrophages are important for the early resolution of *A. baumannii* bacteraemia. A study by Bruhn and colleagues tested the virulence of 33 *A. baumannii* strains using a mouse bacteraemia model and found an inverse relationship between virulence in mice and uptake by RAW 264.7 macrophages *in vitro* (Bruhn et al., 2015). Strains identified as hypervirulent showed reduced uptake by macrophages and increased survival compared to hypovirulent strains (Bruhn et al., 2015). Additionally, bacterial loads of the hypovirulent strains dramatically increased in macrophage depleted mice, identifying macrophages as an important mechanism for clearing infection (Bruhn et al., 2015).

Neutrophils

Neutrophils are phagocytic immune cells which circulate in the blood and are rapidly recruited to sites of inflammation in response to chemoattractant signals, such as TNF-α and MIP-2, which are secreted by epithelial cells, natural killer (NK) cells and macrophages during infection (Tsuchiya et al., 2012, Segal, 2005). Neutrophils eliminate pathogens primarily through phagocytosis and degradation via ROS and antimicrobial proteins such as lysozyme (Kamoshida et al., 2020, Segal, 2005). Other mechanisms, including degranulation and the production of neutrophil extracellular traps (NETs), also contribute to their response against *A. baumannii* (Kamoshida et al., 2018, Kamoshida et al., 2015, Lázaro-Díez et al., 2017). Amazingly, studies have shown a human neutrophil can phagocytise up to 50 *A. baumannii* cells (Lázaro-Díez et al., 2017). *In vitro* studies show neutrophils can neutralise *A. baumannii* cells within 20-30 minutes of co-incubation (Lázaro-Díez et al., 2017). Furthermore, a study by Bruhn and colleagues reported neutrophils were superior to macrophages at killing *A. baumannii* cells, as it took neutrophils and macrophages to neutralise 90% of *A. baumannii* approximately 1 hour and 24 hours, respectively (Bruhn et al., 2015). Although beyond the scope of this thesis, a recent publication by Lazaro-Diez *et al* describes molecular mechanisms involved in neutrophil phagocytosis, including excellent videos and images of human neutrophils engulfing *A. baumannii* cells (Lázaro-Díez et al., 2017).

Neutrophils were first identified as an important component of the host immune response to *A. baumannii* because neutropenic patients showed an increased susceptibility to *A. baumannii* infections (Karim et al., 1991). Animal model studies supported this notion and identified that the early recruitment of neutrophils to the infection site is crucial for clearance of *A. baumannii* pulmonary infections in mice (Qiu et al., 2009, Van Faassen et al., 2007, Tsuchiya et al., 2012). Furthermore, several studies have shown higher lethality in neutrophil depleted mice challenged with *A. baumannii* compared to mice with normal neutrophil numbers (Bruhn et al., 2015, Van Faassen et al., 2007). Paradoxically, one study suggests *A. baumannii* can exploit neutrophils as transport vehicles to other anatomical sites by adhering to the neutrophil surface but escaping the neutrophils defence mechanisms (Kamoshida et al., 2016). The mechanisms for adhering to, yet evading phagocytosis by neutrophils by *A. baumannii*

are unknown, but may involve just a small percentage of “escapees” with the majority of the bacterial inoculum being susceptible to degradation by neutrophils (Kamoshida et al., 2016).

In addition to phagocytosis, neutrophils can protect against *A. baumannii* infection using a defence mechanism known as NETs (Kamoshida et al., 2015). When neutrophils are strongly activated, they form NETs, whereby the nucleus of the neutrophil is destroyed, and nucleic acids and chromatin are released into the cytosol. These NETs are very effective at catching and inactivating invading microbes (Kamoshida et al., 2015). *In vitro* studies suggest *A. baumannii* is capable of inhibiting the formation of NETs by supressing adhesion to neutrophils (Kamoshida et al., 2015, Kamoshida et al., 2018). Furthermore, evidence suggests *A. baumannii* may use neutrophils as a carrier cell to promote disseminated illness by hitching a ride to other locations in the host (Kamoshida et al., 2016).

Epithelial cells

The respiratory epithelium is often the first point of contact between pathogens such as *A. baumannii* and the host. Besides forming a physical barrier against pathogens epithelial cells play an active part in the innate immune response. Airway epithelial cells possess PRRs including the Toll-like receptor (TLR)-4, and TLR-2 which, when activated by *A. baumannii* derived antigens can lead to the production of proinflammatory cytokines, particularly IL-8 (March et al., 2010, Parker and Prince, 2011). Components of invading organisms are often shed into the host environment, allowing them to be detected by intracellular PRRs. The airway epithelium also produces antimicrobial proteins and peptides including lysozyme, lactoferrin, and β defensin in response to interactions with bacterial components (Choi et al., 2008, Yang et al., 2000, Dai et al., 2018, Konstantinidis et al., 2016).

1.3.3 Cell receptors involved in *A. baumannii* recognition

TLRs are a family of receptors produced by many host cells including macrophages and epithelial cells (Gordon and Read, 2002). Each member of the TLR family recognises a specific PAMP. Some TLRs are located on the outer leaflet of the host cell and are activated by extracellular PAMPS; for example, TLR-4 recognises the lipid A portion of lipopolysaccharide (LPS)/LOS and TLR-2 recognises lipopeptides. Activation of TLRs

triggers a complex signal transduction cascade which results in the inflammatory response by releasing cytokines and chemokines and activating the proliferation and recruitment of other immune cells (Wu et al., 2009). Studies have shown that challenge with *A. baumannii* leads to the activation of TLR-4, TLR-2 and TLR-9 in pulmonary epithelial cells and macrophages (García-Patiño et al., 2017, Knapp et al., 2006).

Nucleotide-binding oligomerisation domain (NOD)-like receptors are a family of receptors which detect PAMPs in the host cell cytosol. NOD-1 and NOD-2 are involved in the immune response against *A. baumannii*. Both NOD-1 and NOD-2 recognise bacterial peptidoglycan and respond in a similar manner to TLRs by activating the production of proinflammatory cytokines and antimicrobial peptides via the NF-Kβ pathway, ultimately leading to secretion of TNF-α, β-defensin, Interferon (IFN)-ϒ and IL-1, IL-6, IL-8, IL-10, and IL-10 (Knapp et al., 2006, Moffatt et al., 2013, Lin et al., 2012). Responses to *A. baumannii* are highly variable depending on which bacterial strain used, with some strains showing a more robust immune evasion response compared to other strains analysed (García-Patiño et al., 2017).

Proinflammatory chemokines and cytokines are primarily produced subsequent to the activation of NF-KB, in response to activation to the aforementioned surface receptors (Dikshit et al., 2018). These reactions are kept in check as too much inflammation can lead to the destruction of host tissues. The primary action of NF-KB activation is the release of TNF-α and the cytokine IL-8, which go on to recruit neutrophils to the site of infection (March et al., 2010, Bist et al., 2014).

1.3.4 Soluble secreted factors

Complement

The complement system consists of over 30 host proteins which, in response to activation by cells identified as ‘non-self’ (such as pathogens), undergoes a series of reactions known as the complement cascade (Kim et al., 2009, King et al., 2009, Bruhn et al., 2015, Koenigs et al., 2016, Sanchez-Larrayoz et al., 2017, Sarma and Ward, 2011). There are three known pathways of complement activation, the classical, lectin and alternative pathways. The classical pathway is activated by antibodies bound to their target and the lectin pathway by the presence of lectin bound to specific sugars;

both have similar early pathways of activation (Frank et al., 1987). The alternative pathway is triggered by carbohydrates, lipids, and proteins located on a foreign surface; thus making this pathway most relevant for the innate immune response to capsule (Sarma and Ward, 2011). Although initial steps of each pathway differ, all three activation pathways converge at the cleavage of the complement protein C3 into C3b, which is deposited on the bacterial cell. This results in opsonisation of bacteria and the release of complement-derived cytokines (Sarma and Ward, 2011). Cytokines amplify the response and late acting complement proteins sequentially associate with C3b to form the membrane attack complex, which forms a pore in the bacterial membrane leading to bacterial cell lysis (Sarma and Ward, 2011, Frank et al., 1987).

Levels of complement resistance between *A. baumannii* isolates can be highly variable (García et al., 2000, King et al., 2009). Due to the highly complex nature of the complement response, it is unsurprising *A. baumannii* has co-evolved a range of mechanisms to thwart complement attack either indirectly by the production of biofilms and capsule (García-Patiño et al., 2017) or directly through the degradation of complement components (Koenigs et al., 2016, King et al., 2013). For example, the OMP CipA confers resistance to complement through the degradation of C3b (Koenigs et al., 2016). Additionally, a secreted serine protease, PKF, reduces serum susceptibility by almost 50%, by cleavage of complement components, thus downgrading the response (King et al., 2013). Interestingly, although PKF has an anti-complement response it also inhibits the formation of biofilm, another mechanism used by *A. baumannii* to resist complement lysis (King et al., 2013). Lastly, the binding of factor H may protect against complement lysis, but only two conflicting accounts are available (Kim et al., 2009, King et al., 2009)

Lysozyme

Lysozyme is present in virtually all human secretions, such as respiratory secretions, tears, and skin, as well as neutrophil granules and the phagolysosomes of macrophages (Wiesner and Vilcinskas, 2010, Liu et al., 2015). The primary antimicrobial action for lysozyme is the degradation of peptidoglycan, a component of the bacterial cell envelope, by hydrolysis of specific bonds between N-acetylmuramic acid and N-acetyl glycosamine residues (Niyonsaba and Ogawa, 2005, Liu et al., 2015, Wiesner and Vilcinskas, 2010). Due to its cationic structure, lysozyme also causes cell lysis

independent of peptidoglycan degradation by forming pores in the bacterial envelope (Ragland and Criss, 2017). Several studies have highlighted the importance of lysozyme in limiting bacterial growth at mucosal surfaces, including the respiratory tract; a common site for *A. baumannii* infections (Ragland and Criss, 2017, Ellison 3rd and Giehl, 1991, Dajani et al., 2005, Akinbi et al., 2000).

Alteration in lysozyme susceptibility has previously been associated with modifications in colistin resistance and the production of LOS and capsule (Napier et al., 2013, García-Quintanilla et al., 2014, Tipton et al., 2018, Bao et al., 2018). Furthermore, opaque variants of the *A. baumannii* strain AB5075 show a higher rate of lysozyme resistance (Tipton et al., 2015). Importantly, acapsular mutants of the *A. baumannii* strain AB5075 were found to be significantly less resistant to lysozyme challenge than the WT parent (Tipton et al., 2018). Similar phenomena have been seen in other bacteria. For instance, *Neisseria gonorrhoeae* is only susceptible to lysozyme when membrane integrity is compromised (Ragland et al., 2017), and a study in *Escherichia coli* showed defects membrane morphology also resulted in an increase in lysozyme sensitivity (Heidrich et al., 2002).

Due to the pressing issue of infections with MDR *A. baumannii*, novel methods of treatment such as redesigning components of the immune system are being trialled. A recent paper by Saito and colleagues describes the efficacy of lysozyme in the killing of *A. baumannii* in conjunction with specific oligosaccharide conjugates (Saito et al., 2019). The conjugate, named LYZOX, represented a two-step approach whereby the oligosaccharide conjugate weakened or destroyed the outer cell wall of *A. baumannii*, providing access for the lysozyme portion of the compound to the primary target of the peptidoglycan layer. The lytic action of LYZOX was between 10 to100-fold more lytic than the active lysozyme control (Takoi et al., 2019).

Lactoferrin

Lactoferrin is an iron binding glycoprotein present in many host biological fluids including mucosal surfaces and saliva, with particularly high abundance in milk (Farnaud and Evans, 2003). The primary role of lactoferrin is to bind free iron and minimise the harmful effects of ‘free’ iron to the human host, i.e. the production of damaging free radicals. A secondary effect of the sequestering of iron by lactoferrin is

providing nutritional immunity (See Section 1.2.1). Lactoferrin also possesses direct antimicrobial activity, as it binds to the bacterial cell wall and effects permeability (Farnaud and Evans, 2003, Drago-Serrano et al., 2012).

Beta defensins

A broad range of host peptides have been shown to have antimicrobial effects on *A. baumannii* (Neshani et al., 2020). Antimicrobial peptides are naturally produced compounds; however, we now have the capability to produce them artificially. β defensins are cationic antimicrobial peptides which are important for host defence against respiratory infections (Parker and Prince, 2011) and are predominantly active against Gram-negative bacteria and yeast. These cationic peptides facilitate microbial killing by binding with the bacterial wall, disrupting the membrane and increasing the permeability. There are six types of human β defensins (hβD), but only hβD1 and hβD2 are active against bacterial pathogens such as *A. baumannii* (Feng et al., 2014). The defensin hβD1 is constitutively expressed from several host tissues whereas hβD2 production is induced by bacterial challenge (Parker and Prince, 2011, March et al., 2010). Upon challenge with *A. baumannii*, epithelial cells and neutrophils, upregulates expression of proinflammatory cytokines such as TNF-α and IL-1β and triggers the increased production and secretion of hβD2 (March et al., 2010, Pires and Parker, 2019). Interestingly, one study found that hβD2 was more effective on MDR clinical isolates of *A. baumannii* than non-MDR isolates (Routsias et al., 2010).

1.3.5 The human cathelicidin LL-37

The human cathelicidin LL-37 is a host derived cationic antimicrobial peptide. It is generated primarily by respiratory epithelial cells and neutrophils and shows broad spectrum antimicrobial activity (Parker and Prince, 2011). LL-37 is the most studied member of the cathelicidin family of antimicrobial peptides and is produced by a broad range of cell types (Neshani et al., 2020). Unlike HβD, LL-37 is capable of interfering with the ability of *A. baumannii* to adhere to abiotic surfaces and form biofilms (Feng et al., 2013). Additionally, LL-37 has been found in NETs (Section 1.3.1). These NETs enhance the killing ability of LL-37 and prevent *A. baumannii* biofilm formation (Pires and Parker, 2019). Similar to hβD2, LL-37 shows an increased efficacy against some MDR clinical isolates of *A. baumannii*, especially colistin resistant isolates (García-

Quintanilla et al., 2014).

1.4 Membrane associated glycoconjugates of *A. baumannii*

1.4.1 Lipooligosaccharide

LPS is an integral component of the outer membrane of most Gram-negative bacteria (Raetz and Whitfield, 2002). It is comprised of three distinct domains; a lipid A anchor, inner and outer core oligosaccharide, and O-antigen polysaccharide (Raetz and Whitfield, 2002) (Figure 1.1). The attachment of O-antigen polysaccharide to the lipid-A core is facilitated by the transmembrane protein WaaL (Whitfield, 2006, Wang and Quinn, 2010, Whitfield, 1995). Some bacteria, including *A. baumannii*, do not possess traditional LPS, but a surface glycoconjugate known as LOS (Figure 1.1) (Preston et al., 1996, Kenyon et al., 2014b). LOS is important for survival and forms a major component of the cells outer membrane (Weber et al., 2016). This molecule is similar to LPS in that it is comprised of lipid A, inner and outer core saccharides and a single repeat unit sugar rather than a long oligosaccharide attached O-antigen (Campagnari et al., 1990, Whitfield and Paiment, 2003) (Figure 1.1).

The sugar subunit structure of the outer core (OC) portion of the LOS varies between *A. baumannii* strains. At least 12 OC structures have been confirmed by sequencing and bioinformatic analysis (Wyres et al., 2020, Kenyon et al., 2014b).

Analysis of known *A. baumannii* genome and proteome sequences has failed to find homologues to *waaL*, indicating *A. baumannii* produces LOS rather than LPS (Kenyon et al., 2014b). This is supported by experimental evidence including the absence of distinct banding usually seen of LPS in silver stained SDS-polyacrylamide gel electrophoresis (PAGE) images and the lack of anti-lipid A antibody binding to extracted polysaccharide (Kenyon et al., 2014b, Pantophlet et al., 2002).

Modification of lipid A is a common mechanism used by Gram-negative bacteria to protect themselves against cationic antimicrobial peptides (CAMPs) such as the host derived β-defensin and the antibiotic of ‘last resort’ colistin (Boll et al., 2015). The most common modification is the acetylation of lipid A.

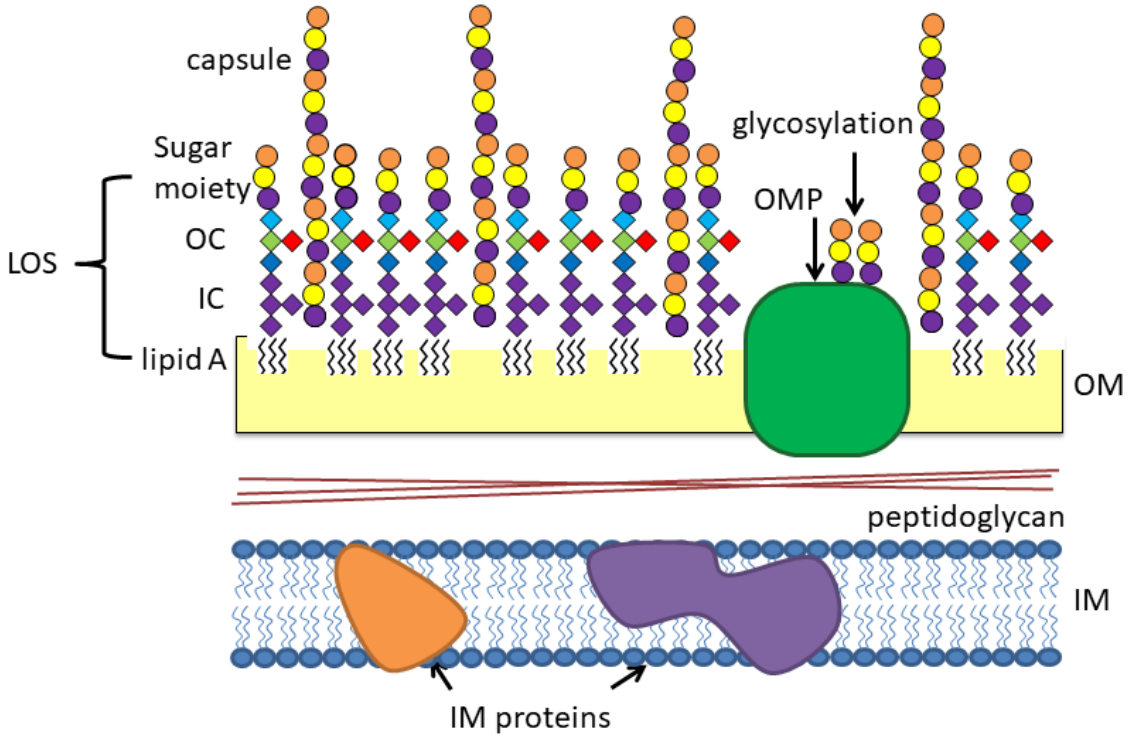

Figure 1.1 Components of the *A. baumannii* cell membrane. The phospholipids of the inner membrane (IM) are represented by small blue ovals with two prongs extending into the centre of the IM. The peptidoglycan layer is represented by thin maroon strands between the IM and outer membrane (OM). The OM is represented by a yellow box decorated with; lipooligosaccharide (LOS) which is comprised of lipid A (three zig zags), inner core (IC, purple diamonds), outer core (OC, multicoloured diamonds) and a single sugar moiety (orange, yellow, and purple circles), capsule which is comprised of repeat sugar moieties and an outer membrane protein (OMP) glycosylated with two sugar moities,

Besides protecting the cell from polymyxin antibiotics, increased acetylation may also protect from desiccation, killing by complement in human serum, and increase activation of the immunostimulatory pathway via TLR-4 signalling (Boll et al., 2015). Lipid A modification can also be driven by the PmrAB system, which when activated can lead to the addition of $GalN^+$ to lipid A, preventing recognition by polymyxin antibiotics. To further increase this resistance mechanism, mutations of the *pmrABC* operon can lead to constitutive expression of the enzymes responsible for this $GalN^+$ addition (Zhang et al., 2017, Arroyo et al., 2011, Chin et al., 2015)

A less common method of LOS modification is the complete removal of lipid A. Many *A. baumannii* can rapidly develop resistance to polymyxin antibiotics by incorporating point mutations into genes which encoding LOS synthesis and export machinery (Moffatt et al., 2010). This results in complete loss of LOS. Evidence suggests not all *A. baumannii* are capable of living in the absence of LOS, but those that can have decreased membrane stability and altered resistance profiles compared to their WT counterparts (Boll et al., 2016b, Moffatt et al., 2010). Furthermore, complete LOS loss has been shown to vastly alter the cell surface by increasing production of lipoproteins, phospholipids, and PNAG (Henry et al., 2011).

Strains of *A. baumannii* which have lost their LOS are typically attenuated, as LOS is involved in cellular fitness and evasion of host immune factors during infection. These include cell membrane stability, enhancing cell motility and adhesion, providing a permeability barrier, preventing killing by opsophagocytes and antimicrobial peptides. In addition to the above, the lipid A portion of LOS is a highly immunogenic endotoxin, triggering a robust inflammatory response in host cells via the TLR-4/ NF-Kβ pathway (Erridge et al., 2007). As expected, LOS-deficient mutants fail to initiate an inflammatory response via TLR-4 (Moffatt et al., 2013). Furthermore, during macrophage challenge, LOS-deficient mutants stimulate lower production of NF-Kβ and secretion of TNF-α compared to the WT *A. baumannii*. Lastly, LOS-deficient mutants showed a higher susceptibility to the human antimicrobial peptide LL-37 than the WT strain (Moffatt et al., 2013).

1.4.2 Protein glycosylation

Glycosylation of proteins is a common post transcriptional modification tool employed

by most prokaryotes including pathogenic bacterial species (Eichler and Koomey, 2017). Two main types of protein glycosylation have been identified in bacteria, N-glycosylation and O-glycosylation, though only O-linked glycosylation has been identified in *A. baumannii* (Scott et al., 2014). O-linked glycosylation involves the attachment of a glycan to a specific amino acid (serene or threonine) of the cognate receptor protein by an O-oligosaccharyltransferase (O-OTase) enzyme (Harding et al., 2015). A 2012 study by Iwashkiw and colleagues identified seven glycoproteins in *A. baumannii* ATCC 17978 which were all glycosylated by the same glycan structure (Iwashkiw et al., 2012).

In *A. baumannii* the glycosyl transferases (GTs) necessary for capsule assembly are part of a bifurcated pathway (Lees-Miller et al., 2013) (Figure 1.2). Therefore, the subunit structure for both capsule and the O-glycan, which decorate surface proteins, have an identical structure (Lees-Miller et al., 2013).

Protein glycosylation contributes to the optimal performance of many cellular functions as well as enhancing pathogenicity. A number of studies have shown protein glycosylation enhances the stability of proteins, increases adherence to surfaces, increases the formation of biofilm, assists in immune system evasion, and promotes overall virulence (Benz and Schmidt, 2002, Schmidt et al., 2003, Iwashkiw et al., 2012, Lees-Miller et al., 2013).

Besides the general O-glycosylation system described above, the gene for a second O-OTase has been identified in most *A. baumannii* strains (Harding et al., 2015). This gene is typically located close to the operon which encodes the Type IV pili, and the O-OTase it encodes is specific for glycosylation of pilin, the protein subunits that compose the Type IV pili (Ronish et al., 2019, Harding et al., 2015).

Poly-β-(1-6)-N-acetylglucosamine

PNAG is an exopolysaccharide which is secreted by most biofilm forming bacteria and forms the “glue” of biofilms, thus making up substantial proportion of the exopolysaccharide matrix (Choi et al., 2009). The volume of PNAG produced by different *A. baumannii* strains varies considerably and the amount of PNAG produced is correlated to the robustness of biofilm formed (Choi et al., 2009).

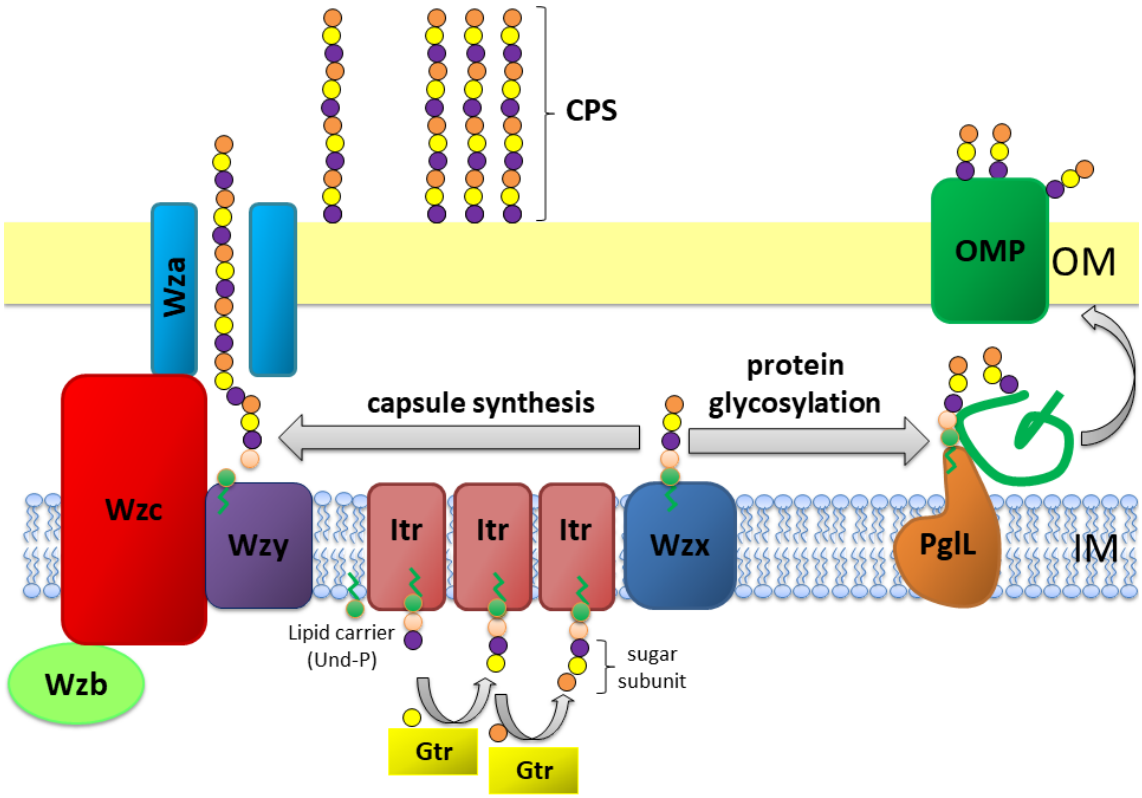

Figure 1.2 Schematic representation of capsule polysaccharide assembly and export in *A. baumannii*. Synthesis begins with the initial transferase (Itr; maroon) located in the inner membrane (IM) transferring the first sugar of the repeating unit to a lipid carrier (Und-P; green circle). Subsequent sugars are then added to the growing unit by specific glycosyltransferases (Gtr; yellow) on the cytosolic side of the inner membrane. The capsule subunit (K unit) is then transferred to the periplasm via the integral membrane protein Wzx (dark blue). The sugar subunits are polymerised by the Wzy protein (purple) and the Wza/Wzb/Wzc complex (cyan, lime, red) coordinates high level polymerisation and export of the growing chain, moving them to the outer membrane (OM). For glycosylation, PglL (orange) links the sugar subunit onto selected outer membrane proteins (OMP; dark green).

Peptidoglycan

Although produced in lower quantities compared to Gram-positive bacteria, peptidoglycan is an essential component of the membrane for Gram-negative bacteria. Forming a thin layer sandwiched between the inner and outer membrane, peptidoglycan is important for Gram-negative bacterial growth and stability (Vollmer and Höltje, 2004, Amera et al., 2020) (Figure 1.1). Furthermore, a recent study has shown that peptidoglycan provides *A. baumannii* with an advantage during bacterial warfare with non-related bacteria species as it provides a barrier against Type 6 Secretion Systems (Le et al., 2020).

1.5 Capsular polysaccharide in *A. baumannii*

An abridged version of this section has been published as a minireview in the journal Frontiers in Microbiology (Section 8 Appendix 1).

1.5.1 Capsule synthesis in *A. baumannii*

Possession of capsular polysaccharide is a virulence trait in bacteria such as *A. baumannii*. Comprised of tightly packed repeat units of oligosaccharides, capsule forms a discrete layer on the bacterial surface. Capsule can be found on both Gram-positive and Gram-negative bacteria and the major differences in the cell wall can affect the mode of capsule synthesis (Yother, 2011, Whitfield, 2006). In general, capsule synthesis and export is more complex in Gram-negative bacteria as they have two membranes compared to a single membrane in Gram-positive bacteria. Furthermore; Gram-negative capsule polymers are hydrophilic and of high molecular weight (10^5-10^6 Da), which are complicated to synthesise and export (Whitfield, 2006, Whitfield and Paiment, 2003). In Gram-negative bacteria the capsule assembly and export process spans the three principal layers of the cell envelope; the IM, the peptidoglycan layer and finally the OM onto which either LPS/LOS and/or capsule is attached (Whitfield, 2006) (Figure 1.2).

There are three primary mechanisms of capsule synthesis; Wzy dependent, ABC transporter dependent, and synthase dependent mechanisms (Yother, 2011). Of these three mechanisms by far the most prominent is the Wzy dependent mechanism, which represents all known *A. baumannii* capsule synthesis mechanisms (Hu et al., 2013,

Kenyon and Hall, 2013). In the Wzy pathway, capsule is synthesised and exported to the cell surface via a series of sequential steps (Figure 1.2). Firstly, capsule repeat (K) units are synthesised on the cytoplasmic surface of the IM, polymerised on the periplasmic side of the IM, and exported to the cell surface. Synthesis of K units is initiated by the IM bound initial transferase (IT) followed by the subsequent transfer of sugars by specific GTs (Figure 1.2). The K unit is generally comprised of 4-6 sugars and the GT determines the addition of a particular sugar. This process occurs on an undecaprenyl pyrophosphate (Und-P) lipid carrier molecule (Whitfield, 2006, Kenyon and Hall, 2013, Lees-Miller et al., 2013). This subunit bound to Und-P is then transferred across to the periplasmic side of the IM by the Wzx translocase. Polymerisation of repeat subunits occurs in the periplasm and is catalysed by the IM bound protein Wzy, which transfers the growing capsule chain from one Und-P carrier to the next incoming subunit (Figure 1.2) (Collins et al., 2007, Whitfield, 2006).

The transport of capsule to the cell surface is a highly co-ordinated process involving the interaction of three proteins; the OM lipoprotein Wza, the IM bound Wzc autokinase, and the phosphotyrosine protein phosphatase Wzb (Figure 1.2) (Obadia et al., 2007, Whitfield and Paiment, 2003, Wugeditsch et al., 2001). Structural studies have revealed a close interaction between Wzc and Wza, which forms a continuous scaffold across the periplasm (Figure 1.2) (Collins et al., 2007). The structure of Wza in the OM forms a large central cavity in which large polar molecules of capsule can be specifically transported (Dong et al., 2006). High level polymerisation and capsule export is therefore largely dependent on the transphosphorylation of Wza and Wzb, as Wzb is responsible for the dephosphorylation of Wzc (Whitfield and Paiment, 2003). The genes, *wza*, *wzb* and *wzc*, are very well conserved between the loci of different K subtypes, both in *E. coli* and *A. baumannii* (Hu et al., 2013, Whitmore and Lamont, 2012). For many bacteria, the Wzi protein is involved in the final stages of Wzy-dependent capsule synthesis (Whitfield, 2006). This protein is not essential for capsule synthesis, but *E. coli* mutants lacking *wzi* show a decrease in surface attached capsule, suggesting a role in surface attachment (Whitfield, 2006). The exact mechanism of capsule attachment or association with the bacterial outer surface is unknown for Wzy-dependent capsules in Gram-negative bacteria. In many strains of the Gram-positive bacterium *Streptococcus pneumoniae* the capsule is covalently attached to the

peptidoglycan layer of the cell wall. This attachment is facilitated by members of the LytR-Cps2A-Psr protein family (Eberhardt et al., 2012)

1.5.1.1 *Genetic organisation of K loci*

As the complete sequences of more *A. baumannii* isolates become available, the extreme diversity of capsule structures between strains of this bacterium are becoming apparent. To date, over 92 unique capsule loci (KL) have been identified in *A. baumannii* (Figure 1.3). These KL regions typically range from 20 to 35 kb in size and are found within a conserved region of the *A. baumannii* genome, between the *fkpA* and *lldP* genes. This high conservation in the regions flanking the KL promotes homologous recombination, thus increasing the adaptive potential of KL in response to environmental cues (Mostowy and Holt, 2018). Analysis of the genes directing capsule synthesis in ten complete *A. baumannii* genomes originally resulted in the designation of nine capsule types, KL1-KL9, which became the basis for a universal typing scheme for these loci (Kenyon and Hall, 2013). The KL of *A. baumannii* contains the genes required for the biosynthesis and export specific to each K type (Figure 1.3a) (Kenyon and Hall, 2013, Hu et al., 2013). Exceptions to this rule are *A. baumannii* strains possessing KL19 and KL39 regions, where the gene encoding the Wzy polymerase, *wzy*, is found on a small genetic island elsewhere on the chromosome (Kenyon et al., 2016a). Additionally, genes which encode enzymes responsible for the synthesis of some common sugars required for capsule production are found outside of the KL.

All KL show a similar genetic configuration, a highly variable cluster of synthesis and transferase genes required for the biosynthesis of unique KL-type complex sugars, flanked on one side by the highly conserved export genes, and on the other side by a set of genes encoding conserved simple sugars and precursors (Figure 1.3a). The *wzx* and *wzy* genes required for repeat-unit processing are highly variable between KL types (Figure 1.3a, light blue), indicating specificity for particular K unit structures and, in general, the order of *gtr* determinants, encoding specific glycosyltransferases within the KL regions, inversely corresponds with the order of action (Kenyon and Hall, 2013).

a)

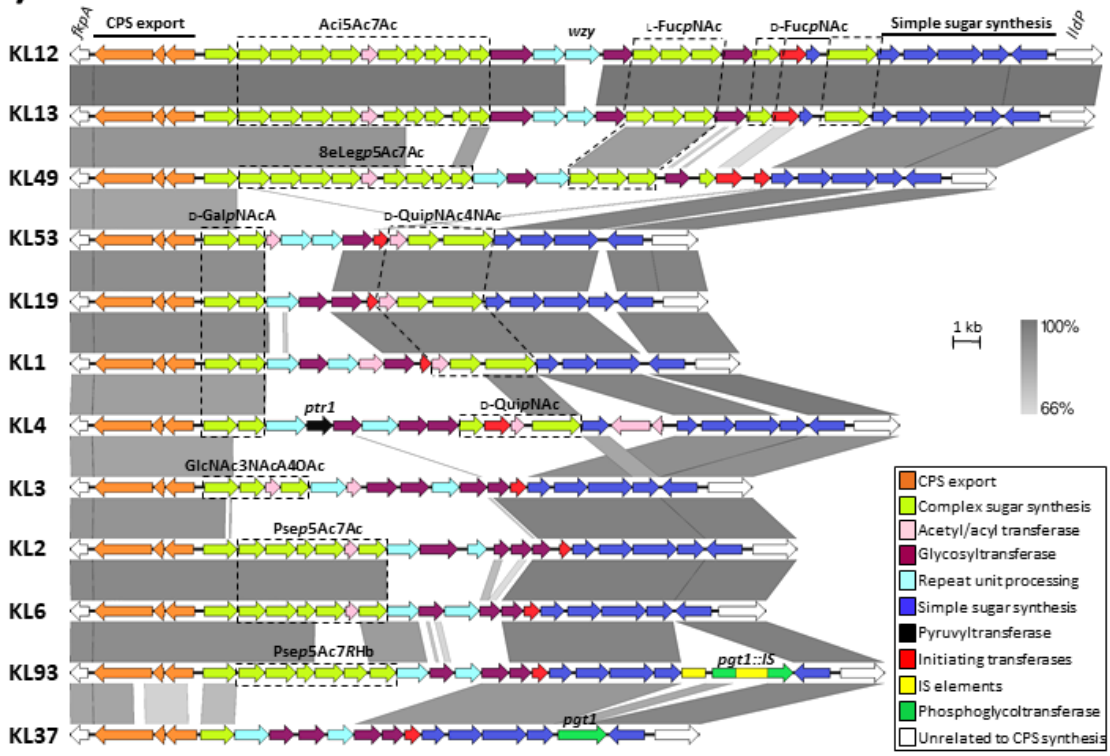

b)

K12
[3)-α-D-GalpNAc-(1→3)-α-L-FucpNAc-(1→3)α-D-FucpNAc-(1→]$_n$
α-Aci5Ac7Ac-(2→6)J

K13
[4)-α-D-Galp-(1→3)α-L-FucpNAc-(1→3)-α-D-FucpNAc-(1→]$_n$
α-Aci5Ac7Ac-(2→6)J

K49
[3)-α-L-FucpNAc-(1→3)-α-D-GlcpNAc-(1→8)-α-8eLegp5Ac7Ac-(2→]$_n$

K53
[3)-α-D-GalpNAcA-(1→3)-β-D-QuipNAc4NAc-(1→]$_n$

K19
[3)-α-D-GalpNAc-(1→4)-α-D-GalpNAcA-(1→3)-β-D-QuipNAc4NAc-(1→]$_n$

K1
[4)-α-D-GlcpNAc-(1→4)-α-D-GalpNAcA-(1→3)-β-D-QuipNAc4N*R*-(1→]$_n$

K4
Pyr(2→4)$_1$
α-D-GlcpNAc-(1→6)$_1$
[4)α-D-GalpNAc-(1→4)-α-D-GalpNAcA-(1→3)-α-D-QuipNAc4NAc-(1→]$_n$

K3
β-GlcNAc3NAcA4OAc-(1→4)$_1$
[3)-α-Galp-(1→6)-β-Glcp-(1→3)-β-GalpNAc-(1→]$_n$
β-GlcpNAc-(1→6)J

K2
[3)-β-D-Galp-(1→3)-β-D-GalpNAc-(1→]$_n$
α-Psep5Ac7Ac-(2→6)-β-D-Glcp-(1→6)J

K6
[4)-β-Pse5Ac7Ac-(2→6)-β-D-Galp-(1→6)-β-D-Galp-(1→3)-α-D-GalpNAc(1→]$_n$

K37
[3)- α -D-Galp-(1→6)-β D-Glcp-(1→3)-β-D-GalpNAc-(1→]$_n$
β-D-Glcp-(1→6) β-D-GalpNAc-(1→4)J

K93
[3)-β-D-Galp-(1→3)-β-D-GalpNAc-(1→]$_n$
β-Psep5Ac7*R*Hb-(2→6)-α-D-Galp-(1→6)J

Figure 1.3 Comparison of representative *A. baumannii* CPS biosynthesis gene clusters and corresponding structures. a) Nucleotide sequences representing different KL regions focusing on genes between *fkpA* and *lldP* were obtained from the National Centre for Biotechnology Information (NCBI) database and aligned using the Easyfig 2.2.2 tool (Sullivan et al., 2011). Genes are depicted by arrows and indicate direction of transcription whilst IS elements are represented by square boxes. Colour scheme is based on homology to the putative function of gene products and are outlined in the key. Nucleotide sequence homology shared between regions is represented by colour gradient. Figure is drawn to scale. Gene modules for sugar synthesis of interest are indicated, where Aci5Ac7Ac represents genes involved in the production of 5,7-di-*N*-acetylacinetaminic acid; L-Fuc*p*NAc, *N*-acetyl-L-fucosaminic acid; D-Fuc*p*NAc, *N*-acetyl-D-fucosaminic acid; 8eLeg*p*5Ac7Ac, 5,7-diacetamido-3,5,7,9-tetradeoxy-L-*glycero*-D-*galacto*-non-2-ulopyranosonic (di-*N*-acetyl-8-epilegionaminic) acid; D-Gal*p*NAcA, *N*-acetyl-D-galactosaminuronic acid; D-Qui*p*NAc4NAc, 2,4-diacetamido-2,4,6-trideoxy-D-glucopyranose (*N*,*N*'-diacetyl-bacillosamine); D-Qui*p*NAc, *N*-acetyl-D-quinovosaminic acid; GlcNAc3NAcA4OAc, 2,3-diacetamido-2,3-dideoxy-α-D-glucuronic acid with an additional O-acetyl group; Pse*p*5Ac7Ac, 5,7-diacetamido-3,5,7,9-tetradeoxy-L-*glycero*-L-*manno*-non-2-ulosonic (pseudaminic) acid and Pse*p*5Ac7*R*Hb, 5-acetamido-3,5,7,9-tetradeoxy-7-(3-hydroxybutanoylamino)-L-*glycero*-L-*manno*-non-2-ulosonic acid. Pyruvyl groups are indicated with pyl. Genes of interest are labelled above corresponding gene, see text for further details. Genbank accession numbers for sequences used in gene alignment are as follows; KL12, JN107991.2 (38.5 kb region; base position range 2332-40832); KL13, MF522810.1 (38.2 kb region); KL49, KT359616.1 (34.5 kb region); KL53, MH190222.1 (23.4 kb region); KL19, KU165787.1 (23.8 kb); KL1, CP001172.1 (24.9 kb; base position range 366401 to 3691388); KL4, JN409449.3 (30.9 kb; base position range 2375 to 33327); KL3, CP012004.1, (25.4 kb; base position range 3762660-3788118); KL2, CP000863.1 (27.1 kb; base position range 77125-104246); KL6, KF130871.1 (25.5 kb); KL93, CP021345.1 30.3 kb (base position range 3338210-3368604) and KL37 KX712115.1 (23.4 kb). **(b** Capsule structures corresponding to KL gene regions in (a are shown. Percentage of O-acetylation of specific glycans from K53, K19, K1 are not represented in structural configurations)(Kenyon et al., 2015c, Kenyon et al., 2017a, Shashkov et al., 2018, Kenyon et al., 2016a, Russo et al., 2010, Kenyon et al., 2016b, Kenyon et al., 2015b, Kasimova et al., 2017, Arbatsky et al., 2015, Talyansky et al., 2021, Vinogradov et al., 2014, Kasimova et al., 2021).

The variable region of some KL gene clusters, such as KL37 and KL14, lack genes for complex sugar synthesis, as they only contain simple sugars in their K units (Kenyon et al., 2015a, Arbatsky et al., 2015). Also adding to their diversity, several KL regions contain redundant genes which are not required for the synthesis of the final K unit. For example KL8 and KL9 contain two *itr* genes (Kenyon and Hall, 2013) and KL37 has the *pgt1* phosphoglyceroltransferase, but no corresponding phosphoglycerol residue in the determined structure (Arbatsky et al., 2015). Furthermore, in KL93, two insertion sequence elements (IS*Aba26* and IS*Aba22*) interrupt the *pgt1* determinant (Figure 1.3) (Kasimova et al., 2017). The genes required for specific sugar biosynthesis will not be discussed as these pathways have been covered previously and are beyond the scope of this thesis (Hu et al., 2013, Kenyon and Hall, 2013). Additionally, other genes located within the KL encode products predicted to be involved in acetylation or acylation modification of specific glycans (Figure 1.3, pink). Although examination of the KL can reveal a lot about K unit structures, chemical analysis and biochemical testing is required to determine exact structures and identify specific linkages between repeat sugars.

1.5.2 Capsule structures

As described above, there is great diversity between *A. baumannii* capsule biosynthesis gene clusters, which translates into the diversity seen in K unit structures (Kenyon and Hall, 2013, Hu et al., 2013). Collectively, over 40 diverse *A. baumannii* K unit structures have been elucidated thus far using NMR spectroscopy and chemical analysis. K unit structures differ in sugar composition and may include derivatives of common UDP-linked sugars such as glucose, galactose and glucuronic acid or rare and atypical sugars such as non-2-ulosonic acids (Figure 1.3b). Structures vary in length and may consist of only two residues, as seen for K53 (Shashkov et al., 2018), or up to five or six monosaccharides, such as that seen in K37 (Figure 1.3b). Structures also differ in the linkages both within and between K units resulting in the production of K units that are linear or involve side branches, as seen in K1 and K93, respectively (Figure 1.3b) (Kenyon et al., 2016a, Kasimova et al., 2017). Differences in the location of specific glycosidic bonds and *O*-acetylation patterns of various oligosaccharides within a structure also contribute to K unit diversity (Figure 1.3).

The incorporation of rare sugars has been identified in many *A. baumannii* K unit structures. For example, pseudaminic, legionaminic or acinetaminic acid derivatives as seen in K2/6, K49, and K12/13 structures, respectively (Figure 1.3b) (Kasimova et al., 2018, Kenyon et al., 2014a, Vinogradov et al., 2014, Kenyon et al., 2015a, Singh et al., 2018). Interestingly, acinetaminic acid derivatives have only been identified in *A. baumannii* and are found nowhere else in nature (Kenyon et al., 2017b). Additionally, some K units incorporate unique derivatives of specific glycans, for instance the pseudaminic acid of K93 is acylated with a (*R*)-3-hydroxybutanoyl group (Kasimova et al., 2017)(Figure 1.3). Other rare K unit motifs have been described in *A. baumannii*, for example K4 has a terminal *N*-acetyl-D-galactosamine (D-Gal*p*NAcA) branch which is capped with a pyruvyl group (Figure 1.3, black) (Kenyon et al., 2016b). As the number of K unit structures identified increases, so does the confidence to infer the K unit structure from analysis of the biosynthesis clusters positioned in the *A. baumannii* KL. However, although informative, an understanding of the role capsule plays in pathogenesis is important to apply this knowledge to improving outcomes of *A. baumannii* infections.

1.6 The role of capsule in environmental persistence

It is beyond doubt that the presence of capsule is essential for *A. baumannii* pathogenicity. Not only is it necessary for evasion of host immune defences (Russo et al., 2010, Geisinger and Isberg, 2015), but it is important for resistance to antimicrobial compounds and survival in adverse environments (Luke et al., 2010, Russo et al., 2010, Geisinger and Isberg, 2015, Tipton et al., 2018).

1.6.1 Oxidative stress

The oxidative stress response in bacteria is important for both survival in the hospital environment as well as surviving the host immune response during infection. Because of its broad spectrum microbiocidal properties, hydrogen peroxide (H_2O_2) based disinfectants are often used to decontaminate patient areas including floors, bed rails and tables. In low concentrations (~3%) it is also used as an antiseptic agent (McDonnell 2014). Hydrogen peroxide is an oxidising agent and the main mechanism of action is to oxidize cellular macromolecules which are important for structure and function, especially DNA and proteins. Previous studies have shown production of

some bacterial polysaccharides, including peptidoglycan and capsule, to be increased under oxidative stress conditions (Wang et al., 2009, Sabra et al., 2002). For example, a 'non-mucoid' *Pseudomonas aeruginosa* PAO1 variant forms a polysaccharide capsule layer in response to oxidative stress (Mathee et al., 1999, Sabra et al., 2002). After treatment with high levels of H_2O_2, *P. aeruginosa* PAO1 biofilms displayed up to 6-fold increased production in the capsule-like polysaccharide alginate.

1.6.2 Desiccation tolerance

As discussed in Section 1.2.3, the ability of *A. baumannii* to persist in the clinical environment has undoubtedly enhanced colonisation and infections in susceptible patients. *A. baumannii* is capable of surviving for months on hospital surfaces such as bed rails, furniture, and medical devices, providing a reservoir that is often the source of transmission and infection (Wendt et al., 1997, Gayoso et al., 2013).

The remarkable desiccation tolerance of *A. baumannii* is thought to be due to a 'bust or boom' strategy, where a persistent subpopulation of cells survive at the expense of dying cells; capsule enhances desiccation tolerance by providing a physical barrier facilitating water retention (Roberts, 1996, Webster et al., 2000, Gayoso et al., 2013, Bravo et al., 2016, Corbett et al., 2010). The protective nature of capsular polysaccharides against desiccation has been known for decades. Superior desiccation tolerance of mucoid strains compared to non-mucoid counterparts have been established for several bacterial species; including *E. coli*, *P. aeruginosa*, *Klebsiella* spp, and non-*baumannii Acinetobacter* spp (Ophir and Gutnick, 1994, Schnider-Keel et al., 2001). More recently, a role for capsule in desiccation resistance of *A. baumannii* was established (Tipton et al., 2018, Chin et al., 2018). A study by Tipton et al investigated the role of capsule in environmental persistence by constructing a *wzc* knock out in the *A. baumannii* strain AB5075. After 12 days desiccation, viability of the capsule deficient mutant decreased by 2.5-fold relative to the WT strain (Tipton et al., 2018).

1.6.3 Motility, adherence and biofilm formation

Capsule production is associated with motility, adherence and biofilm production in *A. baumannii* (Huang et al., 2014, McQueary et al., 2012, Umland et al., 2012, Lees-Miller et al., 2013). Formation of a biofilm on hospital surfaces is a common source of

nosocomial bacterial infections and has been linked to increased survival and antimicrobial resistance (Espinal et al., 2012, Tomaras et al., 2003, Eijkelkamp et al., 2011b). Adherence is the first step in the production of biofilm and invasion of host tissues. Both require attachment to surfaces using exposed appendages such as pili and fimbriae. The capsule extends from the cellular surface and partially conceals these appendages thereby reducing the adherence of the microbe (Favre-Bonte et al., 1999). When capsule is removed from the *A. baumannii* strain ATCC 17978, adherence capability to glass increased by 50% but the morphology of the biofilm significantly changed from a neat uniform growth for the WT to a clumpy rough growth for the acapsular mutant (Lees-Miller et al., 2013). Motility is important for environmental persistence of many bacteria, as it allows for movement towards nutrients (Harshey, 2003). A study by McQueary and colleagues identified a role for capsule production in swarming motility of *A. baumannii* strain 307-0294, as motility was reduced in acapsular variants (McQueary et al., 2012).

1.7 Capsule mediated resistance to disinfectants and antibiotics

The production of capsule enhances antimicrobial resistance in many bacterial species. In *A. baumannii*, capsule increases resistance to a range of antimicrobial compounds, including those used for disinfection in clinical settings (Chen et al., 2017, Geisinger and Isberg, 2015, Tipton et al., 2015, Tipton et al., 2018). For example, an acapsular variant of the *A. baumannii* strain AB5075 exhibited increased sensitivity to the commonly used disinfectants benzethonium, benzalkonium, and chlorhexidine (Tipton et al., 2018). A study by Geisinger and Isberg, compared antibiotic resistance of four distinct capsule knockouts in the *A. baumannii* strain ATCC 17978 (Geisinger and Isberg, 2015). In this study, authors reported reductions in resistance to some antibiotics including; colistin, rifampicin and erythromycin, compared to the WT parental strain. Interestingly the resistance profiles for these antibiotics tested also varied depending on what genes were removed to make the capsule knockout (Geisinger and Isberg, 2015). For example, the capsule deficient *A. baumannii* mutant, KL3, has a large proportion of the K loci removed and was more sensitive to Rifampicin and Erythromycin compared to single gene acapsular mutants (Geisinger and Isberg, 2015). A recent study by Crepin et al, removing the genes *gna-gne2* required for capsule production, identified increased susceptibility to several antimicrobial compounds including amoxicillin, imipenem, and

gentamicin (Crépin et al., 2020).

In addition to the capsule knockout studies described above, it has been suggested that growth of *A. baumannii* in sub-inhibitory levels of antimicrobials influences capsule production. For example, exposure to the antibiotics chloramphenicol or erythromycin led to enhanced capsule synthesis in ATCC 17978 (Geisinger and Isberg, 2015) and meropenem exposure selected for mutations leading to a loss in capsule production in the isolate 37662 (Chen et al., 2017). In *A. baumannii*, increased production of capsule has been associated with higher resistance to antimicrobial treatments and host antimicrobial compounds (Tipton and Rather, 2017, Geisinger and Isberg, 2015).

1.8 Capsule and evasion of host defences

Capsule mediates immune evasion for many bacterial pathogens, including *A. baumannii*, by limiting interactions between immunogenic surface structures of the bacteria and host defences (Preston et al., 1996, Wu et al., 2009, Russo et al., 2010, Lees-Miller et al., 2013, Geisinger and Isberg, 2015, Wang-Lin et al., 2017). In general, although capsule can be recognised by the innate immune system, it is poorly immunogenic (Willis and Whitfield, 2013, Wang-Lin et al., 2017). Because capsule extends further than other more immunogenic surface structures, such as lipid A and specific surface glycoproteins, it masks these antigens from immune detection (Wu et al., 2009, Wang-Lin et al., 2017). This results in a dampening of the host innate immune response as the bacterium evades multiple host defences including; phagocytosis by macrophages and dendritic cells (Fung et al., 2011), complement activation and killing (Geisinger and Isberg, 2015, Sarma and Ward, 2011, Hyams et al., 2010), host antimicrobials including defensins and lysozyme, as well as secreted immune mediators such as cytokines and chemokines (Tipton et al., 2018).

1.8.1 Evasion of macrophage phagocytosis

Several studies have found increased macrophage phagocytosis of acapsular variants compared to WT strains of several bacterial species including *P. gingivalis* (Singh et al., 2011), *Bifidobacterium* (Tahoun et al., 2017), *Mycobacterium tuberculosis* (Stokes et al., 2004) and *K. pneumoniae* (Cortés et al., 2002). One study failed to find a correlation between capsule production and macrophage phagocytosis of *Camplyobacter jejuni* by

human monocyte derived macrophages, yet an increased uptake of acapsular strains by murine macrophages (Kim et al., 2018)

1.8.2 Capsule activation of complement

As discussed in Section 1.3.3, the alternative pathway of the complement system is the most relevant pathway to the complement response to *A. baumannii* (Sarma and Ward, 2011). Activation of the complement system results in opsonisation of bacteria and the release of complement-derived cytokines which amplify the inflammatory response (Section 1.3.3) (Sarma and Ward, 2011). Late acting complement proteins sequentially associate with C3b to form the membrane attack complex, which forms a pore in the bacterial membrane leading to lysis (Frank et al., 1987, Sarma and Ward, 2011). Generally, high amount of capsule protects bacteria, including *A. baumannii*, (Section 1.3.4) (Burns and Hull, 1999, Buckles et al., 2009, Schneider et al., 2004). Furthermore, it has been proposed that capsule effectively hides C3b molecules attached to the cell by sub-capsular localisation, preventing the further deposition of late-acting complement proteins which create the membrane attack complex and the recognition by complement receptors of phagocytic cells that is mediated by the presence of C3b (Roberts, 1996, Cross, 1990, Cortés et al., 2002). The abolition of capsule in multiple different *A. baumannii* strains has shown reduced survival in human serum and acites fluid, and attenuation in rat and murine infection models (Russo et al., 2010, Umland et al., 2012, Lees-Miller et al., 2013, Sanchez-Larrayoz et al., 2017). Furthermore, the up-regulation of capsule production in the commonly utilised *A. baumannii* strain ATCC 17978 increased serum resistance and virulence in a mouse infection model (Geisinger and Isberg, 2015).

1.9 **Regulation of capsule production**

The ability of bacteria to regulate virulence mechanisms, including capsule production, in a location dependant manner is vital as they enter the host environment and initiate infection. This involves the switching on and off of groups of genes involved in survival within a host. There is a limited repertoire of capsule regulatory mechanisms reported in the literature including; phase variation, TCSs, transcription regulators and quorum sensing systems (Mouslim and Groisman, 2003, Cheng et al., 2010, Brimacombe et al., 2013). The regulation of capsule is complex, most of the identified regulators of capsule

expression are not dedicated solely to capsule synthesis, but have extensive regulons (MacRitchie et al., 2008). Furthermore, it is not unusual for several regulatory factors to interact in order to alter *cps* expression.

1.9.1 BfmRS

Environmental cues, such as temperature, osmotic pressure and changes in metabolite and ion availability can influence bacterial capsule production (Hagiwara et al., 2003, Mouslim et al., 2004, Lai et al., 2003, Willenborg et al., 2011). Capsule production is primarily regulated at the post-translational level via the cyclic phosphorylation and dephophorylation of Wzc/b (Willis and Whitfield, 2013) (Figure 1.2). Besides the innate phosphorylation system, only two regulators of capsule production have thus far been identified in *A. baumannii*. These systems are the TCSs BfmRS and OmpR-EnvZ, both which play multiple regulatory roles involved in envelope biogenesis (Tipton and Rather, 2017, Geisinger and Isberg, 2015, Geisinger et al., 2018). When subjected to antibiotic pressure, *A. baumannii* ATCC 17978 capsule gene expression was increased in a BfmRS-dependent manner (Geisinger and Isberg, 2015).

1.9.2 Phase variation and OmpR-EnvZ

The OmpR-EnvZ system in *A. baumannii* AB5075 is important for the regulation of several cell envelope properties including the production of capsule (Tipton et al., 2015). OmpR is a global transcription regulator which alters the expression of many gene targets in response to environmental signals (Tipton and Rather, 2017). The *A. baumannii* strain AB5075 displays phase variation, where the bacterial colonies switch from a translucent to opaque phenotype. OmpR was found to be important for phase variation, as removal of *ompR* results in increased opaque variant switching frequency (Tipton and Rather, 2017). Recent studies have linked the phase-variable phenotype of *A. baumannii* AB5075 with alterations in capsule production, as highly virulent opaque variants produce a capsule layer with twice the thickness of their translucent counterparts (Chin et al., 2018). This transition from translucent to opaque also dramatically increased the pathogenic potential of *A. baumannii* AB5075. Resistance to common hospital disinfectants and a subset of aminoglycoside antibiotics were also increased (Tipton et al., 2015; Chin et al., 2018) and opaque variants were also more resistant to human lysozyme, the cathelicidin-related antimicrobial peptide LL37 and

hydrogen peroxide compared to translucent colonies (Chin et al., 2018). Furthermore, opaque isolates had an increased tolerance to desiccated conditions and out-competed translucent counterparts in a mouse infection model (Chin et al., 2018).

1.10 **Capsule as a potential therapeutic target**

The increase of extremely antibiotic resistant *A. baumannii* isolates, which are difficult to treat and eliminate, is a major concern (Perez and Bonomo, 2014). The need to develop vaccines or treatments against isolates which don't respond to antibiotics has spiked interest in development of alternative treatments for *A. baumannii* including; phage therapy (Schooley et al., 2017), the use of antimicrobial peptides (Jaśkiewicz et al., 2019), photodynamic therapy (Dai et al., 2009) and antibody-based therapies such as prophylactic vaccines and passive immunisation (García-Quintanilla et al., 2013). There are many patient populations which may benefit from prophylactic treatment against *A. baumannii,* including; those at high risk of needing mechanical ventilation, burns patients and military personnel who are at risk of combat wounds (García-Quintanilla et al., 2013, Perez and Bonomo, 2014). At present there are no antibody-based therapies available for *A. baumannii*. The development of such therapies is gaining interest in the medical field as they represent the most promising non-antibiotic treatment against *A. baumannii*. There have been promising results from proof of concept research into vaccines against a number of *A. baumannii* surface antigens including; inactivated whole cell vaccines (KuoLee et al., 2014, McConnell and Pachón, 2010), complete OM complex (McConnell et al., 2011), OmpA (Luo et al., 2012), PNAG (Bentancor et al., 2012), BAP (Fattahian et al., 2011), and capsule (Russo et al., 2013).

Capsular polysaccharide represents an attractive target for the development of new vaccines as it possesses several desirable characteristics for an antigenic target including; surface exposure, broad prevalence, the ability to provoke an immune response and participation in pathogenicity (Russo et al., 2013). Capsule has been a successful target for vaccines and passive immunotherapy for other encapsulated pathogens including; *S pneumoniae*, *N. meningitidis*, *H. influenzae*, and *S. typhi* (Austrian, 2011, Jennings, 1990). Furthermore, there has been several proof-of-concept studies for the use of capsule based vaccines in many other bacterial species including; *C. jejunii*, *Bacillus anthracis*, *N. meningitidis*, *E. coli*, *Pasteurella haemolytica*

(Monteiro et al., 2009, Garufi et al., 2012, Robbins et al., 2011, Russo et al., 2013). Several studies have shown the efficacy of passive immunisation in mice using a capsule-specific antibody, which is protective against bacterial challenge with 13-55% of clinical *A. baumannii* isolates (Russo et al., 2013, Yang et al., 2017, Lee et al., 2018). A study by Russo and colleagues published a paper on their research investigating the potential of monoclonal antibodies (MAb) of K1 capsular polysaccharide as a treatment for *A. baumannii* infection (Russo et al., 2013). The authors generated MAb13D6 against the K1 capsule of *A. baumannii* strain AB307-0294, which resulted in increased opsonisation and neutrophil-mediated bactericidal activity in a mouse model. Furthermore, treating mice with MAb13D6 three and 24 hours pre-bacterial challenge resulted in a four-log decrease of K1 positive *A. baumannii* recovered. the efficacy of using MAb against other *A. baumannii* strains is promising; 13% of the 100 clinical *A. baumannii* isolates tested in the afore mentioned study were reactive to Mab13D6 (Russo et al., 2013). Additionally, inoculation with conjugate vaccines incorporating capsule glycans attached to a protein carrier elicit better immune protection than purified capsule against a diverse range of *A. baumannii* strains (Yang et al., 2017). The effectiveness of MAb against a broader range of *A. baumannii* capsular types still needs to be investigated.

Besides the development of vaccines, a variety of other treatments targeting bacterial capsule have been explored. A 2013 paper by Hsu and colleagues identified a lytic phage which recognises a specific type of capsule in *K. pneumoniae* (Hsu et al., 2013). This phage possesses a polysaccharide depolymerase which degrades capsule, indicating the phage and its enzyme may provide an alternative treatment (Hsu et al., 2013). A polyglutamic acid degrading enzyme, CapD, encoded for on a plasmid from *B. anthracis*, was shown to degrade capsule from a broad range of Bacillus species, resulting in an increase of macrophage phagocytosis and enhancement of neutrophil killing (Scorpio et al., 2007). Lastly, the marine sponge metabolite fascioquinol E was shown to inhibit the protein tyrosine phosphatase CpsB and Wzb in *S. pneumoniae* and *K. pneumoniae*, respectively (Standish et al., 2012). Identifying compounds which either degrade capsule or interrupt the capsule assembly machinery may be useful in treating *A. baumannii* infections, as capsule is an essential trait for invasive disease (Russo et al., 2010).

1.11 **Scope of this thesis**

Capsule is important for both survival in the hospital environment and within the host during infection. Recently, several studies investigating the role of capsule in *A. baumannii* virulence have been published. This has advanced our understanding of the role capsule plays in the survival of this tenacious pathogen (Talyansky et al., 2021, Hu et al., 2020, Tipton et al., 2018). Not only is capsule important for survival in dry environments (Section 1.6.2), but also contributes to resistance against antimicrobial compounds (Section 1.7) and components of the host immune response (Section 1.8). Chapter 3 of this thesis compares the characteristics of 13 *A. baumannii* strains which represent a variety of capsule types. These strains have been challenged in several assays to increase our understanding of how they may vary in their response to environmental and immunological stressors. Chapter 4 of this thesis outlines various methodologies used to create and explore acapsular mutants generated in two *A. baumannii* strains ATCC 17978 and 0411 7201. Chapters 5 and 6 present the results gained from challenge of constructed acapsular mutants to commonly encountered environmental and innate immune stressors, respectively. Lastly, the discussion chapter of this thesis incorporates all the data chapters and expands upon new concepts and ideas gained through the purpose of this research.

2 MATERIALS AND METHODS

2.1 Strains, cell lines, and cloning vectors

Strains, tissue culture cell lines, and plasmids used in this study are listed in Tables 2.1, 2.2, and 2.3, respectively.

2.2 Growth media and conditions

Bacterial strains (Table 2.1) were routinely grown in Lysogeny Broth (LB) or Mueller Hinton (MH) broth (Table 2.4) at 37^{o}C with shaking (120 revolutions per minute [rpm]) unless otherwise stated. The A549 human pneumocyte cell line, RAW 267.4 murine macrophages, and primary human monocytes (Table 2.2.) were routinely cultured in Dulbecco's Modified Eagle Media (DMEM) supplemented with 10% inactivated Foetal Calf Serum (FCS), 2 mM L-glutamine, and 100 µM PenStrep (Table 2.4). Monocyte derived macrophages (MDM) (Section 2.21) were maintained in MDM culture medium (Table 2.4), and U937 macrophages (Table 2.2) were grown in Roswell Park Memorial Institute (RPMI) medium supplemented with 10% inactivated FCS, 2 mM L-glutamine, and 100 µM PenStrep (Table 2.4). Mammalian cell cultures were grown at 37^{o}C and 5% CO_2. *Saccharomyces. cerevisiae* (Table 2.1) was routinely cultured in Yeast Extract–Peptone–Dextrose (YPD) medium at 37^{o}C unless otherwise stated (Table 2.4).

2.3 Buffers, reagents, enzymes, gels, and antimicrobial compounds

Buffers, reagents, enzymes and electrophoresis gel recipies used in this study are listed in Table 2.5. For antibiotic selection of *E. coli* and *A. baumannii*, sterilised media were cooled to approximately 50^{o}C prior to the addition of the required amount of filter sterilised antibiotic stock solution. Typically, selection media contained antimicrobials at the following final concentrations; ampicillin (Amp) 100 µg/mL, tetracycline (Tet) 12 µg/mL, chloramphenicol (Cm) 25 µg/mL, erythromycin (Ery) 25 µg/mL, amikacin (Amk) 40 µg/mL, gentamycin (Gent) and/or potassium tellurite (Tel) 30 µg/mL. All antimicrobials were purchased from Sigma. For blue/white selection agar, 1.25 µg/mL of filter sterilised 5-bromo-4-chloro-3-indoyl-β-D-galacto-pyranoside (X-gal) and 1.6 µg/mL of filter sterilised isopropyl-β-D-galactopyranoside (IPTG), both purchased from Sigma, were included. For selection of yeast containing recombinant clones of pPR2274 (Table 2.3), 2.5 µg/mL of cyclohexamide was added to Sabouraud dextrose (SD) Uracil

(Ura)$^-$ medium (Table 2.4).

2.3.1 *A. baumannii* chromosomal DNA isolation

Chromosomal DNA was isolated from *A. baumannii* cultures using the Bioline ISOLATE Genomic DNA Mini Kit, following the manufacturer's instructions. Briefly, 3 mL of ON culture (Section 2.2) was pelleted by centrifugation (15,000 *xg*/10 min/ room temperature [RT]) and resuspended in 400 µL of Lysis Buffer D and 25 µL of Proteinase K Solution. The suspension was vortexed vigorously for 5 min, incubated at 50^{o}C and vortexed intermittently until it became clear. Binding Buffer D (200 µL) was added to this mixture and vortexed vigorously for 15 sec. The sample was transferred to a spin column and placed in a 2 mL collection tube, centrifuged (10,000 *xg*/ 2 min/ RT), and the collection tube and filtrate was discarded. The spin column was placed in a new collection tube and 700 µL of Wash Buffer D was added. The tube was then centrifuged (10,000 *xg*/ 1 min/ RT), the filtrate discarded and the wash repeated. The sample was further centrifuged (10,000 *xg*/ 2 min/ RT) to remove all traces of Wash Buffer D, and the collection tube discarded. The spin column was placed in a 1.5 mL elution tube and 200 µL of Elution Buffer was added directly to the membrane. The sample was incubated for 5 min at RT before being centrifuged (10,000 *xg*/ 1 min/ RT) to elute the sample. The DNA concentration was quantified using a Thermo Scientific NanoDrop™ 1000 spectrophotometer and the sample stored at 4^{o}C for downstream use.

2.3.2 Polymerase chain reaction

Oligonucleotides (Table 2.6) used for polymerase chain reactions (PCR) were synthesised by Sigma. All PCR reactions were performed in thin-walled 0.5 mL tubes and cycled using a ^{5}PRIME (DKSH technologies) or GenePro™ Thermal cycler.

Table 2.1. Strains used in this study

Strain	Description	Source/reference
A. baumannii		
04117201	Capsule type K2/ international clone II/ tracheal aspirate isolate	Flinders Private Hospital Adelaide, South Australia
04117201Δ*wzy*	*wzy* polymerase deletion mutant in 04117201 background *wzy*::*ery*	This study
307-0294	Capsule type K1/ blood isolate	(Russo et al., 2010)
ACICU	Capsule type K2/ international clone II/ cerebrospinal fluid isolate	(Iacono et al., 2008)
ATCC 17978	Capsule type K3/ non-international clone/ meningitis isolate	(Smith et al., 2007)
Δ*cps*	*cps* and *gna-gtr9* inclusive deletion in ATCC 17978 background *cps*::*ery*	This study
Δ*itrA2*	*itrA2* initial transferase deletion mutant in ATCC 17978 background *itrA2*::*ery*	This study
Δ*wzy*	*wzy* polymerase deletion mutant in ATCC 17978 background *wzy*::*ery*	This study
Δ*wzyC*	*wzy* polymerase deletion mutant in ATCC 17978 background/ pWH1266_wzy	This study
Δ*wzyE*	*wzy* polymerase deletion mutant in ATCC 17978 background/ pWH1266	This study
Δ*itrA2C*	*itrA2* initial transferase deletion mutant in ATCC 17978 background/ pWH1266_itrA2	This study
Δ*itrA2E*	*itrA2* initial transferase deletion mutant in ATCC 17978 background/ pWH1266	This study
ΔΔ*wzy_itrA2*	*wzy* polymerase deletion mutant in ATCC 17978 background/ *itrA2*	This study

inactivated

Table 2.1. Cont.

Strain	Description	Source/reference
A. baumannii		
Δ*Δwzy_itrA2/C*	*wzy* polymerase deletion mutant in ATCC 17978 background/ *itrA2* inactivated/ pWH1266_*itrA2*	This study
Δ*Δwzy_itrA2/E*	*wzy* polymerase deletion mutant in ATCC 17978 background/ *itrA2* inactivated/ pWH1266	This study
ATCC 19606	Capsule type K3/ non-international clone/ urine isolate	(Bouvet and Grimont, 1986)
D36	Capsule type K12	(Kenyon et al., 2015c)
D46	Capsule type K14	(Kenyon et al., 2015a)
D78	Capsule type K4	(Kenyon et al., 2016b)
A1	Capsule type K1	R Hall, University of Sydney, personal communication
A320	Capsule type K9	R Hall, University of Sydney, personal communication
RBH4	Capsule type K6	(Kenyon et al., 2015b)
UMB001	Capsule type K13	R Hall, University of Sydney, personal communication

Table 2.1. Cont.

Strain	Description	Source/reference
Acinetobacter baylyi		
ADP1	Soil isolate	(Barbe et al., 2004)
E. coli		
DH5α	Fφ80, *lacZ* ,ΔM15, Δ(*lacZYA-argF*)U169, *recA1, endA1, hsdR17*(r_k,m_k^+)*phoAsupE44 thi-1 gyrA96, rel*A1λ^-	(Hanahan, 1983)
DH10B	Δ*(ara-leu), 7697 araD139 fhuA* Δ*lacX74, galK16, galE15, e14-* ϕ*80*d*lacZ*Δ*M15, recA1 relA1, endA1, nupG, rpsL, rph spoT1,* Δ*(mrrhsdRMS-mcrBC)*	New England Biolabs
P5993	DH10β Δ*wecA strep*^{R}	(Liu et al., 2017)
S. cerevisiae		
CRY1-2	*S. cerevisiae* recombinational cloning strain/ *MATα, ura3*Δ, *cyh2R*	(Liu et al., 2017)

Table 2.2. Tissue culture cell lines used in this study

Cell line	Description	Source/reference
A549	Human type II pneumocyte/ immortal cell line	(Giard et al., 1973)
RAW 264.7	Murine macrophage adherent immortal cell line ATCC TIB-71™	HPA Culture Collections
U937	Human monocyte cell line derived from a histiocytic lymphoma	(Lehmann, 1998)

Table 2.3. Plasmids used in this study

Plasmid	Description[a]	Source/reference
pAT04	pMMB67EH with *recAb* system/ *tet*^{R}	(Tucker et al., 2014)
pACICU2	Source of the *aphA6* gene	(Hamidian and Hall, 2013)
pEX_04117201_*wzy*	pEX18Tc plasmid containing regions flanking the *wzy* gene of *A. baumannii* 04117201/ *ery*^{R}/ *tet*^{R}	This study
pEX_*wzy*	pEX18Tc plasmid containing regions flanking the *wzy* gene of *A. baumannii* ATCC 17978/ *ery*^{R}/ *tet*^{R}	This study
pGemT_*amk*^{R}	pGEMT- Easy with *aphA6* from ACICU/ *amk*^{R}/ *amp*^{R}	This study
pGEM-T Easy	'T' base overhang cloning vector/ *amp*^{R}	Promega Biotech
pPR2274	pCRG16 with the *Sma*I site in the mini-F *repE* gene eliminated (CCCGGG→CCCGAG)/ *amp*^{R}/ *cm*^{R}/ c*yh*^{S}	(Liu et al., 2017)
pVA819	Source for *ery*^{R} cartridge/ *cm*^{R}/ *ery*^{R}	Invitrogen
pWH1266	*Acinetobacter*/ *E. coli* shuttle vector, generated by ligation of pBR322 and a cryptic *Acinetobacter* plasmid using *Pvu*II digestions/ *amp*^{R}/ *tet*^{R}	(Hunger et al., 1990)

Table 2.3. Cont.

Plasmid	Description[a]	Source/reference
pWH_*itrA2*	pWH1266 with *itrA2* gene from *A. baumannii* ATCC 17978 cloned into *tet*^{R} gene region/ *amp*^{R}	This study
pWH_telR	pWH1266 with *tel*^{R} from *A. baylyi* ADP1 cloned into *tet*^{R} gene region/ *amp*^{R}/ *tel*^{R}	This study
pWH_*wzy*	pWH1266 with *wzy* gene from *A. baumannii* ATCC 17978 cloned into *tet*^{R} gene region/ *amp*^{R}	This study

[a] tetracycline resistance (*tet*^{R}), erythromycin resistance (*ery*^{R}), ampicillin resistance (*amp*^{R}), chloramphenicol resistance (*cm*^{R}), cyclohexamide sensitivity (c*yh*^{S}), amikacin resistance (amk^{R})replication initiator protein (*repE*), *A. baumannii* recombinase system (*recAB*)

Table 2.4. Growth media used in this study

Media	Constituents
DMEM	Prepared as per the manufacturer's instructions
Hanks Balanced Salt Solution, no magnesium, no calcium (HBSS)	Prepared as per the manufacturer's instructions
HBSS plus magnesium and calcium (HBSS+)	Prepared as per the manufacturer's instructions
LB	5 g yeast extract, 10 g tryptone, 10 g NaCl dH_2O to 1 L (pH 7.5)
LB agar	LB broth with 1% (w/v) agar
M9 salt (5X)	64 g $(Na_2 PO_4)7H_2O$, 15 g KH_2PO_4, 2.5 g NaCl, 5 g NH_4Cl, dH_2O to 1 L
M9 minimal medium	200 mL M9 salt (5X), 2 mL 1 M $MgSO_4$, 20 mL of 20 % succinic acid, 100 µL of $CaCl_2$, sterile dH_2O up to 1 L
Maneval's stain	0.05 g fuchsin, 3 g ferric chloride, 0.5 mL acetic acid (glacial), 3.9 mL phenol, 95 mL dH_2O
MH broth	Prepared as per the manufacturer's instructions
MH agar	Prepared as per the manufacturer's instructions
MDM culture medium	10 mM N-2-hydroxyethylpiperazine-N-2-ethane sulfonic acid (HEPES), 10 % (v/v) FCS, 10 % human serum in DMEM

Table 2.4. Cont

Media	Constituents
RPMI-1640 medium	Prepared as per the manufacturer's instructions
MDM adherence medium	10 mM HEPES, 10 % (v/v) FCS, 10 % in DMEM
SD Ura^- broth	6.7g yeast nitrogen base, 1.92 g dropout supplement without uracil, dH_2O to 1 L
SD Ura^- agar	SD Ura^- broth with 2% (w/v) agar
YPD broth	20 g peptone, 10 g yeast extract, 20 g glucose, dH_2O up to 1 L
YPD agar	YPD broth with 2% (w/v) agar

Table 2.5. Buffers, reagents and gels used in this study

Buffer/ reagent/ gel	Constituents
Agarose gel	1-2 % (w/v) agarose in 0.5 % TAE buffer
Agarose gel (low melting point)	1-2% (w/v) agarose in 0.5 % TAE buffer
Alcian blue fixative solution	7% acetic acid, 25% isopropanol in dH_2O
Alcian blue stain	0.05% (w/v) alcian blue, 7% acetic acid, 25% isopropanol in dH_2O
Carbohydrate (COH) stock solution	0.05% (w/v) sucrose, 0.05% (w/v) fructose in dH_2O
Coomassie stain	30% (v/v) methanol, 10% glacial acetic acid, 0.15% Coomassie Brilliant Blue R-250 in dH_2O
CPS lysis buffer	60 mM Tris-HCl (pH 8), 10 mM $MgCl_2$, 50 mM $CaCl_2$ in dH_2O
Crushing buffer	50 mM Tris-HCl (pH 7.5), 10% glycerol, 300 mM NaCl
Destain solution	30% (v/v) methanol, 10% glacial acetic acid in dH_2O
Electrophoresis loading buffer	50% sucrose (w/v), 50 mM ethylenediaminetetra-acetic acid (EDTA) (pH 7.0), 0.05% (w/v) bromophenol blue
80% glycerol solution	80% (v/v) glycerol in dH_2O
GelRed Solution	30 µL of GelRed nucleic acid stain (Biotium), 3.3 mL 3M NaCl in 100 mL dH_2O

Table 2.5 Cont.

Buffer/ reagent/gel	Constituents
SDS-PAGE running buffer (10X)	30.3 g Tris base, 144 g glycine, 10 g sodium dodecyl sulphate (SDS), in 1 L dH_2O
Maneval's stain	15 mL 5% phenol, 5 mL 10% acetic acid, 2 mL 30% ferric chloride (FeIII), 1 mL 1% acid fuchin, 42 mL dH_2O
Metabisulphite solution	0.2 g $Na_2S_2O_5$, 100 mL 5% (v/v) acetic acid in dH_2O
MP Buffer	1 M sorbitol, 1 M NaCl, 10 mM acetic acid (pH 5.5)
PAS fixation solution	10% (v/v) acetic acid, 35% (v/v) methanol in dH_2O
PEG/LiAc solution	8 mL 50% PEG 3350, 1 mL 1M LiAc (pH 7.5), 1 mL 10X TE
Periodate solution	0.7 g periodic acid (H_5IO_6), 100 mL 5% (v/v) acetic acid in dH_2O
Phosphate buffered saline (PBS)	136 mM NaCl, 2.7 mM KCl, 1.76 mM KH_2PO_4, 8.1 mM $(Na_2HPO_4)2H_2O$ in dH_2O
Protoplasting solution	MP buffer containing 10 mg/mL Glucanex® lysing enzyme (Sigma)
Phosphate urea magnesium sulphate (PUM) buffer	22 g/L $K_2HPO_4 .3H_2O$, 7.26 g/L KH_2PO_4, 1.8 g/L urea, 0.02 g/L $MgSO_4.7H_2O$ (pH 7.1)

Table 2.5 Cont.

Buffer/ reagent/gel	Constituents
12% SDS-PAGE gel	1.65 mL dH_2O, 2 ml 30% acrylamide, 1.25 mL 1.5 M Tris-HCl (pH 8.8), 50 µL 10% SDS, 50 µL ammonium persulfate (APS), 2 µL N, N, N′, N′-tetramethylethylenediamine (TEMED)
20% SDS-PAGE gel	350 µL dH_2O, 3.3 mL 30% acrylamide, 1.25 mL 1.5 M Tris-HCl (pH 8.8), 50 µL 10% SDS, 50 µL APS, 2 µL TEMED
SDS-PAGE running buffer stock solution (20X)	0.8 M Tricine, 1.2 M Tris-HCl (pH 8.3), 2% SDS, 50 mM sodium bisulphite (pH 8.2 - 8.3) in dH_2O
SDS-PAGE sample buffer (2X)	0.05 M Tris-HCl (pH 6.8), 5% β-mercaptoethanol, 2% (w/v) SDS, 10% (v/v) glycerol, 0.1% bromophenol blue
SDS-PAGE stacking gel	1.7 mL dH_2O, 420 µL 30% acrylamide, 320 µL 1M Tris-HCl (pH 6.8), 15 µL 10% SDS, 15 µL 10% APS, 2.5 µL TEMED
TAE buffer stock solution (50X)	24.2% (w/v) Tris-base, 50 mM EDTA (pH 8.0), 5.71% (v/v) glacial acetic acid
10X TE	0.1 M Tris-HCl (pH 7.5), 10 mM EDTA
TE/LiAc solution	0.5 mL 10X TE, 0.5 mL 1M LiAc, 4 mL dH_2O
Transformation buffer (TFB) 1	30 mM KCH_3COO, 100 mM KCl, 50 mM $MnCl_2.4H_2O$, 15% (v/v) glycerol in dH_2O
TFB 2	10 mM MOPS, 75 mM $CaCl_2.2H_2O$, 15% (v/v) glycerol in dH_2O

Table 2.5 Cont.

Buffer/ reagent/gel	Constituents
WCL lysis buffer	31.25 mM Tris-HCl (pH 6.8), 4% (w/v) SDS, 0.025% (w/v) bromophenol blue, 20% (w/v) glycerol in dH_2O

Standard cycling conditions were as follows: 5 min initial denaturing step at 94°C, 30 cycles of a 30 sec denaturing step at 94° C, 30 sec annealing step at 55°C, 1 min per kb extension step at 72°C, followed by a final extension step at 72°C for 10 min. Results of PCR were visualised by agarose gel electrophoresis (Section 2.4.8). Prior to downstream applications, PCR products were cleaned (Section 2.4.3) and the DNA concentration was quantified using a Thermo Scientific NanoDrop™ 1000 spectrophotometer. PCR products were stored at 4 °C. For colony PCR, standard conditions for colony PCR were as follows: 5 min initial denaturation step at 94°C, 25 cycles of 30 sec denaturation at 94°C, 30 sec annealing step at 55°C, 1 min per kb extension step at 72°C, followed by a final extension step at 72°C for 10 min (Section 2.4.2.3).

2.3.2.1 *High fidelity PCR*

Velocity DNA polymerase was used for the amplification of PCR products to be cloned into vectors using endonuclease restriction sites. Typically, PCRs using Velocity DNA polymerase were 50 µL in volume and contained 200 ng of either plasmid or genomic template DNA, 0.2 mM of each dNTP (Promega), 0.2 µM of each primer complementary to the 5' and 3' ends of the region to be amplified (Table 2.6), 5 U of Velocity DNA polymerase (Bioline) and 1X Velocity buffer (Bioline).

For the amplification of large DNA fragments over 10 kb, RANGER DNA polymerase (Bioline) was used. Typical 50 µL reactions contained 1X RANGER Reaction Buffer, 1 µL RANGER DNA polymerase, 60 ng template DNA, 0.4 mM of each dNTP and 0.4 µM of each primer (Table 2.6) in dH_2O.

2.3.2.2 *PCR for checking product sizes*

Econotaq (Lucigen) was used for PCR amplifications to check for correct size fragments resulting from cloning and mutagenesis. Amplifications using Econotaq were typically performed in 50 µL reactions with 200 ng of DNA, 0.2 mM of each dNTP (Promega), 0.2 µM of each primer complementary to the 3' and 5' ends of the region to be amplified (Table 2.6), 5 U of Econotaq polymerase (Lucigen) and 1X Econotaq buffer (Lucigen). PCR reactions were performed as per Section 2.4.2 unless otherwise stated.

Table 2.6. Oligonucleotides used in this study

Name	**Nucleotide sequence 5' → 3'[a]**	**Reference**
A1S_0053_F	ATGGACGTAAATGACTCTG	This study
A1S_0053_R	TGCTAATAGTGGATGTGGA	This study
A1S_2565_F	TGGCTCGATATTCAACGTCA	(Eijkelkamp, 2012)
A1S_2565_R	TAACAGCAAACCACCACCAA	
AmikR_F	GAGAGGATCCGCAACTGGTCCAGAACCTTG	This study
AmikR_R	GAGAGTCGACCATCCAGATTTTCCGACAT	This study
AmikR_BamHI_R	GAGAGGATCCCATCCAGATTTTCCGACAT	This study
AVR_up_F	GAGAGTCGACGATGCGTAGTCGCGTTGATA	This study
AVR_up_R	GAGACGGCCGATAATAAATTGATATCTTATACC	This study
AVR_down_F	GAGACGGCCGTTTATTTAGATGAATGGTTGGATTGAG	This study
AVR_down_R	CTCGGGCGATCGGCTCTGCTCATATATTCATTCGTT	This study
A_wzy_UFR_F	GAGAGTCGACCCTAATAATGATGTCGTAGGTG	This study

Table 2.6. cont.

Name	**Nucleotide sequence 5' → 3'[a]**	**Reference**
A_wzy_UFR_R	GAGACTCGAGGAAATAGACTTCAAATACAACGTAC	This study
A_wzy_DFR_F	GAGACTCGAGCTTTGAAGAGTAAATCTGGTTCTG	This study
A_wzy_DFR_R	GAGATCTAGAGTATTGAAATGTTCTGGTTGTTC	This study
A1S_0053_F	ATGGACGTAAATGACTCTG	This study
A1S_0053_R	TGCTAATAGTGGATGTGGA	This study
Cps_NOLall_F	GGCAAGCGAGACAGTTGGTC	This study
Cps_NOLall_R	TACTACACTCACATGCTCAGGC	This study
Cps_NOLup_F	GTTGGCGATGTTAGTGTG	This study
Cps_NOLup_R	CTATCAACACACTCTTAAGCCAGCAGCACCAATTAATGC	This study
Cps_NOLdown_F	CGGAAGGAAATAATTCTATGCTTTAACTGTTCTGTCGCC	This study
Cps_NOLdown_R	GCCAATCCGGAATAGATTG	This study
Ery_check_F	CTAATGCCTATGTTACTAAG	This study
Ery_check_R	CCAATCTCTACTCCTGTTTC	This study
Ery_NOL_F	CTTAAGAGTGTGTTGATAG	This study
Ery_NOL_R	TTATTTCCTCCCGTTAAA	This study

Table 2.6. cont.

Name	**Nucleotide sequence 5' → 3'[a]**	**Reference**
Ery_Xho_F	GAGACTCGAGCTTAAGAGTGTGTTGATAGTGC	This study
Ery_Xho_R	GAGACTCGAGTCATAGAATTATTTCCTCCCG	This study
gent_OAV_F	GAGGTGTTTATAGATAAGGGTGGACATAAGCCTGTTCGG	This study
gent_OAV_R	ACACAAAGGGTCGCGGCTTGAACGAATTGTT	This study
gent_pPR2274_V2_F	GGTCATTGTCTTTTTTCGGCCGAATTGACATAAGCCTGTTCGG	This study
gna_OAV_F	AACAATTCGTTCAAGCCGCGACCCTTTGTGT	This study
gna_OAV_R	AATTATAATTATTTTTATAGCACGTGATGAAAAGGACCGCCAGCACCAATTAAT	This study
IL-6 F	GAACTCCTTCTCCACAAGCG	(Vogel et al., 2012)
IL-6 R	TTTTCTGCCAGTGCCTCTTT	(Vogel et al., 2012)
IL-8 F	CTGCGCCAACACAGAAATTA	(Vogel et al., 2012)
IL-8 R	ATTGCATCTGGCAACCCTAC	(Vogel et al., 2012)

Table 2.6. cont.

Name	**Nucleotide sequence 5' → 3'[a]**	**Reference**
itrA2_comp_F	GAGAGGATCCGTGAATGAAAATATG AAGCG	This study
itrA2_comp_R	GAGAGTCGACGGAATAGACTTACTTG CGGG	This study
itrA2_NOLall_F	GTTTCTGGTACGGTCTGCGT	This study
itrA2_NOLall_R	TAAAACAGCATGCCCTAGGC	This study
itrA2_NOLup_F	CGGGTGATTGCTAAAGGGTA	This study
itrA2_NOLup_R	CTATCAACACACTCTTAAGTTCCGTC CTTACCAGGTCTTT	This study
itrA2_NOLdown_F	CGGAAGGAAATAATTCTATACACGTT TTCTACCCGCAAG	This study
itrA2_NOLdown_R	TCCACAATCCCATATTGATCC	This study
itrA2_OAV_F	ACTTCGTATAGCATACATTATACGAA GTTATATTCGATGCCTTTAACTGTTCT GTC	This study
itrA2_OAV_R	TTTTTTAAAAGATTTTCAAAATCCATA TATAAACATAGGCTTACCTGAGCTAA AC	This study
M13 F	GTAAAACGACGGCCAGT	Sigma
M13 R	GGAAACAGCTATGACCATG	Sigma
N_itr_F	GTTGCTTATAAAGTCCGTAA	This study
N_itr_R	AATCATAAGAAAGATTTCAAG	This study

Table 2.6. cont.

Name	**Nucleotide sequence 5' → 3'[a]**	**Reference**
Node182_F	TTACAACAAGTATCTGTAGGTCCTGACC	(Weber et al., 2015)
Node182_R	AAGTGTCTGAATGTCTATCAATGCC	(Weber et al., 2015)
N_wzy_check_F	CAATCTTATTTAATAGGATTAGCC	This study
N_wzy_check_R	GACAGAATTAAAGAAGCATTCATA	This study
N_wzy_UFR_F	GAGAGTCGACGATATGTTTATTGAGGTTTTGC	This study
N_wzy_UFR_R	GAGACTCGAGGGCTAATCCTATTAAATAAGATTG	This study
N_wzy_DFR_F	GAGACTCGAGTATGAATGCTTCTTTAATTCTGTC	This study
N_wzy_DFR_R	GAGATCTAGACCTATTGTTACCTTTCAAACTA	This study
Peg.2898_F	TAGAAAGCCGTGGCAC	This study
Peg.2898_R	GAAGTAAAGCTTCATACCCAG	This study
pEX18Tc_F	GAGACCTCTTCGCTATTACGCCAG	This study
pEX18Tc_R	GAGAGTTGTGTGGAATTGTGAGCG	This study
pWH1266_OAV_F	CGCACATTTCCCCGAAAAGTGCCACCTGACGTGCCCGGGCGAAACTGGCAGCGAAGAATG	This study

Table 2.6. cont.

Name	**Nucleotide sequence 5' → 3'[a]**	**Reference**
pWH1266_OAV_R	CCGAACAGGCTTATGTCCACCCTTAT CTATAAACACCTC	This study
pWH1266_OAV_V 2_F	CGCACATTTCCCCGAAAAGTGCCACC TGACGTGCCCGGGCCAGA CGATGCAAAACGCAAGATC	This study
pW-Ori_V2_R	CCGAACAGGCTTATGTCAATTCGGCC GAAAAAAGACAATGACC	This study
Tel_BamHI F	GAGAGGATCCGTCTGGTTGAGCTAAG TTATGAC	This study
Tel_BamHI R	GAGAGGATCCCATCGGATGTGTGATA TGCC	This study
Wzy_comp_F	GAGAGCATGCGTACGTTGTATTTGAA GTCTATTTC	This study
Wzy_comp_R	GAGAGTCGACCAGAACCAGATTTACT CTTCAAAG	This study
wzy_NOLall_F	GGGCTAGCATCATTTGGTTTA	This study
wzy_NOLall_R	GCCAATCGTTACAATTTGTTTAC	This study
wzy_NOLup_F	GTTGGCGATGTTAGTGTGG	This study
wzy_NOLup_R	CTATCAACACACTCTTAAGGAAATAG ACTTCAAATACAACGTAC	This study
wzy_NOLdown_F	TTTAACGGGAGGAAATAAGATATGA AAATTCTTTTTTTAA	This study

Table 2.6. cont.

Name	**Nucleotide sequence 5' → 3'[a]**	**Reference**
wzy_NOLdown_R	GCCAATCGTTACAATTTGTTTAC	This study
β-actin F	GGACTTCGAGCAAGAGATGG	(Vogel et al., 2012)
β-actin R	AGCACTGTGTTGGCGTACAG	(Vogel et al., 2012)

[a] Primers are presented in a 5' to 3' direction

[b] Orientation of primers are indicated as F, forward; R, reverse

[c] Underlined regions denote restriction sites

2.3.2.4 *Colony PCR*

For colony PCR, single bacterial colonies from LB plates were picked with a toothpick and resuspended in 8 µL of milli-Q water. The following PCR reagents were then added to the sample: 0.2 mM of each dNTP, 0.2 µM of each primer complementary to the 3' and 5' ends of the region to be amplified (Table 2.6), 5U of Econotaq (Lucigen) DNA polymerase, 1X Econotaq buffer (Lucigen). The PCR was then performed (Section 2.3.2).

2.3.3 PCR clean-up

PCR clean-up systems were used to remove excess buffers, nucleotides and enzymes from PCR products. Either the Wizard SV gel and PCR clean-up system (Promega) or the Isolate PCR and Gel Kit (Bioline) was used as per manufacturers' instructions. Briefly, for the Wizard SV gel and PCR clean-up system, an equal volume of Membrane Binding Solution was added to the product and the mixture transferred to a spin column. The sample was then incubated at RT for approximately 5 min and centrifuged (10,000 *xg*/ 1 min/ RT). Samples were washed twice with 500 µL Membrane Wash Solution by centrifugation (10,000 *xg*/ 1 min/ RT) and resuspended in 50 µL of nuclease free water. For the Isolate PCR and Gel Kit, 500 µL of Binding Buffer A was added to the spin column/ collection tube apparatus together with 45 µL of sample and mixed well by gentle pipetting. The spin column/ collection tube apparatus was then centrifuged (10,000 *xg*/ 1 min/ RT), filtrate removed and centrifuged again (10,000 *xg*/ 2 min/ RT) to remove excess buffer. The spin column was transferred to a new 1.5 mL microfuge tube and 20 µL of elution buffer was added directly to the membrane. The column was incubated at RT for 15 min and then centrifuged (10,000 *xg*/ 1 min/ RT) to elute the sample.

2.3.4 Purification of plasmid DNA from *E. coli*

Plasmid DNA was isolated from ON broth cultures of *E. coli* (Section 2.2) using the Bioline ISOLATE Plasmid DNA Kit as per the manufacturer's instructions. Briefly, 5 mL of ON culture medium was pelleted by centrifugation (15,000 *xg*/ 10 min/ RT), the supernatant was discarded, and the pellet resuspended in 500 uL of Resuspension Buffer by gently pipetting up and down. Lysis Buffer P (500 µL) was added and the suspension mixed gently by inversion six times. Then, 600 µL of Neutralisation Buffer was added

and again mixed by inversion six times. The suspension was centrifuged (13,000 *xg*/ 10 min/ RT) to pellet the cellular debris. Avoiding the pellet, 750 µL of sample supernatant was transferred to a spin column P, placed in a collection tube and centrifuged (10,000 *xg*/ 1 min/ RT). Filtrate was discarded and the remaining sample was added to the spin column. Sample was again centrifuged (10,000 *xg*/ 1 min/ RT). Filtrate was discarded and 500 µL of Wash Buffer AP was added and the sample recentrifuged (10,000 *xg*/ 1 min/ RT). Again, the filtrate was discarded and 700 µL of Wash Buffer BP was added to the spin column and centrifuged (10,000 *xg*/ 1 min/ RT). The filtrate was discarded and the column centrifuged (10,000 *xg*/1 min/ RT) to remove all traces of ethanol. The spin column was placed in a 1.5 mL elution tube and 50 µL of Elution Buffer was added directly to the spin column membrane. The sample was then incubated at RT for 5 min and centrifuged (10,000*xg*/ 1 min/ RT) to elute the plasmid DNA. Plasmid DNA was stored at 4^{o}C for downstream use and the DNA concentration was quantified using a Thermo Scientific NanoDrop^{TM} 1000 spectrophotometer.

2.3.5 Purification of plasmid DNA from yeast

Yeast plasmids were isolated as previously described by Liu et al, (2007). Briefly, yeast containing plasmids of interest (Table 2.3) were grown ON at 30^{o}C on SD Ura^{-} agar plates (Section 2.3). Approximately >100 yeast colonies from the ON plate were transferred to 8 mL of medium containing the relevant nutritional selection, usually SD Ura^{-} (Table 2.4). Cultures were grown ON at 30^{o}C with shaking (200 rpm), cells were harvested by centrifugation (1500 *xg*/ 5 min/ RT) and washed twice with 5 mL dH_2O. Excess dH_2O was removed and the yeast cells were resuspended in 3 mL of 100 mM Tris-HCl (pH 9.3) containing ~17 mM β-mercaptoethanol. The cells were then incubated at 30°C with shaking (200 rpm) for 30 min. Yeast cells were pelleted by centrifugation (1500 *xg*/ 5 min/ RT), resuspended in 3 mL of protoplasting solution (Table 2.5) and incubated overnight at 37°C to promote protoplast generation (Liu et al., 2017).

Protoplast formation was confirmed by a reduction in turbidity of yeast cells diluted in Tris-HCl (pH 9.3) compared to MP buffer (Table 2.5). Briefly, 50 µL of the ON culture was diluted 1:10 in 100 mM Tris-HCl (pH 9.3) and another 50 µL diluted 1:10 in MP buffer. Turbidity between the two samples was compared by eye. Cells were harvested

by centrifugation (1500 *xg*, 8 min, RT) and washed once with MP buffer (Table 2.5), pelleted and re-suspended in 0.5 mL of MP buffer (Table 2.5). Plasmids were isolated using the Bioline ISOLATE Plasmid DNA Kit as per manufacturer's instructions (Section 2.4.4).

2.3.6 Restriction endonuclease digestion of DNA

All DNA restriction endonucleases were purchased from New England Biolabs and used with the supplied corresponding buffer solutions, according to the manufacturer's instructions. Plasmid and PCR DNA were digested at 37^{o}C for 2 and 4 hr, respectively, in 15- 30 µL total volumes. Bovine serum albumin (BSA) was added at 1X concentration required for optimal restriction enzyme performance. Following incubation, digestion reactions were heat inactivated for 5 min at 65^{o}C, when required. Samples were visualised by agarose gel electrophoresis (Section 2.4.8).

2.3.7 DNA ligation

DNA ligation reactions were performed in a 3:1 insert:vector ratio unless otherwise stated. All ligations were performed in a total of 20 µL containing 2 Weiss Units (U) of T4 DNA ligase (New England Biolabs) and 1X T4 DNA ligase reaction buffer, supplied by the manufacturer. All ligation reactions were performed at 4^{o}C ON.

2.3.8 Agarose gel electrophoresis

DNA was subjected to electrophoresis through horizontal agarose gels following standard molecular biological methods (Sambrook and Russell, 2006). Agarose gels (1-2%) were typically used for the visual resolution of DNA products ranging from 0.8-10 kb (Sections 2.4.2, 2.4.6). Gel casts were set for approximately 30 min before loading DNA. Each sample contained a final concentration of 1X Bioline electrophoresis loading buffer and 100-200 ng of the DNA, unless otherwise specified. Typically, 4 µl of Hyperladder I (Bioline) was used as a molecular weight marker covering fragments of 0.2 to 10 kb in length. Electrophoresis was conducted in 0.5X TAE buffer (Table 2.5) at 110 V and stopped when loading buffer dye had run approximately three quarters of the length of the gel. Gels were subsequently stained for 15 min in a 3X Gel Red nucleic acid stain (Biotum) (Table 2.5) and DNA fragments were visualised and photographed using a BioRad Gel Doc^{TM} EZ Imaging system.

2.3.9 Isolation and purification of digested DNA

DNA fragments of interest were excised from unstained, low melting temperature agarose gels (Table 2.5) using a sterile scalpel and transferred to a sterile 1.5 mL microfuge tube. To identify the gel region containing the band of interest, a DNA ladder (typically Hyperladder I) and an additional sample of the digested DNA was run on the gel. The ladder and additional sample were separated from the gel and stained, providing a marker for band excision from the unstained sample. Samples were subsequently purified using the Bioline Isolate PCR and Gel kit, according to the manufacturer's instructions. Briefly, 650 µL of Gel Solubiliser was added to the excised gel fragment and incubated for 10 min at 50^{o}C to dissolve the agarose. Then 50 µL of Binding Optimiser was added and the tube mixed gently by inversion. The solution was added to a spin column/ collection tube apparatus and centrifuged (10,000 *xg*/ 1 min/ RT). Then 700 µL of Wash Buffer A was added to the column and the centrifugation repeated. Filtrate was discarded and the apparatus centrifuged (10,000 *xg*/ 2 min/ RT) to remove residual Wash Buffer A. The spin column was subsequently transferred to a new 1.5 mL microfuge tube and 30 µL of Elution Buffer was added directly to the membrane. The column was incubated at RT for 15 min and then centrifuged (10,000 *xg*/ 1 min/ RT) to elute the sample. The DNA concentration was determined using a Thermo Scientific Nanodrop^{TM} 1000 spectrophotometer (Biolab) and stored at 4^{o}C.

2.3.10 Cloning of PCR products into pGEM T Easy

Purified PCR products were cloned into pGEM T Easy using the T-overhang insertion site as per manufacturer's instructions. Prior to ligation, PCR products were adenosine treated. Typical adenosine treatment reactions included 500 ng of purified PCR product, 0.2 mM of each dNTP, 5 U of Econotaq (Lucigen) DNA polymerase, and 1X Econotaq buffer in 20 µL total. Reactions were incubated at 37^{o}C for 30 min. The following components were added to 20 µL ligation reactions; 10 µL 2X Rapid Ligation Buffer, 1 µL T4 DNA Ligase, 150 ng pGEM T- Easy vector (Table 2.3) and PCR product (Section 2.4.2) to give a 1:3 vector: insert ratio. Ligations were carried out at 4^{o}C for 18 hr prior to transformation into competent *E. coli* DH5α as per section 2.5.1 and plating onto agar plates containing 100 µg/mL Amp, 1.25 µg/mL X-gal and 1.6 µg/mL IPTG (Section 2.3). Plates were incubated at 37^{o}C for 18 hr and colonies were selected by

blue/white screening and verified by colony PCR (Section 2.4.2).

2.4 **Mutagenesis**

2.4.1 Mutagenesis of *A. baumannii* chromosome using homologous recombineering

Mutations in the *A. baumannii* ATCC 17978 chromosome were performed by adapting a recombineering protocol previously developed by Tucker et al (2014). The pAT04 plasmid (Table 2.3) was electroporated into ATCC 17978 and selected for by plating onto agar containing 12 µg/mL Tet (Section 2.3). An Ery resistance (*ery*^{R}) marker and regions flanking the gene/s of interest, approximately 0.3-1 kb, were amplified separately using primers incorporating the required overlapping sequences (Section 2.4.2, Table 2.6). Approximately 50 ng of each product was added to a nested PCR to create a nested overlap (NOL) product incorporating the *ery*^{R} marker sandwiched by the flanking regions of the target gene/s. Approximately 5-10 ng of the NOL product was purified using a Bioline PCR clean-up kit (Section 2.4.3) and resuspended in 10 µL of dH_2O.

A. baumannii ATCC 17978 containing the pATO4 plasmid (Table 2.3) was streaked onto an agar plate containing 12 mg/mL Tet and grown ON. Cells were scraped and resuspended in 200 ml of 12 mg/mL Tet LB broth (Table 2.4). Cells were grown for 45 min at 37^{o}C with shaking (120 rpm) prior to the addition of IPTG to a final concentration of 2 mM. The bacteria were then further incubated (37^{o}C, shaking 120 rpm) until they reached an OD_{600} of 0.4. The sample was then centrifuged (15,000 *xg*/ 10 min/ RT) to pellet cells. The supernatant was removed and cells resuspended in 10 mL of 10% glycerol, centrifuged (10,000 *xg*/ 10 min/ RT) and washed with 10% glycerol X3 prior to resuspension in 200 µl of 10% glycerol. Purified NOL product (5-10 µg) was added to 100 µL of pelleted cells and transferred to electroporation cuvettes and immediately electroporated with a micropulser (1.8 kV, 200Ω, 25 µF). The cells were resuspended in 4 mL of LB containing 2 mM IPTG and recovered for 4 hr (37^{o}C, 120 rpm) before plating on agar containing 25 mg/mL Ery (Tucker et al., 2014).

2.4.2 Mutagenesis using the pEX18Tc plasmid

Mutations in the *A. baumannii* strain 04117201 chromosome were generated using an alternative method using the pEX18Tc shuttle vector (Table 2.3). Upstream and downstream flanking regions of the gene of interest were amplified (Section 2.4.2) from genomic DNA (Section 2.4.1) using specific primer pairs (Table 2.6). Each primer incorporated restriction sites for cloning into pEX18Tc (Table 2.6). The two flanking PCR-derived regions and the pEX18Tc vector were then digested with the appropriate restriction enzymes (Section 2.4.6) and ligated (Section 2.4.7). An *ery*^{R} marker was amplified (Section 2.4.2) using the *ery_Xho*I primer set (Table 2.6) and the plasmid pVA819 (Table 2.3) as a template and cloned in between the flanking regions (Sections 2.4.6 and 2.4.7). The plasmid construct, pEX18Tc plasmid incorporating flanking regions and *ery*^{R} marker, was transformed into competent *E. coli* DH5α (Section 2.5.1) and plated onto agar plates containing Tet (12 µg/mL) and Ery (25 µg/mL). Plates were incubated ON at 37^{o}C. Colonies from ON plates were screened for desired construct via colony PCR (Section 2.4.2). Plasmids were extracted (Section 2.4.4) and sequenced as described elsewhere (Section 2.8).

The pEX18Tc plasmid incorporating flanking regions and *ery*^{R} marker was electroporated into *A. baumannii* as per Section 2.5.1, and homologous recombination selected for by growth on 5% M9 medium with Ery (25 µg/mL) for 24-48 hrs. Gene replacement with the *ery*^{R} marker was confirmed by PCR and Sanger sequencing (Sections 2.4.3 and 2.8).

2.5 **Transformation**

2.5.1 Transformation of *E. coli*

2.5.1.1 *Preparation of competent cells*

ON cultures of *E. coli* were diluted 1:20 in fresh, pre-warmed LB medium and incubated at 37^{o}C for 1 hr, shaking (120 rpm). Cells were further diluted by transferring to 200 mL of fresh, pre-warmed (37^{o}C) LB medium (Table 2.4). Cultures were incubated at 37^{o}C with shaking (120 rpm) until the cell density reached an OD_{600} of 0.6. Cells were then transferred to sterile, pre-chilled centrifuge tubes and incubated on ice for 5 min. Cells were pelleted by centrifugation (15,000 *xg*/ 10 min/ 4^{o}C) and the

supernatant was discarded. Cells were then re-suspended in 40 mL of TFB1 (Table 2.5) and incubated on ice for 10 min. Cells were again pelleted by centrifugation (15,000 *xg*/ 10 min/ 4^{o}C), supernatant removed, and the pellet resuspended in 3.2 mL of TFB2 (Table 2.5). Cells were incubated on ice for 15 min before being dispensed in 100 µL aliquots and stored at -80^{o}C for downstream use (Hanahan, 1983).

2.5.1.2 *Transformation of E. coli*

Chemically competent *E. coli* prepared in Section 2.5.1.1 were used for transformation with plasmid DNA. An aliquot of competent cells was thawed on ice and approximately 150 ng of plasmid DNA or ligated DNA products of interest (Section 2.4.7) added and tubes tapped to mix. Cells were incubated on ice for 30 min before being heat shocked at 42^{o}C for one min. Cells were then incubated on ice for 20 min before the addition of 500 µL of LB medium. Cells were incubated at 37^{o}C for one hr, shaking (120 rpm), plated on selective medium (Section 2.3) and incubated ON (Hanahan, 1983).

2.5.2 Transformation of *A. baumannii*

Plasmids were electroporated into *A. baumannii* for either mutant construction or complementation. Briefly, ON broth cultures were diluted 1:200 in LB medium and grown to an OD_{600} of 0.4. Cultures were centrifuged (10,000 *xg*/ 10 min/ 4^{o}C), supernatant removed, and the pellets resuspended in 10 mL ice cold 10% glycerol. Cells were washed twice more with ice cold 10% glycerol (10,000 *xg*/ 10 min/ 4^{o}C) and the pellet resuspended in 400 µL ice cold 10% glycerol. Approximately 800 ng of plasmid DNA was added to 200 µL of washed cells before the cells were transferred to electroporation cuvettes and immediately electroporated with a micropulser (2.5 kV, 200Ω, 25 µF). Electroporated cells were transferred to 500 µL of LB medium and incubated for 1 hr at 37^{o}C shaking (120 rpm) before plating onto selective media plates (Section 2.3) and incubated ON at 37^{o}C.

2.5.3 Transformation of yeast

Small scale yeast transformations were performed as per methods previously described by Liu et al and Raymond et al (Liu et al., 2017, Liu and Reeves, 2019, Raymond et al., 1999, Raymond et al., 2002).

2.5.3.1 *Preparation of competent yeast*

Briefly, for four transformations, 10 mL of YPD broth (Table 2.4) was inoculated with several colonies of *S. cerevisiae* CRY1-2 (Table 2.1) from an ON YPD agar plate and incubated ON at 30°C shaking (120 rpm). The culture was then transferred to 100 mL of fresh YPD to produce an OD_{600} between 0.2 and 0.3. The culture was incubated for 3 hr at 30°C, shaking (230 rpm), and harvested by centrifugation (1000 x g, 5 min, RT). The supernatant was removed and the yeast cell pellet resuspended in TE (Table 2.5) to a final volume of 10 mL. Yeast cells were then harvested by centrifugation (1000 *xg*, 5 min, RT) and resuspended in 500 µL TE/LiAc (Table 2.5).

2.5.3.2 *Transformation of competent yeast*

For each transformation, 0.1 mg of sonicated salmon sperm DNA (Sigma), 100 ng of digested plasmid DNA (Section 2.4.6), 1 µg of each linear PCR fragment (Section 2.4.2), and 100 µL of competent yeast cells (Section 2.5.3.1), were added to a microfuge tube and mixed by vortexing. PEG/LiAc solution (600 µL) was added and the mixture further vortexed for 10 sec. Transformations were incubated at 30°C for 30 min with shaking at 200 rpm. DMSO (70 µL) was added to each tube and mixed by inversion. Cells were heat shocked for 15 min at 42°C then chilled on ice for 2 min. Cells were harvested by centrifugation (14000 rpm, 5 sec, RT) and the pellet resuspended in 0.5 mL of TE (Table 2.5). Aliquots were plated onto relevant selective SD plates (Section 2.3) and incubated for 2 days at 30°C (Liu et al., 2017, Raymond et al., 1999, Raymond et al., 2002, Liu and Reeves, 2019).

2.6 **RNA methods**

2.6.1 RNA extraction from eukaryotic cells

To analyse the expression of selected genes in eukaryotic cells after interaction with *A. baumannii*, total RNA was extracted. Monolayers of A549 pneumocytes were incubated with *A. baumannii* for 4 hr as per Section 2.2.3 prior to resuspension in 1 mL of Trizol and incubation at RT for 5 min. Chloroform (200 µL) was added and the sample shaken vigorously for 15 sec. The sample was then incubated for 3 minutes at RT before centrifuging (1200 *xg*, 20 min, 4°C). RNA was extracted using the Bioline Isolate II RNA extraction kit as per manufacturer's instructions. RNA samples were stored at -80°C for downstream applications.

2.6.2 Quantitative reverse transcription PCR

RNA samples (Section 2.6.1) were converted to cDNA using the iScript™ cDNA synthesis kit (Bioline) as per manufacturer's instructions. Oligonucleotides used for real-time quantitative PCR (RT-qPCR) are listed in Table 2.6. RT-qPCR reactions were performed on a Rotor-Gene RG-3000 (CorbettLifeScience™, Qiagen) using the DyNAmo SYBR®green qPCR kit, as per manufacturer's instructions (Finnzymes™, ThermoFisher). Typical run parameters were as follows; initial denaturation of 95°C for 15 min followed by 40 cycles consisting of 15 sec at 95°C, 20 sec at 60°C and 10 sec at 72°C. Transcriptional differences were calculated using the $\Delta\Delta C_t$ method (Livak and Schmittgen, 2001). The cycle threshold (C_t) of each experimental sample can then be compared to the C_t of the β-Actin gene to normalise the samples (Vogel et al., 2012).

2.7 Sequencing and bioinformatic analyses

Alignment and manipulation of DNA sequences were performed using SnapGene™. Searches for nucleotide and protein sequences were performed using Blastn (NCBI) and Blastp (NCBI) (Marcher-Bauer 2011). The gene regions of interest for *A. baumannii* strain 04117201 were obtained from the Rapid Annotation using Subsystem Technology (RAST) 2.0 server (Overbeek et al., 2013). Genes and gene regions of interest were identified using the Kyoto Encyclopedia of Genes and Genomes (KEGG) server where specified (Kanehisa and Goto, 2000). Promotor regions of analysed sequences were predicted using the online promotor prediction tool from fruitfly.org (Reese, 2001). Alignments of multiple sequences was performed using EasyFig (Sullivan et al., 2011).

Purified DNA was sequenced by the Australian Genome Research Facility (AGRF) by Sanger sequencing using capillary separation. Up to 500 ng of PCR product or plasmid DNA template and 3.2 pmol of the appropriate sequencing primer were used per reaction (Table 2.6). Nucleotide sequences were analysed using Sequencher™ 4.9 (GeneCodes).

2.8 **Protein and carbohydrate analysis**

2.8.1 Preparation of whole cell lysates

Whole cell lysates (WCL) were prepared as follows. One mL of ON culture was centrifuged (13,000 *xg*/ 10 min/ RT) and the pellet resuspended in 100 µL of WCL lysis buffer (Table 2.5). The sample was then incubated for 1 hr at 50^{o}C before being cooled to RT.

2.8.2 Preparation of membrane fractions

Five hundred µL of ON LB broth culture was transferred to 100 mL of fresh LB broth and incubated at 37^{o}C, shaking (120 rpm), until OD_{600} reached 0.7-1.3. The cells were pelleted by centrifugation (10,000 *xg*/ 15 min/ 4^{o}C) and resuspended in 5 mL crushing buffer (Table 2.5). Cells were disrupted using a high pressure homogeniser (30 per square inch [psi]/ 1 shot head) and samples centrifuged (10,000 *xg*/ 15 min/ 4^{o}C). Supernatant was transferred to an ultracentrifuge tube and centrifuged (134 000 *xg*/1 hr/ 4^{o}C) to pellet the membrane fraction. Supernatant was removed and membrane fractions were resuspended in 400 µL to 1 mL dH_2O and stored at -80^{o}C for future applications. Membrane protein samples were quantified using Biorad protein standards as per manufacturer's instructions.

2.8.3 Extraction of capsule

Capsular polysaccharide was extracted from *A. baumannii* cultures using a method adapted from J Kenyon, Queensland University of Technology (personal communication). Briefly, 10 mL of MH broth (Table 2.2) was inoculated with 100 µL of ON bacterial culture. The sample was incubated at 37^{o}C, shaking (120 rpm) until the culture reached an OD_{600} of 1.0. The sample was centrifuged (10,000 *xg*/ 15 min/ 4^{o}C) and the supernatant transferred to Falcon tubes and stored at -20^{o}C for later analysis. Cell pellets were resuspended in 1 mL of CPS lysis buffer (Table 2.3) with the addition of 250 µg of lysozyme, 500 µg of RNAse and 500 µg of DNAse, and incubated for 1 hr at 37^{o}C. Cells were then disrupted using a high pressure homogeniser (30 psi/1 shot head). Recovered sample (500 µL) was further treated with 250 µg of RNAse and 250 µg of DNAse and incubated at 37^{o}C for 30 min. SDS (0.5% final concentration) was added and the sample incubated at 37^{o}C for 30 min. The samples were processed by

boiling at 100^{o}C for 5 min and cooled to RT prior to the addition of 25 µg of proteinase K. Samples were then incubated at 60^{o}C for 1 hr and stored at -20^{o}C.

2.8.4 SDS-PAGE

2.8.4.1 *SDS-PAGE using pre-cast gels*

For SDS-PAGE gels of WCL (Section 2.9.1) and membrane fractions (Section 2.9.2) 12.5% SDS-PAGE precast gels (Sigma) were used. Membrane fractions were suspended in 1X SDS-PAGE sample buffer (Table 2.5) to a final concentration of 2 mg/mL and incubated at 37^{o}C for 30 min prior to loading. Gels were run at 100-140 V for approximately 2-3 hr, buffered with 1X SDS-PAGE running buffer (Table 2.5). Protein samples were quantified using Biorad protein standards as per manufacturer's instructions. A molecular weight marker, the Precision Plus Protein^{TM} Prestained Protein Standard (Biorad), was included to determine the size of bands.

2.8.4.2 *SDS-PAGE*

For electrophoresis on longer gels, SDS-PAGE gels of 20% acrylamide gel layered with an SDS-PAGE stacking gel was poured and used (Table 2.5) to resolve extracted CPS (Section 2.9.3). CPS was suspended in 1X SDS-PAGE sample buffer and incubated at 37^{o}C for 30 min prior to loading samples. SDS-PAGE gels were run at 90 V for approximately 12 hr. For electrophoresis of membrane fractions a 12.5% acrylamide gel layered with SDS-PAGE stacking gel was used (Table 2.5). Membrane fractions (Section 2.9.2) were suspended in 1X SDS-PAGE sample buffer (Table 2.5) and incubated at 37^{o}C for 30 min prior to loading samples. Membrane fraction SDS-PAGE gels were run at 90-140 V for approximately 3 hr. A molecular weight marker, the Precision Plus Protein^{TM} Prestained Protein Standard (Biorad), was included to determine the size of bands**.**

2.8.5 Coomassie blue stain

WCL (Section 2.9.1) and membrane fractions (Section 2.9.2) were run on 12.5% SDS-PAGE (Section 2.9.4.1, 2.9.4.2) and stained with Coomassie stain (Table 2.5) ON at RT with gentle rotation. Gels were destained with destain solution until bands visible (Table 2.5) and scanned using a Gel Doc EZ system (Biorad).

2.8.6 Alcian blue stain

Alcian blue staining methods were adapted from previous studies (Min and Cowman, 1986, De Castro et al., 2010). Extracted CPS (Section 2.9.3) was run on a 20% SDS-PAGE gel (Section 2.9.4) and fixed with Alcian blue fixative solution (Table 2.5) for 1 hr with gentle agitation. The gel was then stained with Alcian blue stain (Table 2.5) ON with gentle agitation and decolourised with Alcian blue fixative solution ON (Table 2.5) and scanned using Gel Doc EZ system (Biorad).

2.8.7 Periodic acid-Schiff stain

Periodic acid-Schiff (PAS) stains were conducted as previously described (Cagatay and Hickford, 2008). All steps were carried out at RT in the dark and under gentle agitation. Briefly; SDS-PAGE gels (Section 2.9.4) of membrane fractions (Section 2.9.2) were washed with 50% (v/v) ethanol (ETOH) in dH_2O for 30 min and fixed with PAS fixation solution (Table 2.5) for 1 hr. Fresh PAS fixation solution was then added and the gel fixed ON. Fixation solution was removed, and the gel was incubated with for 30 min with Periodate solution (Table 2.3) before washing with dH_2O for 5 min a minimum of six times with agitation. The gel was then incubated in metabisulphite solution (Table 2.3) for 5-10 min. The solution was replaced with fresh metabisulphite solution and incubated for a further 10 min. The gel was then incubated with Schiffs reagent (Sigma) for 2 hrs before incubation and storage in 0.1% $Na_2S_2O_5$ in 10 mM HCl. The gel was photographed using the Gel Doc EZ system (Biorad) and stored in 7.5% acetic acid, 5% methanol.

2.8.8 Phenol sulphuric acid assay

A phenol sulphuric acid assay was adapted to quantify bacterial surface carbohydrate levels (Nielsen, 2010). Bacterial cells were grown to an OD_{600} of 1.0 in LB medium as per Section 2.2 and then 1 mL of this culture was centrifuged (10, 000 *xg*/ 2 min/ RT) and washed 3 times in 50 mM NaCl. Cells were resuspended in 1 mL of 50 mM EDTA (pH 7) and incubated, shaking (120 rpm) for 30 min. Cells were pelleted by centrifugation (10,000 *xg*/ 2 min/ RT) and 400 µL of the supernatant was added to 400 µL of 5% phenol in dH_2O in a glass tube. To each sample, 2 mL of sulphuric acid was then added. Samples were incubated at RT for 10 min before absorbance was measured

at 490 nm. A standard curve was generated to quantify the concentrations of surface carbohydrate using serial dilutions of COH stock solution (Table 2.5) (Nielsen, 2010) in place of bacterial supernatants.

2.9 **Microscopy**

2.9.1 Gram stain

Three to eight colonies of bacteria grown ON on MH agar were resuspended in a drop of dH_2O on a clean microscope slide. Samples were air dried and heat fixed by passing the slide through a Bunsen burner flame 3 times. Two to three drops of 1% crystal violet was added to each bacterial sample and incubated for 30 sec at RT. The samples were washed with tap water to remove crystal violet and two to three drops of Mordant with Jensens iodine was added for 30 sec. Samples were washed with tap water and decolourised with 95% ETOH for 15 to 30 sec. Slides were rinsed with tap water and three drops of Safranin Orange (0.1%) was added for 30 sec. Samples were briefly rinsed again and blotted with tissue before allowing to dry. Bacteria were visualised at 1000X magnification using a BX53 Brightfield microscope (Olympus). Images were analysed using Fiji ImageJ software (Schneider et al., 2012).

2.9.2 Maneval's stain

Two to four colonies were resuspended in a drop of dH_2O on a clean glass microscope slide. One drop of 1% Congo Red dye (Sigma) was added and smeared across the slide and allowed to air dry. Slides were flooded with Maneval's stain (Table 2.5) and incubated at RT for 2 min. Excess dye was removed and slides allowed to air dry. Bacteria were visualised at 1000X magnification using a BX53 Brightfield microscope (Olympus). Images analysed using Fiji ImageJ software (Schneider et al., 2012).

2.10 **Bacterial growth curves**

2.10.1 Standard growth curves

Bacterial growth was assessed by growth curves. Briefly, ON bacterial cultures were diluted 1:200 in 10 mL of MH medium and incubated for 8 hr at 37^{o}C shaking (120 rpm). The OD_{600} was determined every hour using a either a DU 640 (Beckman) or

Spectronic 200E (Thermofisher Scientific) spectrophotometer. Growth curves were performed in duplicate on a minimum of three separate occasions.

2.10.2 Growth under pH stress

To assess the effect of extracellular pH on bacterial survival, growth curves were performed as per Section 2.11.1 with the pH of the MH medium adjusted using acetic acid to 5.5. The OD_{600} was determined every hr for the first 8 hr then at 12, 24 and 48 hr.

2.10.3 Growth under temperature stress

To assess the effect of temperature on bacterial survival, growth curves were performed as per Section 2.11.1 at varying temperatures between 37-47^{o}C for 8 hrs. The OD_{600} was determined every hr.

2.10.4 Growth under oxidative stress

Bacterial strains were grown to an OD_{600} of 0.6 in MH medium, shaking (120 rpm) at 37^{o}C. Cultures were diluted 1:200 in fresh MH medium and 2 mL of diluted culture was added to each well of a 24 well plate. The required stock solution of paraquat (200 mM) was added to each well to give the final concentrations of paraquat (0-500 µL). Plates were covered and the assay monitored using a Fluostar Omega spectrometer (BMG Labtech). Plates were agitated at 5 min intervals and OD_{600} was recorded every hour for 18 hrs.

2.10.5 Viability growth curves

To ascertain the maximum viability of bacterial strains, ON bacterial cultures (Section 2.2) were diluted 1:200 in fresh MH medium (Table 2.4). Serial dilutions of each culture were plated onto LB agar at 1 hr intervals for 14 hr. Plates were incubated ON at 37^{o}C and total viable counts (TVC) were determined as colony forming units (CFU)/mL.

2.11 **Antimicrobial resistance assays**

For all antimicrobial resistance assays, bacterial cultures were grown ON in MH medium (Table 2.4, Section 2.2), diluted 1:200 in 5 mL of fresh MH medium, and

grown to an OD_{600} of 0.6 (Section 2.2). Three different methods were used to assess bacterial resistance:

The minimal inhibitory concentration (MIC) of bacterial strains to antimicrobial compounds was investigated using a microplate dilution method in a 96 well plate as described previously (Wiegand et al., 2008). ON bacterial cultures were diluted 1:1000 in MH broth. For each antimicrobial compound, a 2-fold dilution series was prepared in wells containing 200 µL of diluted bacterial cultures. The 96 well plates were then incubated at 37^{o}C with gentle shaking. Bacterial growth was determined after 18 hr by measuring the absorbance OD_{600} using a Fluostar Omega spectrometer (BMG Labtech).

Bacterial cultures (OD_{600} of 0.6) were serially diluted in 10-fold intervals. Bacterial aliquots (5 µL) of the neat to 10^{-5} dilutions were plated on MH agar plates containing increasing concentrations of antibiotic. Plates were incubated ON at 37^{o}C.

For disk diffusion assays, MH agar plates (Table 2.4) were inoculated with 100 µL of bacterial culture, plates were allowed to dry, and a paper disk impregnated with 5 µL of antibiotic was placed on the plate. Plates were incubated ON at 37^{o}C and zones of inhibition (diameter) were measured (Srinivasan et al., 2012).

2.12 **Hydrogen peroxide killing assay**

ON bacterial cultures (Section 2.2) were diluted 1:50 in MH medium and grown to an OD_{600} of 0.4 at 37^{o}C, shaking (120 rpm). To each bacterial sample (1 mL), 3 µL of 30% H_2O_2 was added and the sample was incubated with gentle shaking at 37^{o}C. Serial dilutions of each sample, including the starting culture before treatment, were plated after 10, 20 and 30 min. An untreated control containing no H_2O_2 was prepared in parallel with the treatment arm and used for comparison.

2.13 **Serum survival assay**

Serum survival assays were performed as previously described (Kim et al., 2009). Briefly, ON bacterial cultures (Section 2.2) were diluted 1:50 in LB medium and grown to an OD_{600} of 0.6. Cells were washed twice with PBS and resuspended in PBS to a final OD_{600} of 0.6. Serial dilutions of the initial suspension were plated to determine pre-treatment viability. Bacterial suspensions (10 µL) were added to; 200 µL of 40%

human serum (Sigma), 200 μL of inactive serum (serum heated to 56°C for 30 min), or 200 μL of PBS (Table 2.5). Samples were incubated for two hr with gentle shaking at 37°C and serial dilutions were plated on LB agar. Percentage survival was determined by dividing the CFU/ mL of serum treated by the CFU/ mL of the sample treated with inactivated serum.

2.14 **Lysozyme killing assay**

ON bacterial cultures (Section 2.2) were diluted 1:50 in LB medium and grown to an OD_{600} of 0.6. Cultures were then further diluted to an OD_{600} of 0.05 and serial dilutions of this culture were plated on LB agar plates (Table 2.4) to obtain the initial CFU/ mL. Cultures were incubated for 1 hr in 1 mg/mL final concentration of human lysozyme (Sigma) and serial dilutions were plated on LB agar and incubated ON at 37°C. An untreated control, containing no lysozyme, was prepared in parallel with the treatment arm and used for comparison.

2.15 **Static biofilm assay**

The static biofilm assay was modified from a method previously described (Eijkelkamp et al., 2011b). Briefly, 5 mL of MH medium was inoculated 1:200 with an ON broth culture of *A. baumannii* and grown to an OD_{600} of 0.6. Cultures were then further diluted 1:100 in 5 mL of MH medium and incubated statically at 37°C for 72 hr in the dark. After incubation, the OD_{600} of the culture containing planktonic growth was measured. Adherent cells were washed once with PBS and stained with 6 mL 0.1% crystal violet for 30 min at 4°C. Cells were then washed three times in PBS. Dye was released from adherent cells by the addition of 5 mL of 80% ethanol, 20% acetone and absorbance at OD_{595} using a Fluostar Omega spectrometer (BMG Labtech).

2.16 **Desiccation assay**

2.16.1 Long-term desiccation

For long-term desiccation (>100 days), experimental procedures were adapted from Jawad et al (1998). Glass cover slips were first washed with 0.01% SDS, followed by dH_2O and finally 80% ETOH before sterilisation in an oven at 160°C for 2 hr (Jawad et al., 1998). Initially, 30 cover slips were prepared for each of the strains to be tested. The

relative humidity (RH) of the chamber was controlled using saturated $CaCl_2$ in an open beaker. A hygrometer was used to ensure the RH remained at 38-40%; additional $CaCl_2$ was added when necessary. Strains were grown to their maximum density (Section 2.11.5) and 1 mL of each strain was centrifuged (10 000 *xg*, 5 min, RT). Supernatant was removed and bacterial pellets were washed in 1 mL dH_2O. Samples were again centrifuged (8 000 *xg*, 5 min, RT), the supernatant was removed and the pellet was resuspended in 1 mL of H_2O. Aliquots (20 µL) of bacterial suspension were added to the middle of each cover slip. Slips were placed in an uncovered petri dish inside an airtight chamber (transparent plastic box). Serial dilutions of this suspension were plated onto LB agar and incubated ON at 37ºC to obtain a T_0 sample. For each time point, two slides for each strain were rehydrated in 5 mL of sterile water by vigorously vortexing for 3 min. Serial dilutions of the rehydrated bacteria was then plated onto LB and incubated ON at 37ºC (Jawad et al., 1998).

2.16.2 Short term desiccation

For short-term desiccation experiments (30 days), methods were adapted from Gayoso et al (2013). Briefly, ON bacterial cultures were grown in duplicate to an OD_{600} of 0.6 and washed twice with sterile dH_2O before diluting to an OD_{600} of 0.1. Bacterial samples (300 µL) were added to each well of a six well tissue culture tray and allowed to air-dry. Samples were then incubated at 21ºC and a relative humidity of 30% (+/- 2%). Bacteria were recovered at 0, 2, 3, 5, 7, 9, 15, 21, and 30 days by rehydration in 1 mL of PBS. Serial dilutions were plated onto LB agar plates and survival calculated by dividing the CFU/mL of each time point by the day 0 CFU/mL (Gayoso et al., 2013).

2.17 **Hydrophobicity assay**

Cell surface hydrophobicity was examined as described previously by Rosenberg et al (1980). ON bacterial cultures (Section 2.2) were diluted 1:10 in LB medium (Table 2.4) and incubated at 37ºC for 2 hr at 120 rpm (shaking). Cells were washed twice with potassium urea magnesium (PUM) buffer (Table 2.5) and incubated at 30ºC for 30 min. The cell suspension was adjusted to an OD_{600} of 0.25 ($OD_{initial}$) in PUM buffer in glass vials. Xylene (3 mL) was added and samples were vortexed for 2 min. The two phases were allowed to separate for 15 min at RT. The OD_{600} of the aqueous phase (OD_{final}) was measured using a Beckman DU 640 spectrophotometer. Three independent assays

were conducted for each bacterial strain in duplicate. The hydrophobicity index (HI) was expressed as a percentage and calculated using the following formula: HI (%)=($OD_{initial}$-OD_{final}/$OD_{initial}$)*100 (Rosenberg et al., 1980).

2.18 **Heat shock assay**

Heat shock assays were adapted from Aranda et al (2011). Briefly, ON bacterial cultures (Section 2.2) were diluted 1:200 in MH medium (Table 2.4) and incubated at 37^{o}C with shaking at 120 rpm until an OD_{600} of 0.5 was reached. Samples (1 mL) of this culture was then incubated at 55^{o}C statically. At 0, 20, and 40 min time points serial dilutions were plated on LB agar and incubated ON at 37^{o}C to obtain TVCs (Aranda et al., 2011).

2.19 **Isolation of human monocyte derived macrophages**

Approximately 40 mL of buffy coats (obtained from Red Cross Blood Bank) were mixed with RT Hanks Balanced Salt Solution (HBSS) (Gibco) up to a total of 100 mL. In 50 mL Falcon tubes, 20 mL of Lymphoprep^{TM} (Stemcell Technologies^{TM}) was added and overlayed with 25 mL of buffy coat. Tubes were centrifuged (1200 *xg*/ 30 min/ RT) with the break on low to avoid disruption of layers. Leukocyte bands were removed with a Pasteur pipette and pooled in two fresh Falcon tubes. Leukocytes were washed in HBSS and pelleted by centrifugation (300 *xg*/ 10 min/ RT). Supernatant was removed and cells washed in HBSS and pelleted by centrifugation (300 *xg*/ 5 min/ RT). Supernatant was again removed and cells resuspended in 20 mL HBSS. Monocyte yields were counted using a haemocytometer and cells were centrifuged (300 *xg*/ 5 min/ RT), supernatant removed, and resuspended at a concentration of 1 x 10^7 cells/mL in monocyte derived macrophage (MDM) adherence medium (Table 2.4). Cells were transferred to tissue culture flasks and incubated at 37^{o}C under 5% CO_2 for 1 hr. Adherent cells were gently washed with HBSS+ (Gibco) and the MDM adherence medium replaced whilst non-adherent cells were transferred to a clean flask. This was repeated up to three times before pooling of adherent cells in the original culture flask with the addition of MDM culture medium (Table 2.4). Cells were incubated at 37^{o}C under 5% CO_2 for 48 hours. Two days post-isolation supernatant was removed and centrifuged (350 *xg*/ 5 min/ RT). The cell pellet, consisting of MDM cells, was resuspended in fresh MDM culture medium (Table 2.4) and returned to the original

flask. Five to six days post isolation, MDM cells were detached using 10 mL of cold HBSS and a cell scraper. Cells were centrifuged (350 *xg*/ 5 min/ RT) and resuspended in 10 mL MDM culture medium. Yields were determined using a haemocytometer and additional MDM culture medium was added to cells to obtain 1.5 x 10^5 monocytes/mL. Aliquots (200 µL) were added to each well of 48 well plates and incubated 24-72 hr at 37^{o}C under 5% CO_2 for downstream applications.

2.20 **Adherence and invasion of pneumocytes**

Adherence of *A. baumannii* strains to A549 cells (human type 2 pneumocytes) was performed as previously described (Talbot et al., 1996). Cell lines were grown in DMEM (Invitrogen) supplemented with 10% FCS, 2 mM L-glutamate, and 100 µg/mL PenStrep (Table 2.4) in 24 well plates. Prior to use, cell monolayers were examined microscopically to ensure >90% coverage of the bottom surface of the wells. Washed A549 cells were then infected with a bacterial inoculum of ~1x10^7 CFU and incubated at 37^{o}C for 4 hr. Monolayers were washed three times with PBS to remove non-adherent bacteria. A549 cells were detached from the plate by treating with 0.25% trypsin and lysed using 0.025% Triton X-100. Serial dilutions were plated onto LB agar to determine the CFU of adherent bacteria per well. For invasion assays, Gent 16 mg/mL was added to the wells after the incubation period (4 hr) to kill any bacterial cells outside the A549 cells. Data from adherence and invasion assays were collected from three independent experiments and represent the data points for each experiment of quadruplicate wells.

2.21 **Invasion and intracellular killing by macrophages**

2.21.1 Phagocytosis assay using RAW 264.7 murine macrophages

Bacterial strains were grown ON in MH medium and diluted to a concentration of 10^7 CFU/mL in DMEM. Lawns of RAW 264.7 macrophages in 24 well plates were inoculated with 200 µL of bacterial suspension (Section 2.21). Plates were centrifuged (200 *xg*/ 5 min/ RT) to settle bacteria onto the macrophage lawns. Plates were incubated at 37^{o}C for 1 hr. Medium was removed, and macrophages washed twice with PBS. Fresh DMEM supplemented with 400 µg/mL Amk was added to each well and plates were incubated for a further 1-3 hrs at 37^{o}C. Wells were then washed with PBS, cells

were detached from the plate by the addition of 100 µL of 0.25% trypsin and monocytes lysed using 400 µL of 0.025% Triton X-100. Serial dilutions were plated onto LB agar to determine the CFU of phagocytised bacteria.

2.21.2 Macrophage phagocytosis assay using human monocyte derived macrophages

Bacterial strains were grown in MH medium at 37ºC with shaking (120 rpm) until they reached an OD_{600} of 0.6. The concentration of the bacterial sample was adjusted to an OD_{600} of 0.4- 0.5. Then, 10 µL of bacterial culture was added to 990 µL MDM culture media (without penstrep) (Table 2.4). MDMs (Section 2.20) were gently washed with PBS prior to the addition of 200 µL of bacterial suspension to each well (Section 2.21). Cells were incubated for either 1 hr (first time point [T1]) or 2 hr (second time point [T2]) at 37ºC, then media containing the bacterial suspension was removed and the MDMs were washed with PBS. Media containing 16 µg/ mL Gent was added for a further 1 hr incubation to kill extracellular bacteria. MDMs were lysed with 500 µL of 0.025% Triton X-100 and plated on LB agar plates to determine intracellular bacterial counts.

2.22 **Statistical analyses**

Data were analysed using the IBM SPSS statistical software package (SPSS, 2007). Datasets were analysed for normal distribution using the Shapiro Wilk method ($p > 0.05$). For those datasets unevenly distributed, a pairwise comparison using the Kruskal-Wallis method was employed (McKight and Najab, 2010). A student's T-test was used determine if the mean of two sets of data were significantly different ($p < 0.05$). A one-way analysis of variance (ANOVA) and Tuckey's post hoc test were used to determine if the mean of three or more sets of data were significantly different ($p < 0.05$).

3 ANALYSIS OF *A. BAUMANNII* CLINICAL ISOLATES POSSESSING VARIOUS CAPSULE TYPES

3.1 Introduction

Clinical isolates of *A. baumannii* vary greatly in their pathogenic potential. For example, comparative analyses have revealed extreme diversity between clinical isolates in their ability to produce biofilms, adhere to human cells and resist human complement (Eijkelkamp et al., 2011b, King et al., 2009, Lee et al., 2008). Although correlations between capsule type and pathogenicity potential have been reported in other bacterial species (Section 1.6), no studies have previously investigated this in *A. baumannii*.

The aim of the work presented in this chapter is to compare the response of 12 *A. baumannii* strains, representing nine capsule types, under stress conditions which may be encountered in the nosocomial environment or within the host during infection. Assays include: cell surface hydrophobicity, which is linked to survival in dry environments (Section 1.6); growth under acidic stress, which has been associated with adaptation to changing environmental conditions (Section 1.6); and desiccation tolerance, which is vital for *A. baumannii* to survive for extended periods of time in drying environments (Section 1.6.2). This chapter also examines resistance of *A. baumannii* to two important host antimicrobial compounds, lysozyme and complement, which both play important roles in the innate immune response against *A. baumannii* (Section 1.8). The desiccation assays were only performed on eight of the twelve A. baumannii strains as replicates of the given strains were not consistent (Section 3.2.3, Figures 3.6 and 3.7). Due to time constraints, serum resistance assays were only performed on 10 of the 12 strains included in this study (Section 3.2.5). The strains included were chosen to ensure all nine capsule types were represented.

The strains assessed in this chapter were chosen from our strain collection as the genome regions of the K loci are available and the K structures have been determined (except for for K9) (Kenyon and Hall, 2013, Kenyon et al., 2015a, Kenyon et al., 2014a, Kenyon et al., 2015c, Kenyon et al., 2016b, Kenyon et al., 2015b) (Table 2.1). These

strains represent a wide variety of capsule types and three of the capsule types assessed, K1, K2 and K3, are represented by more than one strain (Figures 3.1, 3.2). Generally, all capsule types have a net negative charge due to the incorporation of acidic sugar residues. Broadly, the represented capsule types can be divided into two general groups; those which incorporate non-2-ulosonic acids such as pseudaminic or acinetaminic non-2-ulosonic acids (K2, K6, K12 and K13) and those without these acid residues (K1, K3, K9, K4 and K14).

Some of the capsule types can also be grouped based on structural similarity. For instance, K12 and K13 differ only by the linkage of two glycans (Figure 3.2), which requires the use of an alternate Wzy polymerase; accordingly, the K loci of both strains are identical except for the *wzy* gene (Figure 3.1). Similarities exist between some other K loci. For example, the K3 and K14 representatives are composed only of simple sugars (Figure 3.2) and correspondingly, their variable gene regions in the KL contain no genes for specific sugar synthesis (Figure 3.1). Uniquely, the K4 structure of D78 is uncommon as it is composed only of amino-sugars, one of which is capped with a rare pyruvyl group (Kenyon et al., 2016b) (Figure 3.1). Several of the strains analysed have one or more side linkages which branch from the main repeating sugar unit (Figure 3.2). Furthermore, a broad variety of glycosidic linkages are seen between the sugars that compose the K structures of selected strains (Figure 3.2).

3.2 **Results and Discussion**

3.2.1 Cell surface hydrophobicity of *A. baumannii* clinical isolates

Cell surface hydrophobicity is an important factor which has been correlated to bacterial pathogenicity (Section 1.2.4). Surface hydrophobicity can vary vastly between *A. baumannii* strains. A previous study reported approximately 20% of clinical isolates tested to display high levels of hydrophobicity (Giles et al., 2015). A more recent study identified IC I strains of *A. baumannii* as being more hydrophobic than IC II strains, interestingly, the IC I strains in this study also produced more capsule than the IC II strains (Skerniškytė et al., 2018) (Section 1.2.4).

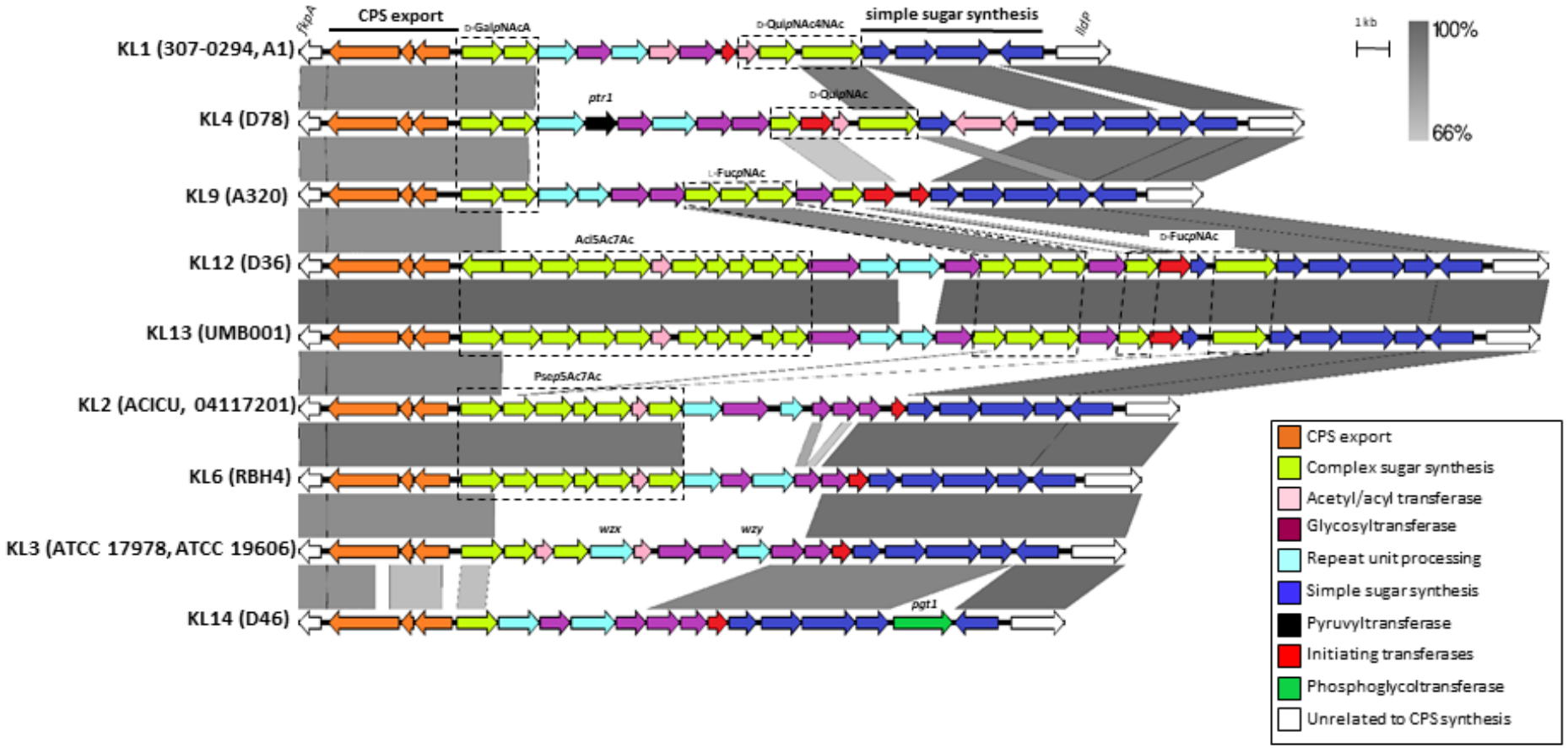
fkpA
CPS export
D-GalpNAcA
D-QuipNAc4NAc
simple sugar synthesis
lldP
1 kb
100%
66%
KL1 (307-0294, A1)
KL4 (D78)
KL9 (A320)
KL12 (D36)
KL13 (UMB001)
KL2 (ACICU, 04117201)
KL6 (RBH4)
KL3 (ATCC 17978, ATCC 19606)
KL14 (D46)
ptr1
D-QuipNAc
L-FucpNAc
AcI5Ac7Ac
D-FucpNAc
Psep5Ac7Ac
wzx
wzy
pgt1
CPS export
Complex sugar synthesis
Acetyl/acyl transferase
Glycosyltransferase
Repeat unit processing
Simple sugar synthesis
Pyruvyltransferase
Initiating transferases
Phosphoglycoltransferase
Unrelated to CPS synthesis

Figure 3.1 Comparison of *A. baumannii* CPS biosynthesis gene loci. Nucleotide sequences of KL regions, between *fkpA* and *lldP* were obtained from the NCBI database and aligned using Easyfig (Sullivan et al., 2011). Genes are depicted by arrows and indicate direction of transcription. Colours are outlined in the key and based on homology to the putative function of gene products. Homology of nucleotide sequences are represented by grey shading. Strains representing the various KL types are named in parentheses. Further information on *A. baumannii* strains represented can be found in Table 2.1. Genes required for variable sugar synthesis and other genes of interest are indicated above the corresponding region, where Aci5Ac7Ac represents genes involved in the production of 5,7-di-*N*-acetylacinetaminic acid; L-Fuc*p*NAc, *N*-acetyl-L-fucosaminic acid; D-Fuc*p*NAc, *N*-acetyl-D-fucosaminic acid; D-Gal*p*NAcA, *N*-acetyl-D-galactosaminuronic acid; D-Qui*p*NAc4NAc, 2,4-diacetamido-2,4,6-trideoxy-D-glucopyranose (*N*,*N*'-diacetyl-bacillosamine); D-Qui*p*NAc, *N*-acetyl-D-quinovosaminic acid; Pse*p*5Ac7Ac, 5,7-diacetamido-3,5,7,9-tetradeoxy-L-*glycero*-L-*manno*-non-2-ulosonic (pseudaminic) acid. Genbank accession numbers for sequences used in gene alignment are as follows; KL12, JN107991.2 (38.5 kb region; base position range 2332-40832); KL13, MF522810.1 (38.2 kb region); KL1, CP001172.1 (24.9 kb; base position range 366401 to 3691388); KL4, JN409449.3 (30.9 kb; base position range 2375 to 33327); KL3, CP012004.1, (25.4 kb; base position range 3762660-3788118); KL2, CP000863.1 (27.1 kb; base position range 77125-104246); KL6, KF130871.1 (25.5 kb); KL9, JN247441 (27.8 kb base position range 2338-30186); KL14, JN247441 (23.5 kb). Figure is drawn to scale (Kenyon and Hall, 2013, Kenyon et al., 2015a, Kenyon et al., 2014a, Kenyon et al., 2015c, Kenyon et al., 2016b, Kenyon et al., 2015b).

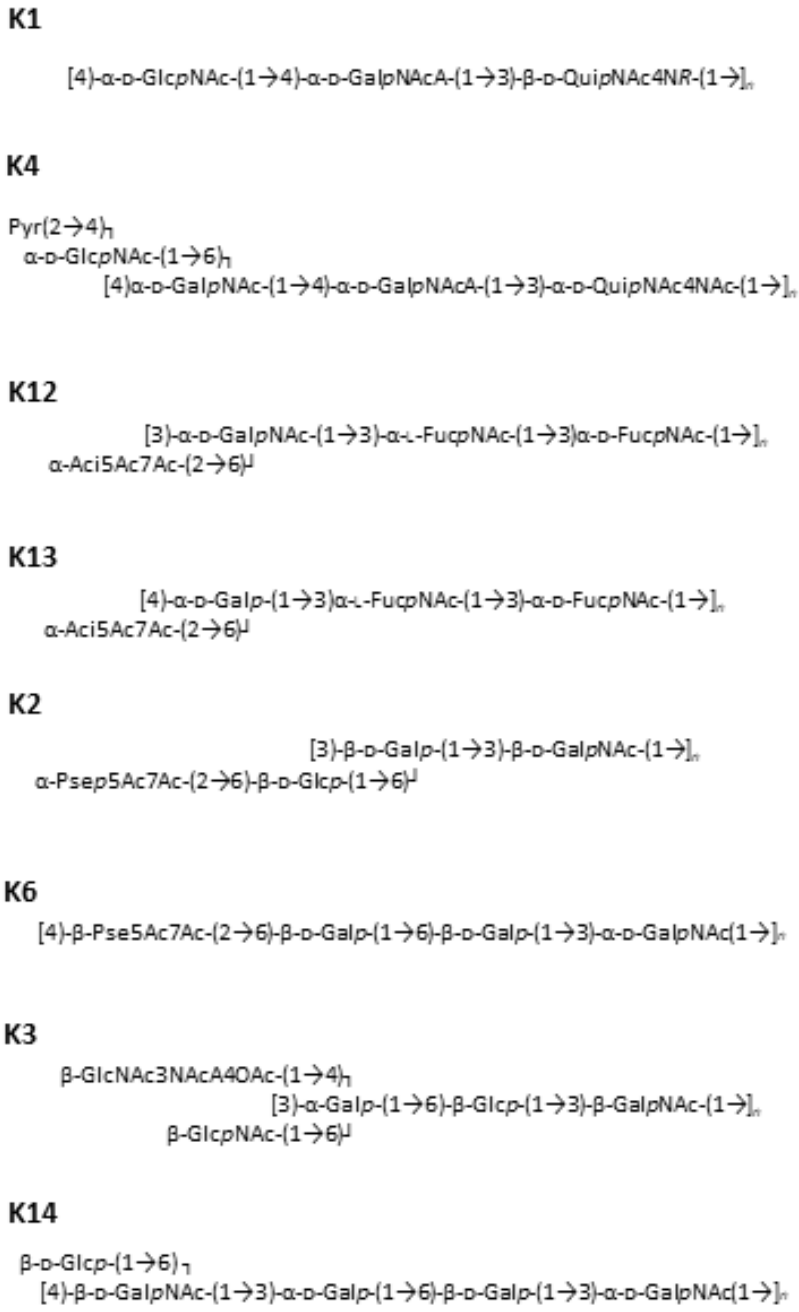

Figure 3.2 Comparison of *A. baumannii* CPS repeat unit structures. Capsule structures correspond to the KL types shown in Figure 3.1. Numbers and arrows in parentheses represent the position of glyosidic linkages between individual sugars. Full names of sugar subunits are listed in Figure 3.1 (Kenyon et al., 2015a, Kenyon et al., 2014a, Kenyon et al., 2015c, Kenyon et al., 2016b, Kenyon et al., 2015b, Russo et al., 2010, Talyansky et al., 2021, Kenyon et al., 2017b, Lees-Miller et al., 2013).

In this study, cell surface hydrophobicity was determined for twelve *A. baumannii* strains by testing their affinity to the hydrocarbon xylene in comparison to an aqueous buffer (Rosenberg et al., 1980) (Section 2.18). Briefly, bacteria were grown to an OD_{600} of 0.6 and resuspended in PUMS buffer (Table 2.5). Xylene was added and the samples vortexed before allowing the phases to separate. The hydrophobicity was then calculated by the decrease in turbidity of the aqueous phase (Section 2.19) (Rosenberg et al., 1980). Cell surface hydrophobicity varied across the isolates tested, five strains were classified as hydrophobic (> 70%) and seven as hydrophilic (< 30%) (Figure 3.3).

In some instances, correlations were seen between *A. baumannii* strains possessing the same capsular type. For example, both K1 strains, 307-0294 (96.9%) and A1 (96.5%), showed similar levels of hydrophobicity ($p = 1$), as did the K3 strains ATCC 17978 (1.4%) and ATCC 19606 (9.4%) ($p = 1$). Furthermore, two strains, UMB001 and D36, which have highly similar K unit structures (Figure 3.2) show a similar hydrophobicity index (Figure 3.3). On the other hand, one K2 strain, 04117201 (0%) was completely hydrophilic, whereas another K2 strain, ACICU (91.9%), was highly hydrophobic (Figure 3.3).

It was hypothesised that those with capsule that incorporate non-ulosonic acids and thus additional acidic residues, may show lower hydrophobicity to those than those without. Correlations between capsule charge and cell surface hydrophobicity were analysed statistically. Overall, strains possessing acidic K types incorporating non-ulosonic acid were less hydrophobic (25%) compared to the strains with neutral K types (64%) ($p = 0.002$; p-value < 0.05 is significant using the Student's t-test). Most of the K types incorporating non-ulosonic acid were hydrophilic, including, 04117201, RBH4 and D78, whereas only oneK type strain incorporating non-ulosonic acid were, ACICU, showed high levels of hydrophobicity (Figure 3.3). Previous studies suggested that many cell surface moieties play a role in *A. baumannii* hydrophobicity, including BAP and lipid A (Brossard and Campagnari, 2012, Zhang et al., 2017). The specific capsule type may still play a role in cell surface hydrophobicity of *A. baumannii*, but too few strains belonging to the same capsule type were assessed to draw any firm conclusions.

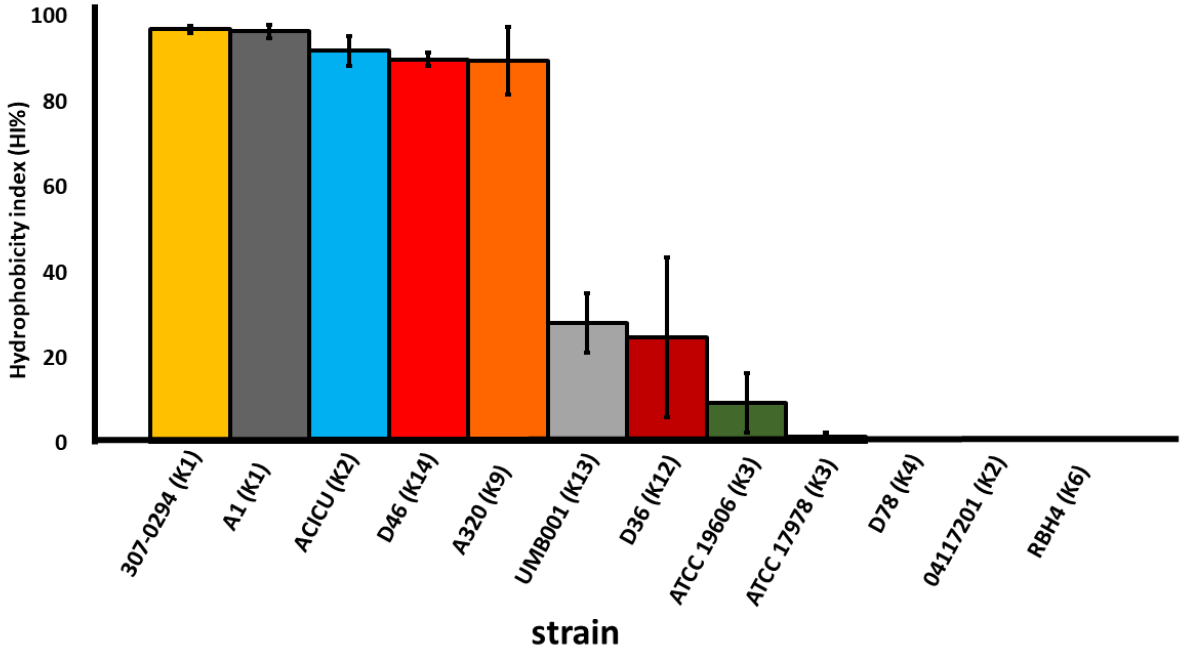

Figure 3.3. Cell surface hydrophobicity of *A. baumannii* clinical isolates. Cell surface hydrophobicity was determined by cellular affinity to xylene over an aqueous buffer and represented as a percentage. No visible bar indicates a completely hydrophilic strain. Each bar represents the average of three independent replicates. Error bars represent the standard deviation.

3.2.2 The response of *A. baumannii* clinical isolates to acidic stress

Tolerating fluctuations in pH is vital for bacterial adaption to changing environmental conditions. Increased environmental acidity can cause damage to the outer membrane and disrupt cytoplasmic pH homeostasis, leading to interference in the synthesis of cellular components, DNA damage, enzyme denaturation and ultimately cell death. Most studies assessing acid tolerance of virulent bacteria have focused on gastric pathogens such as *E. coli* and *Helicobacter pylori*, as passage through the highly acidic stomach is the primary route of infection (King et al., 2010, Valenzuela et al., 2011). During colonisation and infection, *A. baumannii* may encounter many low pH environments. For example, the phagolysosomes of macrophages contain acid to degrade invading pathogens, and transmission of *A. baumannii* via the hands of hospital staff (pH ~5.5) has been identified as the most important factor contributing to patient infection (Joly-Guillou, 2005, Luebberding et al., 2013).

Additionally, it has been hypothesised that bacteria with high pH tolerance, such as *A. baumannii*, may be aspirated from the stomach into the lung, which is a common route of respiratory infection in patients undergoing pulmonary ventilation (Cendrero et al., 1999). This is further supported by the reduction in stomach acidity seen in many Intensive Care Unit patients, which would allow for *A. baumannii* survival within the stomach (Cendrero et al., 1999). Lastly, although atypical, *Acinetobacter* has been identified as a causative agent for gastritis (Rathinavelu et al., 2003).

Despite this, little study has been conducted on acid tolerance in *A. baumannii*. Thus, the growth of twelve *A. baumannii* strains was compared at typical laboratory pH of 7.5 and under acidic stress at a pH of 5.5. This was assessed by incubation of the strains in MH media (pH 5.5 or 7.5), at 37^{o}C for 48 hours (Section 2.11.2). At pH 7.5, UMB001, ACICU, D78 and D46 lagged in growth compared the other strains tested (Figure 3.4). The strains which showed the fastest growth under these conditions were 04117201, ATCC 17978 and A320 (Figure 3.4).

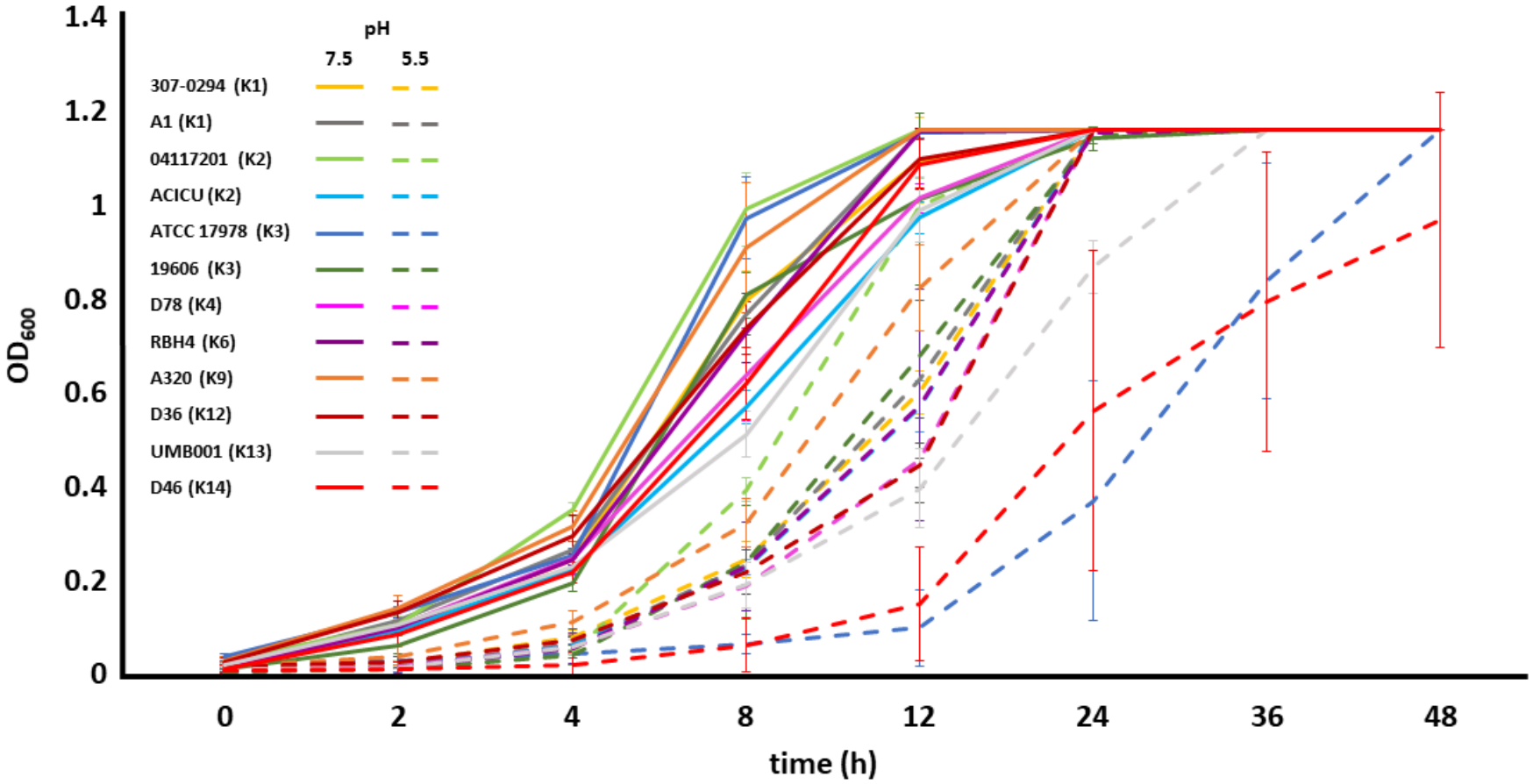
pH
7.5
5.5
307-0294 (K1)
A1 (K1)
04117201 (K2)
ACICU (K2)
ATCC 17978 (K3)
19606 (K3)
D78 (K4)
RBH4 (K6)
A320 (K9)
D36 (K12)
UMB001 (K13)
D46 (K14)
OD600
1.4
1.2
1
0.8
0.6
0.4
0.2
0
0
2
4
8
12
24
36
48
time (h)

Figure 3.4 Growth curve of *A. baumannii* strains at pH 7.5 and 5.5. Cultures were grown in MH medium at 37^{o}C shaking at 120 rpm. MH media was adjusted to a pH of 5.5 with acetic acid. Bold lines represent cultures grown at a pH of 7.5 (bold lines) and perforated lines a pH of 5.5 (perforated lines) by adjustment with acetic acid. Growth over 48 hrs was recorded as turbidity at OD_{600}. Data represent the average of three independent replicates, error bars represent the standard deviation. See the key to identify the different strains.

As growth rates at pH 7.5 varied considerably between the strains tested, the relative growth at pH 5.5 compared to pH 7.5 was determined as a percentage after 12 hours growth (Section 2.11.2, Figure 3.5).

Compared to growth at pH 7.5, a wider distribution of growth rates was seen between the *A. baumannii* strains under acidic stress (Figures 3.4 and 3.5). Two strains, D46 and ATCC 17978, displayed severe growth defects at pH 5.5, though the variability between replicates of these two strains was substantial (Figure 3.5). Reasons for the high variation between the replicates of D46 and ATCC 17978 under acid stress are unknown, but it can be postulated that this stressor may occasionally lead to mutations resulting in higher stress tolerance (Vandecraen et al., 2017). As growth of the various strains in pH 7.5 media was unequal, growth under acidic conditions could not be directly compared between strains.

Therefore, the growth of each strain under acidic conditions was compared to the growth of the same strain under optimal pH at a specific time point. For each strain, the OD_{600} after 12 hrs growth in acidic conditions was expressed as a percentage of optimal growth, i.e. growth at pH 7.5 was equal to 100%. The 12 hr time point was determined to be the best fit for comparison because most strains were actively growing under both tested conditions.

The *A. baumannii* strains D46 and ATCC 17978 had a low tolerance for a change in pH and increased acidic stress, 12 hrs incubation in medium at pH 5.5 cell density for these two strains were 14% and 9% of the growth in medium at pH 7.5, respectively (Figure 3.5). Some strains, including 04117201, A320 and ATCC 19606, showed high tolerance to acidity with 85%, 71% and 67% relative growth at pH 5.5 after 12 hrs compared to the pH 7.5 controls (Figure 3.5). After 12 hours, most strains grew at 50% (+/- 10%) in acidic conditions compared to that at pH 7.5 (Figure 3.5).

Multiple comparisons using a one-way ANOVA revealed only a few of the strains varied significantly in relative growth under acidic conditions after 12 hours (Section 2.23). High rates of variability were seen between replicates of the pH 5.5 growth curves, which likely contributes to the lack of statistically sound results and thus questions the reproducibility and validity of results obtained.

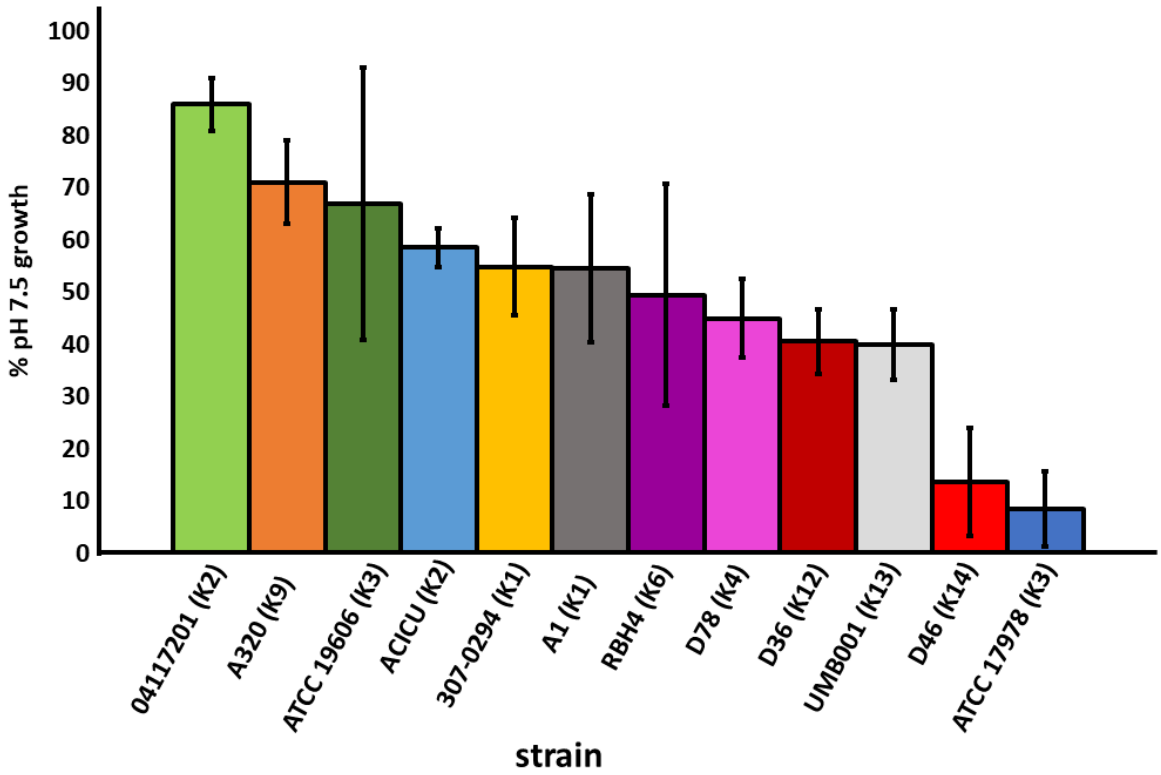

Figure 3.5. Growth of *A. baumannii* isolates under acid stress (pH 5.5) represented as a percentage of growth under optimal pH (pH 7.5). Cultures were grown in MH medium at 37^{o}C shaking at 120 rpm for 12 hrs. For acid stress, MH media was adjusted to a pH of 5.5 with acetic acid, for the control, pH was adjusted pH 7.5. Growth was measured by turbidity at OD_{600}. Percentage growth was calculated by (pH 5.5 OD_{600}/ pH 7.5 OD_{600}) *100. Data represents the average of three independent replicates, error bars represent the standard deviation.

Nonetheless, D46 showed significantly lower growth compared to 04117201 ($p = 0.005$), ATCC 19606 ($p = 0.03$), and A320 ($p = 0.05$). ATCC 17978 showed significantly lower growth compared to 04117201 ($p = 0.003$), ATCC 19606 ($p = 0.02$), and A320 ($p = 0.02$). Both K1 strains analysed, 307-0294 and A1, showed a similar relative growth under acid stress ($p = 1$) (Figure 3.5). No other correlations were identified for strains possessing the same K type, yet two strains with similar capsule structures, UMB001 (K13) and D36 (K12) displayed similar relative growth in acidic conditions ($p = 1$) (Figure 3.5). No correlation between resistance to low pH and incorporation of non-ulosonic acid within the capsule structure was found.

Previously, acid resistance in *A. baumannii* has only been investigated in the K3 strain ATCC 19606. A study by Peleg and colleagues (2012), identified that ATCC 19606 is more resistant to acid stress than other Acinetobacter species including *A. nosocomialis*, *A. pittii*, and *A. calcoaceticus*. This study also found higher rates of metabolism under pH stress in *A. baumannii* than the other *Acinetobacter* strains mentioned above (Peleg et al., 2012). In the current study, ATCC 19606 displayed high acid tolerance compared to other *A. baumannii* strains, supporting the findings of Peleg et al. The great variability in acid resistance between *A. baumannii* strains tested shows the need for caution when generalising the *A. baumannii* response to environmental stressors based on a single *A. baumannii* strain. (Figure 3.5).

3.2.3 Desiccation tolerance of *A. baumannii* isolates

Capsule production is an important factor in preventing desiccation of bacteria, allowing them to survive for extended periods of time in drying environments (Roberson and Firestone, 1992, Roberts, 1996, Ophir and Gutnick, 1994, Tipton et al., 2018, Chin et al., 2018) (Section 1.6.2). In this study desiccation tolerance was assessed over 30 days for eight *A. baumannii* isolates representing seven distinct capsule types (Figure 3.6) (Section 2.17.2). All *A. baumannii* strains remained viable over the 30-day incubation period, supporting previous evidence of the high desiccation tolerance seen for this pathogen (Gayoso et al., 2013, Jawad et al., 1998) (Figure 3.6).

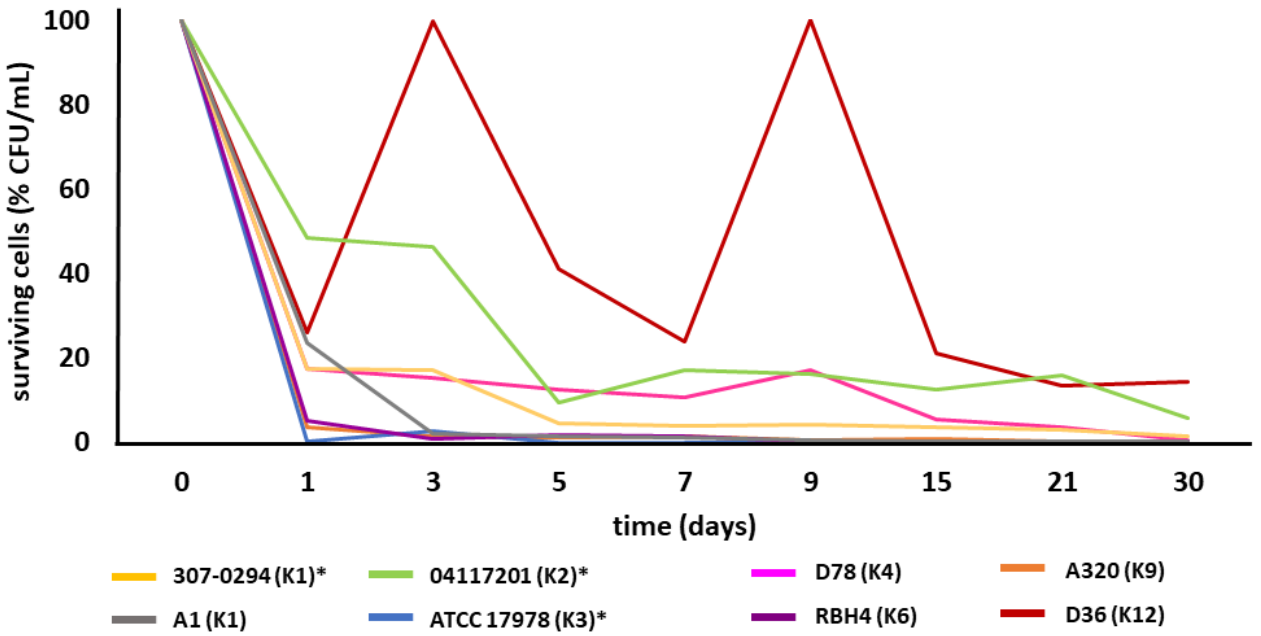

Figure 3.6 Desiccation tolerance of *A. baumannii* isolates. Strains were grown to an OD_{600} of 0.6 prior centrifugation to concentrate a pellet and resuspension in dH_2O and drying. Bacterial samples were rehydrated and enumerated at the given time points. Data are represented as the % CFU/mL of surviving cells compared to day 0. Data represent a single replicate except for three strains denoted by * in which assay was performed in duplicate (see Figure 3.7).

After 24 hours, the number of viable cells decreased to approximately 10% of the initial inoculum for RBH4 and A320, 0.01% for ATCC 17978, and between 20-45% for 04117201, D36, A1, and D78 (Figure 3.6). After this initial drop, the viability for most strains remained stable over the duration of the experiment. For some strains, including ATCC 17978, D36 and RBH4, increases in viability was seen for some time points (Figure 3.6). Because of the inconsistency between time points, a second biological replicate was only performed for three of the eight strains, 307-0294, 04117201, and ATCC 17978. Extreme variability was seen for all three strains between biological replicates (Figure 3.7).

Several factors may have influenced the inconsistencies seen in the desiccation experiment including phase variation within strain replicates (Tipton et al., 2018) (see Section 1.2.3) and the growth phase of the bacterial inoculum during the desiccation procedure (Zeidler and Müller, 2019b) (Figure 3.7, Section 2.16).

Contamination of the assays was considered as a potential source of variation between replicates but the uniform appearance of recovered colonies suggests this was not the case. One study suggests a 'bust or boom' strategy for *A. baumannii* survival under desiccating conditions whereby only a few remaining cells lay dormant until they encounter more favourable conditions (Gayoso et al., 2013). These persister cells show a range of differentially expressed proteins compared to growth in favourable conditions, thus unknown factors between replicates may account for some of the discrepancies in cell viability between time points.

After desiccation experiments were completed for this study, new methods for a potentially more robust desiccation assay in *A. baumannii* were published. Studies by Chin et al and Tipton et al established desiccation assays that involved smaller bacterial aliquots and a larger number of replicates, ultimately increasing the sample size and thus diluting outlier replicates that can confound results (Chin et al., 2018, Tipton et al., 2018). Given more time, using this method of increased replicates of smaller bacterial samples may have helped to elevate some of the reproducibility issues with desiccation assays (Chin et al., 2018, Tipton et al., 2018).

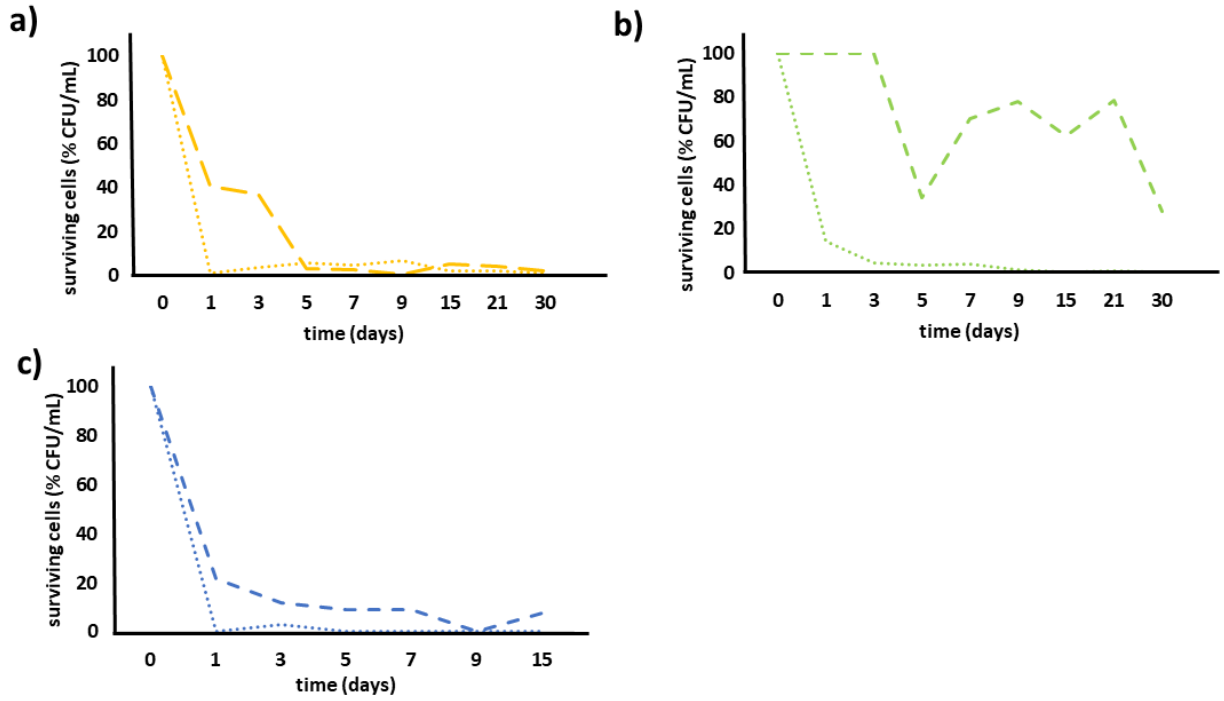

Figure 3.7 Variation between biological replicates of *A. baumannii* desiccation tolerance assays Strains were grown to an OD_{600} of 0.6 prior to centrifugation to concentrate a pellet, resuspension in dH_2O and drying. Bacterial samples were rehydrated at the given time points and surviving cells (CFU/mL) enumerated and represented as a percentage of day 0 survival. Perforated and dotted lines represent replicate 1 and 2, respectively. a) 307-0294 (yellow), b) 04117201 (green), c) ATCC 17978 (blue).

3.2.4 Resistance to human lysozyme

The antimicrobial protein lysozyme plays an important role in the innate immune response against bacterial pathogens (Section 1.8). A recent study found acapsular variants of the *A. baumannii* strain AB5075 to be more susceptible to lysozyme killing than the encapsulated parental strain (Tipton et al., 2018). None-the-less, no studies have assessed a panel of *A. baumannii* strains for lysozyme resistance. Resistance to lysozyme was determined for twelve *A. baumannii* strains by incubating the bacteria in 1 mg/mL human lysozyme for one hour (Section 2.15) before plating and enumerating.

The total viable count (CFU/ mL) was determined for the initial inoculate and bacterial samples with/ without the addition of 1 mg/mL human lysozyme (Section 2.15). The viability of all isolates decreased by at least 10-fold after lysozyme treatment, though levels of resistance varied greatly between isolates (Figure 3.8). The highest level of resistance was seen for ATCC 17978 followed by 04117201 and RBH4, with 2.8 X 10^5, 4.2 X 10^4, and 4.2 X 10^4 CFU/mL recovered, respectively. Two strains, D46 and D36 showed drastically lower resistance to lysozyme compared to the other *A. baumannii* strains (Figure 3.8). Although differences were seen in lysozyme resistance of the various strains only ATCC 17978 was significantly higher than most (8/11, $p = < 0.05$). Furthermore, D36 and D46 were the only strains significantly less lysozyme resistant than most of the others strains (7/10, $p = < 0.05$). No correlation between capsule type or capsule charge and lysozyme resistance was identified ($p = 0.01$).

3.2.1 Serum resistance of *A. baumannii* isolates

Complete sensitivity to lysis by complement proteins found in serum has been well documented in acapsular variants of *A. baumannii* (Russo et al., 2010) (Section 1.8.2). Therefore, in this study serum resistance was determined for a panel of *A. baumannii* strains to assess variation in serum resistance for a range of K types. The serum resistance of ten *A. baumannii* strains in 40% human serum over a two-hour incubation period was determined (Section 2.14). This was compared to survival in a heat-inactivated serum control to eliminate differences seen in growth rates between the strains, and demonstrate that active complement is required for bactericidal action (Kim et al., 2009) (Figure 3.9).

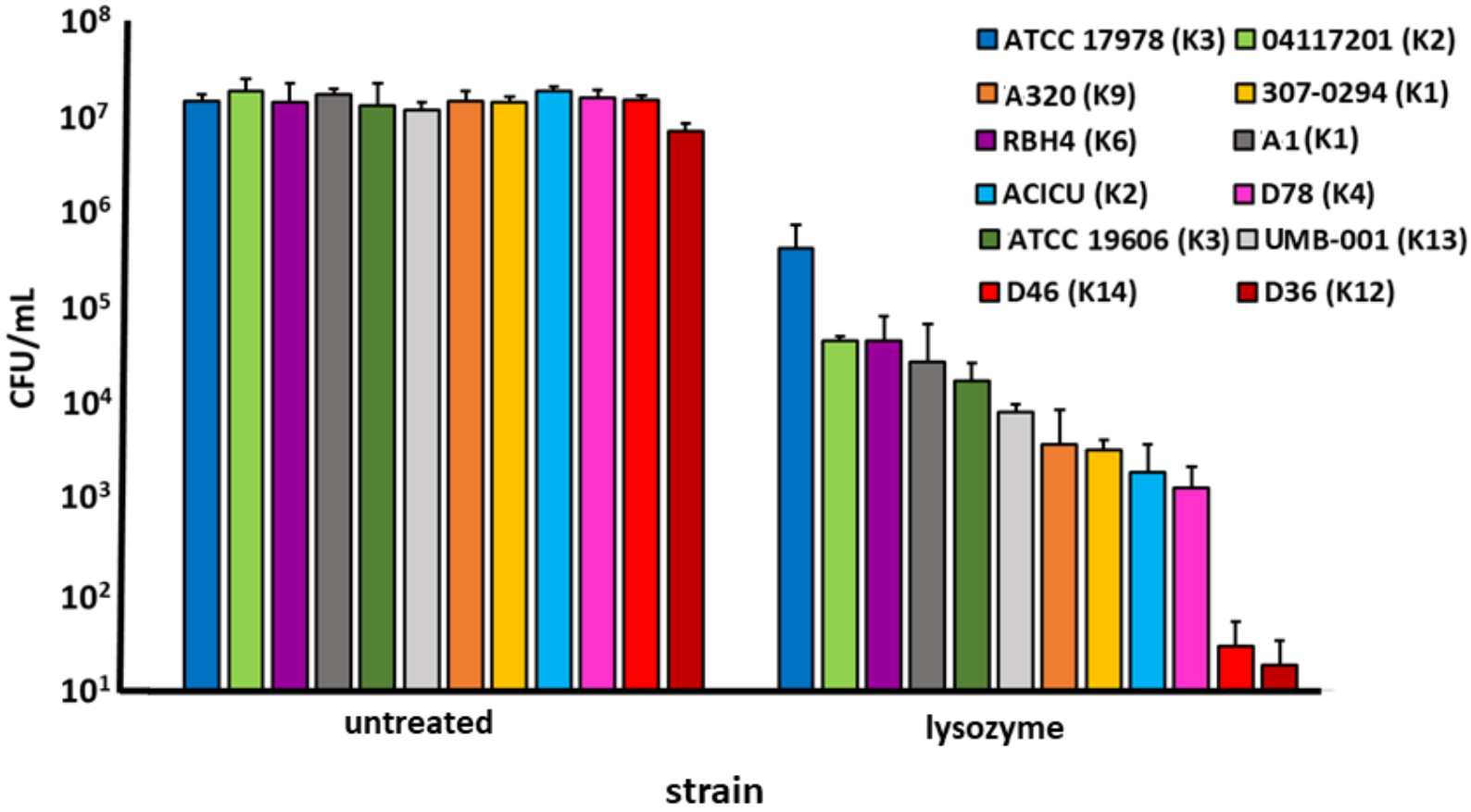
10^8
10^7
10^6
10^5
10^4
10^3
10^2
10^1
CFU/mL
ATCC 17978 (K3)
04117201 (K2)
A320 (K9)
307-0294 (K1)
RBH4 (K6)
A1 (K1)
ACICU (K2)
D78 (K4)
ATCC 19606 (K3)
UMB-001 (K13)
D46 (K14)
D36 (K12)
untreated
lysozyme
strain

Figure 3.8 Resistance of *A. baumannii* isolates to human lysozyme. Bacterial strains were grown to an OD_{600} of 0.6 before treatment with 1 mg/mL human lysozyme at 37^{o}C with gentle shaking for 2 hr. Serial dilutions of bacterial samples were then plated on LB agar, incubated ON at 37^{o}C and enumerated. Untreated controls are represented to show differences in growth rates between strains in the absence of lysozyme. Data represent the average of three independent replicates. Error bars represent the standard deviation.

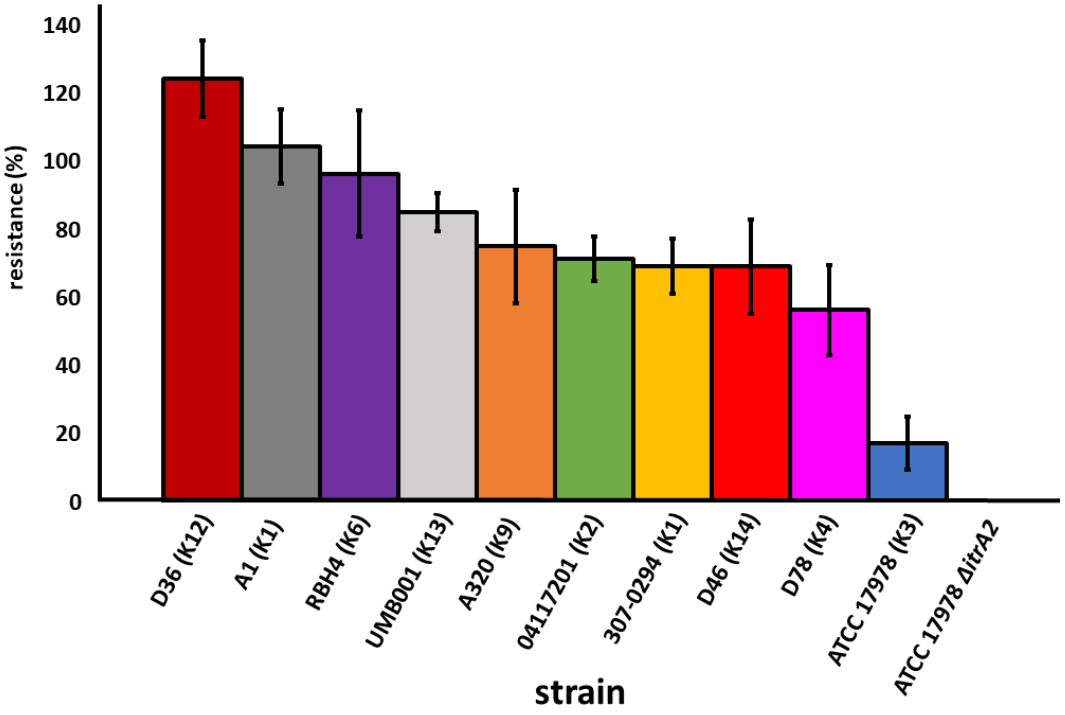

Figure 3.9. Resistance of *A. baumannii* isolates to serum complement. Bacterial strains were grown to an OD_{600} of 0.6 and incubated with 40% human serum at 37ºC slowly shaking for 2 hr. Resistance is given as a percentage of recovered cells compared to the inactivated control. Data represent the average of three independent replicates. Error bars represent the standard deviation.

During this study, the bactericidal activity of human serum was found to be extremely heat labile. Even when stored at -20^{o}C or -80^{o}C in single use aliquots, serum would show reduced bactericidal activity after one-month storage. To further preserve complement activity the serum was stored aliquoted at -150^{o}C. Because of this, a positive control strain, ATCC 17978Δ*itrA2* (Table 2.1), a generated acapsular derivative (see Section 4.2.5.2) that exhibits 100% sensitivity to 40% human serum was used as a control during this study (Figure 3.9). For each serum assay, a neat sample of ATCC 17978Δ*itrA2* was plated on LB agar and no viable colonies were recovered (Figure 3.9).

All strains showed significantly higher resistance to serum than the ATCC 17978Δ*itrA2* control ($p < 0.001$). A range of resistance levels was seen between the *A. baumannii* isolates tested, with two strains, D36 and A1, showing complete resistance to 40% human serum (Figure 3.9). A third strain, RBH4, showed near complete resistance with an average survival of 96% compared to the inactivated serum control (Figure 3.9). The K3 strain ATCC 17978 showed the lowest level of resistance to serum with only 17% survival. All other strains showed resistance levels > 50%, demonstrating the overall high resistance of capsulated *A. baumannii* to human complement (Figure 3.9).

No significant correlations were identified between capsule type or charge and the ability of the strain to resist complement killing ($P = 0.1$). The results of this study correspond with a previous study which found 12/15 *A. baumannii* strains tested to be highly resistant to human serum (Sanchez-Larrayoz et al., 2017). Although capsule is a major factor involved in resistance to human serum, a number of other cell components are thought to be involved serum resistance including; membrane lipids (Sanchez-Larrayoz et al., 2017), signal transduction proteins (Liou et al., 2014), and PKF (King et al., 2013).

3.3 Conclusions

In this chapter, twelve *A. baumannii* clinical isolates, and in particular a subset, representing nine distinct capsular types, were assessed for cell surface hydrophobicity, response to acidic stress, desiccation tolerance, resistance to human lysozyme and survival in human complement. A summary of the capsule types and observations collected on the *A. baumannii* strains are summarised in Table 3.1. A significant correlation was identified between cell surface hydrophobicity and the incorporation of

non-ulosonic acid (Section 3.2.2) but no correlations were identified between capsule type and resistance to any of the stressors tested (Table 3.1). For example, the K1 strain 307-0294 showed intermediate levels of resistance to all stressors whereas the K1 strain A1 showed high levels of resistance to both human lysozyme and serum (Table 3.1). Furthermore, these data suggest the ability of an *A. baumannii* strain to resist a given stress does not increase its ability to resist other stressors likely to be encountered. For example, the *A. baumannii* strain ATCC 17978 (K3) showed high levels of resistance to lysozyme but low resistance to acid stress and human serum compared to other strains. Despite this, the data presented highlight the extreme phenotypic variability seen between *A. baumannii* isolates when encountering various stressors. Importantly, this is the first study to our knowledge which compares acid tolerance and resistance to human lysozyme in a range of *A. baumannii* strains.

Importantly, the amount of capsule produced by each strain was not assessed and this may contribute greatly to a given strains ability to withstand various stressors. In hindsight, assessing the quantity of capsule produced by each strain in conjunction with comparison of capsule types would provide additional insight into the results gained. Regulation of capsule production, irrespective of capsule type, undoubtedly plays a role in *A. baumannii* survival under environmental stressors. For example, phase variation and regulation by two component systems influence capsule production and responses to various stressors (Section 1.9) (Geisinger et al., 2018, Geisinger and Isberg, 2015, Tipton and Rather, 2017, Tipton et al., 2015).

A limitation of this study was the low number of stains assessed; thus it is difficult to draw firm conclusions based on only twelve strains. Furthermore, only three of the capsule types were represented by more than one strain. Comparing a larger range of isolates with multiple strains representing each capsule type would provide a better basis for correlating virulence attributes with a given capsular type. However, increasing the number of strains analysed may not fully compensate for the multifactorial nature of phenotypic variation, regardless of the role different capsule types may play.

Table 3.1 CPS type and virulence determinants of *A. baumannii*

Strain	K type	non-ulosonic acid	Cell surface hydrophobicity[a,b]	Acid stress tolerance[a,c,f]	Lysozyme resistance[a,d]	Serum resistance[a,e]
307-0294	1	no	+++	+	+	+
A1	1	no	+++	+	+++	+++
04117201	2	yes	-	+++	+++	+++
ACICU	2	yes	+++	+	+	n.d.
ATCC 17978	3	no	-	-	+++	-
ATCC 19606	3	no	-	+++	+++	n.d.
D78	4	no	-	+	+	+
RBH4	6	yes	-	+	+++	+++
A320	9	no	+++	+++	+	+++
D36	12	yes	-	+	-	+++
UMB-001	13	yes	-	+	+	+++
D46	14	no	+++	-	-	+

[a] high (+++), intermediate (+), low (-), not done (n.d.)

[b] high >70%, intermediate 30-70%, low <30%

[c] high >60%, intermediate 30-60%, low <30%

[d] high >10^4 CFU/ml, intermediate >10^3 CFU/ml, low <10^3 CFU/ml;

[e] high >70%, intermediate 30-70%, low <30%.

[f] acid stress determined as growth under acidic conditions (pH 5.5) compared to normal conditions (pH 7.5) after twelve hours incubation.

Additionally, due to the ever increasing number of identified capsule types for *A. baumannii* isolates, it may not be feasible to determine the role of capsule type in virulence by comparing clinical strains (Hu et al., 2013, Kenyon and Hall, 2013, Singh et al., 2018) (Section 1.5.3). Alternatives to this strategy include constructing capsule gene deletion mutants within a given *A. baumannii* strain and/or generating a panel of isogenic mutants expressing a variety of capsular types. Chapter four outlines the generation and analysis of acapsular variants in two of the *A. baumannii* strains assessed, 04117201 (K2) and ATCC 17978 (K3). This chapter will also discuss techniques to construct capsule-swapped mutants in *A. baumannii* ATCC 17978 and 04117201.

4 MANIPULATION OF GENES WITHIN THE CAPSULE LOCI OF *A. BAUMANNII* ATCC 17978 AND 04117201

4.1 Introduction

The ability to manipulate bacterial genomes is essential for advancing our understanding of infectious diseases. Historically, genetic manipulation of *A. baumannii* has been difficult, as limited molecular tools have been available compared to those for other pathogenic bacterial species (Tucker et al., 2014, Muyrers et al., 2001). Genetic manipulation of *A. baumannii* is further complicated by the high levels of antimicrobial resistance seen in clinical isolates which limits the availability of suitable resistance markers available for use as selection markers when modifying the genome (WHO, 2014).

A close relative to *A. baumannii*, *A. baylyi* has previously been used as a model organism for genetic manipulation, as it is naturally transformable and can express a wide variety of foreign genes (Palmen and Hellingwerf, 1997, Barbe et al., 2004, Metzgar et al., 2004, Young et al., 2005) . Despite these advantages, *A. baylyi* is a poor representative for *A. baumannii* virulence as it is non-pathogenic. Accordingly, efforts have been made to develop and improve upon tools available to manipulate *A. baumannii*. Over the last decade, many advancements in genetic manipulation of *A. baumannii* have occurred including the development of transposon mutant banks (Smith et al., 2007, Gallagher et al., 2015) and application of various recombination strategies such as double cross-over recombination (Choi et al., 2009, Aranda et al., 2010), marker-less recombination (Amin et al., 2013), and genetic recombineering (Tucker et al., 2014). These genetic tools have revolutionised the study of *A. baumannii* pathogenesis, though the application of such tools in the study of many virulence factors, including capsular polysaccharides, remain in its infancy.

Previous studies investigating the role of capsule in the virulence of *A. baumannii* have involved the removal or interruption of specific genes or entire regions within the K loci (Russo et al., 2010, Geisinger and Isberg, 2015, Tipton et al., 2018). In the *A. baumannii* strain ATCC 17978 single gene deletion mutants have previously been

constructed for *wza*, *wzc*, *itrA*, *galU* and the gene region spanning from *wzc* to *galU* (Geisinger and Isberg, 2015, Iwashkiw et al., 2012), all producing acapsular variants (Figure 3.1). However, a limitation of studying capsule deficient mutants such as these is that the influence of a specific capsule type on *A. baumannii* pathogenesis cannot be distinguished.

Using capsule-swapped mutants is the gold standard in assessing the role of a specific capsule type in virulence as it eliminates differences between strains based on non-capsule related mechanisms. Capsule-swapped mutants are derivatives that have been constructed where only the genetic region encoding the capsule is replaced by a capsule-encoding region from another strain, producing isogeneic variants that only differ in their CPS region. Differing levels of homology exist between the variable regions of capsule loci of *A. baumannii* strains, (Kenyon and Hall, 2013) (Figure 1.2). In some instances, this reflects similarities of sugar moieties used in capsule structures. Therefore, depending on which strains are selected for capsule-swap experiments, the requirements for knock-out/knock-in gene regions swapped are strain specific (Section 1.5.3). Several capsule swapping studies have been performed on *S. pneumoniae* and *K. pneumoniae* (Kabha et al., 1995, Hyams et al., 2010), but similar studies have not been undertaken in *A. baumannii*. Although in some species, such as *S. pneumoniae*, certain capsular types have been highly correlated to virulence potential, there seems to be little correlation in other bacteria. Thus, generation of capsule-swapped variants would provide a valuable foundation for investigating the role of specific capsule types in *A. baumannii* pathogenesis.

This chapter outlines the generation, confirmation, and growth characteristics of capsule deficient mutants in two *A. baumannii* strains; 04117201 (KL2) and ATCC 17978 (KL3). Also described are attempts to identify and clone appropriate resistance markers for genetic manipulation of the multidrug resistant 04117201 strain and generate capsule-swapped variants of 04117201 and ATCC 17978.

4.2 Results and discussion

4.2.1 Identification of K loci in *A. baumannii* strains 04117201 and ATCC 17978

Two *A. baumannii* strains 04117201 (KL2) and ATCC 17978 (KL3) were selected for

genetic manipulation as they are both fully sequenced, possess different capsular types, and vary in their disease potential based on *in vitro* virulence assays (Section 3.2). Access to the genome sequence of 04117201 strain was kindly provided by R. Hall and K. Holt via the online server RAST (Section 2.8) (Overbeek et al., 2013). The genome sequence for ATCC 17978 was obtained from NCBI (Accession number CP053098.1) (Section 2.8). The K loci of ATCC 17978 was found using Blastn to identify the conserved genes, *fkpA* and *lldP*, which flank all known K loci in *A. baumannii* (Section 2.8) (Figure 4.1) (Altschul et al., 1990, Kenyon and Hall, 2013).

The K loci of 04117201 was determined by locating the genes between *fkpA* and *lldP* genes in the RAST server. Annotated open reading frames (ORFs) were confirmed using SnapGene™ (Section 2.8), and gene names allocated by comparison to previously determined KL2 and KL3 regions (Pruitt et al., 2006, Kenyon and Hall, 2013) (Figure 4.1). The genetic organisation of the ATCC 17978 K loci has previously been described (Kenyon and Hall, 2013). Prior to genetic manipulation, the ATCC 17978 strain in our collection was screened for the presence of the pAB04-1 multidrug resistance plasmid, as the loss of this plasmid is known to effect virulence in this strain and its loss would skew any results obtained (Weber et al., 2015) (Section 2.3.2, Table 2.4, Appendix 1). PCR amplification of the Node 182 region, of the plasmid was amplified with Node_182 F and R primers (Table 2.6) and yielded a product approximately 500 bp in ATCC 17978, this was absent in 04117201 (data not shown). Thus ATCC 17978 possesses the pAB04-1 plasmid but 04117201 does not. Once the K loci of 04117201 and ATCC 17978 were identified these regions were used as a template to construct various capsule mutants. The next section will focus on the generation of a *wzy* deletion in 04117201.

4.2.1 Generation of 04117201Δ*wzy* by homologous recombination

The *wzy* gene of *A. baumannii* 04117201 was removed using the homologous recombination method outlined in Section 2.5.2. The *wzy* gene was selected as the target for gene deletion as it encodes a protein essential for capsule production but is not required for protein glycosylation (Section 1.5.1).

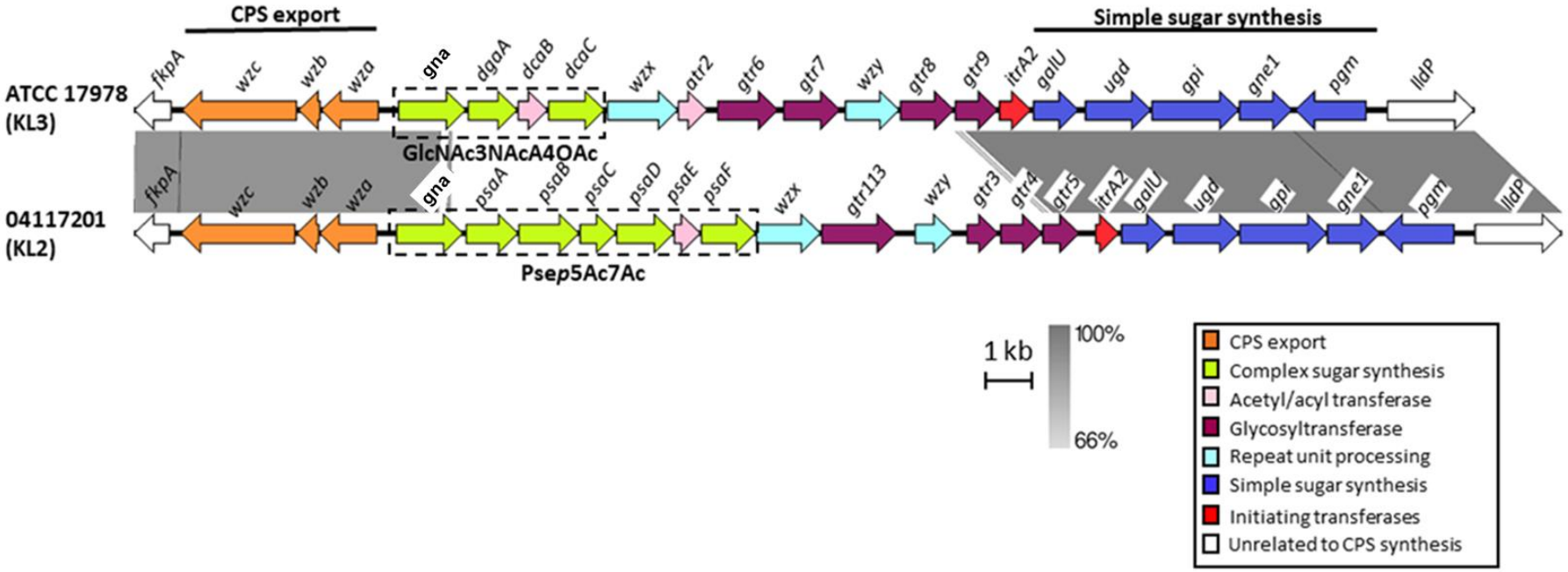

Figure 4.1 Comparison of ATCC 17978 (KL3) and 04117201 (KL2) CPS biosynthesis gene clusters. Nucleotide sequences representing KL3 and KL2 different KL regions were obtained from the NCBI database and aligned using the Easyfig 2.2.2 tool (Sullivan et al., 2011). Genes are depicted by arrows and indicate direction of transcription. Gene names are denoted above the corresponding arrows. Colour scheme is based on homology to the putative function of gene products and are outlined in the key. Nucleotide sequence homology shared between regions is represented by the grey gradient between the K loci. Figure is drawn to scale.

Briefly, regions flanking *wzy* in the 04117201 chromosome were amplified using N_wzy_UFR and N_wzy_DFR primer pairs (Table 2.6). Primers were designed to non-coding regions to minimise potential knock on effects on non-targeted genes (Figure 4.2a). Subsequent PCR products were then digested and ligated into the *A. baumannii* shuttle vector pEX18Tc (Table 2.3, Figure 4.2b, Sections 2.4.6 and 2.4.7). An *ery*^{R} cartridge was amplified from using the PVA plasmid as a template (Table 2.3) and Ery_Xho_F and Ery_Xho_R primers (Table 2.6). This cartridge was then cloned between the flanking regions to aid in the selection of mutants (Figure 4.2b, Section 2.4.6 and 2.4.7). The resulting plasmid, pEX_04117201_*wzy*, was electroporated into *A. baumannii* 04117201 cells and colonies selected on Ery12 plates (Section 2.5.2).

The pEX18Tc plasmid contains a *sacB* gene (Table 2.3), which makes the expression of this plasmid lethal when cells are grown in the presence of sucrose. Therefore, the loss of the pEX18Tc shuttle vector was selected for by serial plating *ery*^{R} 04117201 colonies onto medium containing 10% sucrose and Ery10. After three successive sucrose treatments, colony PCR (Section 2.4.2.3) with primers designed outside of the flanking regions, N_*wzy*_check_F and N_*wzy*_check_R (Table 2.6), revealed one isolate with the *ery*^{R} replacing *wzy* in the chromosome. This strain was denoted 04117201Δ*wzy* (Table 2.1). The PCR reaction was repeated using extracted chromosomal DNA (Section 2.4.2.1) and resulting product sequenced and compared to the WT sequence using Sequencher™ 4.9 (Section 2.8, Figure 4.2c), confirming the gene replacement.

4.2.1 Verification of capsule synthesis disruption in 04117201Δ*wzy*

To confirm that the removal of *wzy* results in loss of capsule, a phenol sulphuric acid assay was used to determine the quantity of surface polysaccharide for the *A. baumannii* 04117201 parent and its acapsular variant (04117201Δ*wzy*) (Section 2.7.8). The phenol sulphuric acid assay was employed as it is a quick and simple method which can determine the concentration of a range of carbohydrates based on absorbance at 490 nm (Nielsen, 2010, Cuesta et al., 2003). Although this method was unable to verify the presence or absence of capsule *per se*, it indicated that the parental 04117201 possesses approximately twice the amount of surface polysaccharide as the 04117201Δ*wzy* variant (Figure 4.3a).

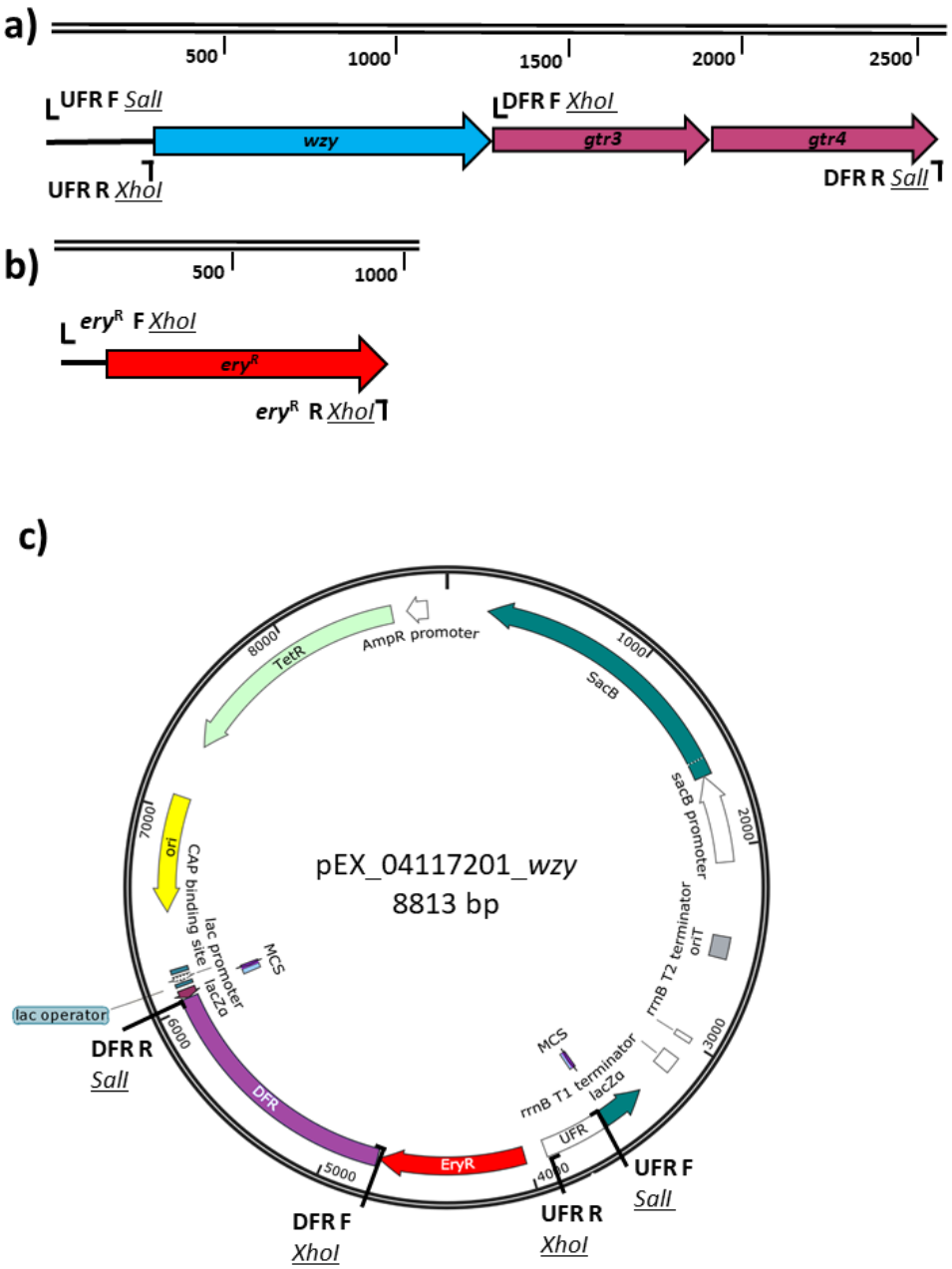
a)
500
1000
1500
2000
2500
UFR F SalI
wzy
DFR F XhoI
gtr3
gtr4
UFR R XhoI
DFR R SalI
b)
500
1000
eryR F XhoI
eryR
eryR R XhoI
c)
pEX_04117201_wzy
8813 bp
AmpR promoter
TetR
SacB
sacB promoter
rrnB T2 terminator
oriT
ori
CAP binding site
lac promoter
lacZα
MCS
lac operator
DFR
EryR
rrnB T1 terminator
UFR
DFR R SalI
DFR F XhoI
UFR R XhoI
UFR F SalI
d)
500
1000
1500
2000
2500
eryR
gtr3
gtr4

Figure 4.2 Cloning strategy for removal of the *wzy* gene from *A. baumannii* 04117201. Sequences were obtained from the RAST server and analysed using SnapGene™. Genes are represented by arrows and indicate the length (bp) and direction of gene transcription. Gene names/locus tags are denoted within the arrows. Scale above linear DNA represents size (bp). Solid black lines represent non-coding regions. Location of primers used for amplification are represented by solid black corner symbols (⌜ or ⌟); incorporated restriction sites are underlined. N_wzy_UFR_F *SalI* (UFR F), N_wzy_UFR_R *XhoI* (UFR R), N_wzy_DFR_F *XhoI* (DFR F), and N_wzy_DFR_R *SalI* (DFR R), Ery_F_Xho *XhoI*, Ery_R_Xho *XhoI*. a) chromosomal *wzy* gene region indicating location of primers for the upstream and downstream flanking regions, b) *ery*^{R} cartridge amplified from the PVA819 plasmid (Table 2.3) c) pEX18Tc vector harbouring *wzy* flanking regions and *ery*^{R} (pEX_04117201_*wzy*), d) location of *wzy* replaced in the 04117201 chromosome with *ery*^{R} (04117201Δ*wzy*). Figures are drawn to scale.

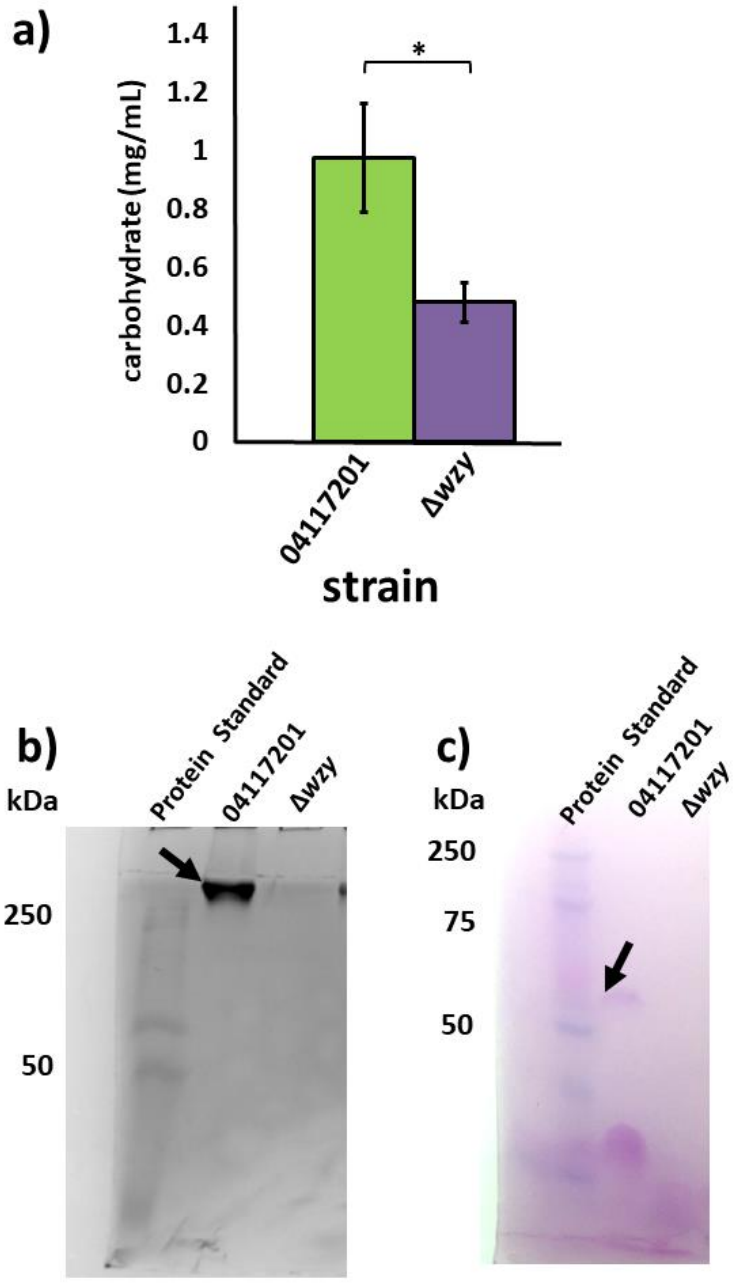

Figure 4.3. Surface polysaccharide analysis of 04117201 and 04117201Δ*wzy*.

a) Phenol sulphuric acid quantification of surface polysaccharides. Data represent assays performed in triplicate; error bars represent the standard deviation. Statistical significance was assessed using the two-tailed student T-Test (*= p value <0.05) b) Alcian blue stain of extracted capsular polysaccharide run on a 20% polyacrylamide gel. Arrow indicates stained capsular polysaccharide (c) PAS stain of extracted membrane fractions run on a 12.5% polyacrylamide gel. Arrow indicates band of stained glycosylated protein A Precision Plus Protein™ Standard (Stained) (Bio-Rad) was used for size determination of capsule and protein bands.

A more robust method of determining capsule presence is by staining with Alcian blue, a cationic dye which stains polysaccharide capsule which can then be visualised as a band of high molecular weight on a polyacrylamide gel (Section 2.9.6). This method has previously been successfully used to identify capsule deficient *A. baumannii* mutants (Lees-Miller et al., 2013, Geisinger and Isberg, 2015, Tipton et al., 2018). Alcian blue stains of purified capsular fractions verified the presence and absence of capsule production of the 04117201 parental and Δ*wzy* strains, respectively (Figure 4.3b, Section 2.9.6).

A PAS stain, which selectively stains only glycosylated proteins, was performed on the membrane fractions of 04117201 and 04117201Δ*wzy* to test whether deletion of *wzy* inadvertently influences glycosylation of membrane proteins (Section 1.4.2, Section 2.9.7). As previously described, capsule synthesis is part of a branched pathway with protein glycosylation, and thus shares certain synthesis machinery (Section 1.4.2). Previous studies in other bacterial species have shown that removing certain capsule genes can lead to secondary non-target mutations which influence protein glycosylation (Xayarath and Yother, 2007). The *wzy* gene is involved only in capsule production and not protein glycosylation (Figure 1.1); therefore, a PAS strain of the *wzy* mutant membrane fraction should resemble that of the WT. A band representing protein glycosylation was seen on the PAS stain for the WT 04117201 but not the Δ*wzy*, demonstrating that the 04117201Δ*wzy* has interrupted protein glycosylation (Figure 4.3c). This may indicate the presence of a secondary mutation affecting function of the protein glycosylation pathway in Δ*wzy* (Section 1.5.1, 1.4.2). Previously, secondary non-target mutations supressing protein glycosylation have been identified in the initial transferase gene of acapsular mutants in some bacterial species (Xayarath and Yother, 2007, Burrows and Lam, 1999). To see if a secondary mutation had occurred in the initial transferase gene of 04117201Δ*wzy*, the *itrA2* gene was amplified using the N_itr primer pair (Table 2.6). The resulting PCR product was sequenced and compared to the known sequence of the *itrA2* gene of the WT 04117201 (Section 2.7). No mutations were identified in the *itrA2* sequence of 04117201Δ*wzy* and further genetic analysis of this strain was not undertaken due to time constraints. Instead efforts focused on attempts to complement *A. baumannii* 04117201Δ*wzy* with a clone of the whole capsular region, as this construct would then serve the dual function of restoring capsular in both the 04117201Δ*wzy* derivative and form a basis for a capsule swap into

ATCC 17978 (Section 4.2.7).

Complementation experiments are essential to confirm results obtained are due to targeted gene deletions. For instance, the WT *wzy* gene may be re-introduced into the 04117201Δ*wzy* variant on a plasmid. To select for transformed colonies a suitable resistance marker needs to be incorporated into the plasmid alongside the WT *wzy* gene. The next section outlines attempts made to identify and clone two resistance genes, for tellurite and amikacin resistance, to use in 04117201 complementation experiments.

4.2.2 Identification and attempts to clone resistance markers to aid complementation of 04117201Δ*wzy*

To evaluate the results of gene deletion mutations on *A. baumannii* phenotypes it is prudent to reintroduce the gene/s of interest into the mutant strain. This is to ascertain that any differences observed in the mutant can be attributed solely to the introduced mutation. Complementation experiments of *A. baumannii* mutants are typically performed by expressing the WT gene/s on a shuttle vector such as pWH1266 (Table 2.3) (Moffatt et al., 2010, Hunger et al., 1990, Smani et al., 2013). Isolates transformed with pWH1266 containing the WT gene/s of interest are primarily selected for using an antibiotic resistance marker. Although pWH1266 harbours both amp^R and tet^R resistance genes, an alternative resistance cassette may be required for selection in highly drug resistant strains (Srinivasan et al., 2015). *A. baumannii* 04117201 is resistant to many commonly used antibiotics employed in selection including kanamycin, tetracycline, ampicillin, and gentamicin. Therefore, identification and trial of alternative resistance markers was necessary to attempt complementation of 04117201Δ*wzy* (Table 2.1).

The toxic compound potassium tellurite has previously been used as a selection marker for multidrug resistant *P. aeruginosa* and *A. baumannii* (Amin et al., 2013, Sanchez-Romero et al., 1998). A colleague, S. Giles, had previously determined *A. baumannii* 04117201 showed sensitivity to tellurite (Personal Communication). Therefore, attempts to clone tellurite resistance markers (tel^R) into plasmid constructs was undertaken (Figure 4.4).

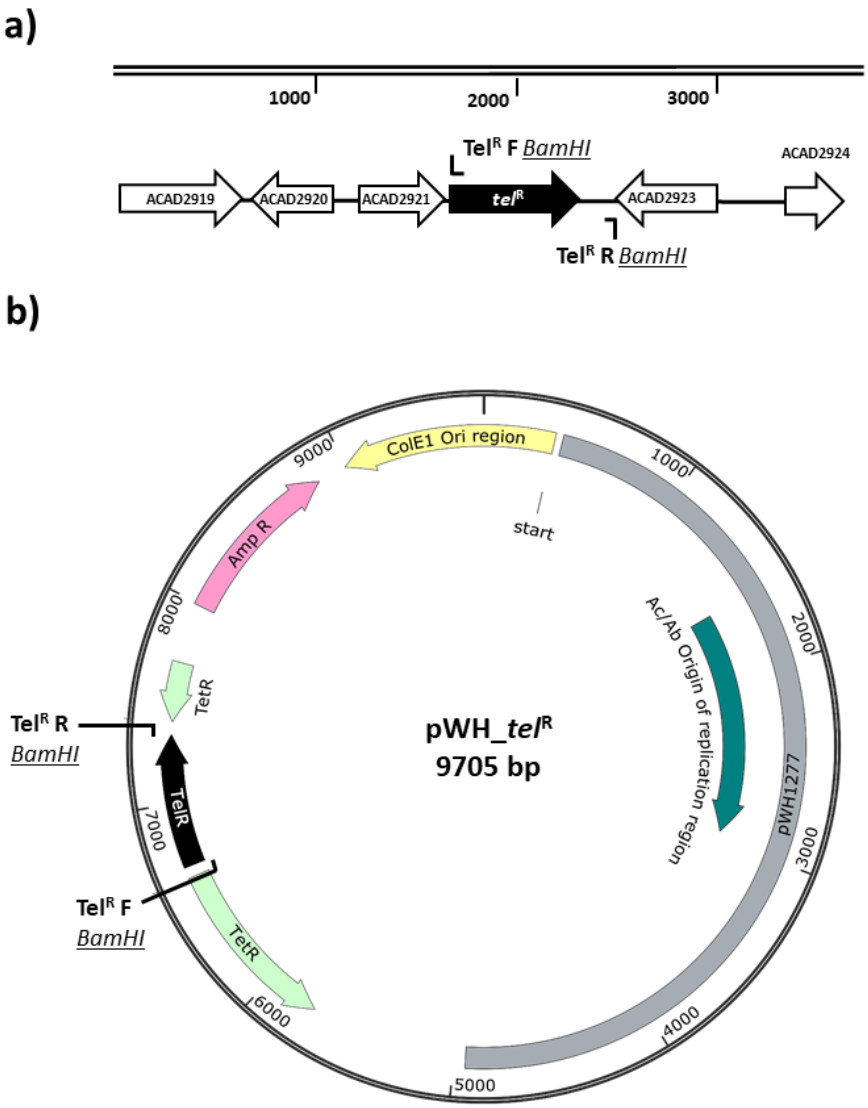

Figure 4.4 Identification and cloning of tellurite resistance gene from *A. baylyi* ADP1 into pWH1266. Sequences were obtained from the NCBI database and analysed using SnapGene™. Genes are represented by arrows and indicate the length (bp) and direction of gene transcription. Gene names/locus tags are denoted within the arrows. Solid black lines represent non-coding regions. The *tel*^{R} genes are represented by a black arrow, surrounding genes represented by white arrows. Location of primers used for amplification are represented by a solid black corner symbols (⌝ or ⌟), Tel^R F and Tel^R_R represent TelR_BamHI_F and TelR_BamHI_R primers, respectively. a) Region of *A. baylyi* ADP 1 harbouring *tel*^{R}, White arrows upstream from *tel*^{R} represent a putative transcriptional regulator, putative membrane protein and a hypothetical protein. White arrows downstream from *tel*^{R} represent hypothetical proteins (Altschul et al., 1990). The scale above linear DNA represent size (bp). b) Plasmid construct containing the *tel*^{R} gene cloned into *tetR* of pWH1266 to produce pWH1266 (pW_*tel*^{R}).

The *tel*^{R} gene (locus tag ACIAD2922), encoding a thiopurine methyltransferase was identified using KEGG (Section 2.8) was amplified from *A. baylyi* strain ADP1 chromosomal DNA using the TelR_BamHI primer pair (Table 2.6) and cloned into *BamH*I restricted pWH1266 (Section 2.4, Table 2.3, Figure 4.4). The resulting construct (pWH1266_*tel*^{R}) was then electroporated into 04117201Δ*wzy* cells and tellurite resistant isolates were selected by plating the electroporated cells onto LB agar plates containing 30 µg/mL tellurite (Section 2.5.2). Only approximately 10% of tellurite resistant isolates harboured pWH1266_*tel*^{R} when screened for using the TelR_BamHI primer pair (data not shown). Furthermore, upon re-isolation of pWH1266_*tel*^{R} containing isolates the plasmid was lost from the bacteria. Because of the instability of the pWH1266_*tel*^{R} plasmid, a different compound, amikacin, was investigated for potential use as a resistance marker for use in 04117201 mutants.

The aminoglycoside amikacin is one of the few compounds to which 04117201 displays sensitivity. Many other *A. baumannii* isolates display amikacin resistance via expression of the *aac(6')-Ib* or *aphA6* amikacin resistance genes (Lopez et al., 2015, Hamidian and Hall, 2013). These genes are widely distributed amongst *A. baumannii* and may be encoded on the chromosome or mobile genetic elements including plasmids and transposons (Lopez et al., 2015, Nigro and Hall, 2014, Nigro et al., 2014). The *aphA6* gene, encoding an aminoglycoside 3'-phosphotransferase from a conjugative plasmid in ACICU (pACICU2) was investigated as a potential resistance marker (Table 2.3) (Hamidian and Hall, 2013). Thus, the *aphA6* gene was amplified from pACICU2 using the AmkR_F and AmkR_R primer pair and attempts were made to clone the PCR product containing *aphA6* into pWH1266 (Figure 4.5, Table 2.6, Section 2.4). After several failed attempts to obtain the desired construct (pWH1266_*amk*^{R}) and alternative strategy was employed where the first step was to clone the *aphA6* gene into pGEM T-easy using the same primer pair (Section 2.4.10, Table 2.3). Ligated plasmids were transformed into competent *E. coli* DH5α cells (Section 2.5.1), the DNA extracted and the presence of *aphA6* confirmed via digestion with *Bam*HI and *Sal*I (Sections 2.4.4 and 2.4.6). *E. coli* DH5α cells containing the pGem_*amk*^{R} plasmid showed a 4-fold increase in amikacin resistance, indicating the *aphA6* gene product confers amikacin resistance. Despite several attempts, transferring gel-excised *aphA6* from pGEM T-easy into pWH1266 was unsuccessful (Section 2.4.9).

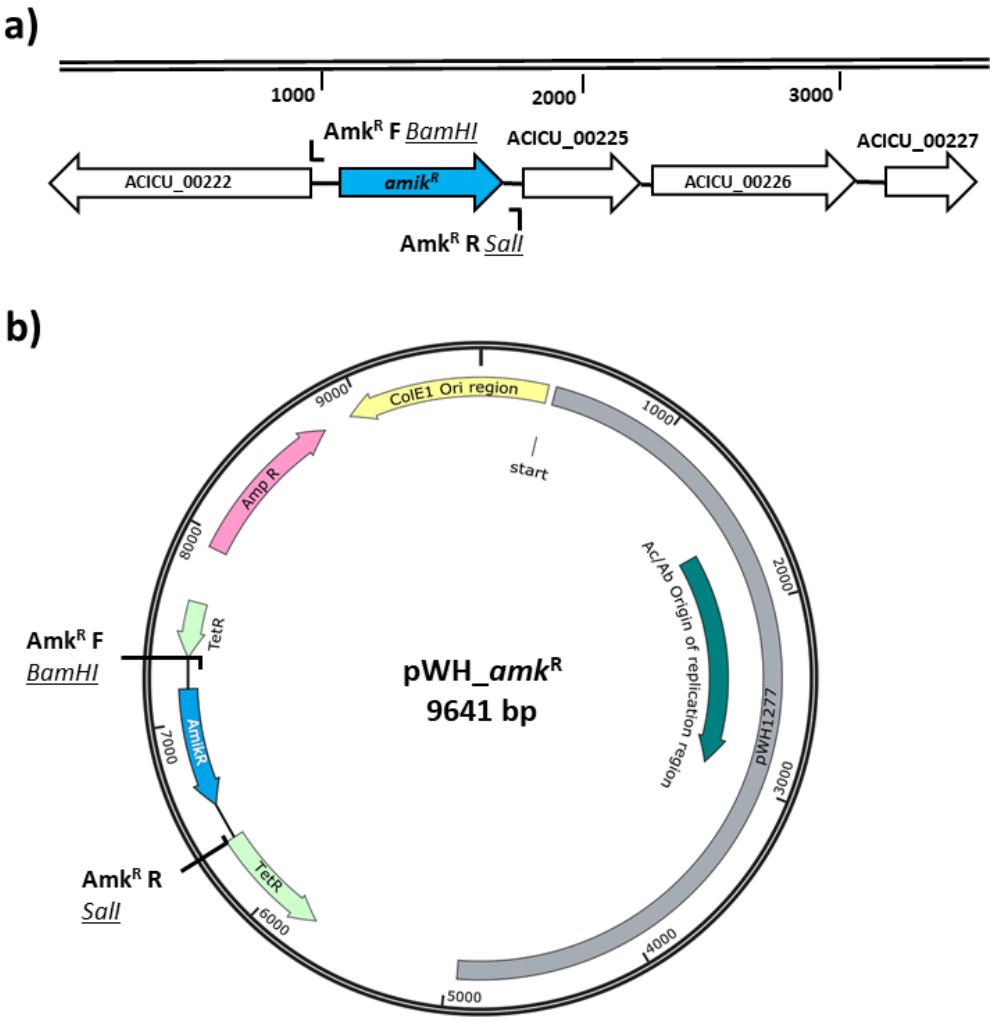

Figure 4.5 Identification and attempted cloning of the amikacin resistance gene from pACICU2 into pWH1266. Sequences were obtained from the NCBI database and analysed using SnapGene™. Genes are represented by arrows and indicate the length (bp) and direction of gene transcription. Gene names/locus tags are denoted within the arrows. Location of primers used for amplification are represented by a solid black corner symbols (⌝ or ⌟). The scale above the linear DNA represents size (bp). Solid black lines represent non-coding regions. The *aphA6* (*amk*^{R}) gene is represented by a light blue arrow, surrounding genes represented by white arrows. Location of primers used for amplification are represented by a solid black corner symbols (⌝ or ⌟); Amk^R_F. *Bam*HI (Amk^R F), Amk^R_R *Sal*I (Amk^R R) a) Region of pACICU2 harbouring *amk*^{R}, White arrows downstream from *amkR* represent three putative antibiotic resistance related genes, white arrow upstream from *amkR* represents a divergently transcribed intergrase gene. b) Plasmid construct containing the *amkR* gene cloned into the *tetR* gene of pWH1266 (pW_*amkR*).

No further attempts to complement the 04117201Δ*wzy* were made. Instead efforts concentrated on generating mutants in the *A. baumannii* strain ATCC 17978, which already has various resistance markers available for cloning purposes. The following section details the generation of acapsular mutants in ATCC 17978 by deletion of various genes within the K loci.

4.2.1 Generation of acapsular mutants in *A. baumannii* ATCC 17978

4.2.1.1 *Generation of an A. baumannii ATCC 17978 wzy deletion mutant by plasmid recombination*

Initially, removing the *wzy* gene of ATCC 17978 was attempted using the method outlined in Section 4.2.2. Regions flanking *wzy* were amplified using A_*wzy*_UFR and A_*wzy*_DFR primer pairs (Table 2.6). These PCR products, incorporating *Xho*I and *SalI* restriction sites (Figure 4.6a), were then digested with *Xho*I and *SalI* and cloned into *Xho*I and *SalI* digested pGEM T-easy. An *ery*^{R} cartridge was then incorporated into this construct using *Xho*I restriction sites (Table 2.5, Section 2.4.10, Figure 4.6b). The flanking regions and *ery*^{R} were then excised from this construct, pGem_ATCC17978_*wzy*KO by digestion with *Sal*I and *Xba*I (Figure 4.6). This excised product was then cloned into pEX18Tc digested with *Sal*I and *Xba*I to produce pEX_ATCC17978_*wzy*KO (Table 2.3, Figure 4.6c).

The resulting plasmid was isolated from *E. coli* and sequenced using the Ery_check_F and Ery_check_R primer pair, which bind to the *ery*^{R} and read outward into the cloned flanking regions (Table 2.6, Section 2.8, Figure 4.6c). This confirmed the successful construction of the clone. Despite this, there were difficulties electroporating pEX_ATCC17978_*wzy* into *A. baumannii* ATCC 17978 cells (Section 2.5.2). Several steps were taken to troubleshoot this issue including optimising plasmid concentration and electroporation parameters, the addition of 10% glycerol to samples, and the re-cloning of the pEX_ATCC17978_*wzy* plasmid, but none proved successful. Subsequently, a new method involving the homologous recombination of the WT *wzy* gene region with a linear PCR fragment, as opposed to a plasmid construct, was employed (Section 2.5.1).

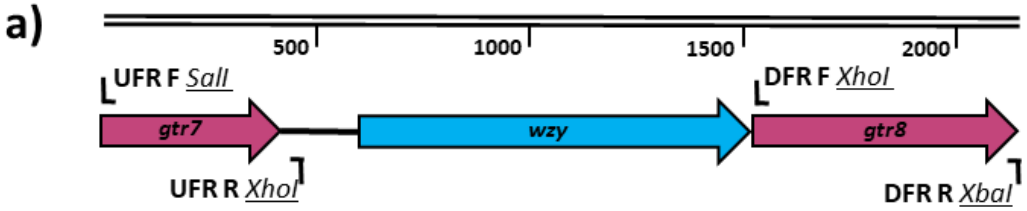
a)
500
1000
1500
2000
UFR F SalI
DFR F XhoI
gtr7
wzy
gtr8
UFR R XhoI
DFR R XbaI

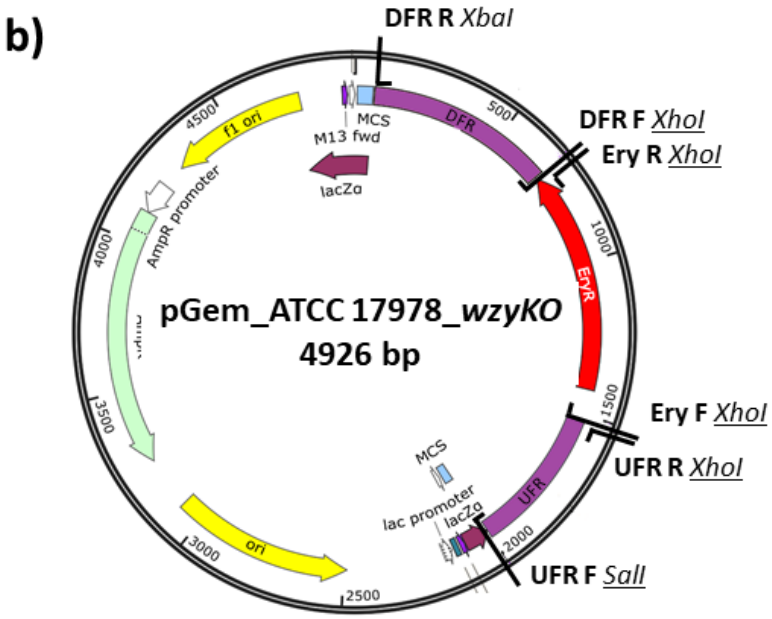
b)
DFR R XbaI
DFR F XhoI
Ery R XhoI
Ery F XhoI
UFR R XhoI
UFR F SalI
pGem_ATCC 17978_wzyKO
4926 bp
MCS
M13 fwd
lacZα
DFR
EryR
UFR
ori
f1 ori
AmpR promoter
lac promoter
500
1000
1500
2000
2500
3000
3500
4000
4500

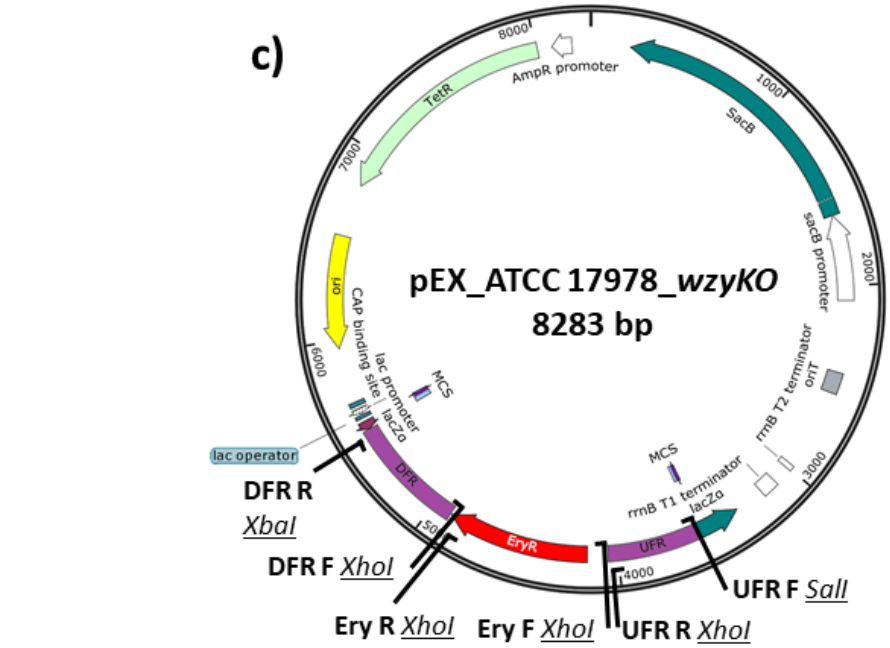
c)
pEX_ATCC 17978_wzyKO
8283 bp
AmpR promoter
TetR
SacB
sacB promoter
ori
CAP binding site
lac promoter
MCS
lacZα
lac operator
DFR
EryR
UFR
rrnB T1 terminator
rrnB T2 terminator
oriT
DFR R XbaI
DFR F XhoI
Ery R XhoI
Ery F XhoI
UFR R XhoI
UFR F SalI
1000
2000
3000
4000
6000
7000
8000

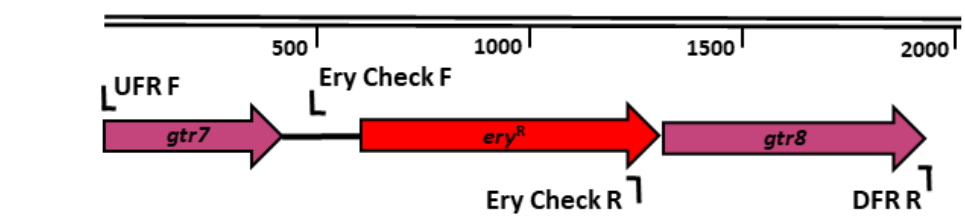
d)
500
1000
1500
2000
UFR F
Ery Check F
gtr7
eryR
gtr8
Ery Check R
DFR R

Figure 4.6 cloning of ATCC 17978 *wzy* flanking regions and *ery*^{R} into the pEX18Tc cloning vector. Sequences were obtained from the NCBI database and analysed using SnapGene^{TM}. Genes are represented by arrows and indicate the length (bp) and direction of gene transcription. Gene names/locus tags are denoted within the arrows. The scale above linear DNA represents size (bp). Solid black lines represent non-coding regions. Location of primers used for amplification are represented by a solid black corner symbols (⌝ or ⌟) and incorporated restriction sites are underlined; A_wzy_UFR_F *Sal*I (UFR F), A_wzy_UFR_R *Xho*I (UFR R), A_wzy_DFR_F *Xho*I (DFR F), A_wzy_DFR_R *Xba*I (DFR R), Ery_F *XhoI*, Ery_R *XhoI*. Figures are drawn to scale. a) chromosomal region of *wzy* in ATCC 17978 indicating primers to amplify upstream and downstream flanking regions b) Plasmid construct of *ery*^{R} (See Figure 4.2b) and flanking regions in pGEM T Easy vector (pGem_ATCC17978_*wzy*KO) c) Plasmid construct of *ery*^{R} and flanking regions in pEX18Tc vector (pEX_ATCC17978_*wzy*KO) d) desired chromosomal gene arrangement in successful ATCC 17978Δ*wzy* mutant showing location of the sequencing primers, Ery Check F and R.

4.2.1.1 *Generation of acapsular mutants in A. baumannii ATCC 17978 using recombination-mediated genetic engineering*

During the course of this study, a recombination-mediated genetic engineering (recombineering) protocol for the generation of *A. baumannii* gene deletion mutants became available (Tucker et al., 2014). Recombineering involves expressing a plasmid encoded recombinase and the addition of large quantities of linear DNA template to bacterial cells to stimulate recombination (Section 2.5.1) (Tucker et al., 2014). This method was adopted to make three separate deletion mutants in ATCC 17978 by replacing the following gene/s with *ery*^{R}; the *wzy* polymerase (Δ*wzy*), the initial transferase gene (Δ*itrA2*) and the variable region genes from *gna-itrA2* (Δ*cps*) (Figure 4.7).

Firstly, linear fragments containing regions flanking target genes and *ery*^{R} NOL PCR products were generated (Figure 4.7, Section 2.5.1). Flanking regions were amplified with target gene specific NOL_up and NOL_down primer pairs (Table 2.6, Section 2.4.1, Figure 4.7). The linear construct was then amplified by NOL PCR using target gene specific NOL_all primer pairs, flanking regions, and *ery*^{R} PCR products as a template DNA (Figure 4.7, Section 2.5.1). The size of the NOL product was confirmed via gel electrophoresis (Section 2.4.8) prior to electroporation into *A. baumannii* ATCC 17978 cells containing the pAT04 plasmid (Table 2.3). The pAT04 plasmid contains a recombinase gene which enhances recombination of the target sequence (Tucker et al., 2014). Mutants were then grown on selective solid media (Ery) to select for Ery^{R} cells which have replaced the target gene/s with the *ery*^{R} marker. Mutants were confirmed by Sanger sequencing with appropriate primers over the region targeted for deletion (Section 2.8).

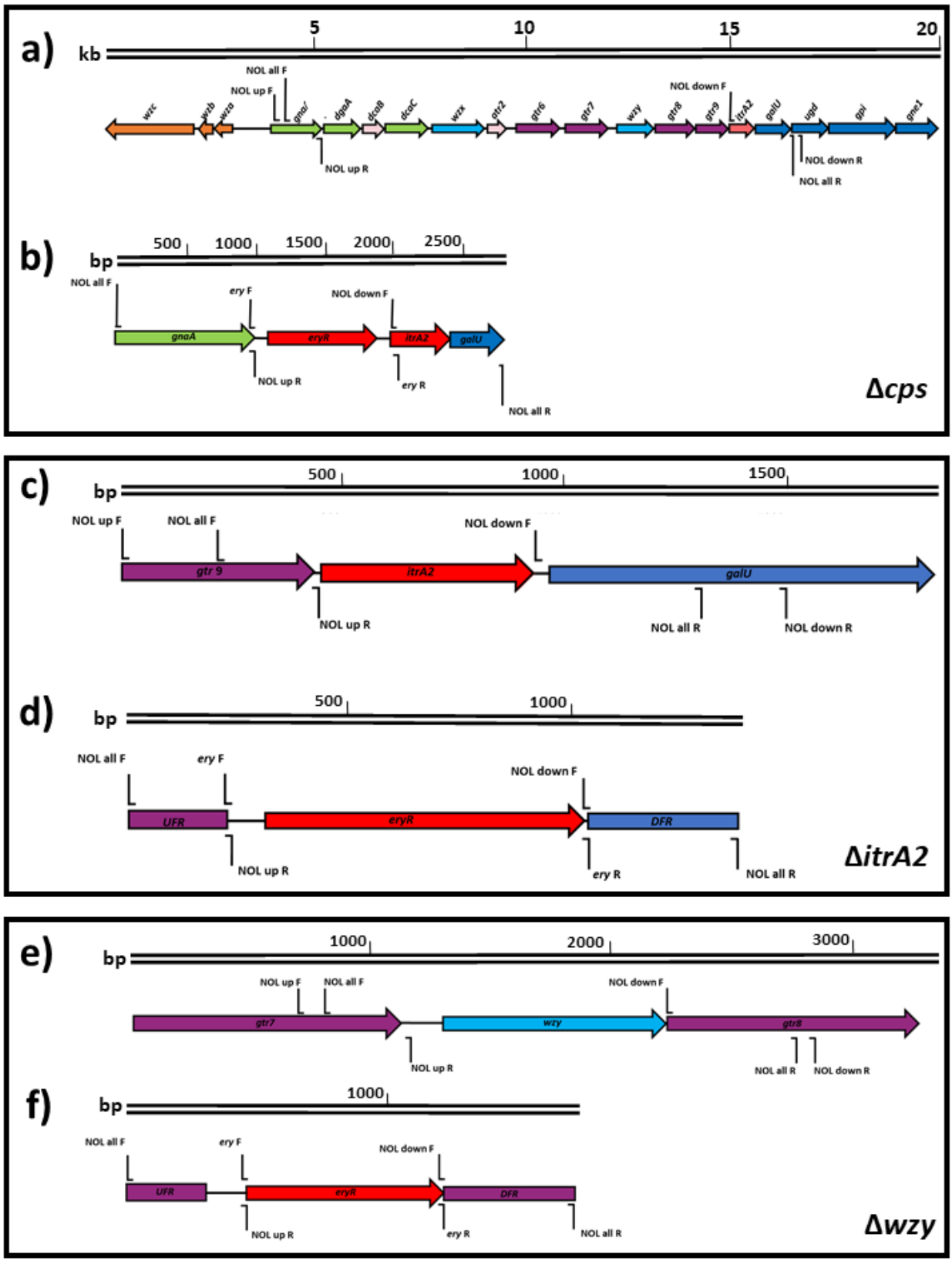
a)
kb
5
10
15
20
NOL all F
NOL up F
NOL down F
wzc
wzb
wza
gnaA
dgaA
dcaB
dcaC
wzx
gtr2
gtr6
gtr7
wzy
gtr8
gtr9
itrA2
galU
ugd
gpi
gne1
NOL up R
NOL down R
NOL all R
b)
bp
500
1000
1500
2000
2500
NOL all F
ery F
NOL down F
gnaA
eryR
itrA2
galU
NOL up R
ery R
NOL all R
Δcps
c)
bp
500
1000
1500
NOL up F
NOL all F
NOL down F
gtr 9
itrA2
galU
NOL up R
NOL all R
NOL down R
d)
bp
500
1000
NOL all F
ery F
NOL down F
UFR
eryR
DFR
NOL up R
ery R
NOL all R
ΔitrA2
e)
bp
1000
2000
3000
NOL up F
NOL all F
NOL down F
gtr7
wzy
gtr8
NOL up R
NOL all R
NOL down R
f)
bp
1000
NOL all F
ery F
NOL down F
UFR
eryR
DFR
NOL up R
ery R
NOL all R
Δwzy

Figure 4.7 Recombination mediated genetic engineering 'Recombineering' chromosomal template regions and nested overlap products for acapsular mutant construction in *A. baumannii* ATCC 17978. Sequences were obtained from the NCBI database and analysed using SnapGene™. Genes are represented by arrows and indicate the length and direction of gene transcription. Gene names/locus tags are denoted within the arrows. The scale above linear DNA represents size. Solid black lines represent non-coding regions. Only generic primer names are used, specific names of primers can be found in Table 2.6. Figures are drawn to scale. Black boxes separate the DNA templates for the various acapsular mutants constructed. a) chromosomal template Δ*cps*, b) linear NOL construct for Δ*cps*, c) chromosomal template DNA for Δ*itrA2*, d) linear NOL construct for Δ*itrA2*, e) chromosomal template DNA for Δ*wzy*, f) linear NOL construct for Δ*wzy*.

4.2.1.2 *Complementation of acapsular ATCC 17978 mutants*

Complementation of Δ*wzy* and Δ*itrA2* was achieved by cloning the respective WT gene from *A. baumannii* ATCC 17978 into pWH1266 (Table 2.3) for expression in the acapsular mutant background (Figures 4.8 and 4.9). The *wzy* gene was amplified from the WT ATCC 17978 chromosome with the Wzy_comp_F and Wzy_comp_R primer pair and cloned into the Tet^R region of pWH1266 using *Sal*I and *Eag*I restriction sites (Table 2.5, Sections 2.4.6 and 2.4.7, Figure 4.8). This construct included upstream non coding regions to ensure any promotor sequences were captured in the complementation plasmid. This plasmid, denoted pWH_*wzy*, was then electroporated into Δ*wzy* cells (Section 2.5.2, Figure 4.8). A pWH1266 empty vector was similarly electroporated into Δ*wzy* cells to generate a complementation negative isolate for comparison (Section 2.5.2, Table 2.6). Complemented strains were selected for using Amp^R that is carried on pWH1266. The retention of the complementation plasmid was verified by passage on non-selective media three times followed by confirmation of Amp^R. Complementation of Δ*itrA2* was performed in a similar manner except the WT gene was amplified using the ItrA2_comp_F and ItrA2_comp_R primer set and was cloned into pWH1266 using *Bam*HI and *Sal*I restriction sites, generating pWH_*itrA2* (Table 2.6, Sections 2.4.6 and 2.4.7, Figure 4.9).

Complemented stains of Δ*itrA2 and Δwzy* were used for downstream experiments to ensure phenotypes observed are a result of removing the gene of interest and not off target mutations of modifications. The complimented strains of Δ*itrA2* and Δ*wzy* are denoted as Δ*itrA2C* and Δ*wzyC*, respectively (Figures 4.8, 4.9).

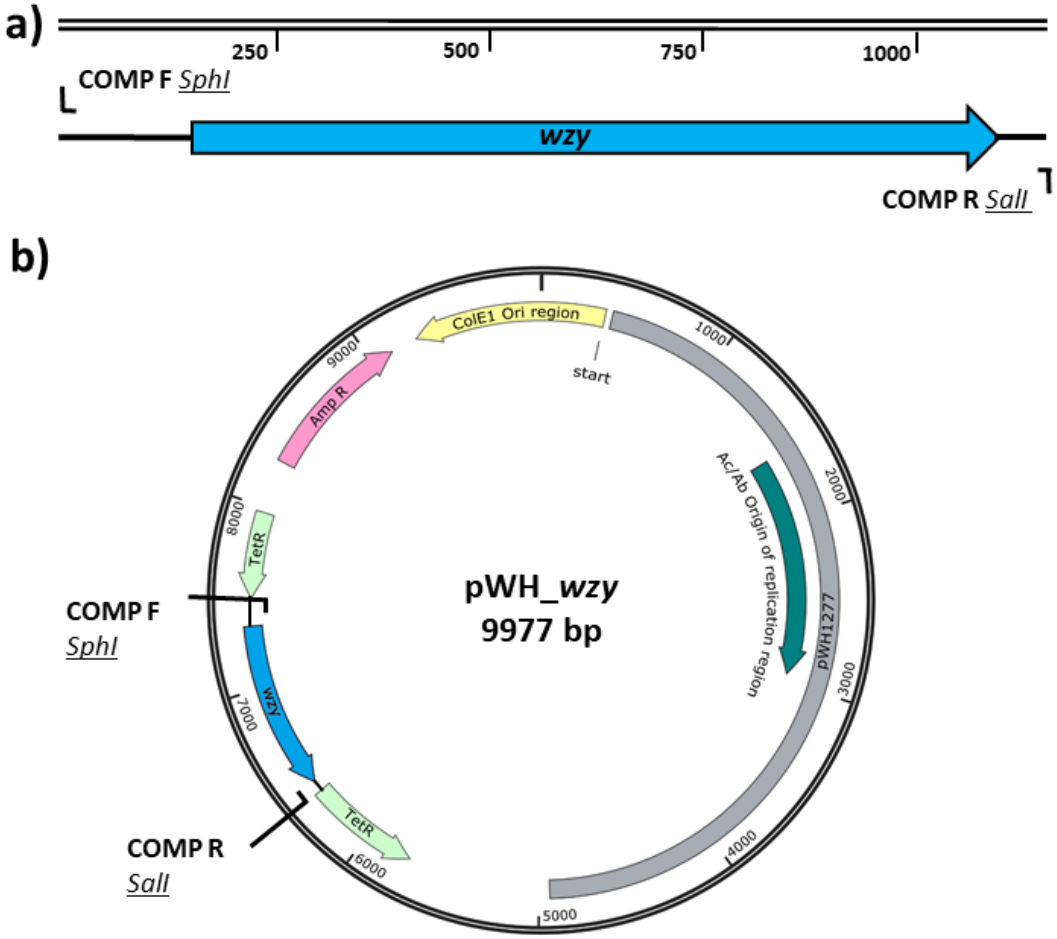

Figure 4.8 Complementation of a Δ*wzy* mutant in ATCC 17978. Sequences were obtained from the NCBI database and analysed using SnapGene™. Genes are represented by arrows and indicate the length and direction of gene transcription. Gene names/locus tags are denoted within the arrows. The scale above linear DNA represents size. Solid black lines represent non-coding regions. Figures are drawn to scale. Location of primers used for amplification are represented by a solid black corner symbols (⅂ or ⅃) and incorporated restriction sites are underlined; wzy_comp_F Sph*I* (COMP F), wzy_comp_R Sal*I* (COMP R). The gene of interest *wzy*, is in blue. a) chromosomal template DNA (ATCC 17978 WT) used for preparation of a *wzy* containing plasmid to be used for complementation, b) location of *wzy* cloned into the pWH1266 shuttle vector, producing pWH_*wzy*.

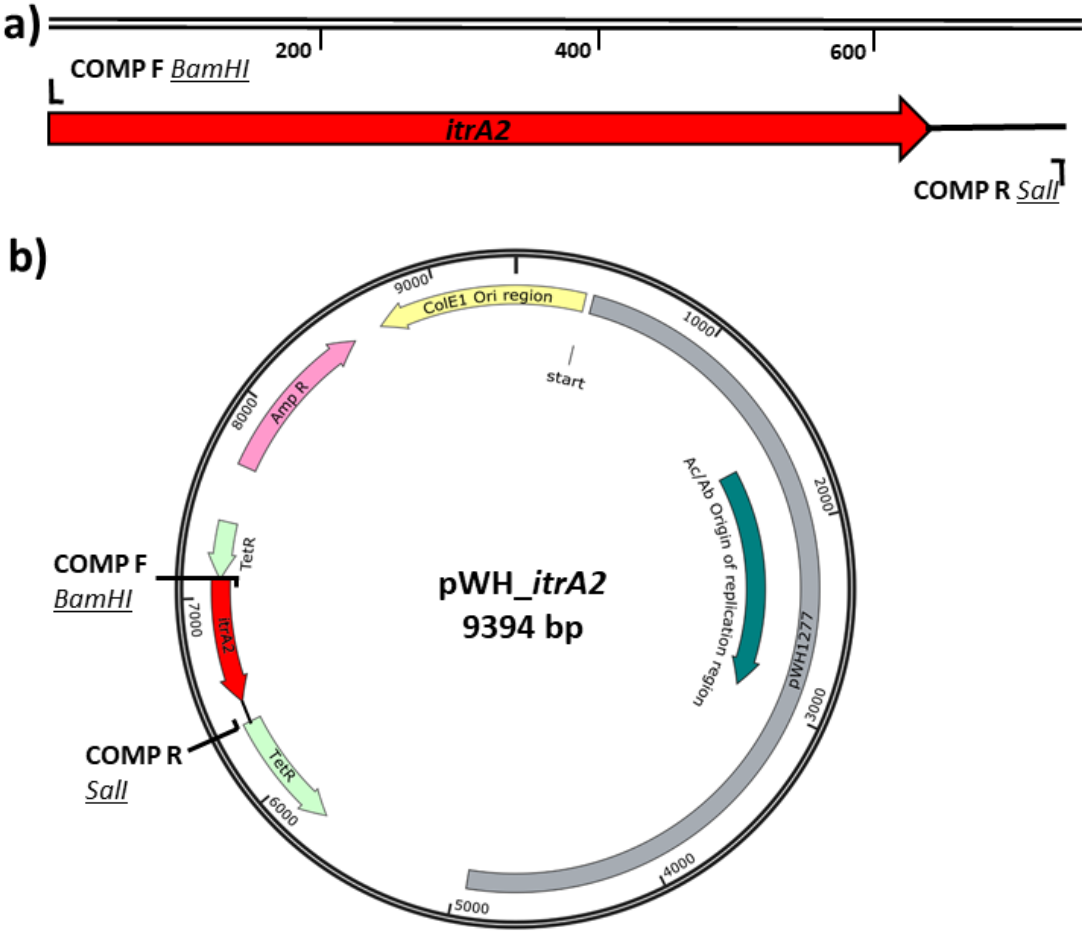

Figure 4.9 Complementation of Δ*itrA2*. Sequences were obtained from the NCBI database and analysed using SnapGene™. Genes are represented by arrows and indicate the length and direction of gene transcription. Gene names/locus tags are denoted within the arrows. The scale above linear DNA represents size. Solid black lines represent non-coding regions. Figures are drawn to scale. Location of primers used for amplification are represented by a solid black corner symbols (⌜ or ⌟) and incorporated restriction sites are underlined; *itrA2*_comp_F *BamHI* (COMP F), *itrA2*_comp_R *SalI* (COMP R). The gene of interest, itrA2 is in red. a) chromosomal template DNA (ATCC 17978 WT) for *itrA2* complementation, b) location of *itrA2* insertion into the pWH1266 vector (pWH_*itrA2*).

The strains of Δ*itrA2* and Δ*wzy* containing the empty pWH1266 vectors (i.e. negative controls) are denoted as Δ*itrA2E* and Δ*wzyE*, respectively (Table 2.3).

4.2.1.3 *Confirmation of loss of capsule production in acapsular ATCC 17978 variants*

To confirm the absence of capsule in the knockout strains, capsular material was extracted from the appropriate strains, separated on a 20% SDS-PAGE gel and stained with Alcian blue (Section 2.9.6, Figure 4.10). A molecular weight marker, the Precision Plus Protein™ Prestained Protein Standard (Biorad), was included to determine the size of bands. As expected, a distinct band of high molecular weight can be seen for the WT ATCC 17978 strain representing the stained capsule (Figure 4.10). No band can be observed in all three capsule mutants confirming the loss of capsule production (Figure 4.10). By reintroducing the WT *itrA2* gene back into the Δ*itrA2* via an expression vector, pWH*itrA2* (Table 2.3), capsule production is restored (Figure 4.10a). Similarly, when a vector expressing the *wzy* gene is reintroduced into the Δ*wzy* variant capsule production is similarly restored (Figure 4.10c).

As the *itrA2* gene is involved in both protein glycosylation and capsule production (Figure 1.5.1), a PAS stain of the membrane fraction extracted from Δ*itrA2* cells was performed (Section 2.9.7). PAS stains are commonly used to confirm protein glycosylation as only proteins which are glycosylated will result in a band (Cagatay and Hickford, 2008). A Precision Plus Protein™ Prestained Protein Standard (Biorad), was included to determine the size of bands. After staining, a band was present at approximately 37 kDa for the WT strain but not the *itrA2* mutant, indicating the loss of protein glycosylation in Δ*itrA2* as expected (Figure 4.11a). Complementation of Δ*itrA2* (Δ*itrA2*C*)* restored protein glycosylation to WT levels (Figure 4.11a).

Previous experiments showed that generation of a *wzy* mutant in *A. baumannii* 04117201 led to abolition of protein glycosylation (Section 4.2.3). Similarly, a PAS stain identified a lack of protein glycosylation in the first attempt to construct a *wzy* mutant in ATCC 17978 (Figure 4.11). Sequencing of the *itrA2* gene in the *wzy* mutant revealed a point mutation approximately 600 bp from the start of the gene which resulted in an early stop codon, preventing expression of the full ItrA2 product (Section 2.7). This isolate was then denoted ΔΔ*wzy_itrA2* (Table 2.3, Figure 4.11).

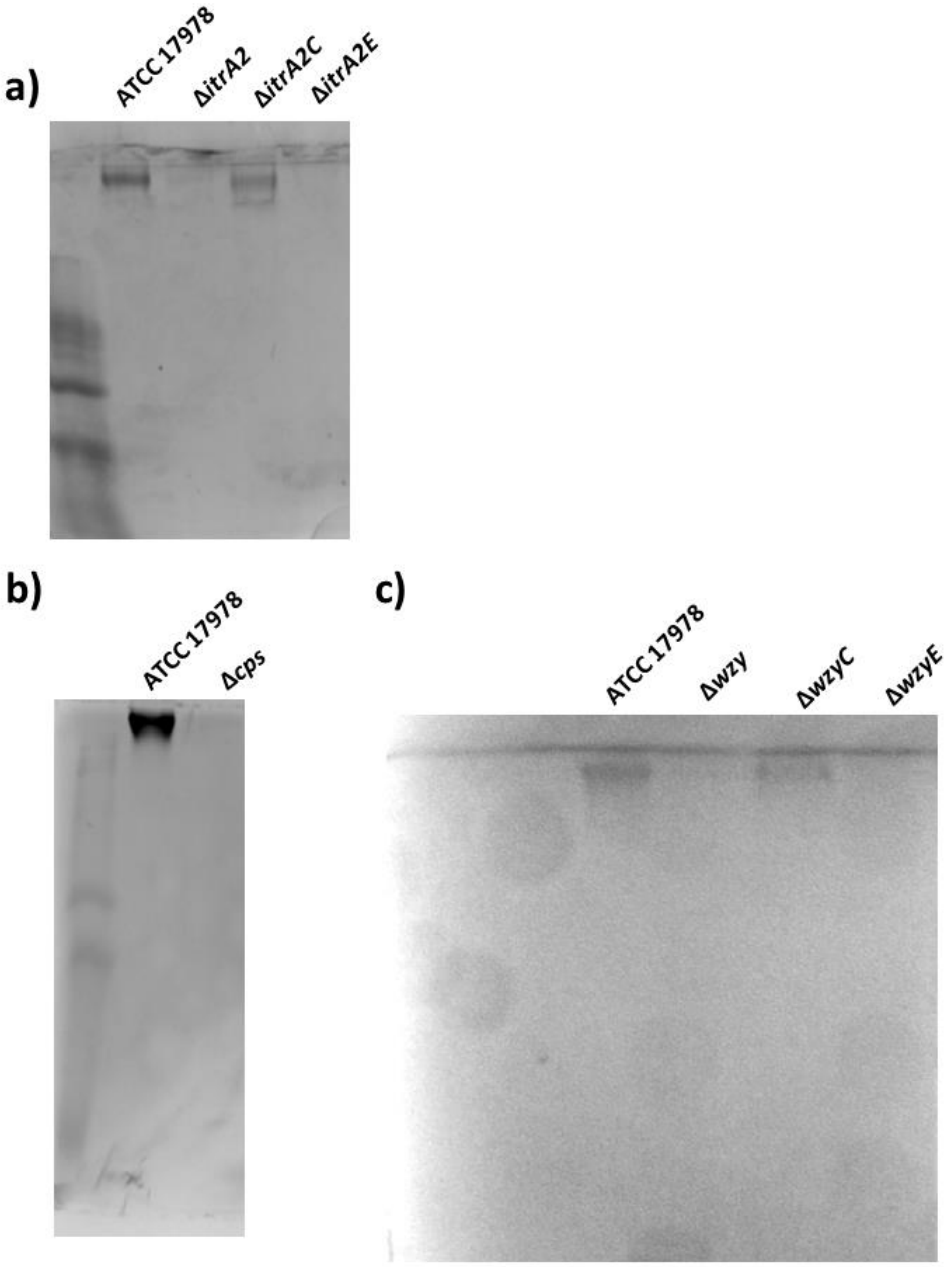

Figure 4.10 Alcian blue stain of capsular polysaccharide extracted from acapsular mutants in *A. baumannii* ATCC 17978. Extracted capsular polysaccharide was run on a 20% polyacrylamide gel prior to staining. A molecular weight marker, the Precision Plus Protein™ Prestained Protein Standard (Biorad), was included to determine the size of bands. a) ATCC 17978 WT strain compared to isogenic derivatives: *itrA2* inactivated, Δ*itrA2*; complemented Δ*itrA2*, Δ*itrA2*C; and Δ*itrA2* carrying the empty pWH1266 vector, Δ*itrA2*E, b) ATCC 17978 WT strain compared to *cps* deletion strain, Δ*cps*, c) ATCC 17978 WT strain compared to *wzy* inactivated, Δ*wzy*; complemented *wzy*, Δ*wzy*C; and Δ*wzy* carrying the empty pWH1266 vector, Δ*wzy*E.

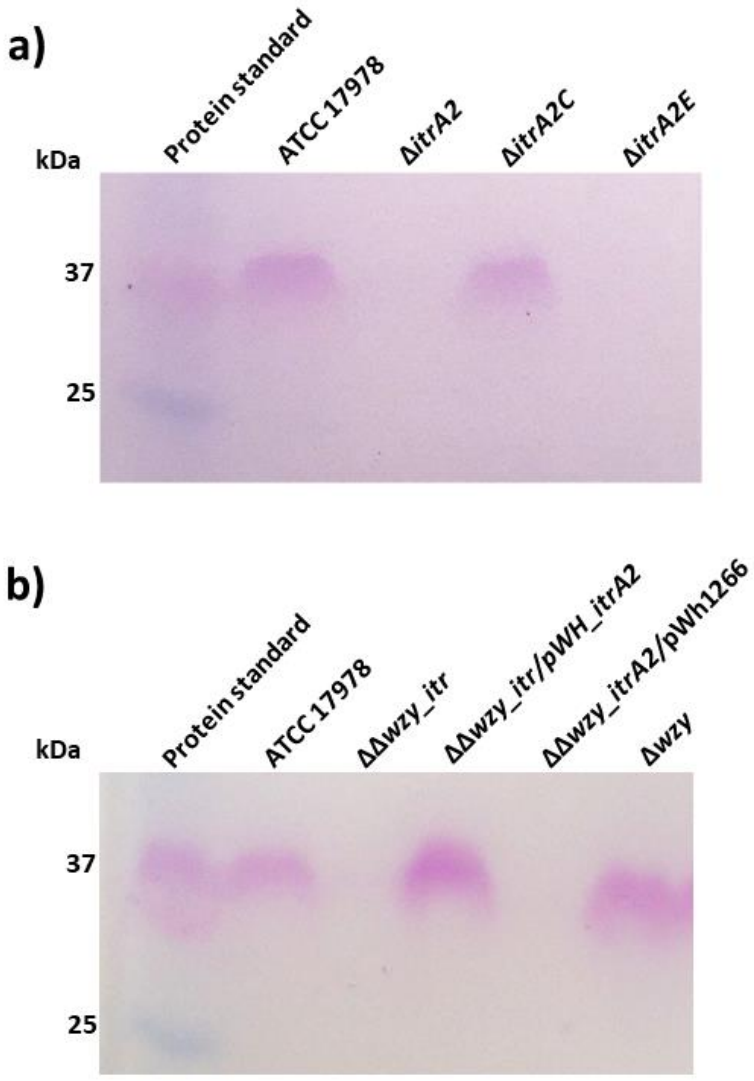

Figure 4.11 PAS stain of membrane fractions extracted from acapsular variants of ATCC 17978. Extracted membrane fractions were run on a 12.5% polyacrylamide gel prior to PAS staining. A molecular weight marker, the Precision Plus Protein™ Prestained Protein Standard (Biorad), was included to determine the size of bands. a) ATCC 17978 WT compared to isogenic derivatives: *itrA2* inactivated, Δ*itrA2*; complemented Δ*itrA2*, Δ*itrA2*C; and Δ*itrA2* carrying the empty pWH1266 vector, Δ*itrA2*E Δ*itrA2*, Δ*itrA2*C and Δ*itrA2*E. b) ATCC 17978 WT compared to a *wzy* mutant containing a point mutation in *itrA2* (ΔΔ*wzy_itrA2*), ΔΔ*wzy_itrA2* complemented with the WT *itrA2* gene (ΔΔ*wzy_itrA2*/pWH_*itrA2)*, ΔΔ*wzy_itrA2* empty vector control (ΔΔ*wzy_itrA2*/pWH1266) and Δ*wzy*

The phenomenon of secondary suppressor mutations has been identified in other bacteria when genes involved in capsule production are removed (Xayarath and Yother, 2007). This is hypothesised to occur when deletion of the primary gene, such as *wzy* in *Streptococcus*, is extremely detrimental or lethal (Xayarath and Yother, 2007). To investigate whether a *wzy* only deletion mutant would be viable in ATCC 17978 the *itrA2* gene was re-introduced into ΔΔ*wzy_itrA2* via the pWH_*itrA2* plasmid (Figure 4.2). Re-introduction of the WT *itrA2* gene (ΔΔ*wzy_itrA2*/C) restored protein glycosylation to WT levels, indicating the deletion of *wzy* is possible without the presence of secondary mutations (Figure 4.11).

Using the recombineering protocol outlined in previous sections several new *wzy* deletion mutants were made in the *A. baumannii* ATCC 17978 strain (Section 2.5.1). To investigate the efficiency of *wzy* mutant generation, *itrA2* mutants were generated in parallel to *wzy* mutants as a comparison. The transformation efficiency of the *itrA2* deletion was six-fold that of *wzy* (data not shown). Furthermore, only one of the four acquired *wzy* mutants displayed a band for protein glycosylation when membrane extracts were PAS stained (Figure 4.11b, Section 2.9.7). Complementation of this glycosylation positive Δ*wzy* derivative restored capsule production when analysed by Alcian blue staining (Figure 4.10). To assess the stability of Δ*wzy*, the strain was serially passaged on selective (Ery) and non-selective media several times prior to PAS staining to check for protein glycosylation (Section 2.9.7, Figure 4.11). There was no detectable effect of serial passage of Δ*wzy* on protein glycosylation, as indicated by a band present at approximately 37 kDa on the PAS stain for Δ*wzy* (Figure 4.11b, far right). Therefore the mutation seemed stable and downstream experiments were performed on this isolate.

4.2.1.4 *Cell morphology of capsule deficient ATCC 197978 mutants*

There have been many methods of capsule staining published which use a variety of dyes to visualise capsular polysaccharide. In this study, a number of methods, were trialled including using India ink, Congo Red staining, and Maneval's stain (Breakwell et al., 2009, James and Swanson, 1977, Hughes and Smith, 2007). In the India ink method cells are stained with crystal violet and counterstained with India ink. As the ink cannot penetrate the capsule layer the capsule should be represented by a halo of white on a background of black ink (Breakwell et al., 2009). However, here the India ink

method was unsuccessful as acapsular mutants could not be reliably differentiated from the encapsulated WT cells. Negative staining with Congo red dye (Breakwell et al., 2009) was also unsuccessful in determining the presence of capsule in the WT and acapsular mutants ATCC 17978 variants. Thus, a method involving Maneval's staining was used which also allows for visualisation of the capsule (Hughes and Smith, 2007). Briefly, cells were fixed onto glass slides and stained with crystal violet. Cells were then counterstained with Maneval's stain which, similar to India ink, can't penetrate the capsule layer and results in a white halo of capsule around the pink cells on a blue background (Section 2.10.2, Figure 4.12b). As predicted, a white halo was seen for the WT *A. baumannii* cells, which was absent for the Δ*itrA2* mutant (Figure 4.12b). Unexpectedly, a white halo was observed around the *A. baumannii* Δ*cps* and Δ*wzy* cells, but this is likely due to shrinking of the bacterial cells during the staining process rather than the presence of capsule (Figure 4.12b). This is evidenced by the much smaller cell size of Δ*cps* and Δ*itrA2* (represented in pink) compared to the WT and Δ*itrA2* cells after Maneval's staining (Figure 4.12b). The cellular morphology of *A. baumannii* ATCC 17978 appeared to be affected by the removal of genes required for capsule synthesis. Both the Δ*itrA2* and Δ*cps* mutants exhibited an enlarged, swollen morphology compared to the typical coccobacilli shape of the WT ATCC 17978 (Fig 4.12a). The cell morphology of the Δ*wzy* mutant was dramatically perturbed compared to the ATCC 17978 WT, as Δ*wzy* cells were grossly enlarged, elongated, and showed a tendency of forming chains (Figure 4.12a). The size for a random sample of 10 cells from each mutant and WT *A. baumannii* were measured using Fiji ImageJ software (Figure 4.12c) (Schneider et al., 2012).

Complementation of Δ*itrA2* restored WT cellular morphology whereas complementation of Δ*wzy* showed reversion to a more typical *Acinetobacter* coccobacillus morphology but cells remained enlarged and bloated compared to the WT (Figure 4.12a).

The peculiar phenomenon of cell elongation in response to the removal of genes involved in surface polysaccharide synthesis has been seen previously in *E. coli* (Jorgenson et al., 2016, Jorgenson and Young, 2016, Ranjit and Young, 2016). The removal of genes involved in the production of *E. coli* colanic acid and O-antigen results in gross morphological defects including; elongated, filamentous, and branched cells (Jorgenson et al., 2016, Jorgenson and Young, 2016).

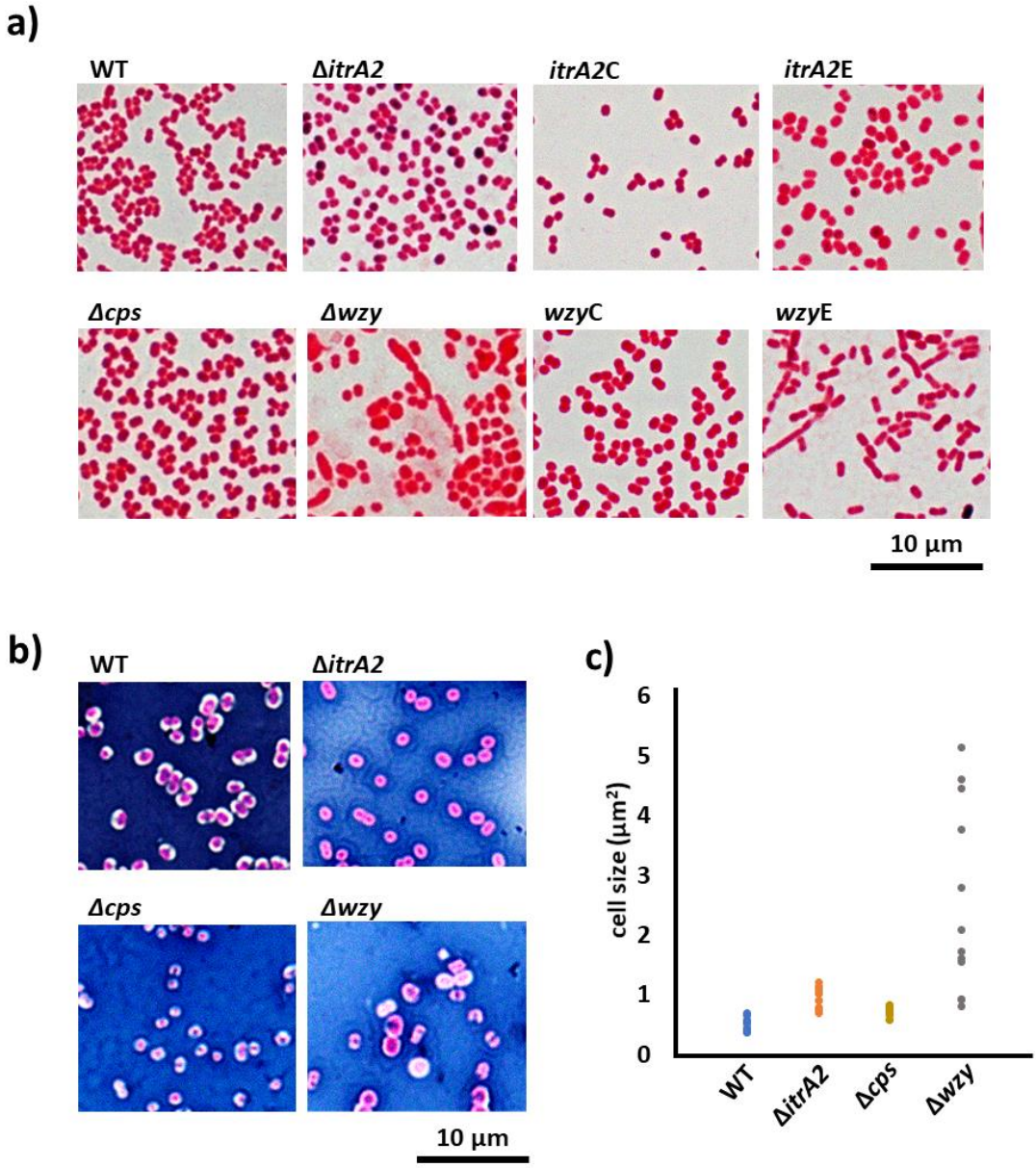

Figure 4.12 Cell morphology of ATCC 17978 WT and acapsular variants. Strains were grown on MH agar at 37ºC for 18 hours. Bacteria were resuspended in dH_2O, air or heat fixed and stained. Slides were visualised using a Brightfield Olympus BX50 microscope, 1000X objective Scale bars (10 µm) are included for size comparison between strains. Images were analysed using ImageJ software. a) Gram stain images of ATCC 17978 WT, acapsular mutants and complemented strains. b) Manevals stain for capsule of ATCC 17978 WT and acapsular variants. c) Quantitative analysis of bacterial cell sizes taken from a random sample of Gram stained *A. baumannii* (n=12).

The most likely reason for this phenomenon is that removing certain genes in the synthesis pathway of colanic acid, O-antigen, and capsule results in a build-up of Und-P linked intermediates (Jorgenson et al., 2016, Jorgenson and Young, 2016). Und-P is a lipid carrier essential for the synthesis of many cellular carbohydrates in Gram-negative bacteria including; colanic acid, O-antigen, core polysaccharide, capsule and peptidoglycan (Tatar et al., 2007).

Bacteria possess a limited pool of Und-P and accumulation of dead-end intermediates in colanic acid and O-antigen synthesis greatly reduce the free Und-P required for synthesis of other carbohydrates, particularly peptidoglycan. Peptidoglycan plays an essential role in determining the size and shape of Gram-negative cells, thus interruption of the peptidoglycan synthesis process can result in significant morphological abnormalities (Jorgenson et al., 2016). Furthermore, *E. coli* mutants with defective colanic acid and O-antigen synthesis systems, are strikingly similar in morphology to the Δ*wzy* mutant generated in this study (Figure 4.12) (Jorgenson et al., 2016, Jorgenson and Young, 2016).

Although assessing phenotypic changes in capsule knockout strains provides significant insight into the role of capsule in *A. baumannii* survival and virulence, it is unable to identify if a specific capsule type plays a role. The following section summarises attempts made to produce capsule swapped derivatives of two *A. baumannii* strains ATCC 17978 and 04117201 which possess KL3 and KL2 capsules, respectively.

4.2.2 Attempts to produce capsule swapped mutants

Several attempts were made to swap the KL regions of the *A. baumannii* strains ATCC 17978 and 04117201 that used plasmid vectors, recombineering, and a yeast cloning system. Although the strategies above were different in their approach to constructing capsule swapped mutants, they all shared the common principal of replacing the variable capsule genes from one strain, and replacing them with the variable genes of another. The strains used for these studies shared common genes both upstream and downstream of the central variable gene regions, thus providing naturally homologous flanking regions for double homologous recombination to occur. By using the capsule knock out strains to receive the donated variable region DNA, several methods of selection including the loss of Ery^R, and gain of serum resistance (Section 3.2.5, Section 6.1.3). This section provides a brief overview of approaches used and results during

these studies.

4.2.2.1 *Amplification and cloning of the variable capsule region of ATCC 17978 into pEX18Tc and pWH1266*

Prior to the capsule swap, efforts were focused on complementing the Δ*cps* strain in ATCC 17978 (Section 4.2.5). Additionally, a construct to complement Δ*cps* would also serve to make a capsule swap in the 04117201 Δ*wzy* strain (Section 4.2.2), as homology would select for replacement of all genes variable between the two strains. The primers AVR_up_F and AVR_down_R were designed to amplify the 13.6 kb ATCC 17978 KL variable region (AVR) (Table 2.6). This amplicon was designed to include regions upstream and downstream of the AVR which are homologous to the 04117201 K loci to allow for recombination (Figure 4.13a). Primers were designed to include the restriction sites *Sal*I and *Pvu*I to allow cloning of the AVR into the *E. coli-A. baumannii* shuttle vector pEX18Tc (Figure 4.13). The restriction site *Ava*I was also included in the AVR_down_R primer to allow for cloning into pWH1266 (Table 2.6). As an additional measure, internal primers, AVR_up_R and AVR_down_F, were designed incorporating an *Eag*I restriction site in a non-coding region to amplify the large region as two separate sections which could subsequently be ligated (Table 2.6, Figure 4.13). Using Ranger DNA polymerase (Bioline) a fragment of approximately 13.6 kb was initially successfully amplified using AVR_up_F and AVR_down_R primers (Table 2.6, Section 2.4.2.1, Figure 4.13). Ranger DNA polymerase is a hot start, high fidelity polymerase specifically designed to reliably amplify long DNA fragments between 10 and 25 kb in length (Maridian-Bioscience, 2020).

Further attempts to reamplify this product proved unsuccessful and strategies to troubleshoot the PCR included modifying the constituents of the PCR including the concentration of template DNA or $MgCl_2$, use of various DNA polymerases, and the addition 2-5% DMSO. Attempts to optimise the cycling conditions of the PCR included decreasing the extension time or annealing temperature and adjusting the number of cycles (Section 2.4.2.1). Despite these measures, the ability to amplify the AVR product was inconsistent, and yields were generally low and included non-specific amplification.

a)

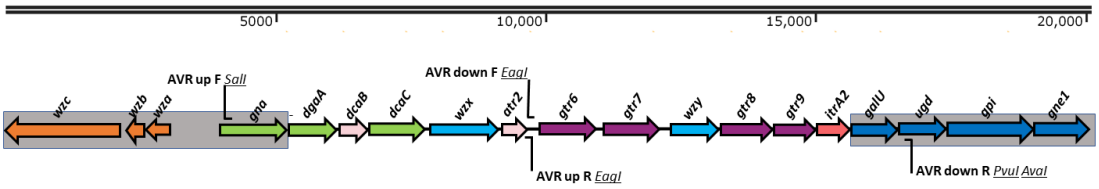
5000
10,000
15,000
20,000
AVR up F SalI
AVR down F EagI
wzc
wzb
wza
gna
dgaA
dcaB
dcaC
wzx
atr2
gtr6
gtr7
wzy
gtr8
gtr9
itrA2
galU
ugd
gpi
gne1
AVR up R EagI
AVR down R PvuI AvaI

b)

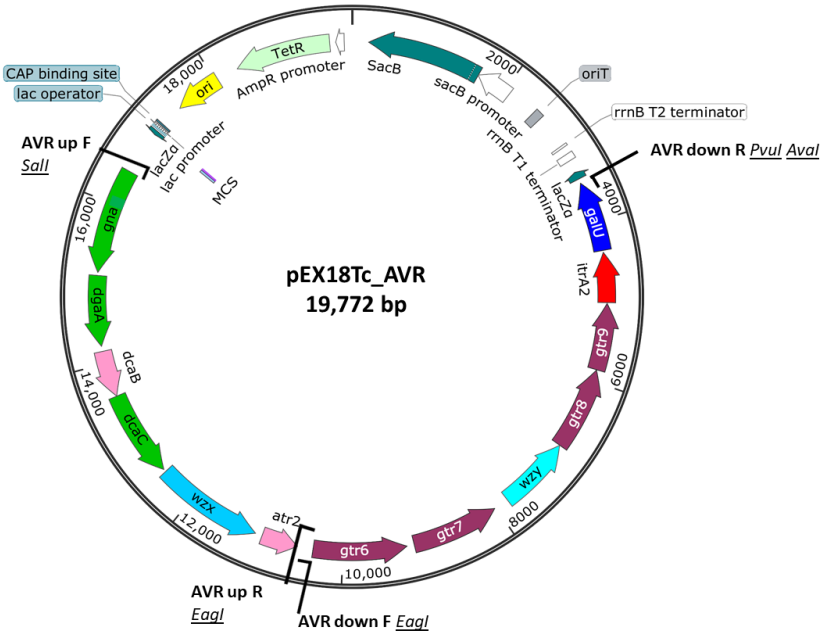
pEX18Tc_AVR
19,772 bp
TetR
AmpR promoter
SacB
sacB promoter
oriT
rrnB T2 terminator
rrnB T1 terminator
lacZo
galU
itrA2
gtr9
gtr8
wzy
gtr7
gtr6
atr2
wzx
dcaC
dcaB
dgaA
gna
ori
CAP binding site
lac operator
lacZo
lac promoter
MCS
AVR up F
SalI
AVR down R PvuI AvaI
AVR up R
EagI
AVR down F EagI

C)

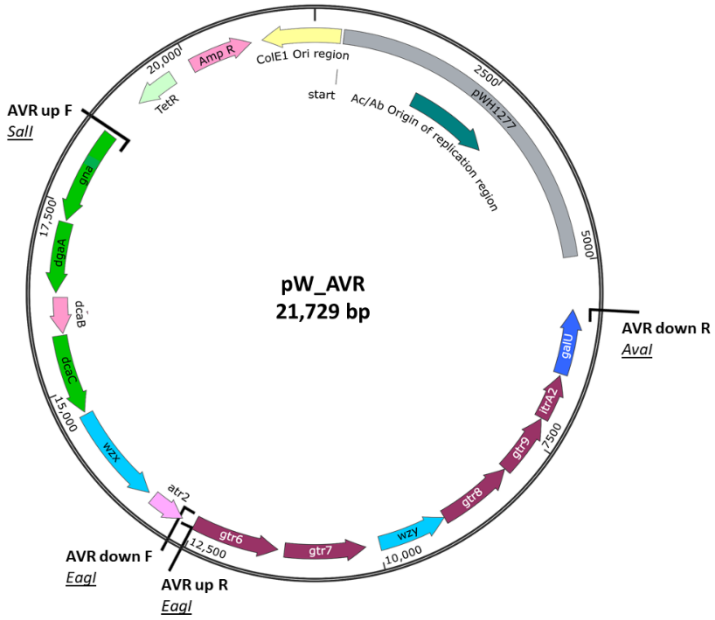
pW_AVR
21,729 bp
Amp R
ColE1 Ori region
start
Ac/Ab Origin of replication region
pWH1277
TetR
gna
dgaA
dcaB
dcaC
wzx
atr2
gtr6
gtr7
wzy
gtr8
gtr9
itrA2
galU
AVR up F
SalI
AVR down R
AvaI
AVR down F
EagI
AVR up R
EagI

Figure 4.13 Amplification and cloning of the ATCC17978 capsule variable region. Sequences were obtained from the NCBI database and analysed using SnapGene™. Genes are represented by arrows and indicate the length (bp) and direction of gene transcription. Gene names/locus tags are denoted within or above the arrows. The scale above linear DNA represents size (bp). Solid black lines represent non-coding regions. The colour scheme is based on homology to the putative function of gene products (refer to Figure 4.1). Location of primers used for amplification are represented by a solid black corner symbols (⌜ or ⌟) and incorporated restriction sites are underlined; AVR_up_F SalI (AVR up F), AVR_up_R EagI (AVR up R), AVR_down_F EagI (AVR down F), AVR_down_R PvuI AvaI (AVR down R). Figure is drawn to scale. a) Chromosomal template DNA of the ATCC 17978 KL variable region (AVR), nucleotide sequence homology shared between KL2 and KL3 regions are represented by grey boxes. b) Desired construct of AVR cloned into the pEX18Tc plasmid vector (pEX_AVR). c) Desired construct of AVR cloned into pWH1266 plasmid vector (pW_AVR).

This process was tedious and time consuming so the second strategy of amplifying the AVR as two smaller regions was undertaken. The up and down regions of the AVR were separately amplified using the AVR_up and AVR_down primer sets (Table 2.4, Figure 4.13a). The AVR_up product was then adenosine treated and cloned into pGEM T-easy using T-A cloning, producing pGem_AVR_up (Section 2.4.10). After several unsuccessful attempts to clone the AVR_down product into both pGEM T-easy and pGem_AVR_up this line of work was abandoned.

Attempts to clone the whole AVR product into pWH1266 were also undertaken as this construct could perform the dual function of complementing Δ*cps* (Section 4.2.5.2) and expressing the KL3 (ATCC 17978) genes in the 04117201 acapsular background. Although this method of KL3 gene expression would not produce a product as clean as homologous recombination, it would act as proof of principle for making a capsule swap in *A. baumannii*. Several attempts were made to clone the AVR amplicon into pWH1266 using *Sal*I and *Ava*I restriction sites (Figure 4.13c), but ultimately this proved unsuccessful. Cloning of a suitable resistance cassette would have been necessary to provide a selection for this plasmid in the 04117201 acapsular mutant. Attempts to introduce tel^R and amk^R into the tetracycline region of pWH1266 were also unsuccessful (Section 4.2.4). As previous attempts to introduce the AVR amplicon into a plasmid vector failed, efforts were redirected to producing a capsule swapped *A. baumannii* via recombineering (Section 2.5.1).

4.2.2.2 *Recombineering ATCC 17978 and 04117201 variable capsule regions*

As the recombineering protocol was previously successful in generating mutants in the *A. baumannii* strain ATCC 17978 attempts to produce a capsule swap in the ATCC 17978Δ*cps* background was initially undertaken (Section 4.2.5.2). As primers for the amplification of AVR were designed in regions homologous to both ATCC 17978 and 04117201 they could be used to generate a 04117201 variable region (NVR) amplicon (Figure 4.14). The pAT04 plasmid was electroporated into Δ*cps* and the NVR amplified using the AVR_up_F and AVR_down_R primers (Tables 2.3 and 2.6, Figure 4.14). Concurrently, the AVR was amplified for the complementation of ATCC 17978Δ*cps*. The NVR and AVR amplicons were then electroporated separately into ATCC 17978Δ*cps* containing pAT04 as per Section 2.5.1. The antimicrobial resistance profile for Δ*cps* (See Section 5.2.9) was analysed to identify a suitable antibiotic to aid in the selection of complemented and capsule swapped strains.

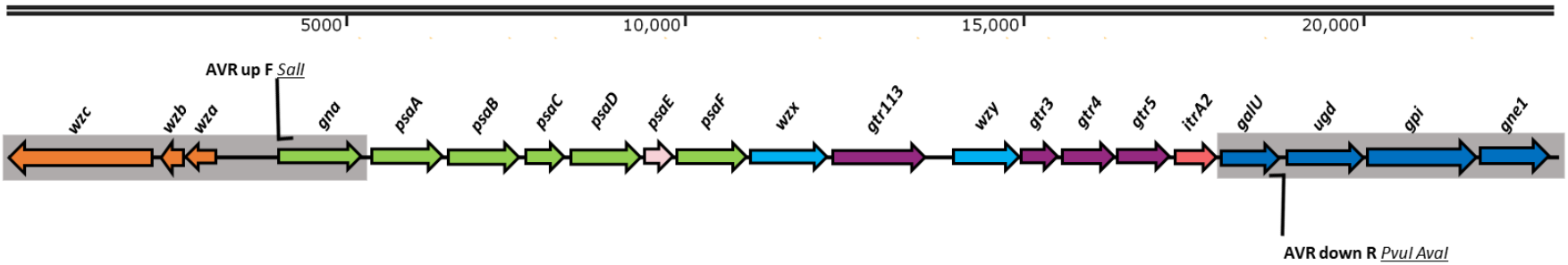

Figure 4.14 Amplification of the 04117201 capsule variable region using AVR primers. Sequences were obtained from the RAST database and analysed using SnapGene™. Genes are represented by arrows and indicate the length (bp) and direction of gene transcription. Gene names/locus tags are denoted above the arrows. The scale above linear DNA represents size (bp). Solid black lines represent non-coding regions. The colour scheme is based on homology to the putative function of gene products (see Figure 4.1). Regions homologous with KL3 are shaded grey. Location of primers used for amplification are represented by a solid black corner symbols (⌉ or ⌋) and incorporated restriction sites are underlined; AVR_up_F *SalI* (AVR up F), AVR_down_R *PvuI AvaI* (AVR down R). Figure is drawn to scale. a) Chromosomal template DNA of the 04117201 K loci variable region (NVR), nucleotide sequence homology shared between KL2 and KL3 regions are represented by grey boxes.

The Δ*cps* strain displayed a two-fold reduction in kanamycin resistance compared to the capsular parental strain, therefore, ex-transformants were plated onto solid media containing 5 µg/mL of kanamycin after recovery. Approximately 300 resultant colonies from both the NVR and AVR transformations were patched onto LB plates containing ery as a negative selection, as recombination of either NVR or AVR would result in the loss of the *ery*^{R} cassette. All isolates screened retained *ery*^{R} indicating recombination had not occurred. The protocol was repeated and colonies were pooled and screened via PCR for KL3 and KL2 specific genes using the primer pairs A1S_0053 and peg.2898, respectively (Table 2.6, Section 2.4.2). Amplification of both KL3 and KL2 genes from the recombination experiments proved unsuccessful (data not shown).

As recombination of AVR and NVR into ATCC 17978 was unsuccessful, attempts were made to introduce a new resistance marker into pAT04 to allow for recombineering into *A. baumannii* 04117201 (Section 2.5.2.2). Primers for *amk*^{R} and *tel*^{R} incorporating *Bam*HI restriction sites were used for cloning into the *tet*^{R} region of pAT04. Cloning either *amk*^{R} or *tel*^{R} into this region would allow for the expression of the new resistance marker from the *tet*^{R} promotor. After several attempts, cloning *amk*^{R} and *tel*^{R} into pAT04 proved unsuccessful (data not shown). Although the PCR products for *amk*^{R} and *tel*^{R} were amplified successfully, they failed to be incorporated into the pAT04 vector.

4.2.3 Construction of capsule swapped mutants using yeast recombinational cloning

A major hurdle in creating a plasmid or linear fragment for ‘knocking in’ large DNA constructs into *A. baumannii* was difficulties amplifying and cloning large DNA fragments. In addition, limited restriction site availability and multiple steps required to construct required plasmids proved problematic in creating a capsule ‘knock in’ strain. During this study, colleagues from the University of Sydney developed an operon assembly protocol (OAP) which utilised the natural homologous recombination DNA repair pathway of *S. cerevisiae* (Liu et al., 2017, Liu and Reeves, 2019). Liu *et al* used the OAP they developed to construct O-antigen deletions and replacements in *E. coli*. The method involves the modification of the yeast-*E. coli* shuttle vector pPR2274 to incorporate ‘hook’ regions homologous to the adjacent DNA sequence of the O-antigen region of *E. coli* to be ‘knocked in’ (Liu et al., 2017). The pPR2274 vector contains selective (URA3) and counter selective (CYH2) genes for *S. cerevisiae*, single (mini-F)

and high copy (ColEI) origins of replication (*ori*) for *E. coli*, as well as resistance makers for *cml*^{R} and *amp*^{R} (Fig 4.15a). The pPR2274 plasmid also contains two *Not*I sites for cloning the hook regions, and a 'stuffer' region which gets removed via digestion with *Sma*I upon incorporation of the operon of interest (Fig 4.15a).

The major advantage of using the OAP to 'knock in' capsule regions is the need to create the operon assembly vector (OAV) only once, as the hook regions contain DNA sequence which is highly homologous to all sequenced *A. baumannii* strains. Therefore, the same base can be used to create plasmids with various K loci.

Initially it was decided to first try and complement the ATCC 17978Δ*cps* mutant with the WT ATCC 17978 K loci as a proof of concept (Figures 4.15, 4.16). The first step involves cloning 'hooks' into the pPR2274 plasmid which are designed to capture a series of PCR products with regions of overlapping sequence (Figure 4.15). The hooks consist of the regions flanking the removed genes, *gna* to *itrA2* into the pPR2274 plasmid, as well as a resistance cartridge (*gent*^{R}) and an origin of replication (pW_*ori*) that would allow for replication of the plasmid in *A. baumannii* (Figure 4.15c) The pPR2274 plasmid with hook regions incorporated is called the OAV. The second cloning event involves introducing *Not*I digested OAV, and the overlapping PCR products encoding the KL3 region to be recombined, into yeast cells (Figure 4.16). Through homologous recombination the yeast cells will naturally repair the double stranded break in the pPR2274 plasmid with the overlapping KL3 PCR products, resulting in a plasmid which expresses all the genes removed from the ATCC 17978 Δ*cps* mutant. During the capture of the KL3 PCR products the plasmid loses a 'stuffer' region which contains the counter-selective CYH2 gene and an *amp*^{R} marker, allowing for the selection of the recombination event (Figure 4.16).

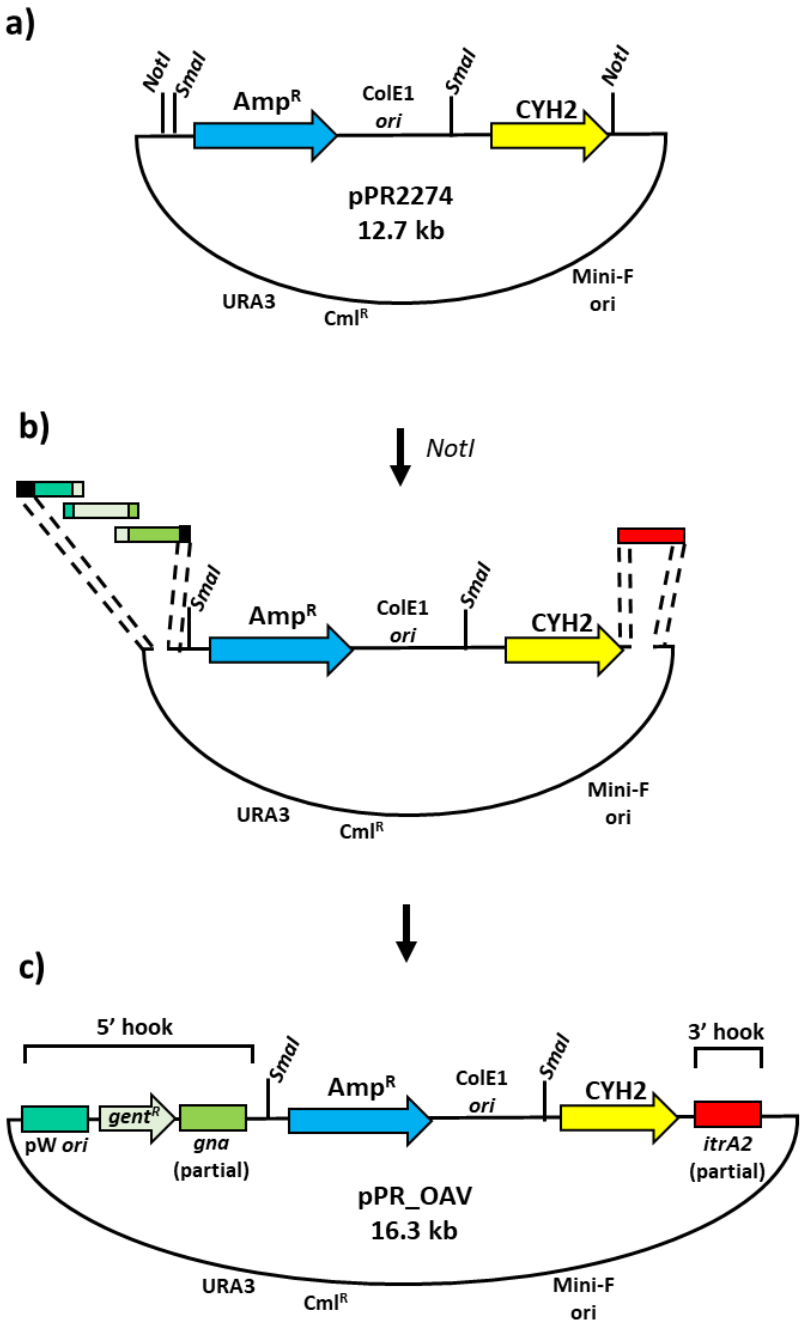

Figure 4.15 Construction of the Operon Assembly Vehicle for the capture of ATCC 17978 variable region. Sequences for ATCC 17978 derived PCR products were obtained from the NCBI database and analysed using SnapGene™. Sequence of pPR2274 was obtained from Liu et al (2017). Complete genes are represented by arrows and incomplete genes by boxes. Gene names/locus tags are denoted within, above, or below arrows/boxes. a) plasmid map of pPR2274. b) Plasmid map of pPR2274 including location of PCR products to be incorporated into the OAV. c) Desired construct of the OAV required to capture AVR genes.

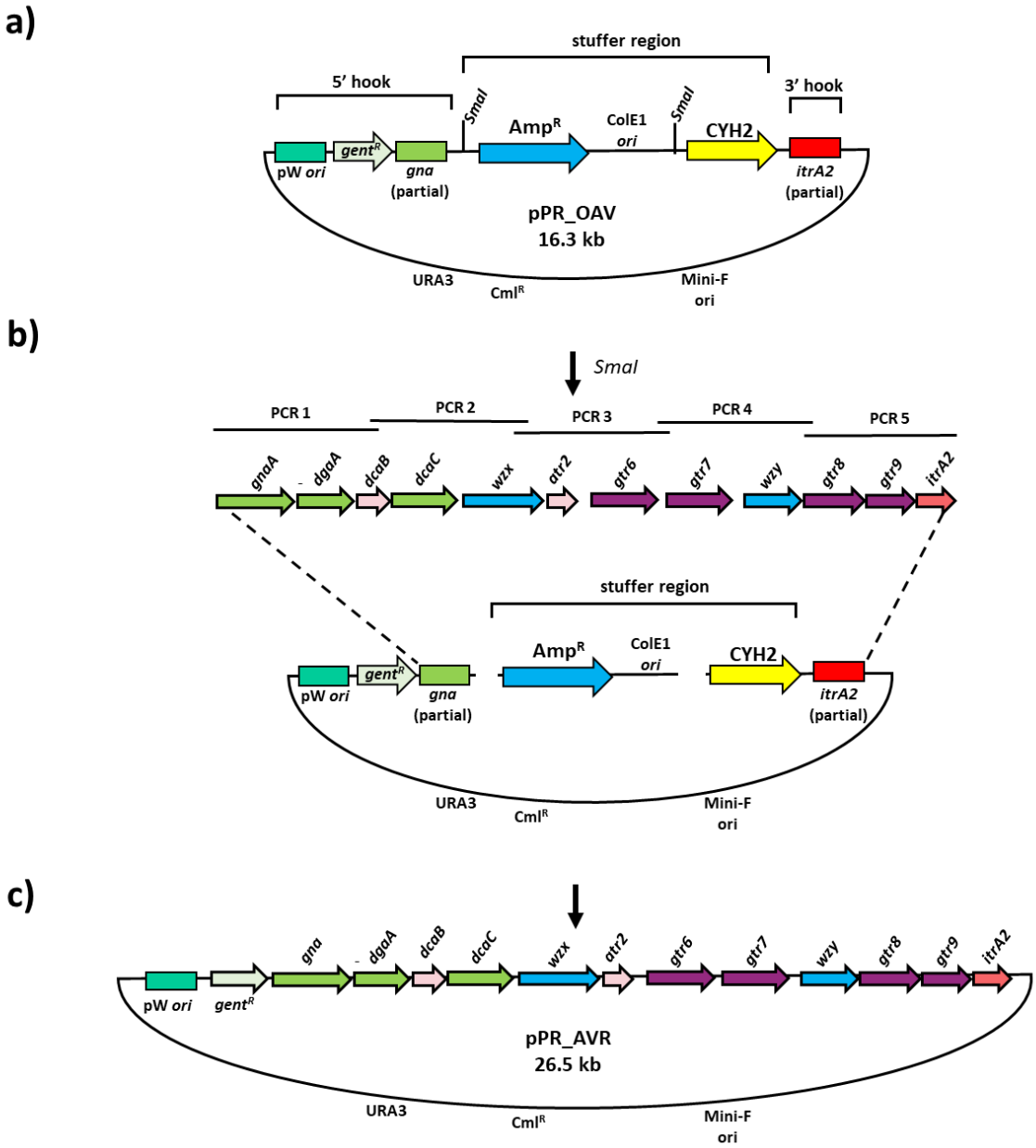

Figure 4.16 Capture of the AVR using the OAV pPR_OAV. Sequences for ATCC 17978 derived PCR products were obtained from the NCBI database and analysed using SnapGene™. Complete genes are represented by arrows and incomplete genes by boxes. Gene names/locus tags are denoted within, above, or below arrows/boxes. a) pPR_OAV for capturing the AVR genes including *Sma*I restriction sites. b) hypothetical location of overlapping PCR products to be cloned into the OAV. c) Desired construct incorporating the AVR for expression in Δ*cps* (pPR_AVR).

Primers were designed to amplify the four PCR products required to make the OAV in a single cloning procedure (Table 2.6, Section 2.4.2). These PCR products were designed to contain overlapping segments that would be recombined by the *S. cerevisiae* DNA repair pathway into the desired vector (Figure 4.16). Upstream from the stuffer region an overlapping series of three PCR products; pWH_*ori*, *gent*^{R}, and upstream hook containing homology to *gna*, were amplified (Figure 4.15b). Two potential promoter regions identified upstream of *gna* using the online promoter prediction tool fruitfly.org (Reese, 2001) were incorporated into the upstream hook region to ensure expression of the KL from the OAV plasmid. Downstream from the stuffer region a single PCR product was designed which consisted of homology to *itrA2* and overhanging regions with the stuffer region and downstream portion of the pPR227 plasmid (Figure 4.15b). Each of these products overlaped 20-40 bp with the neighbouring PCR product to be cloned into the OAV (Fig 4.15, Table 2.6). The hook regions were designed to incorporate all missing genes to ensure expression of capsule when expressed in Δ*cps*. All amplicons were checked to ensure no *Sma*I site was present in their sequence, as digestion with *Sma*I will be needed to create a double stranded break in the plasmid and allow for recombinational repair by yeast (Figure 4.16a).

Briefly, pPR2274 was extracted from *E. coli* JM109 and digested with *Not*I. Cultures of *S. cerevisiae* were harvested and resuspended in TE/LiAc solution (Section 2.5.3, Table 2.5). *Not*I digested pPR2274, PCR products, and sonicated salmon sperm DNA was added to yeast samples. Sonicated salmon sperm DNA acts as a non-specific DNA carrier and increases the uptake of plasmid DNA into the yeast cell (Tripp et al., 2013). Other constituents of the transformation including PEG, LiAC, and DSMO were also added to the transformation buffer to chemically assist in DNA uptake by the yeast (Tripp et al., 2013). After heat shock the cells were recovered on SD ura- plates to select for plasmid uptake (Liu et al., 2017, Liu and Reeves, 2019). A positive control of undigested pPR2274 and negative controls of no plasmid DNA and *Not*I-digested pPR2274 were also prepared. Approximately 50 colonies were recovered from the transformation of *S. cerevisiae* with the pPR2274 plus PCR product hooks. No colonies were recovered from the DNA control, ~50 colonies were recovered from the *Not*I-digested negative control, and ~100 colonies were recovered on the positive (pPR2274) undigested control. Although a similar recovery of cells was seen for the *Not*I digested negative control and the OAV sample, indicating the procedure may not have been

successful, the *S. cerevisiae* recovered from the OAV sample were processed regardless, to check for successful recombination. Colonies were pooled from the SD ura- plates, plasmids extracted and retransformed into competent *E. coli* DH10B cells (Section 2.5.1)

Transformed *E. coli* DH10B cells were plated on Gent 12 agar plates and incubated for 24-48 hrs. No colonies were formed on the Gent 12 plates after 24 hrs, at 48 hrs 12 colonies had formed and a colony PCR using primers for the *gent*^{R} cartridge was performed (Section 2.4.2.3, Table 2.6) on these cells. None of the resulting colonies amplified a PCR product, thus this attempt at making an OAV was unsuccessful.

Shortly after this attempt to create an OAV for complementation of Δ*cps*, the full sequence and annotation of the pWH1266 plasmid was made available (Lucidi et al., 2018). Prior to this many regions of the plasmid remained cryptic. The sequencing of pWH1266 revealed a toxin/antitoxin system close to the *ori*. It is suspected this may be the reason for the failure to modify the OAV for replication in *A. baumannii* and future attempts would require the incorporation of a much larger portion of pWH1266 to ensure cell viability and plasmid stability. Shortly after this discovery a member of our group successfully cloned a larger segment of pWH1266 into pPR2274, including the toxin/antitoxin system, and showed this plasmid could be expressed in both *E. coli* and *A. baumannii* (data not shown). Due to time constraints, the OAV experiment was abandoned and studies were focused on characterising the acapsular mutants.

4.3 Conclusions

A total of four *A. baumannii* acapsular mutants were generated in this study, three in the strain ATCC 17978 and one in 04117201. In ATCC 17978 three deletion mutants were generated which interrupted different steps of the capsule biosynthesis pathway, laying a firm base for comprehensive analysis of the role of capsule in *A. baumannii* virulence. Furthermore; this is the first-time successful generation of a stable Δ*wzy* mutant in *A. baumannii* has been reported. The ability to produce mutants in ATCC 17978 was greatly enhanced by applying a new streamlined recombineering method which allowed for the construction of mutants without the necessity of cumbersome and time-consuming cloning steps (Tucker et al., 2014).

A major limitation of this study was the failure to identify and clone a resistance

cassette suitable for use as a selection marker in the *A. baumannii* strain 04117201. Due to high levels of resistance to all but one commonly used resistance marker incorporation of either *tel*^{R} or *amk*^{R} was vital to the production of a capsule swap or complementation of acapsular mutants in 04117201. Another limitation of this study was the failure to produce a capsule swapped mutant. Although amplification of the operon assembly protocol (OAP) KL2 and KL3 variable regions was successful neither were cloned into a plasmid vector. The employment of recombineering also failed to produce a capsule swap. Some progress was made on adapting a yeast homologous recombination system for use in *A. baumannii* but ultimately this experiment was set aside due to time constraints.

Whilst capsule deficient mutants have previously been investigated in *A. baumannii* these studies have lacked an in-depth analysis of the role capsule plays in environmental persistence and host-pathogen interactions. The following chapter investigates the role capsule plays in ability of *A. baumannii* to withstand a range of environmental stressors that may be encountered.

5 THE ROLE OF CAPSULE IN ENVIRONMENTAL PERSISTENCE OF *A. BAUMANNII*

5.1 Introduction

The ability to survive harsh environmental conditions has undoubtedly contributed to the success of *A. baumannii* as an opportunistic pathogen by facilitating persistence on hospital surfaces and maintaining reservoirs which are often the source of transmission and infection (Wendt et al., 1997). Additionally, the ability to produce biofilms on indwelling devices and ventilator tubing as well as the capacity to actively move towards sources of nutrients enhance the pathogenic potential of many *A. baumannii* strains (Eijkelkamp et al., 2011b). Though only limited evidence is available, studies suggest surface exposed polysaccharides such as capsule are protective against environmental stressors and contribute to antimicrobial resistance (Section 1.6, 1.7). For instance, a recent study showed a protective role for *A. baumannii* capsule against many environmental stressors including desiccation and common hospital disinfectants (Tipton et al., 2018). Furthermore, abolition of capsule has been linked to changes in the ability of *A. baumannii* to produce biofilm and display a motile phenotype (McQueary et al., 2012, Lees-Miller et al., 2013).

In this chapter, the role of capsule in the survival of *A. baumannii* under environmental stress was investigated. Acapsular variants were generated in the *A. baumannii* strains ATCC 17978 and 04117201 as they have diverse capsule types, vary considerably in their virulence potential (Chapter 3), and have previously been genetically manipulated (Section 3, Section 4.2.1). Three acapsular variants were generated in ATCC 17978 by removing the capsule polymerase (Δ*wzy*), initial transferase (Δ*itrA2*), and variable region (Δ*cps*) of the K loci (Section 4.2.5). Strains complemented with a WT copy of the gene of interest, generated for two of the ATCC 17978 acapsular mutants, Δ*wzy* and Δ*itrA2*, were also assessed (Section 4.2.5.3). Additionally, a single acapsular mutant constructed for the *A. baumannii* strain 04117201 (Δ*wzy*) was included for some of the environmental stress assays (Section 4.2.5.3). This was because it was later identified that *A. baumannii* strain 04117201Δ*wzy* had a secondary mutation elsewhere which

affected off target processes (Section 4.2.3). Phenotypes assessed included planktonic growth rates, biofilm production, desiccation survival, and resistance to temperature, osmotic and acidic stressors. Additionally, resistance to selected antimicrobial compounds was determined. These stressors and phenotypes were designated as 'environmental' as they affect survival of *A. baumannii* outside of the human host. It is, however, important to note that the response to some of these stressors, e.g. temperature and acidic stress, also affect survival within the human host and the designation given is somewhat arbitrary.

5.2 Results and discussion

5.2.1 Growth in rich media

Prior to evaluation of environmental stress tolerance, the growth of *A. baumannii* WT and acapsular variants in rich media was determined. For liquid cultures, typical conditions involved inoculation of MH medium with ON culture and incubation at 37^{o}C with shaking (Section 2.2, Table 2.4). Typical growth on solid medium involved inoculation of 1% MH agar plates and incubation at 37^{o}C for 18 hrs (Table 2.4).

When grown on solid MH medium (Table 2.4), WT *A. baumannii* colonies were smooth and glossy, whereas colonies of the acapsular variants were smaller in size and friable, especially the Δ*wzy* variant of ATCC 17978 (Figure 5.1). Furthermore, Δ*wzy* colonies varied greatly in size, from punctiform to colonies 2 mm in diameter (Figure 5.1). The growth of *A. baumannii* ATCC 17978 WT and acapsular variants in liquid medium was compared to identify any growth defects (Section 2.2, Table 2.4). Strains were grown for 8 hrs and cell density was determined by the OD_{600} at given time points (Section 2.11.1). Both Δ*itrA2* and Δ*wzy* acapsular mutants showed slightly extended lag phases compared to the ATCC 17978 WT (Figure 5.2a), whereas this pattern was less prominent for the Δ*cps* mutant (Figure 5.2b). The same pattern (as shown in Fig 5.2a) was seen between the 04117201 strains, as the lag phase of the Δ*wzy* derivative was slightly extended compared to the WT parent (Figure 5.2c). All acapsular variants showed quicker sedimentation than the WT strains and a tendency to form cell clusters in liquid media (data not shown).

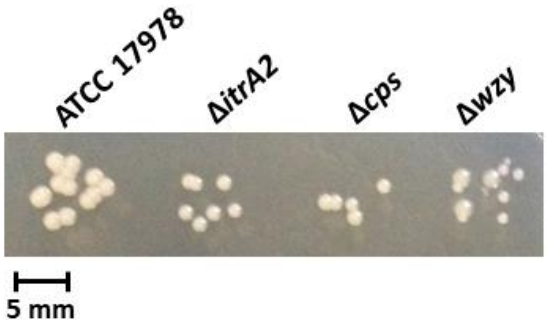

Figure 5.1. Growth of *A. baumannii* ATCC 17978 WT and acapsular variants on solid medium. Strains were grown in liquid MH medium at 37ºC shaking for 4 hrs then diluted equal amounts of each culture were spotted onto 1% MH agar. Plates were incubated at 37ºC for 18 hrs and photographed. Figure is representative of results obtained.

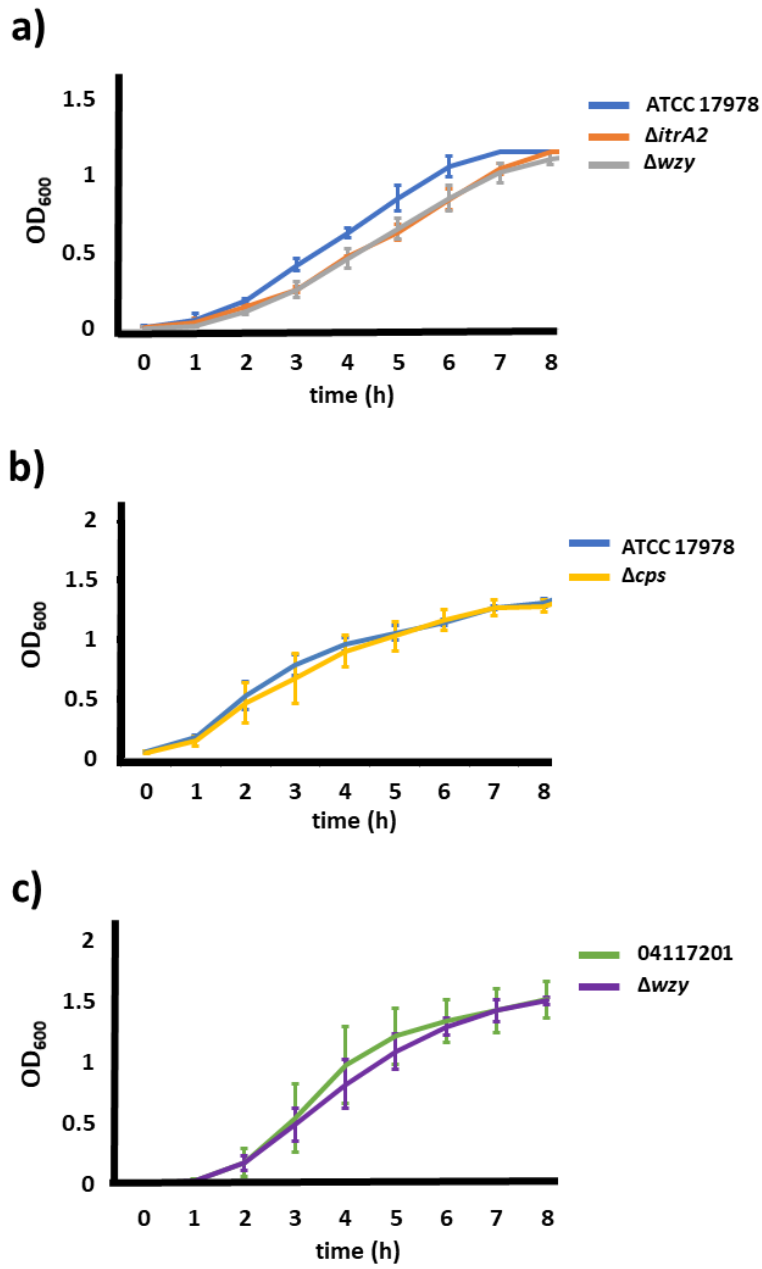

Figure 5.2. Growth curves of WT and acapsular *A. baumannii* strains. Strains were grown in MH medium at 37ºC shaking at 120 rpm for 8 hrs. Cell density (OD_{600}) was measured by spectrophotometer to determine growth. a) WT ATCC 17978 (blue), Δ*itrA2* (orange) and Δ*wzy* (grey). b) WT ATCC 17978 (blue) versus ATCC 17978Δ*cps* (yellow). c) WT 04117201 (green) and 04117201Δ*wzy* (purple). The OD_{600} was recorded using either a Spectronic 200E (Thermofisher Scientific) or DU 640 (Beckman) spectrophotometer. Data represents assays performed in triplicate, error bars represent the standard deviation.

This phenotype has been seen previously in acapsular mutants of other bacterial strains, yet no previous studies investigating *A. baumannii* capsule have mentioned this phenomenon (Tahoun et al., 2017). Increased aggregation and sedimentation of the acapsular *A. baumannii* variants may be associated with the increase in cell surface hydrophobicity described later in this chapter (Section 5.2.2).

Growth of ATCC 17978 Δ*itrA2* and Δ*wzy* acapsular variants was partially restored to WT levels upon complementation, when compared to the respective mutant containing the empty vector (Figure 5.3). Both the complemented (Δ*itrA2*C, Δ*wzy*C) and empty vector pairs (Δ*itrA2*E, Δ*wzy*E) for Δ*itrA2* and Δ*wzy*, respectively, showed lower growth rates compared to the WT and acapsular variants (Figure 5.3). This effect may be due to the presence of the pWH1266 plasmid. When the pWH1266 plasmid was introduced into the WT ATCC 17978 strain, no growth defect was seen (data not shown). Incomplete complementation of growth defects has previously been seen when re-introducing a WT gene into an *A. baumannii* deletion mutant on pWH1266 (Li et al., 2016b, Funahashi et al., 2012). Furthermore, a number of studies have shown only partial complementation for a range of phenotypes by re-introduction of a WT gene into *A. baumannii* on pWH1266 (Saroj et al., 2012, Liou et al., 2014, Wang et al., 2018).

5.2.2 Capsule alters cell surface hydrophobicity and perturbs biofilm formation

As capsule forms the outer-most layer of the bacterial cell, removing the capsule is bound to have implications for cell surface properties such as hydrophobicity and adherence capability. In Chapter 3 it was determined that both 04117201 and ATCC 17978 WT *A. baumannii* strains have hydrophilic cell surfaces (Section 3.2.2). It was hypothesised that acapsular variants of both strains would display increased cell surface hydrophobicity compared to their WT counterparts as capsule masks many hydrophobic structures on the bacterial cell surface including BAP and lipid A (Brossard and Campagnari, 2012, Powers and Trent, 2018). To investigate whether capsule production influences cell surface hydrophobicity in *A. baumannii*, the WT and acapsular strains of 04117201 and ATCC 17978 were assessed for their affinity to the hydrocarbon xylene compared to water (Section 2.18).

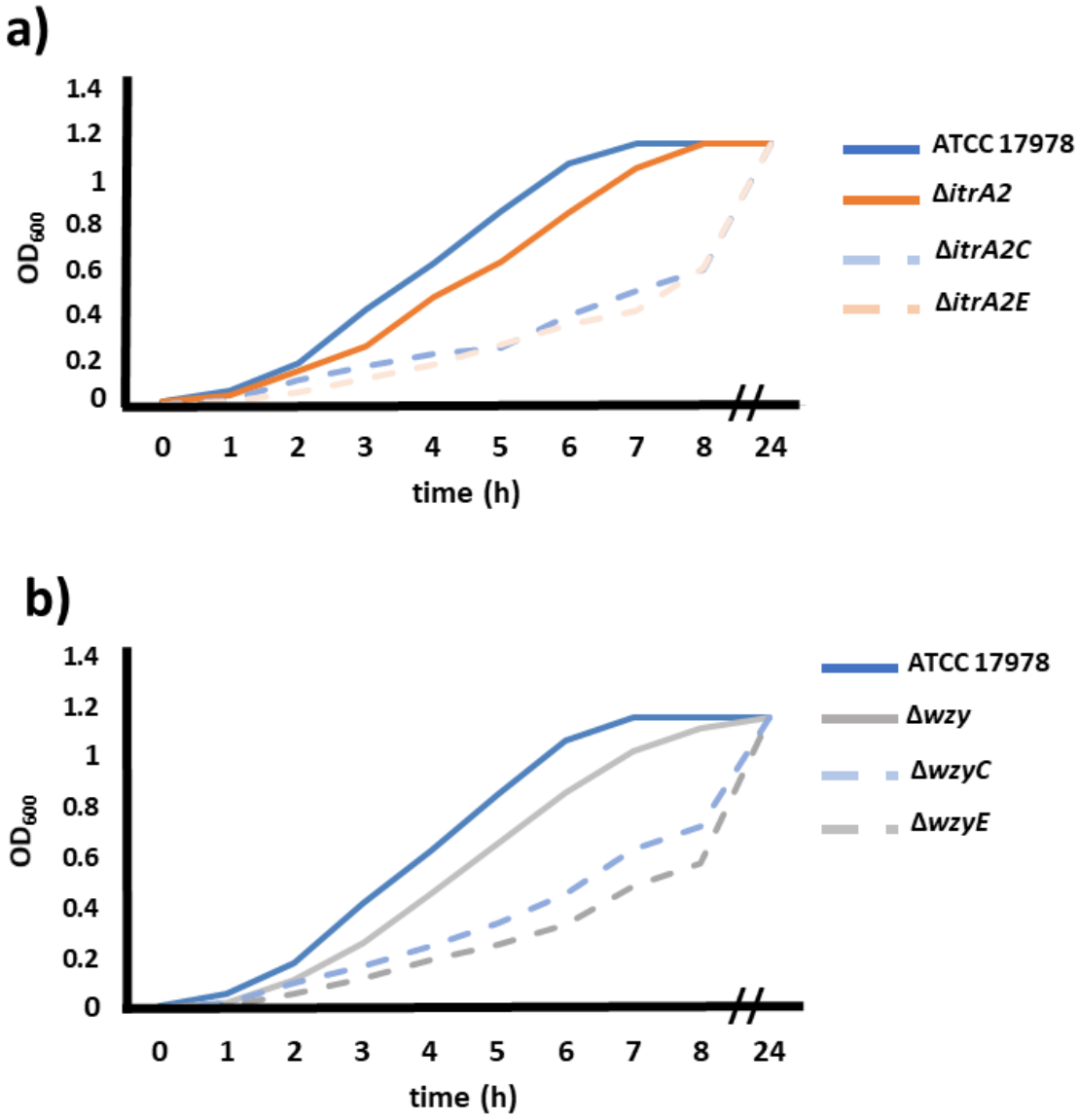

Figure 5.3. Growth curves of complemented *A. baumannii* ATCC 17878 acapsular mutants. Strains were grown in MH medium at 37ºC shaking for 24 hrs. a) ATCC 17978 WT (blue) and ATCC 17978 Δ*itrA2* (orange), complemented ATCC 17978 Δ*itrA2* (Δ*itrA2*C [light blue perforated]) and ATCC 17978 Δ*itrA2* containing the pWH1266 empty vector (Δ*itrA2*E [light orange perforated]). b) ATCC 17978 WT (blue) and ATCC 17978 Δ*wzy* (grey), complemented ATCC 17978 Δ*wzy* (Δ*wzy*C [light blue perforated]) and ATCC 17978 Δ*wzy* containing the pWH1266 empty vector (Δ*wzy*E [light grey]). OD_{600} was recorded using the DU 640 spectrophotometer (Beckman). Data is displayed as a representative growth curve.

The cell surface hydrophobicity was expressed as the HI (%), which represents the percentage of bacterial cells associated with the xylene layer of the assay (Section 2.18) (Rosenberg, 2017).

The 04117201 WT was completely hydrophilic with a HI of 0%, whereas the acapsular Δ*wzy* variant of 04117201 had an average HI of 10% (Figure 5.4a). The change in hydrophobicity by removing capsule in 04117201 was modest and highly variable between replicates. There was no significant difference in hydrophobicity between the WT 04117201 and Δ*wzy* variant using a two tailed student T-Test (Figure 5.4a). Contrastingly, all acapsular mutants of ATCC 17978 showed high levels of hydrophobicity (HI >90%) compared to their hydrophilic (HI 0%) WT parent (Figure 5.4b). When the ATCC 17978 WT *itrA2* and *wzy* genes were re-introduced the hydrophilic phenotype was restored, Δ*itrA2*C had a HI of 20% compared to 85% for Δ*itrA2*E, and Δ*wzy*C a HI of 2% compared to 92% for Δ*wzy*E (Figure 5.4b).

These results suggest that the effect of capsule on cells surface hydrophobicity is strain dependent, as removal of capsule in 04117201 resulted in only a modest change in hydrophobicity whereas for ATCC 17978 a drastic difference in hydrophobicity was seen between the WT and acapsular variants. Various cell surface components or variations in capsule produced may mask the influence of capsule on surface hydrophobicity for some *A. baumannii* strains including 04117201 (Section 1.4), (Tipton et al., 2015, Giles et al., 2015).

Biofilms are an alternate growth state where bacteria adhere to a surface and form an enclosed community surrounded by a protective extracellular matrix (Longo et al., 2014). This enhances persistence of bacterial colonies in the nosocomial environment by providing protection from environmental stressors and antimicrobial compounds (Høiby et al., 2011). Biofilm production is a multifactorial process and is influenced by environmental cues including light, temperature, cell density, iron availability and quorum sensing (Section 1.2.2).

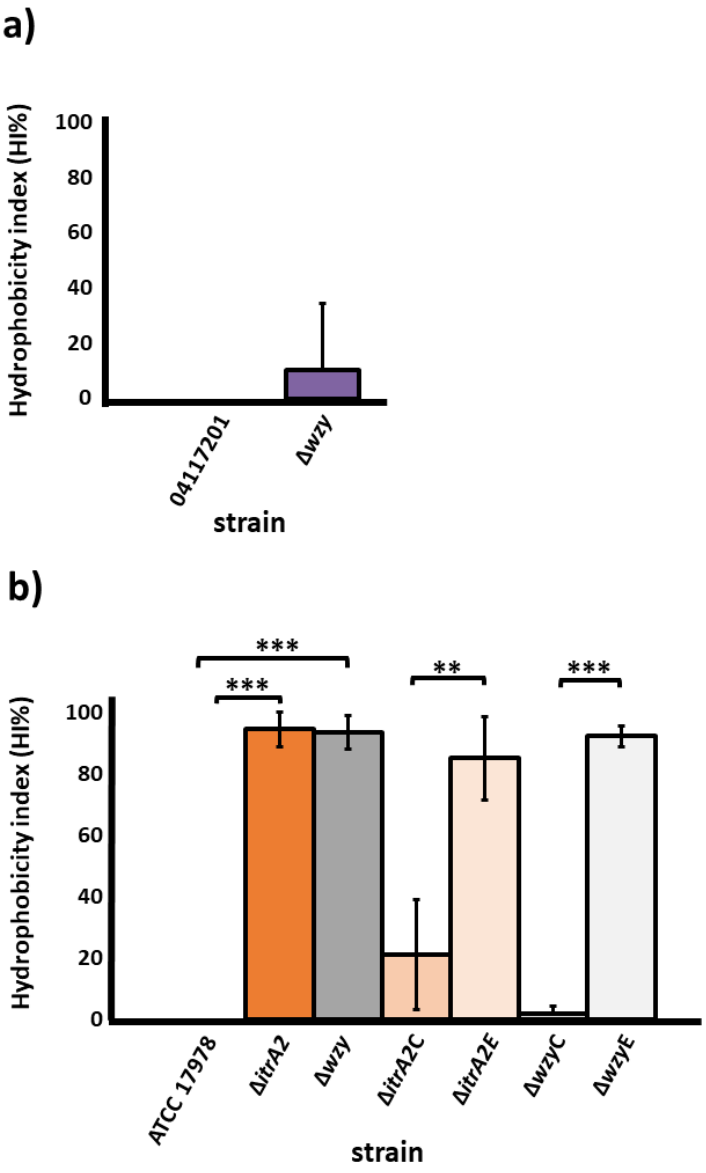

Figure 5.4. Cell surface hydrophobicity of *A. baumannii* ATCC 17978, 04117201 and acapsular variants. Hydrophobicity was measured by cell affinity to xylene. No visible bar indicates a completely hydrophilic strain. a) hydrophobicity of 04117201 and acapsular variant 04117201Δ*wzy* (purple). b) hydrophobicity of ATCC 17978, acapsular variants Δ*itrA2* (orange) and Δ*wzy* (grey), complemented strains for Δ*itrA2* (Δ*itrA2*C [medium orange]) and Δ*wzy* (Δ*wzy*C [grey]), and acapsular variants with empty vector for Δ*itrA2* (Δ*itrA2*E [light orange]) and Δ*wzy* (Δ*wzy*E [light grey]). Data represent assays performed in triplicate; error bars represent the standard deviation. Statistical significance was assessed using the two-tailed student T-Test (**= p value <0.01, ***=p value <0.001).

Biofilm formation was assessed for the acapsular mutants using a static biofilm assay (Section 2.16). Capsule production was found to impede biofilm formation for 04117201 as the acapsular mutant produced 2.6-fold more biofilm than the WT parental strain, though this difference was not statistically significant as judged by a two-tailed student T-Test (Figure 5.5a). Substantial variability was seen between biofilm assay replicates for 04117201 WT and the acapsular strain, this may have been caused by inconsistencies in bacterial starting concentrations or metabolic differences between samples (Figure 5.5a). Additionally, slight changes in environmental conditions could also have affected biofilm production between replicates (Wood et al., 2018, Tomaras et al., 2003, Bhargava et al., 2014).

Previous studies have demonstrated that ATCC 17978 is a weak biofilm producer compared to other *A. baumannii* strains (Eijkelkamp et al., 2011b). Because of this, large differences in biofilm production were not expected between the *A. baumannii* ATCC 17978 WT and acapsular strains (Figure 5.5b). The ATCC 17878 acapsular variants, Δ*itrA2* and Δ*wzy*, displayed increased biofilm production of 2.9- and 2.4-fold compared to the WT parent, respectively (Figure 5.5b). Furthermore, a difference in biofilm production was seen between the ATCC 17978 Δ*itrA2* and Δ*wzy* variants, suggesting the removal of these genes differentially impacts on biofilm production (Figure 5.5b). Unexpectedly, the Δ*cps* strain showed no difference in biofilm production compared to the WT ATCC 17978. Complementation of Δ*itrA2* and Δ*wzy* with a WT copy of the removed gene resulted in partial restoration of the parental phenotype (Figure 5.5b). Previous studies have demonstrated biofilms produced by *A. baumannii* acapsular mutants are rough and disordered, suggesting the biofilm structure in the absence of capsule may not provide the protective factors of a typical biofilm (Lees-Miller et al., 2013). Further analysis of the biofilm structure using scanning electron microscopy (SEM) would be useful to determine whether the biofilm structures produced by the acapsular strains represent typical biofilm architecture.

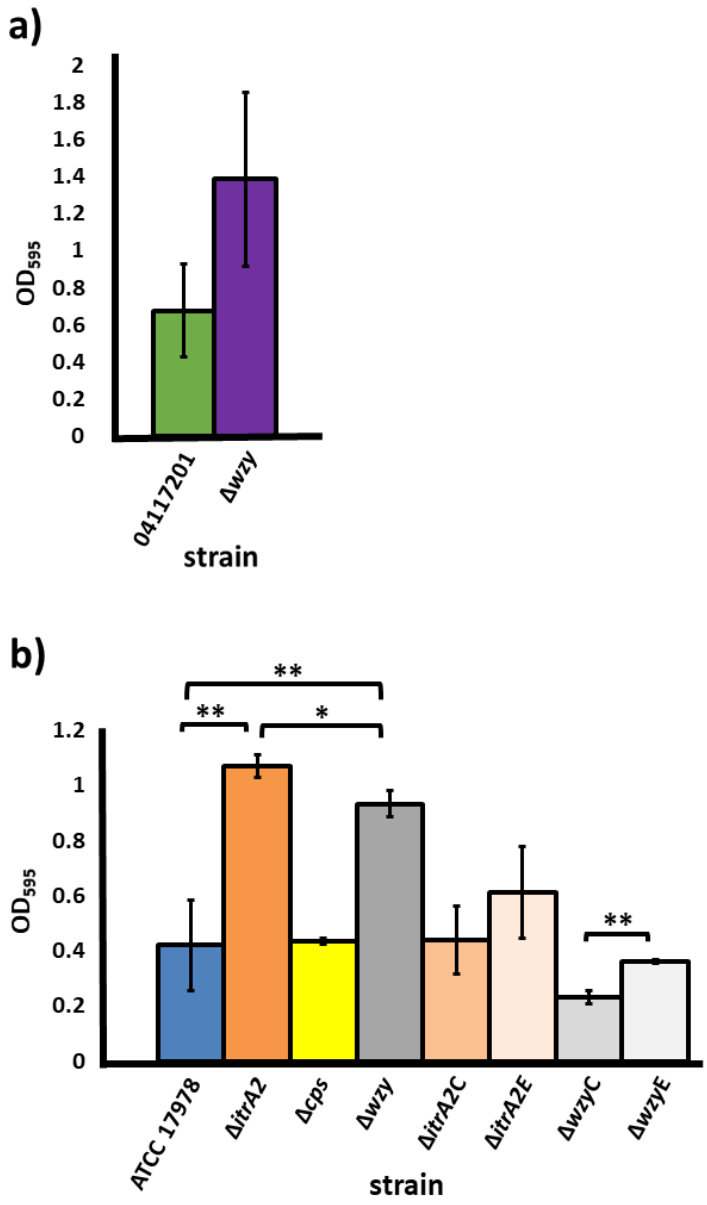

Figure 5.5. Biofilm production by *A. baumannii* ATCC 17978, 04117201 and acapsular mutants. Biofilm production was measured as absorbance of crystal violet at 595 nm (OD_{595}). a) biofilm production of 04117201 (green) and acapsular variant 04117201Δ*wzy* (purple). b) biofilm production of ATCC 17978 (blue), acapsular variants Δ*itrA2* (orange) and Δ*wzy* (gray), complemented strains for Δ*itrA2* (Δ*itrA2*C [medium orange]) and Δ*wzy* (Δ*wzy*C [medium grey]), and acapsular variants with empty vector for Δ*itrA2* (Δ*itrA2*E [light orange]) and Δ*wzy* (Δ*wzy*E [light gray]). Data represents assays performed in triplicate, error bars represent the standard deviation. Statistical significance was assessed using the two-tailed student T-Test; ** <0.01, * <0.001.

5.2.3 The role of capsule in protection against acidic pH stress

Tolerating fluctuations in acidity is an important trait of many pathogens. Acidic environments that may be encountered by *A. baumannii* include human skin and the phagolysosomes of macrophages (Luebberding et al., 2013, Joly-Guillou, 2005). In other bacterial species, the production of surface polysaccharides aid survival in acidic conditions. For example, the removal of genes required for exopolysaccharide production in the gastric pathogen *E. coli* O157:H7 led to a reduction in acid tolerance (Mao et al., 2006, Mao et al., 2001). Similarly, production of capsule and exopolysaccharide are required for tolerating low pH by the probiotic bacterium *Bifidobacterium longum* (Tahoun et al., 2017).

In Section 3, the ability to survive and grow in acidic environments was identified in a range of *A. baumannii* strains (Section 3.2.3). The 04117201 strain showed high tolerance to acidic stress compared to other strains, whereas ATCC 17978 displayed a relatively low tolerance (Section 3.2.3). (Mao et al., 2006, Mao et al., 2001, Tahoun et al., 2017). It was hypothesised that a reduction in growth for the acapsular variants compared to the WT parents would be seen, as the barrier between the cell cytosol and the external environment would be compromised, making it more difficult for the bacterium to maintain internal pH homeostasis. The WT *A. baumannii* strains 04117201 and ATCC 17978, and their respective acapsular variants, were grown in MH medium at optimal pH (pH 7.5) and acidic pH (pH 5.5) at 37^{o}C for 48 hours (Section 2.11.2). A similar growth rate was seen for 04117201 and Δ*wzy* under acidic stress (pH 5.5) compared to optimal pH (7.5) (data not shown). Growth of ATCC 17978 WT and acapsular variants was substantially impeded at a pH of 5.5 compared to a pH of 7.5 (Figure 5.6).

Both the Δ*itrA2* and Δ*cps* ATCC 17978 acapsular mutants failed to grow at pH 5.5, whereas the WT and Δ*wzy* were capable of growth under acidic stress, albeit slower than at pH 7.5 (Figure 5.6). Interestingly, the ATCC 17978 Δ*wzy* variant grew better than the WT strain at pH 5.5, though this was not deemed statistically significant due to variation between replicates. The ability of Δ*wzy* to grow under acidic conditions better than the Δ*itrA2* and Δ*cps* variants may be due to Δ*wzy* retaining protein glycosylation or single K units being exported to the cell surface (Figure 5.6).

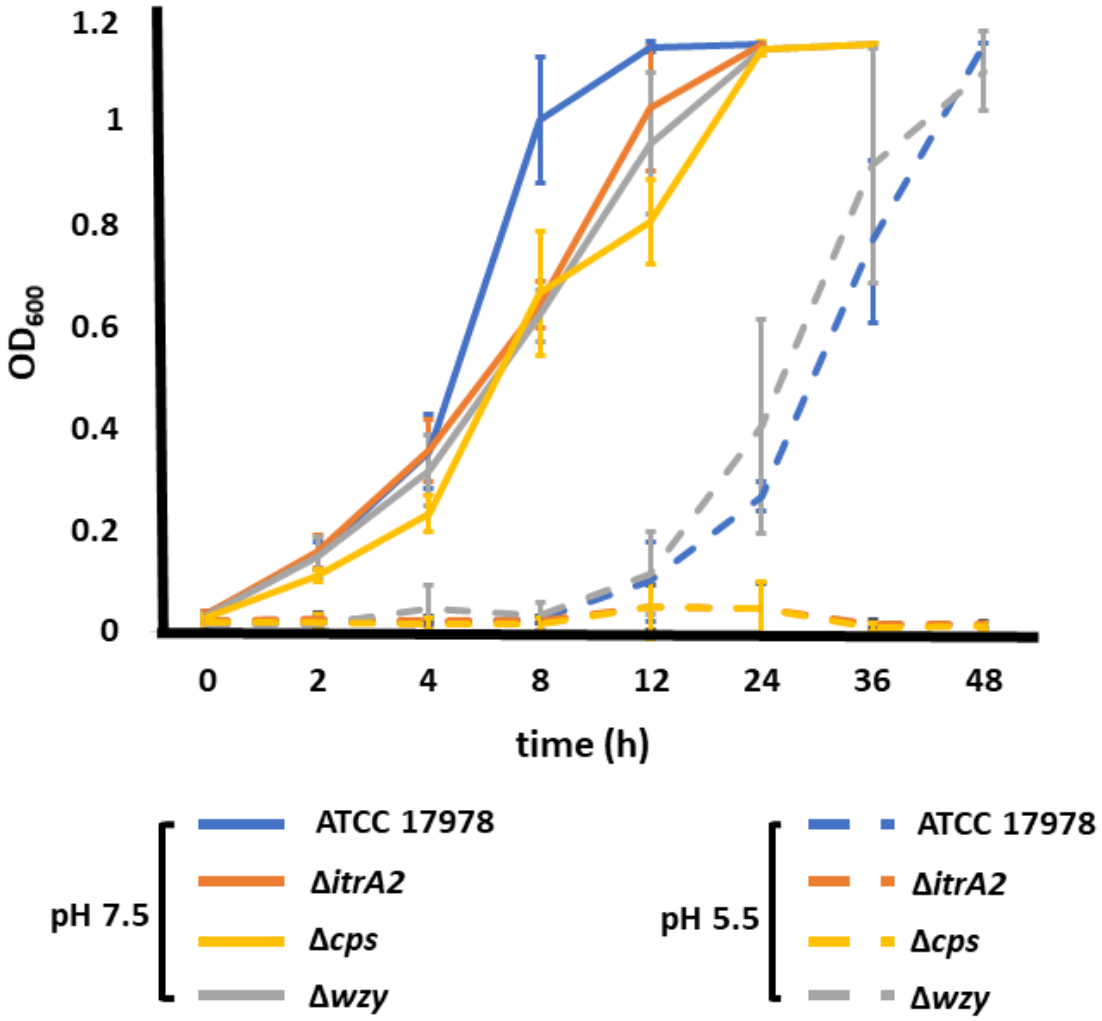

Figure 5.6. Growth of *A. baumannii* ATCC 17978 WT and acapsular mutants under acidic pH stress. Strains were grown in MH medium for at 37ºC shaking at 120 rpm for 48 hours. Solid lines represent growth in medium at pH 7.5 and perforated lines growth in medium at pH 5.5, ATCC 17978 WT (blue), Δ*itrA2* (orange), Δ*cps* (yellow), Δ*wzy* (grey). OD_{600} was recorded using a DU 640 spectrophotometer (Beckman). Data represents assays performed in triplicate; error bars represent the standard deviation.

The increased acid tolerance of Δ*wzy* compared to Δ*itrA2* and Δ*cps* could be due to the significant perturbation of the cell wall seen in Δ*wzy* compared to the other ATCC 17978 derived acapsular strains (See Section 4.2.5.5), or downstream effects of *wzy* deletion in ATCC 17978 not directly linked to capsule production. These differences may also be due to protein glycosylation remaining intact for Δ*wzy* but not Δ*itrA2* and Δ*cps*. Additionally, single K units may be exported to the cell surface for Δ*wzy* but not in the Δ*itrA2* and Δ*cps* strains.

Overall, the results for ATCC 17978 Δ*itrA2* and Δ*cps* variants support these previous studies that associate the production of surface polysaccharides with increased tolerance of acidic conditions.

5.2.4 The role of capsule in the response to osmotic stress

A. baumannii can persist within environments of varying osmolarity and fluctuating concentrations of solutes. For instance, the osmolarity between the external environment and within different host niches varies considerably thus tolerating differences in osmolarity is essential for *A. baumannii* colonisation and infection. Several properties of *A. baumannii* including low membrane permeability, the production of stabilising compounds, and modification of membrane lipids aid in its ability to withstand osmotic stress (Zeidler and Müller, 2019b, Zeidler and Müller, 2019a, Breisch and Averhoff, 2020, Sand et al., 2014). In some bacterial species, such as *K. pneumoniae* and *E. coli*, capsule is involved in resistance to osmotic stress (Wang et al., 2013, Kuzhiyil et al., 2012). Therefore, the role of capsule in withstanding osmotic stress was investigated for *A. baumannii*.

The osmotic stress response of the WT and acapsular variants of *A. baumannii* 04117201 and ATCC 17978 were evaluated using two osmolytes, sucrose and NaCl. Two methods were employed to assess growth under osmotic stress, growth curves in MH medium containing additional osmolytes (Section 2.11), and growth of bacteria on solid MH medium containing increasing levels of osmolyte (Table 2.4).

There was no difference in the growth curves of 04117201 WT compared to the Δ*wzy* mutant under osmotic stress (20% sucrose or 20% NaCl) (Figure 5.7).

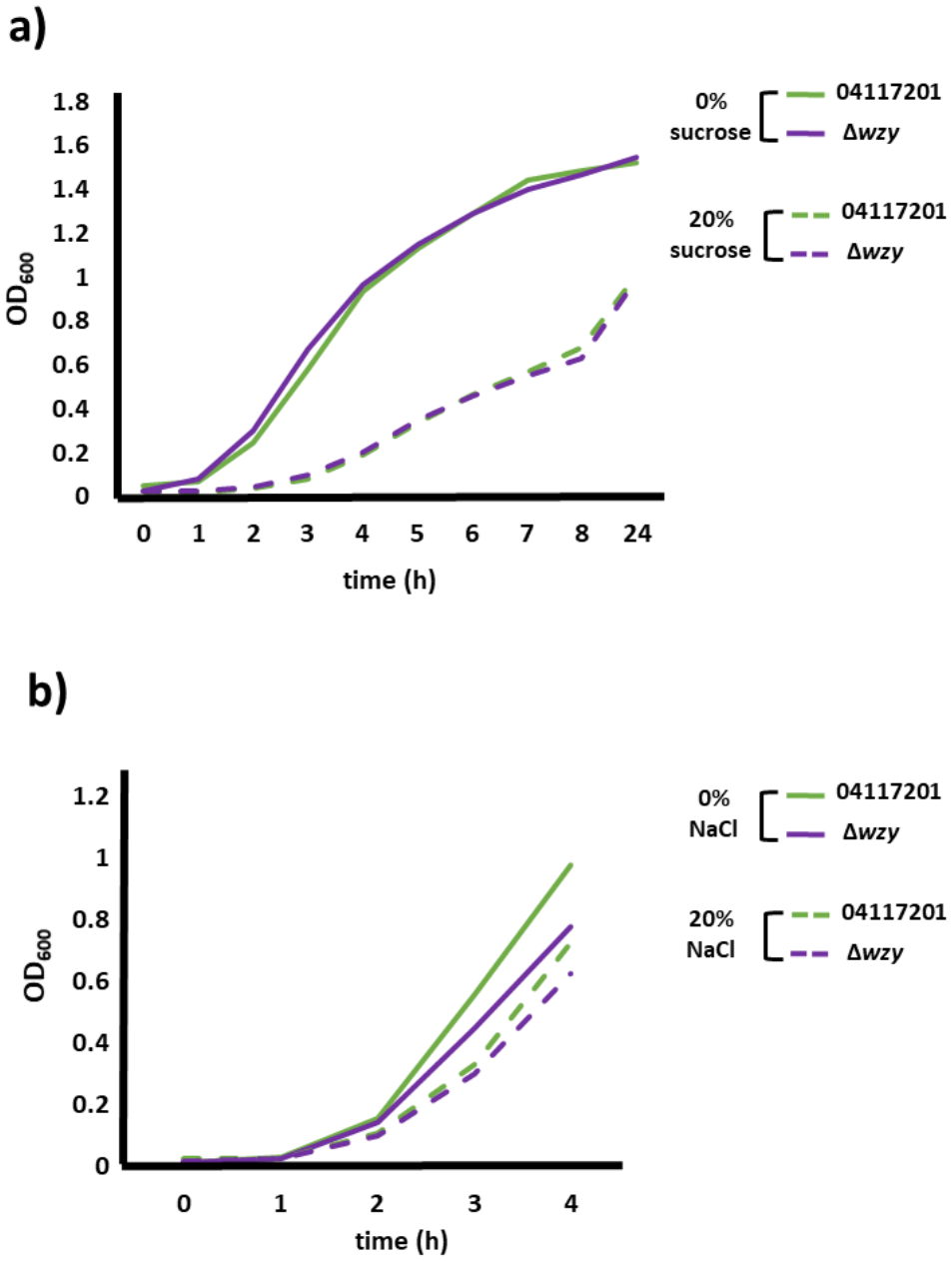

Figure 5.7 Osmotic stress tolerance of 04117201 and 04117201Δ*wzy*. Solid lines represent growth in the absence of osmotic stress and perforated lines growth in the presence of osmotic stress, WT 04117201 (green) and 04117201Δ*wzy* (purple). a) growth curves in MH broth supplemented with 20% sucrose at 37ºC shaking for 12 hours. b) Growth in MH medium supplemented with 20% NaCl at 37ºC shaking at 120 rpm for 4 hours. OD_{600} was recorded using the DU 640 spectrophotometer (Beckman). Data represent the average of two replicates.

Growth in MH containing 20% sucrose was severely impaired for both 04117201 WT and 04117201Δ*wzy* (Figure 5.7a). A slightly reduced growth rate was seen for both 04117201 WT and 04117201Δ*wzy* in the presence of 20% NaCl (Figure 5.7b).

Because no difference in the osmotic stress response was seen between 04117201 WT and 04117201Δ*wzy* these assays were performed only in duplicate (Figure 5.7). When grown in media containing 20% NaCl no differences were observed between the WT ATCC 17978 and acapsular variants (data not shown). Growth of ATCC 17978 WT and acapsular variants was initially tested in liquid medium supplemented with 20% sucrose, however all isolates failed to grow after 8 hours incubation (data not shown). However, when grown in media supplemented with 15% sucrose the ATCC 17978 WT lagged in growth compared to the Δ*itrA2* and Δ*cps* strains (Figure 5.8a). This result was mirrored on solid MH medium containing increasing concentrations of sucrose and complementation of Δ*itrA2* with the WT *itrA2* gene restored the WT phenotype (Table 2.4, Figure 5.8b). This unexpected result could be due to the increased accessibility of cell surface proteins known to contribute to osmotic stress survival in *A. baumannii* such as the EmrAB efflux pump (Lin et al., 2017) and the TolC-like OMP, AbuO (Srinivasan et al., 2015). Another reason for this increased osmotic stress tolerance seen in the Δ*itrA2* and Δ*cps* strains could be due to changes in cellular morphology where cells are more rounded and compared to WT ATCC 17978, decreasing their surface to volume ratio (Section 4.2.5.5) (Zeidler and Müller, 2019a).

For the Δ*wzy* variant, growth was limited compared to that of the WT ATCC 17978 strain in the presence of 15%-20% sucrose (Figure 5.8, grey). Although Δ*wzy* is capable of growth in MH broth containing 15% sucrose, it was markedly reduced compared to the ATCC 17978 WT, Δ*itrA2* and Δ*cps* strains. When grown on solid media containing 15% sucrose a reduction in cell density of Δ*wzy* compared to the ATCC 17978 WT strain was evident (Figure 5.8b). It is likely that the reduction in osmotic stress tolerance of Δ*wzy* is linked to the gross cellular morphology changes and probable membrane perturbations seen in this mutant (Section 4.2.5.5). The Δ*wzy* cells were larger and deformed compared to the WT ATCC 17978, increasing the surface area and perhaps interfering with the function of cell surface proteins which contribute to osmotic regulation (Zeidler and Müller, 2019a, Zeidler and Müller, 2020).

a)

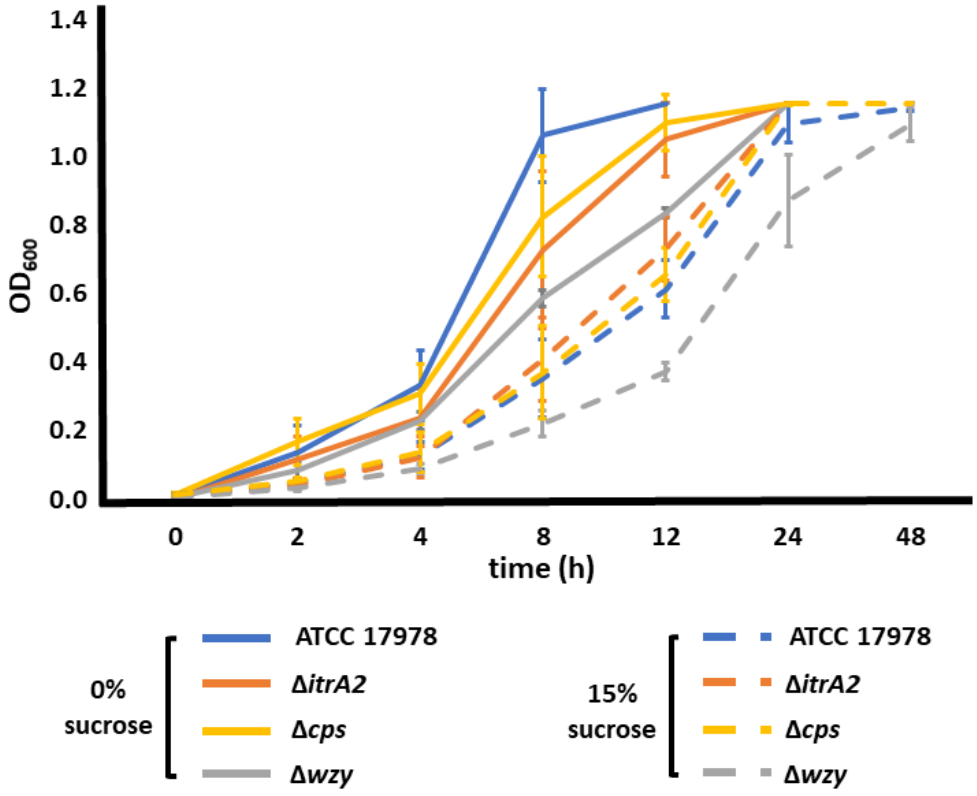
1.4
1.2
1.0
0.8
0.6
0.4
0.2
0.0
OD600
0
2
4
8
12
24
48
time (h)
0% sucrose
ATCC 17978
ΔitrA2
Δcps
Δwzy
15% sucrose
ATCC 17978
ΔitrA2
Δcps
Δwzy

b)

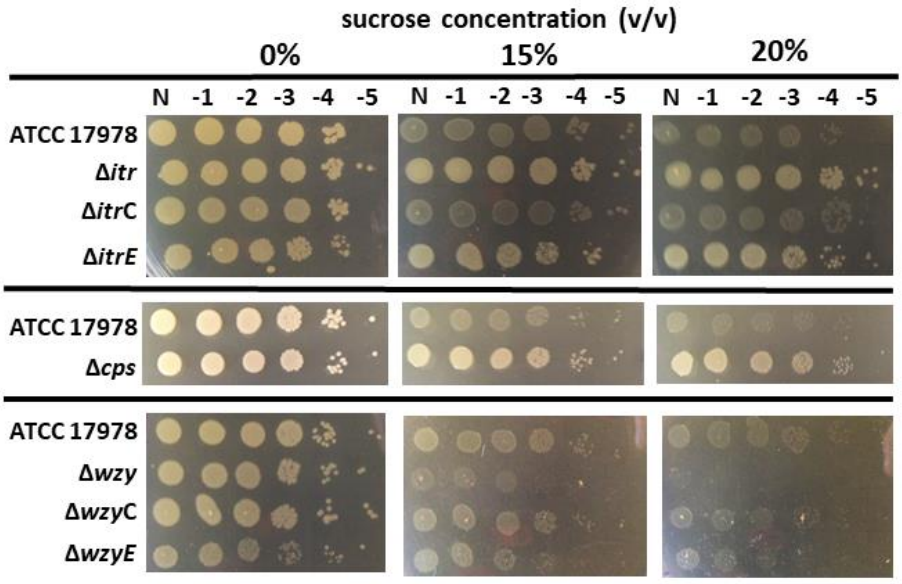
sucrose concentration (v/v)
0%
15%
20%
N -1 -2 -3 -4 -5
N -1 -2 -3 -4 -5
N -1 -2 -3 -4 -5
ATCC 17978
Δitr
ΔitrC
ΔitrE
ATCC 17978
Δcps
ATCC 17978
Δwzy
ΔwzyC
ΔwzyE

Figure 5.8 Osmotic stress tolerance of ATCC 17978 WT and acapsular mutants. a) growth curve of WT and acapsular mutants in MH broth supplemented with 15% sucrose. Bacterial strains were incubated in MH broth at 37ºC shaking for 48 hrs. Solid lines represent growth at 0% sucrose and perforated lines growth at 15% sucrose, ATCC 17978 WT (blue), Δ*itrA2* (orange), Δ*cps* (yellow), Δ*wzy* (grey). Data represent assays performed in triplicate, error bars represent the standard deviation. b) 10-fold dilution series of WT, Δ*itrA2*, Δ*cps*, Δ*wzy*, and complemented strains, on MH agar containing increasing concentrations of sucrose; N represents undiluted cells. Bacteria were grown to an OD_{600} of 0.6 prior to dilutions and plates incubated at 37ºC ON. OD_{600} was recorded using the DU 640 spectrophotometer (Beckman). Assays were performed in triplicate; figures are representative of results obtained.

Although complementation of Δ*wzy* in ATCC 17978 with the WT *wzy* gene partially restored sucrose tolerance on solid media containing 15% sucrose, an increase in sucrose tolerance was also seen for the Δ*wzy* containing the empty pWH1266 vector. This suggests the re-introduction of *wzy* was not responsible for the increased sucrose tolerance of the complemented Δ*wzy* strain. *wzy* (Figure 5.8b).

5.2.5 Response of acapsular variants to temperature stress

Resistance to heat within the nosocomial environment is an often overlooked but important factor in bacterial persistence, as heat is frequently used to decontaminate surfaces and resistant bacteria are more likely to persist on heat-generating medical devices such as endoscopes and monitors (Boll et al., 2016a, Boll et al., 2017). As capsule forms a protective coating around the bacterial cell it was hypothesised that it may protect the bacterium from heat stress. It has previously been demonstrated in certain strains of *E. coli* that the amount of capsule produced is higher at 37ºC compared to 20ºC, though it is yet to be determined if capsule plays a thermotolerance role at higher temperatures for any bacterial species (Willis and Whitfield, 2013).

All growth curves were performed with cells in MH medium, shaking at 120 rpm (Section 2.11.1). Heat tolerance of *A. baumannii* 04117201 and the acapsular 04117201Δ*wzy* variant was assessed by comparing the growth rate of the two strains at 37ºC and 42ºC (Figure 5.9).

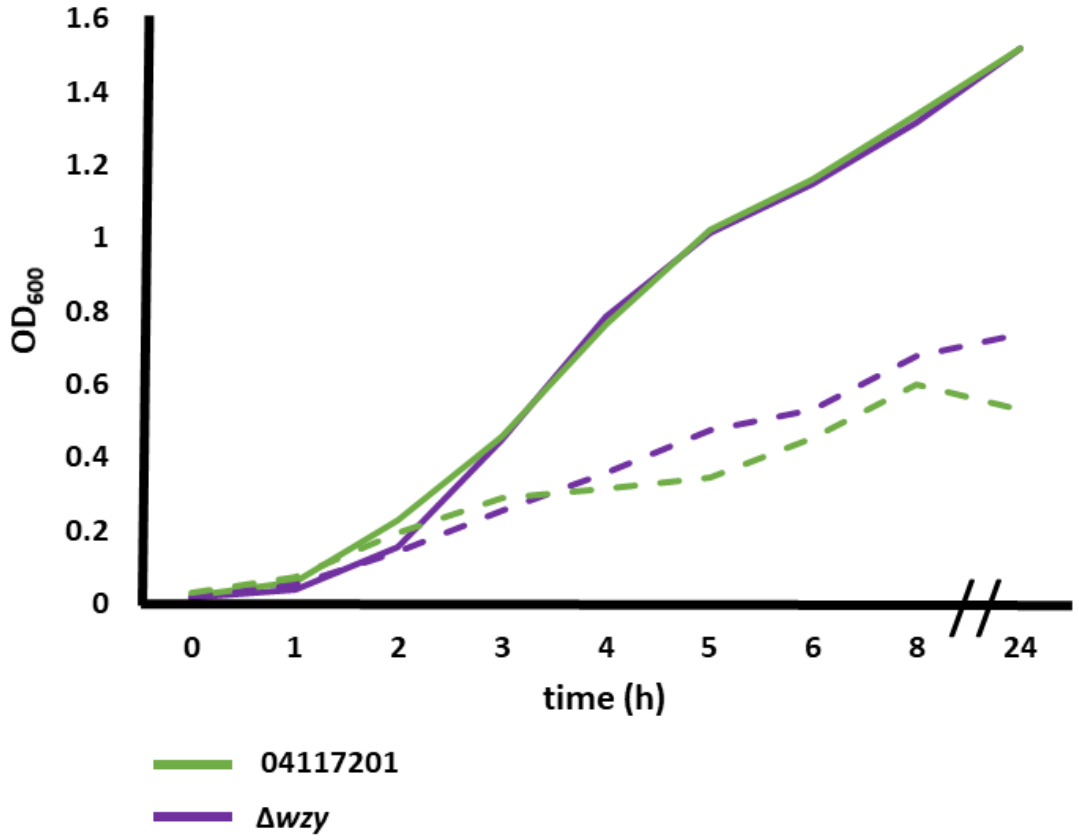

Figure 5.9. Thermotolerance of 04117201 and 04117201Δ*wzy*. Strains were grown in MH medium shaking for 24 hours at either 37°C (solid lines) or 42°C (perforated lines), WT 04117201 (green) and 04117201Δ*wzy* (purple). Growth was measured as OD_{600} using a DU 640 spectrophotometer (Beckman). Data represents the average of two replicates.

Both strains showed reduced growth at 42^{o}C compared to 37^{o}C over 24 hrs. The 04117201Δ*wzy* strain grew slightly better at 42^{o}C compared to the WT 04117201 strain (Figure 5.9). In contrast, there was no difference in growth between the ATCC 17978 WT and acapsular variants at 37^{o}C compared to 42^{o}C. (Figure 5.10a). As more capsule is produced by *E. coli* when grown at 20^{o}C compared to 37^{o}C, the growth of WT and acapsular mutants was also assessed at 20^{o}C. All strains showed reduced growth at 20^{o}C compared to 37^{o}C but no difference was seen between the isolates (data not shown). Due to the high heat tolerance of the ATCC 17978 WT and acapsular strains a heat shock assay at 55^{o}C was performed to identify any difference in thermotolerance between strains (Section 2.19). All strains saw a decrease in viability at 30-, 60- and 90-minutes post heat shock (Figure 5.10b). Although the Δ*itrA2* strain showed slightly higher levels of heat resistance compared to the ATCC 17978 WT and Δ*wzy* strains there was significant variability between the replicates and the differences seen may not be a true representation of a difference in heat tolerance.

5.2.6 Desiccation tolerance of acapsular *A. baumannii*

Desiccation tolerance is a major factor in the sustained colonisation of *A. baumannii* seen within health care settings. Strains of *A. baumannii* can remain viable for months on hospital surfaces, facilitating the spread of infection and reducing the capability to control outbreaks (Jawad et al., 1998). Desiccating environmental conditions poses numerous challenges to bacterial cells including starvation, dehydration, osmolyte imbalances, and disruption of the cellular structure (Wang et al., 2020). A number of factors including growth phase (Zeidler and Müller, 2019b, Chiang et al., 2017), acetylation of lipid A (Boll et al., 2015), protein aggregation (Wang et al., 2020) and production of surface polysaccharides (Chin et al., 2018, Tipton et al., 2018, Tipton et al., 2015, Gayoso et al., 2013) have been identified as promoting desiccation survival in *A. baumannii*. C (Section 1.6.2). A recent study has shown that capsule production enhances desiccation tolerance in the *A. baumannii* strain AB5075, as removal of the capsule export gene *wzc* in this strain resulted in a 2.5-fold reduction in desiccation survival (Tipton et al., 2018).

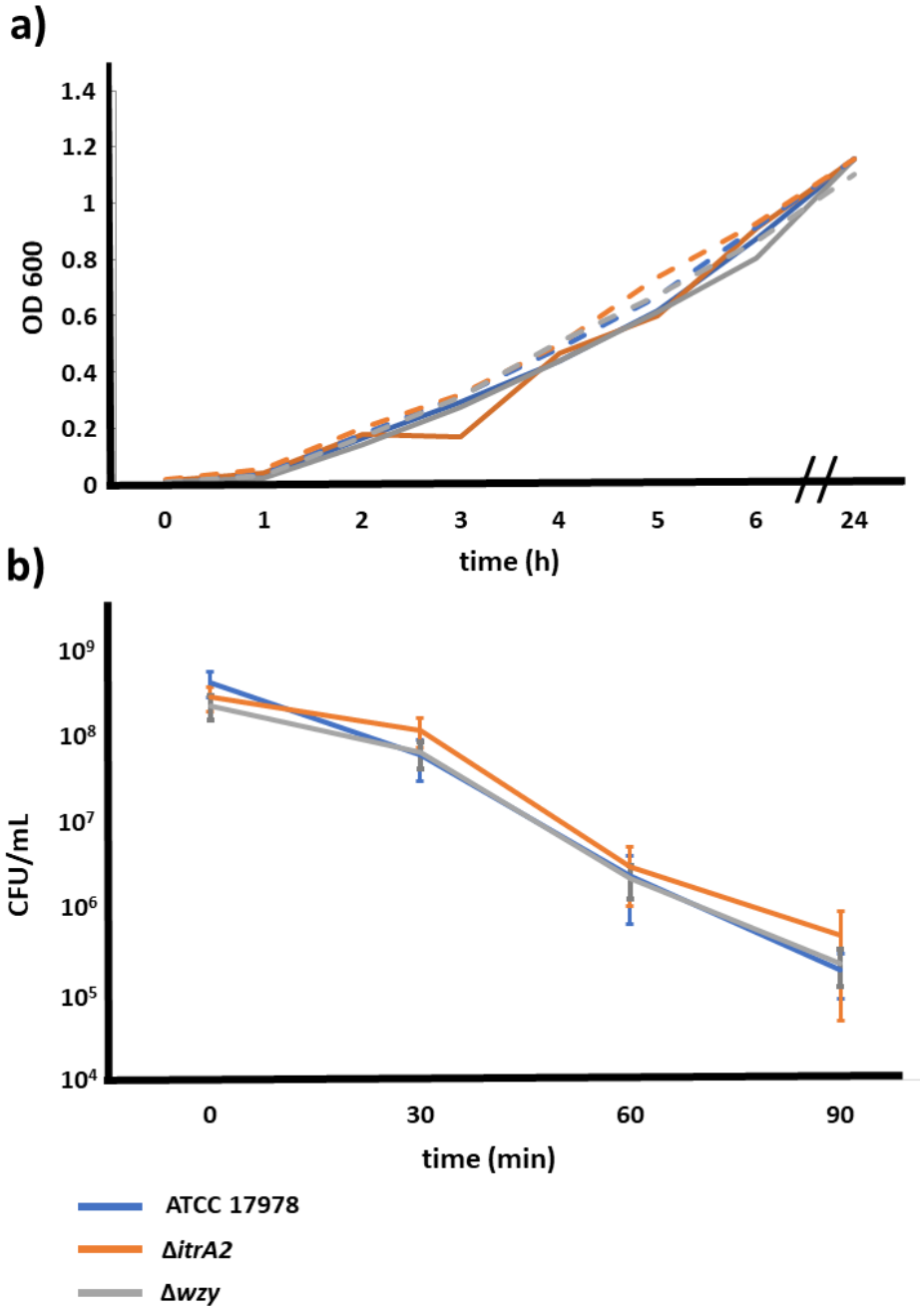

Figure 5.10. Thermotolerance of ATCC 17978 acapsular mutants. a) Strains were grown for 24 hours in MH broth shaking at either 37ºC (solid lines) or 42ºC (perforated lines). b) To assess heat shock tolerance strains were grown in MH broth at 37ºC to mid-log phase prior to incubation at 55ºC for 90 min. CFU/ mL at each time point was determined by the TVC of serial dilutions of each sample. Strains are represented by: ATCC 17978 WT strain (blue), Δ*itrA2* (orange), and Δ*wzy* (grey). Data represent the average of three independent experiments. Error bars represent standard deviation of replicates.

In this study, the role of capsule in desiccation survival in the *A. baumannii* strains 04117201 and ATCC 17978 was investigated using two different desiccation assays, a long-term desiccation assay which recorded cell viability over approximately 100 days (Jawad et al., 1998) and a short-term desiccation assay spanning 30 days (Gayoso et al., 2013) (Section 2.17).

Determining the maximum cell viability of the *A. baumannii* strains was required prior to performing the long-term desiccation assays (Section 2.11.5). The TVC (CFU/mL) was determined for WT 04117201 and ATCC 17978 at various time points (Figure 5.11, Section 2.11.5). Briefly, bacteria were grown in MH broth (37^{o}C, 120 rpm) and aliquots of bacterial cells were diluted, plated and counted for each time point (Section 2.11.5). Peak viability for both 04117201 and ATCC 179789 was reached after approximately 9-10 hrs (Figure 5.11). The number of viable cells of 04117201 remained consistently higher than ATCC 17978 over the 14 hr growth period and the peak viability of 04117201 (~1 X 10^{12} CFU/mL) was 10-fold higher than ATCC 17978 (~1 X 10^{11} CFU/mL) (Figure 5.11).

Initially, a long-term desiccation assay was employed using just the 04117201 and ATCC 17978 WT strains (Jawad et al., 1998) (Figure 5.12a). This involved air drying high cell density aliquots of bacteria onto sterile glass cover slides and re-hydrating samples at given time points (Section 2.17.1). Samples were plated onto LB agar for enumeration in duplicate on days 0-9, every second day for days 10-22 and every 5 days thereafter (Figure 5.12a). Viability was determined as the percentage survival compared to the initial inoculum. Both strains saw a sharp decline in survival over the first 24 hours then then remained stable throughout the experiment. In the first desiccation assay, viability dropped to 0.03% for the 04117201 WT and 0.02% for the ATCC 17978 WT after 24 hours (Figure 5.12a). After 16 days desiccation, the assay for the ATCC 17978 strain was halted due to contamination of samples evidenced by unexpected colony morphologies present on agar plates of revived samples (data not shown). The 04117201 strain remained viable up to day 102, when the experiment was ended (Figure 5.12a).

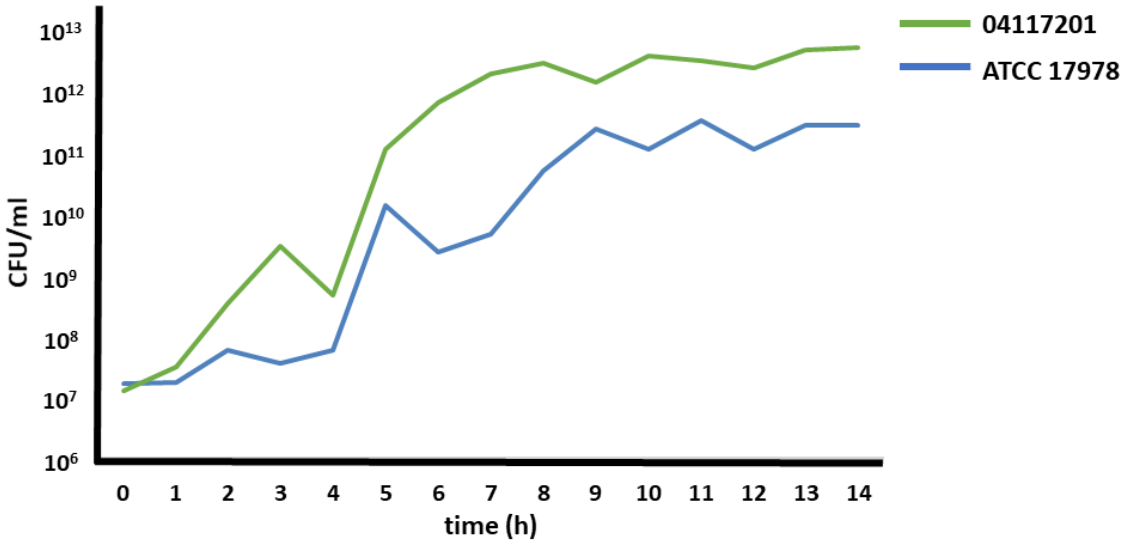

Figure 5.11. Viability of ATCC 17978 and 04117201. Cultures were grown in MH medium at 37°C shaking at 120 rpm for 14 hrs. Viability was determined as CFU/mL by plating serial dilutions of aliquots at each time point onto LB agar and incubating ON at 37°C. Data represents the average of two replicates.

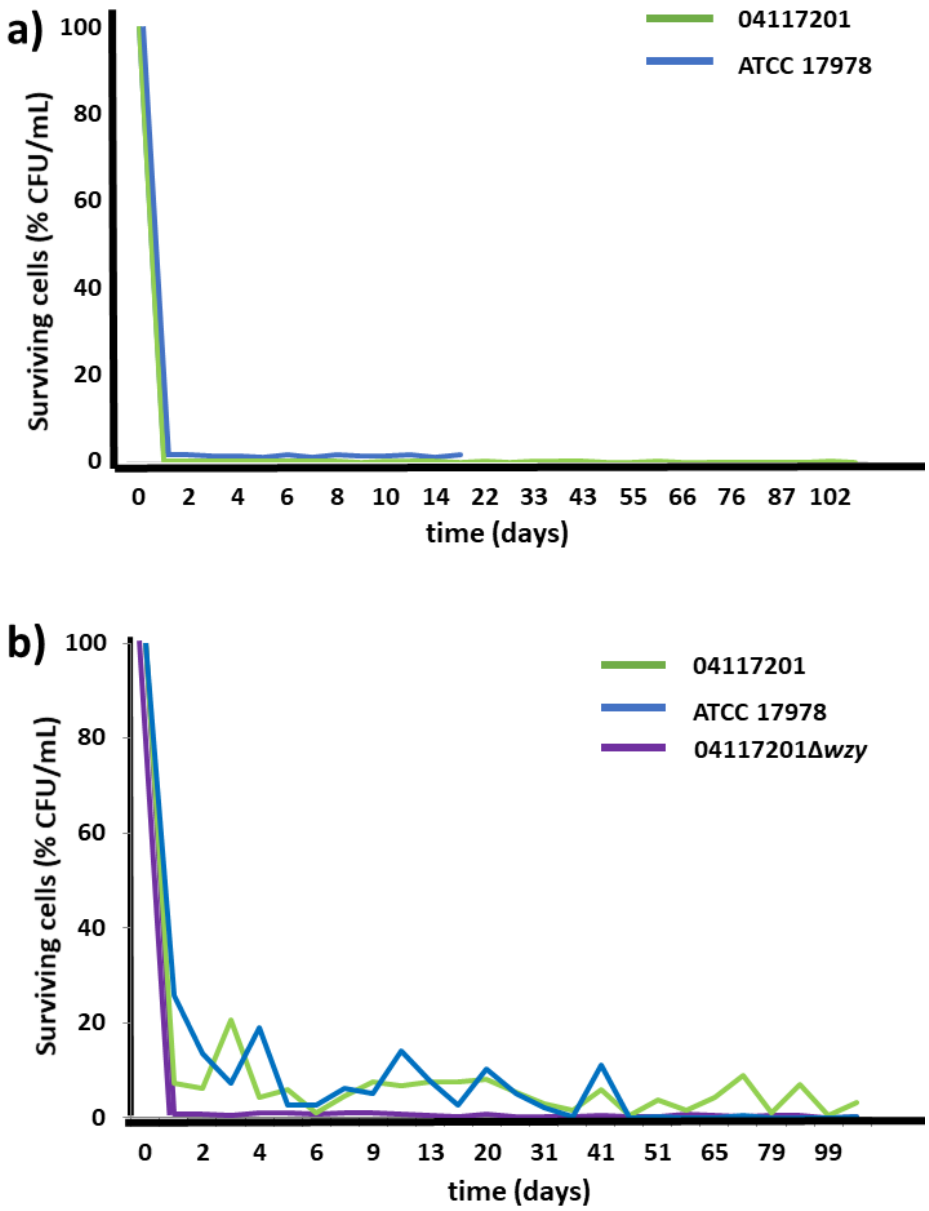

Figure 5.12. Long-term desiccation survival of *A. baumannii* strains 04117201 and ATCC 17978. Strains were grown in MH medium 37ºC with shaking for 9 hrs. Cells were washed with sterile H_2O prior to inoculation of glass coverslips with 20 µL of culture. Slips were incubated at 21ºC and 38-40% RH for the indicated time. Serial dilutions of rehydrated bacteria were plated onto LB agar and incubated ON at 37ºC to determine viability (CFU/mL) for each time point. ATCC 17978 (blue) and 04117201Δ*wzy* (purple). a) initial long-term desiccation assay, initial inoculums 1.4 x 10^{11} CFU/mL (ATCC 17978) and 4 x 10^{12} CFU/mL (04117201). b) second long-term desiccation assay, initial inoculum 1.6 x 10^{9} CFU/mL (ATCC 17978) and 3.7 x 10^{9} CFU/mL (04117201). Assays were performed in duplicate.

A second long-term desiccation assay was performed using the 04117201 and ATCC 17978 WT strains plus the addition of the 04117201 Δ*wzy* acapsular mutant (Figure 5.12b). The 04117201Δ*wzy* strain showed a significant decrease in survival over the first 24 hours of desiccation (0.8%), cell viability stabilised over the remaining 105 days at a similar level to the WT 04117201. Survival of the ATCC 17978 and 04117201 WT strains was highly erratic between each time point during the second long-term desiccation assay, suggesting a high rate of variability of survival between each inoculum. Compared to the first long-term desiccation assay, survival of the ATCC 17978 and 04117201 WT strains was much higher after 24 hours, 25% and 7%, respectively.

The initial inoculum of ATCC 17978 and 04117201 varied greatly between the first and second long-term desiccation assays. For the first desiccation assay the initial inoculum was 1.4 X 10^{11} CFU/mL and 4 X 10^{12} CFU/mL for ATCC 17978 and 04117201, respectively. The initial inoculum for the second long-term desiccation assay was over 100-fold lower than the first for both ATCC 17878 and 04117201, 1.6 X 10^{9} CFU/mL and 3.7 X 10^{9} CFU/mL, respectively. Difficulties standardising each sample, as the concentration of bacterial cells was high (between 10^{11} and 10^{12} CFU/mL) and accuracy in preparing samples of small volume (20 µL), may have influenced the variability seen (Figure 5.12, Section 2.17.1).

Because of the lengthy nature of the long-term desiccation assay, difficulty in standardising initial inoculum, and potential for contamination of samples, an alternative short-term desiccation assay was employed for the acapsular variants of both 04117201 and ATCC 17978 *A. baumannii* strains (Gayoso et al., 2013) (Section 2.17.2). This involved inoculating wells of a polystyrene tray with a lower density inoculum of bacterial culture, which was then re-hydrated at given time points of up to 30 days (Section 2.16). A similar starting inoculum was used for each strain, with the ATCC 17978 WT and acapsular variants ranging from 1.0 X 10^{7} and 2.1 X 10^{7} CFU/well and the 04117201 WT and *wzy* mutant 5.0 X 10^{7} and 1.0 X 10^{8} CFU/well, respectively. Similar to the long-term desiccation assay, all strains showed a dramatic drop in viability over the first 24 hours (Figure 5.13). No differences in desiccation tolerance was seen between the WT 04117201 or ATCC 17978 and their respective acapsular mutants using the short-term assay (Figure 5.13).

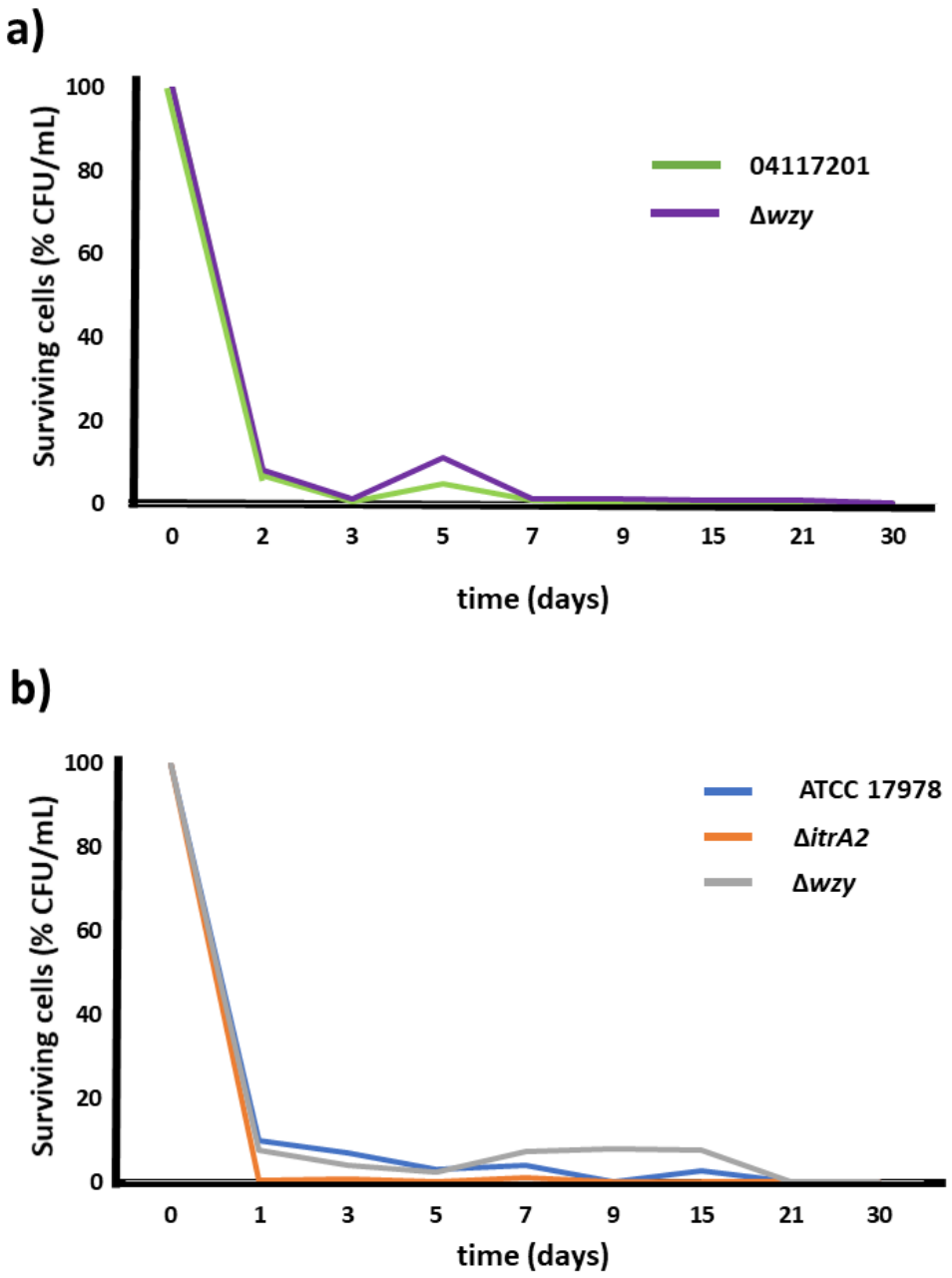

Figure 5.13 Short term desiccation assay of 04117201, ATCC 17978 and acapsular variants. Bacterial suspensions were dried onto 6 well tissue culture plates and incubated at 21°C at relative humidity 30% (+/- 2%) for 30 days. Serial dilutions of rehydrated bacteria were plated onto LB agar and incubated ON at 37°C to obtain the TVC for each timepoint. Each data point represents the average of two replicates. a) 04117201 (green) and 04117201Δ*wzy* (purple). b) ATCC 17978 (blue), Δ*itrA2* (orange) and Δ*wzy* (grey).

Inconsistent recovery of viable cells was seen during the short-term desiccation experiment for all strains, with viability increasing for some time points (Figure 5.13). Large variations (over 100-fold) were seen between some technical replicates for all strains, because of these inconsistencies only 2 replicates were performed for each strain (Figure 5.13). Comparatively, disparity between replicates was also seen for the desiccation assay on the various KL strains as discussed in Chapter 3 of this thesis (Section 3.2.3). Small changes to temperature and humidity may have influenced the consistency of the assay, as these factors are known to drastically impact *A. baumannii* desiccation tolerance (Zeidler and Müller, 2019a). Variations in the incubation conditions between samples may have occurred despite efforts to maintain consistency, for example the position within the incubator may affect humidity and temperature. Additionally, the discrepancies seen may be a result of the 'bust and boom' phenomena suggested by Gayoso and colleagues whereby a small proportion of the bacterial cells can survive on the corpses of the dead majority (Gayoso et al., 2013).

5.2.7 Susceptibility of acapsular mutants to oxidative stress

ROS are toxic to bacteria by causing major damage to membranes, proteins and DNA. Pathogenic bacteria are subject to oxidative stress within the nosocomial environment as many disinfectants are oxidative agents (e.g. bleach) and within the host as immune cells release ROS during infection (Section 1.3). *A. baumannii* possess a number of mechanisms which contribute to oxidative stress resistance, notably the production of superoxide dismutase (Heindorf et al., 2014), universal stress proteins (Zimbler et al., 2012, Soares et al., 2010), and the RecA DNA repair protein (Aranda et al., 2011) (Section 1.6.1). For some Gram-negative bacteria, such as *P. aeruginosa* and *K. pneumoniae*, the production of bacterial polysaccharides, including peptidoglycan and capsule, are increased under oxidative stress (Wang et al., 2009, Sabra et al., 2002, Wang et al., 2013). The role of capsule in protecting *A. baumannii* from oxidative stress has not been previously been studied, but it is hypothesised that the production of capsule on the bacterial surface creates a physical barrier against diffusion of ROS from the external environment.

Subsequently, the role of capsule in resistance to oxidative stress was investigated for the *A. baumannii* 04117201 and ATCC 17978 WT strains and their acapsular variants.

Three methods were employed to assess resistance to oxidative stress; disk diffusion assays, growth curves in the presence of paraquat, and hydrogen peroxide killing assays. Firstly, disk diffusion assays using both hydrogen peroxide and paraquat were employed to measure and compare the zone of inhibition for the parental and acapsular strains (Section 2.12). The 04117201 Δ*wzy* mutant was more sensitive to both paraquat and hydrogen peroxide than the parental strain, though the difference was small and was not statistically significant (Figure 5.14). The disk diffusion assay was not performed for the Δ*wzy* mutant in ATCC 17978 as it had not yet been constructed when disk diffusions were performed.

Two ATCC 17978 acapsular strains, Δ*wzy* and Δ*itr*, showed a small increase in sensitivity to hydrogen peroxide and paraquat compared to the WT and the Δ*cps* strains (Figure 5.14b). Again, there was no statistical difference in the disk diffusion between the ATCC 17978 WT and Δ*itrA2* or Δ*cps* for either oxidising compound.

Hydrogen peroxide is a highly reactive compound and therefore is not suitable for testing the response to oxidative stress in broth cultures. Because of the instability of hydrogen peroxide, growth curves of ATCC 17978 WT and acapsular strains were conducted in various concentrations of paraquat (Figure 5.14c). ATCC 17978 WT, Δ*itrA2*, and Δ*cps* were grown in liquid broth for 18 hours in the presence of paraquat. Although Δ*itrA2* displayed higher growth than the Δ*cps* and ATCC 17978 WT strains at 200-300 µM paraquat, variations between replicates hindered the identification of meaningful differences (Figure 5.14c). This variation may have been due to the small volume of each sample (2 mL of liquid culture) and may be improved by repeating the assay in a higher volume of medium. The hydrogen peroxide growth curve did not include diffusion the Δ*wzy* in ATCC 17978 as this mutant had not yet been constructed at the time the assay was performed.

Studies have shown that during the stationary phase of growth, bacteria increase production of various enzymes and antioxidants that may increase oxidative stress resistance compared to cells in an actively growing state (Soares et al., 2010). For this reason, a third method, a hydrogen peroxide killing assay, was employed to test resistance during exponential phase.

a)

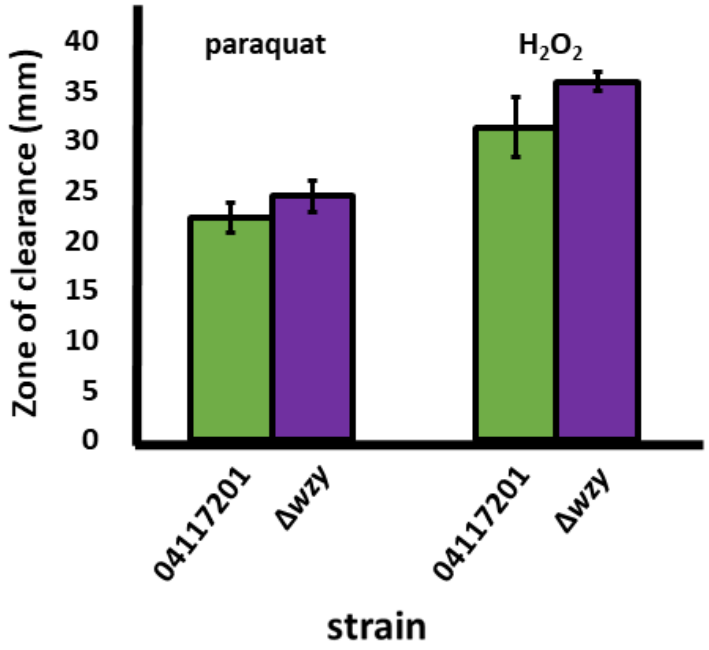
paraquat
H_2O_2
Zone of clearance (mm)
40
35
30
25
20
15
10
5
0
04117201
Δwzy
04117201
Δwzy
strain

b)

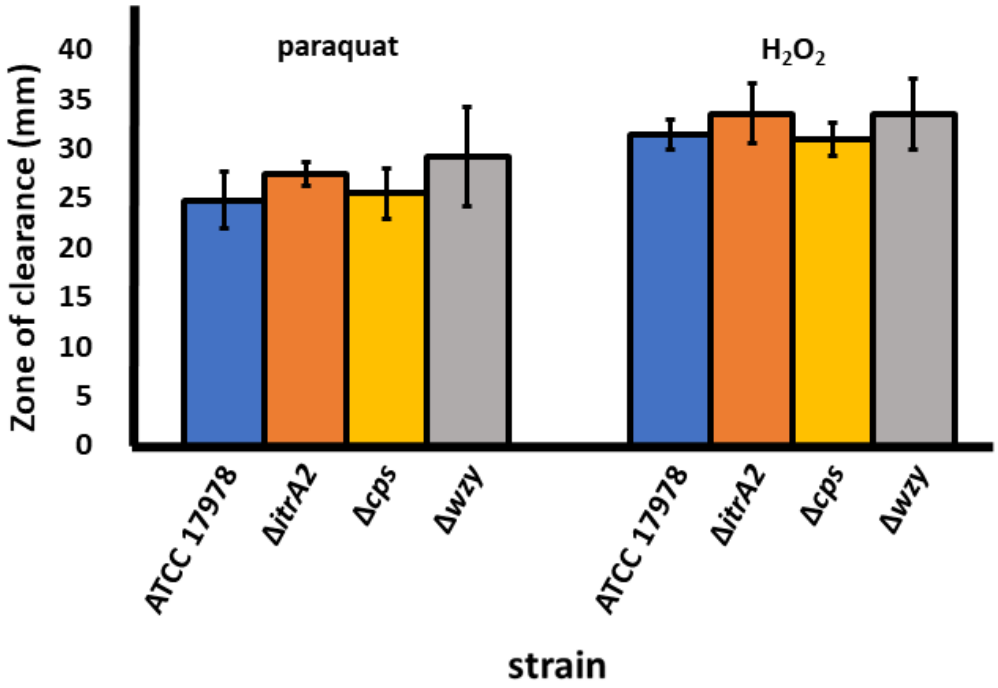
paraquat
H_2O_2
Zone of clearance (mm)
40
35
30
25
20
15
10
5
0
ATCC 17978
ΔitrA2
Δcps
Δwzy
ATCC 17978
ΔitrA2
Δcps
Δwzy
strain

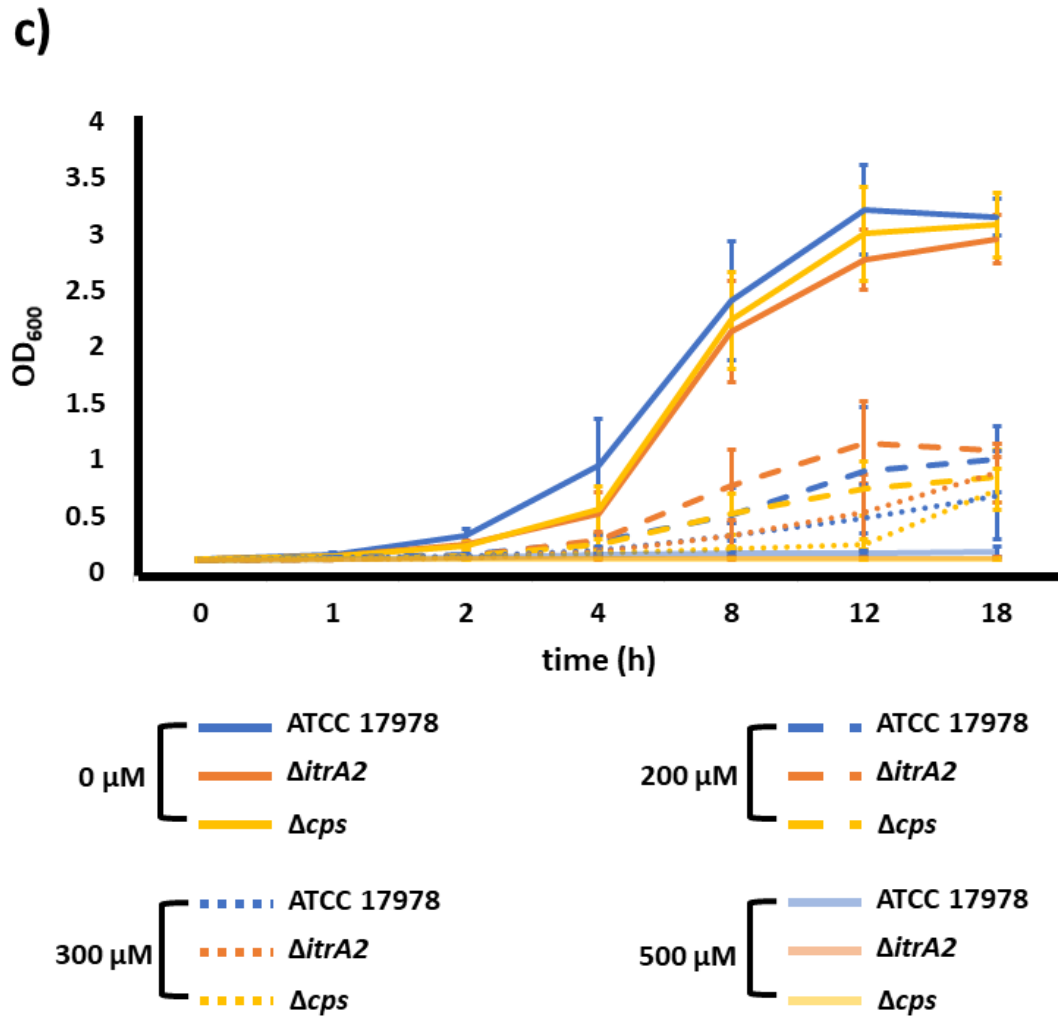

Figure 5.14. Disk diffusion susceptibility assays and growth curves of 04117201, ATCC 17978 and acapsular variants under oxidative stress. For disk diffusion assays, MH agar plates were inoculated with 100 µL of respective bacterial strains grown to an OD_{600} of 0.6 and disks impregnated with either 5 µL of 200 mM paraquat or 30% H_2O_2, placed onto the agar plates and incubated ON at 37ºC. Zones of clearance were measured as the highest value diameter obtained of the clear zone surrounding the disks. a) Average zone of clearance of 04117201 compared to the Δ*wzy* variant. b) Average zone of clearance of ATCC 17978 compared to acapsular variants. c) For growth curves, ATCC 17978 and acapsular variants were incubated MH medium in the presence of different concentrations of paraquat (0, 200, 300, and 500 µM) in 2 ml wells for 18 hours at 37ºC with intermittent shaking every 5 minutes. Growth was determined by OD_{600} measured using a FLUOstar Omega microplate reader (BMG Labtech). Assays were performed in triplicate. Error bars represent the standard deviation.

Briefly, ATCC 17978 and acapsular variants were grown to an OD_{600} of 0.6 before exposure to 0.09% hydrogen peroxide (Section 2.11.4). Results of the killing assay were inconsistent between the five replicates performed (data not shown). The highly reactive nature and small concentrations of hydrogen peroxide used may account for the poor accuracy of the assay.

Most studies on *A. baumannii* determine susceptibility to ROS using a simple disk diffusion method (Ajiboye et al., 2018, Heindorf et al., 2014, Srinivasan et al., 2015). In this study, disk diffusion methods were not sensitive enough to determine statistically significant differences in oxidative stress responses. Despite this, a trend of lower resistance was seen for acapsular variants using the disk diffusion method (Figure 5.14a,b). Experiments using alternative methods were undertaken though both the hydrogen peroxide killing assay and paraquat growth curve were unable to elucidate a role for capsule in oxidative stress resistance in *A. baumannii*.

5.2.8 Susceptibility of acapsular mutants to ethanol treatment

Ethanol is frequently used as an antimicrobial agent, for example it is the primary component of many hand sanitisers (Chiang et al., 2017). A concentration of 70-80% is recommended for effective disinfection of hands and surfaces (Kampf, 2018). Despite this, evaporation and variation in volumes used to sanitise hands and surfaces can lead to ineffective disinfection and thus ineffective killing of intrinsically ethanol resistant microbes such as *A. baumannii* (Chiang et al., 2017). Additionally, biofilm formation can further increase ethanol resistance of MDR *A. baumannii* strains (Chiang et al., 2017), and low concentrations of ethanol promote pathogenicity by inducing the expression of stress proteins (Camarena et al., 2010). Although no evidence has previously been found for a link between the production of capsule and resistance to ethanol, it was hypothesised that capsule may provide a barrier between the plasma membrane and extracellular ethanol, dampening the deleterious effects of ethanol on the membrane. Furthermore, a recent study has shown mutations in genes required for LOS production in the *A. baumannii* strain ATCC 19606 leads to a 2-8-fold reduction in ethanol resistance (Carretero-Ledesma et al., 2018).

To ascertain the ethanol resistance capacity of the WT strain ATCC 17978, bacterial cultures were grown to an OD_{600} of 0.6 before being treated with a range of ethanol

concentrations for 5 min. It was found that growth of the WT ATCC 17978 was uninhibited in 20% ethanol, slightly inhibited in 25% ethanol, and completely inhibited in 30% ethanol (Figure 5.15a).

Resistance to treatment with 20% and 25% ethanol was also assessed for the acapsular ATCC 17978 strains, as this range moderately affected the WT strain (Figure 5.15). When treated with 20% ethanol no difference was seen between the acapsular mutants and the WT ATCC 17978 strain, however, at 25% ethanol growth of Δ*cps* and Δ*wzy* was more inhibited than the WT strain (Figure 5.15b).

To verify that the deletion of *wzy* was responsible for the decreased resistance to ethanol, Δ*wzy* with the WT *wzy* gene in pWH1266 (Δ*wzy*C) as well as Δ*wzy* cells containing the empty pWH1266 vector (Δ*wzy*E) were treated with 20% and 22.5% ethanol. When treated with 20% ethanol there was no difference in viability for Δ*wzy*C and Δ*wzy*E, whereas Δ*wzy*C grew slightly better on 22.5% ethanol compared to Δ*wzy*E (Figure 5.15c)

As previously described, both Δ*wzy*C and Δ*wzy*E showed poor growth rates compared to the WT ATCC 17978 and *Δwzy*, which may account for the lack of viability when treated with 25% ethanol. To circumvent this issue Δ*wzy*C and Δ*wzy*E were treated with 22.5% ethanol, the Δ*wzy*C variant showed increased viability compared to Δ*wzy*E after treatment suggesting the reintroduction of *wzy* into Δ*wzy* partially improves ethanol resistance (Figure 5.15c).

Unexpectedly, no difference between the WT and Δ*itrA2* variant was seen (Figure 5.15b). Reasons for why ethanol resistance was not perturbed in the Δ*itrA2* variant of ATCC 17978 but reduced in the Δ*cps* and Δ*wzy* strains remains to be investigated. It may be due to differences in the composition of the outer membrane between the acapsular variants. Although Δ*cps* and Δ*itrA2* halt capsule production at the same stage (Figure 1.1) and thus theoretically should display the same phenotype, the downstream effects of their specific mutations on the production of other surface structures, such as LOS, remain unknown.

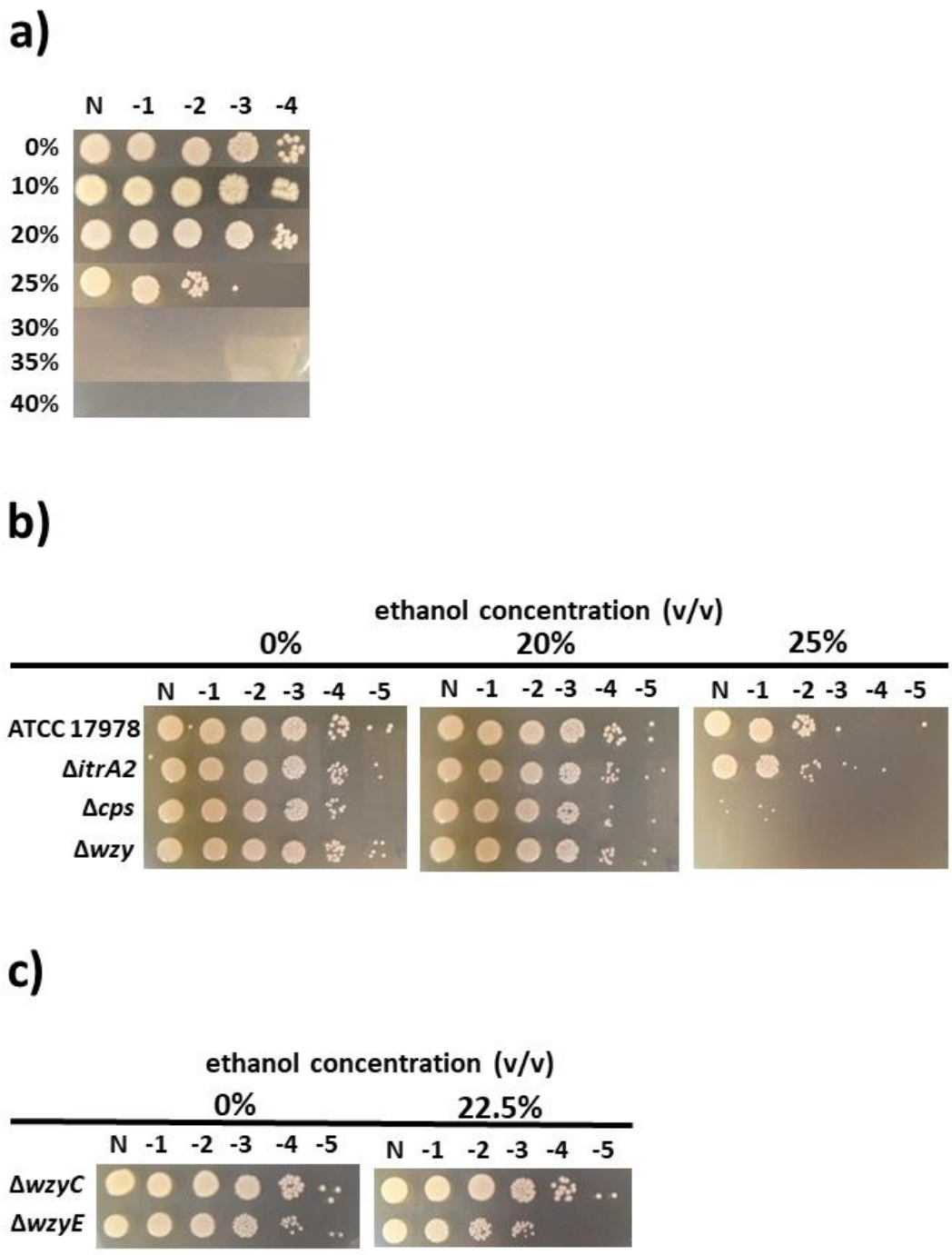

Figure 5.15. Resistance to ethanol treatment of ATCC 17978 and acapsular variants. Cells were grown to an OD_{600} of 0.6 and incubated in the presence of ethanol for 5 minutes prior to plating 10-fold dilution series on MH agar and incubation ON at 37°C; N represents undiluted cells. a) ATCC 17978 WT strain treated with increasing concentrations of ethanol, b) acapsular mutants treated with 20% and 25% v/v ethanol, c) complemented ATCC 17978Δ*wzy* (Δ*wzy*C) and Δ*wzy* containing the empty vector (Δ*wzy*E) treated with 22.5% ethanol. Figures are a representative of the results obtained.

Other factors may involve differential expression of stress related genes by the various capsule mutants, which may indirectly augment the response to ethanol treatment (Camarena et al., 2010). Analysing the transcriptome of the various mutants under ethanol stress may elucidate the mechanisms behind these incongruous results.

5.2.9 Role of capsule in *A. baumannii* resistance to antimicrobial compounds

Effective antimicrobial treatment is critical to reduce mortality due to *A. baumannii* infections and adequate environmental disinfection during outbreaks significantly reduces patient to patient transmission. However, due to the high frequency of resistance, *A. baumannii* infections are difficult to treat and hospital disinfection in response to outbreaks often unsuccessful. Antimicrobial resistance mechanisms of *A. baumannii* include the production of multidrug efflux pumps (Lin et al., 2017, Yoon et al., 2015), β-lactamases (Gupta et al., 2006), and aminoglycoside modifying enzymes (Hamidian and Hall, 2013). Additionally, intrinsic properties of *A. baumannii* isolates including low membrane permeability (Zahn et al., 2016), LOS (Powers et al., 2019) and capsule (Geisinger and Isberg, 2015, Tipton et al., 2018) contribute to resistance to various compounds. Surprisingly, the number of studies investigating the role of capsule on antimicrobial resistance is limited. One study found capsule contributes to the resistance of *A. baumannii* to various antimicrobials, , as acapsular mutants; Δ*wzc*, Δ*itrA*, Δ*cps*, were more susceptible to colistin, rifampicin and erythromycin (Geisinger and Isberg, 2015). Another found removal of capsule decreases resistance to the commonly used disinfectants benzethonium, benzalkonium and chlorhexidine (Tipton et al., 2018).

In this study, resistance to three compounds; chloramphenicol, colistin, and polymyxin B, were assessed for the 04117201 mutant (Δ*wzy*). The antimicrobial peptides colistin and polymyxin B were chosen as they directly affect the cells OM (Campos et al., 2004) and the antibiotic chloramphenicol was included as a control, as this compound is small and likely to penetrate capsule and enter the bacterial cell (Geisinger et al., 2019). No difference in resistance between the WT 04117201 and the Δ*wzy* mutant was found for any of the compounds tested (Table 5.1). No further compounds were assessed because

Table 5.1 Minimal inhibitory concentrations of 04117201 and the Δ*wzy* acapsular variant for selected compounds (µg/ mL)

	WT	Δ***wzy***
Compound[a]		
chl	50	50
col	24-48	24-48
pol	3.75	3.75

[a] chl chloramphenicol, col colistin, pol polymyxin B

the complementation of the 04117201 Δ*wzy* strain was not achieved (Section 4.2.4) and therefore direct comparison to not be achieved. This decision was also due to the suspicion that the Δ*wzy* mutant in 04117201 possessed a secondary mutation elsewhere in the K Loci (Section 4.2.3). Subsequently the work focussed on the ATCC 17978 variants.

Resistance to 18 various compounds was determined for the ATCC 17978 WT and acapsular variants. Compared to the ATCC 17978 WT, the Δ*itrA2* acapsular mutant showed reduced resistance to several compounds including the aminoglycosides kanamycin and streptomycin, and the polymyxin colistin (Table 5.2).

Compared to the ATCC 17978 parental strain, both the Δ*wzy* and Δ*cps* variants showed decreased resistance to the aminoglycosides kanamycin, gentamycin, amikacin and streptomycin. Compared to the WT parental strain, all acapsular variants of ATCC 17978 displayed a moderate reduction in resistance to the polymyxin antibiotic colistin (Table 5.2). The complementation of colistin resistance assays for Δ*itrA2* and Δ*wzy* were inconsistent using a 96 well plate dilution method (Section 2.12). This could be a result of colistin induced mutations in genes encoding lipid A (Moffatt et al., 2010) and the PmrAB (Beceiro et al., 2011) two component system, as seen in other studies (Zhang et al., 2017) (Section 1.2.5). Resistance to colistin was restored to WT levels consistently for both complemented strains using an agar plate dilution method (Figure 5.16).

Unexpectedly, both the Δ*wzy* and Δ*cps* variants displayed an increase in resistance to several compounds, including ciprofloxacin, trimethoprim, and the disinfectant chlorhexidine, compared to the ATCC 17978 WT. Interestingly, in this study acapsular mutants were more resistant to chlorhexidine, whereas another study showed a reduction in resistance for their *A. baumannii* acapsular variant (Tipton et al., 2018). This result may be due to differences in methodology, strain variation, or choice of knock out gene to produce acapsular mutants. An alternative reason for the increased resistance of the acapsular mutants to various compounds are the effects gene deletions may have on regulation of other cellular processes. For example, the removal of capsule may lead to an increase in other surface polysaccharides or protein glycosylation (Boll et al., 2016b, Iwashkiw et al., 2012)

Table 5.2 Minimal inhibitory concentrations of ATCC 17978 and acapsular variants for selected compounds (µg/ mL)

	WT	**Δ*itrA2***	**Δ*wzy***	**Δ*cps***	**Δ*itrA2*C**	**Δ*itrA2*E**	**Δ*wzy*C**	**Δ*wzy*E**
Compound[a]								
chl	50	50	50	50	n.d.	n.d.	n.d.	n.d.
ben	5	5	5	5	n.d.	n.d.	n.d.	n.d.
cip	0.8-1.6	0.8-1.6	3.2	3.2	n.d.	n.d.	3.2	3.2
trim	8.25-16.5	8.25-16.5	33	33	n.d.	n.d.	33	16.5
amp	150	150	150	150	n.d.	n.d.	n.d.	n.d.
gent	1.6-3.2	1.6	1.6	1.6	n.d.	n.d.	0.8	0.4
kan	1.6	0.8	0.8	0.8	0.8	0.4	0.8	0.4
strep	25	6.25	12.5	12.5	12.5	6.25	12.5	3.13
tet	1	1	1	1	n.d.	n.d.	n.d.	n.d.
nal	6.3	6.3	6.3	6.3	n.d.	n.d.	n.d.	n.d.
amik	12.5	12.5	6.25	6.25	n.d.	n.d.	6.25	1.56
col[b]	4	2-4	2-4	2-4	2	2	2	2
rif	2	2	2	2	n.d.	n.d.	n.d.	n.d.
pol	2	2	2	2	n.d.	n.d.	n.d.	n.d.
tri	1.25	1.25	1.25	1.25	n.d.	n.d.	n.d.	n.d.
chx	6.25	6.25	12.5	12.5	n.d.	n.d.	3.13	6.25
pent	62.5	62.5	62.5	62.5	n.d.	n.d.	n.d.	n.d.
nov	10	10	10	10	n.d.	n.d.	n.d.	n.d.

[a] chl chloramphenicol, ben benzalkonium, cip ciprofloxacin, trim trimethoprim, amp ampicillin, gent gentamycin, kan kanamycin, strep streptomycin, tet tetracycline, nal nalidixic acid, amik amikacin, col colistin, rif rifampicin, pol polymyxin B, tri triclosan, chx chlorhexidine, pent pentamidine, nov novobiocin, n.d. strain not tested

[b] complementation using agar plate dilution

[c] MICs which differ from WT are shaded in grey

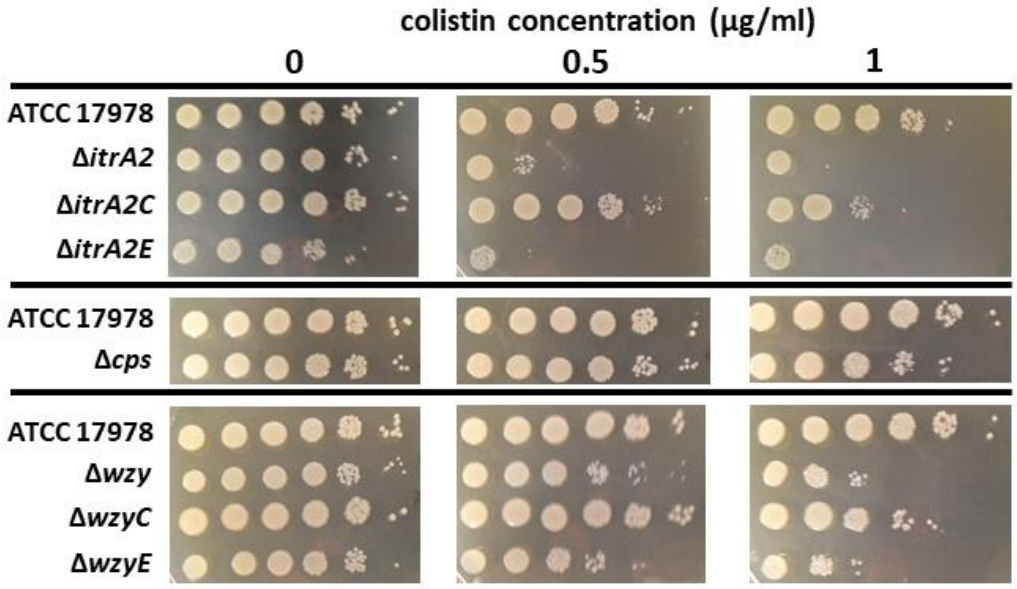

Figure 5.16. Agar plate dilutions of ATCC 17978 and acapsular variants on increasing concentrations of colistin sulphate (µg/ mL). Cells were grown to an OD_{600} of 0.6 and 10-fold dilution series were plated on MH agar containing increasing concentrations of colistin sulphate, then incubated ON at 37°C; N represents undiluted cells. OD_{600} was recorded using the DU 640 spectrophotometer (Beckman). Assays were performed in triplicate, figures are representative of results obtained.

Difficulties arose with the complementation of MICs using the microplate dilution method (Section 2.12). Using this method only partial complementation was achieved for many of the MIC experiments. For example, in the case of chlorhexidine the following MICs were determined; 6.25 µg/mL for the WT ATCC 17978, 12.5 µg/mL for the Δ*wzy* variant, 3.15 µg/mL for Δ*wzy*C and 6.25 µg/mL for Δ*wzy*E. Although a 2-fold difference was seen between the WT and Δ*wzy*, and between Δ*wzy*C and Δ*wzy*E, the MICs of the latter were 2-fold lower than expected (Table 5.2). Complementation did not restore the increased resistance to ciprofloxacin seen in Δ*wzy* using the 96-well plate dilution method or the agar plate dilution method.

Reasons why only partial complementation of resistance profiles were seen are unknown. A likely contributor of this 2-fold difference between the WT and complemented strain is a growth defect observed in both Δ*itrA2* and Δ*wzy* harbouring pWH1266 derivatives (Section 5.2.1). Mutants containing the pWH1266 derivatives failed to reach MICs resembling the WT and acapsular variants when the incubation time was extended to 48 hours, therefore the phenotype is most likely not due to a lack of growth alone. Previous complementation studies using pWH1266 to re-introduce deleted genes into *A. baumannii* have also shown only partial complementation to a number of antimicrobial compounds including ciprofloxacin (Saroj et al., 2012, Liou et al., 2014, Li et al., 2016b), imipenem (Liou et al., 2014), amikacin, colistin, ceftazidime, and chloramphenicol (Li et al., 2016b). Conversely, other studies were able to fully complement changes in resistance profiles in gene deletion strains using WT genes expressed on pWH1266 (Ravasi et al., 2011, Chen et al., 2013, Moffatt et al., 2010).

5.3 **Conclusions**

A key determinant of the clinical success of *A. baumannii* is the ability to thrive in hostile environments. This study investigated the effect of environmental stressors on the growth and survival of acapsular mutants in the *A. baumannii* strains ATCC 17978 and 04117201. Responses to the environmental stressors assessed varied not only between the WT and acapsular mutants, but between the acapsular variants of both strains.

Growth of all *A. baumannii* acapsular mutants lagged slightly in rich media compared to the parental strains and had a tendency to aggregate and sediment quickly (Figure 5.2).

A dramatic increase in hydrophobicity was seen for all the ATCC 17978 acapsular variants, whereas removal of capsule did little to affect cell surface hydrophobicity in 04117201 (Figure 5.4). Levels of biofilm formation was increased for most acapsular strains compared to the WT parents, indicating that interactions between *A. baumannii* and surfaces required for biofilm formation are perturbed by capsule production (Figure 5.5).

There was no difference between the WT 04117201 and Δ*wzy* variant under osmotic stress (Figures 5.7). Conversely, differences in growth under osmotic and acidic stress were identified between the WT ATCC 17978 strain and acapsular variants. Interestingly, growth under sucrose induced osmotic stress differed between the ATCC 17978 acapsular strains, with higher than WT growth for the Δ*itrA2* and Δ*cps* variants and decreased growth for Δ*wzy* (Figure 5.7). Furthermore, the Δ*wzy* strain showed higher growth than its parent under acidic conditions, whereas both Δ*cps* and Δ*itrA2* were unable to grow at all. Lastly, both Δ*cps* and Δ*wzy* were less tolerant to treatment with 25% ethanol than the WT ATCC 17978 and Δ*itrA2* (Figure 5.14). No differences were seen in the MIC analysis between the 04117201 WT and Δ*wzy* variant, though only three compounds were tested. The MIC to several compounds varied between ATCC 17978 and the acapsular mutants assessed, Δ*itrA2*, Δ*cps*, and Δ*wzy*. The varied responses between acapsular ATCC 17978 mutants to hyper-osmotic, acidic and antimicrobial stress was not expected and suggest that removal of genes involved in different stages of capsule synthesis differentially affect the response to environmental stressors. This may indicate that inhibition of capsule synthesis is not the direct cause of all the results seen, and that the response of acapsular mutants of *A. baumannii* to environmental stress differs depending on what specific gene/s are removed.

A primary factor in the persistence of *A. baumannii* is the ability to withstand desiccation. Although desiccation experiments were unsuccessful in this study, the extreme toughness of *A. baumannii* in the dry environment was validated as viable cells of both 04117201 and ATCC 17978 were recovered after three months in dry conditions.

The human host is perhaps the most important environment to consider when studying *A. baumannii* from a clinical perspective. Many of the environmental stressors

investigated in this chapter such as fluctuating pH, osmotic stress, and the presence of antimicrobial compounds, as well as altered physiological states such as biofilm, are relevant to survival in both external environments and within the human host. The next chapter will investigate the role capsule plays in interactions between *A. baumannii* and the host immune system.

6 CAPSULAR POLYSACCHARIDE OF *A. BAUMANNII* MODULATES HOST-MICROBE INTERACTIONS

6.1 Introduction

A prominent characteristic of many virulent *A. baumannii* strains is the ability to dampen the immune response, enhancing bacterial proliferation and increasing infection severity and the risk of dissemination (De Breij et al., 2012) (Section 1.8). Capsule is one of the first components of the bacterial cell to encounter the host during infection. Therefore, it is not surprising that capsule plays a vital role in protecting the bacterium from a range of host immune defences, especially those of the innate immune system (Section 1.8). During infection, a range of protective measures are employed by the host to impede microbial colonisation. These defences involve an intricate interplay between cellular components such as epithelial cells, macrophages, neutrophils and humoral defences such as antimicrobial peptides, lysozyme, and complement, and secreted immune mediators such as cytokines and chemokines (Section 1.8).

The production of capsule has been identified as a key determinant in the evasion of several host immune defences by *A. baumannii* (Geisinger and Isberg, 2015, Tipton et al., 2018). One study reported that deletion of the initial transferase (Δ*itrA*) in the *A. baumannii* strain 307-0294 resulted in the strain becoming susceptible to human complement (Geisinger and Isberg, 2015). Another study in the *A. baumannii* strain AB5075 showed reduced resistance to lysozyme and reduced virulence in a Δ*wzc* mutant compared to the WT parent (Tipton et al., 2018). In this chapter, the role of capsule in immune evasion by the *A. baumannii* strains ATCC 17978 and 04117201 was investigated by comparing the response of various acapsular mutants, as described in Chapter 4, to the WT strains under a variety of stressors including iron limitation, lysozyme and complement. Furthermore, adherence to adherence to pneumocytes, macrophage phagocytosis and immune gene expression by tissue cultures under bacterial challenge was examined.

6.2 Results and Discussion

6.2.1 Growth of *A. baumannii* ATCC 17978 acapsular mutants under iron-limiting conditions

Iron is a limited, yet essential resource required by *A. baumannii* to cause infection (Section 1.2.1). Within the host, free iron is extremely scarce, as the vast majority of iron is stored in a complex with iron-binding molecules such as the heme of red blood cells (Parrow et al., 2013). In addition to preventing iron toxicity, the sequestering of iron by host molecules provides nutritional immunity by limiting iron availability to invading organisms (Nwugo et al., 2011). An inverse correlation between surviving iron-limiting conditions and the production of capsule has previously been found in *K. pneumoniae*, as the iron-regulating protein FUR represses capsule production (Lin et al., 2011). A previous study in *A. baumannii* ATCC 17978 reported that under iron limitation, *FUR* was upregulated but no change in the expression of capsule genes was seen (Eijkelkamp et al., 2011a). Despite this, capsule production is not entirely regulated at the transcriptional level (See Section 1.9) and the role of capsule in growth under iron limitation has not previously been explored for *A. baumannii*. Therefore, the acapsular *A. baumannii* ATCC 17978 strains were subjected to iron-limiting conditions by growth on agar plates containing increasing concentrations of 2,2' dipyridyl (DIP), a synthetic iron chelator (Section 2.12).

All acapsular strains and WT ATCC 17978 were capable of growing on <225 µM DIP (Figure 6.1). Growth of the Δ*itrA2* and Δ*wzy* strains were severely inhibited when grown on agar containing 250 µM DIP. This can be seen by the comparative translucency of these two strains compared to the WT (Figure 6.1). Interestingly, the results for Δ*cps* were no different to the WT strain.

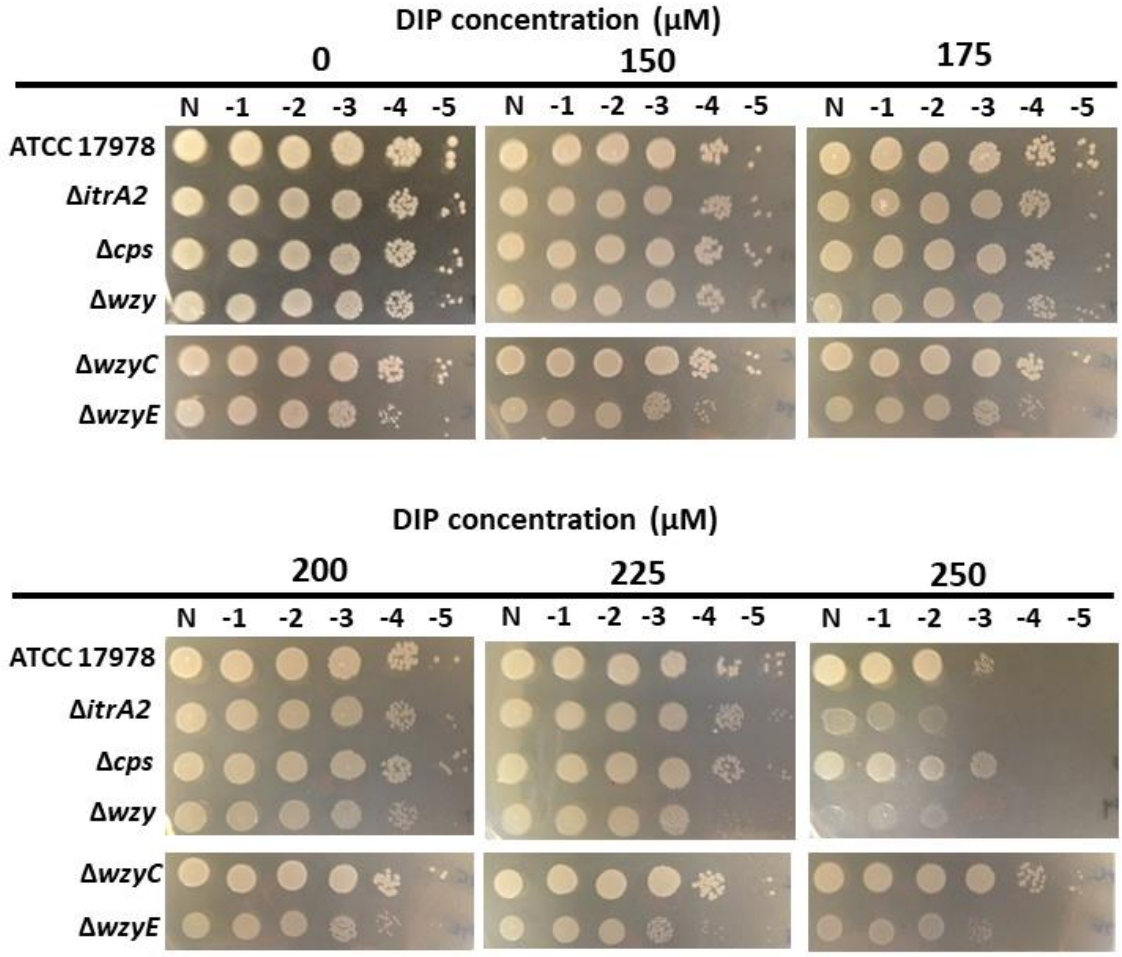

Figure 6.1. Growth of ATCC 17978 WT and acapsular mutants under iron-limiting conditions. Strains were grown in MH broth at 37ºC shaking until reaching an OD_{600} of 0.6 prior to plating 10-fold dilution series on MH agar containing increasing concentrations of DIP prior to incubation ON at 37ºC; N represents undiluted cells. OD_{600} was recorded using the DU 640 spectrophotometer (Beckman). Assays were performed in triplicate; figures are representative of results obtained.

The WT results differ slightly from a previous study which showed showed growth of the *A. baumannii* strain ATCC 17978 was uninhibited in the presence of 100 µM DIP, moderately inhibited in 200 µM DIP, and severely inhibited in 300 µM DIP (Eijkelkamp et al., 2011a). In this study the WT and Δ*itrA2* were moderately inhibited at 250 µM DIP. No assays using 300 µM DIP carried out in this study.

Upon complementation of the Δ*wzy* strain with a WT version of the *wzy* gene (Δ*wzy*C) cell growth under iron limitation was restored to WT levels (Figure 6.1). It can therefore be hypothesised that the decreased growth seen in iron depleted conditions for Δ*wzy*, and to a lesser extent Δ*itrA2*, may be somehow associated with dysregulation of iron uptake systems. In the Δ*wzy* variant specifically, abnormalities seen in the cell structure (Chapter 4.2.5.5) may alter the ability of this mutant to efficiently take up iron when this resource is scarce, for example by reducing the secretion of iron scavenging siderophores or affecting the efficiency or number of iron transport systems (Eijkelkamp et al., 2011a). This could be investigated by comparing transcription levels of siderophores and iron transport genes of the Δ*wzy* and Δ*itrA2* mutants compared to the WT under iron limitation. Furthermore, analysis of iron transport proteins in the membrane fractions, under iron limitation, may detect whether the membrane abnormalities play a role in the phenotype of Δ*wzy*.

6.2.2 Capsular polysaccharide increases resistance of *A. baumannii* ATCC 17978 to human lysozyme

The primary mode of action for lysozyme is the degradation of peptidoglycan, a component of the bacterial cell envelope, by hydrolysis of specific bonds between N-acetylmuramic acid and N-acetyl glycosamine residues (Niyonsaba and Ogawa, 2005, Liu et al., 2015, Wiesner and Vilcinskas, 2010). Due to its cationic structure, lysozyme also causes cell lysis independent of peptidoglycan degradation by forming pores in the bacterial envelope (Ragland and Criss, 2017). Lysozyme is present in virtually all human secretions, as well as neutrophil granules and the phagolysosomes of macrophages (Wiesner and Vilcinskas, 2010, Liu et al., 2015). It is hypothesised that the removal of capsule would make *A. baumannii* more susceptible to lysozyme killing as the peptidoglycan layer would be more of readily accessible to lysozyme (Section 1.3.4). In a previous chapter it was shown that *A. baumannii* is susceptible to lysozyme

killing, though variations in resistance were seen between different clinical isolates (Section 3.2.4). Furthermore, a recent study by Tipton et al found the removal of capsule (Δ*wzc*) in the *A. baumannii* strain AB5075 resulted in a 100-fold reduction in lysozyme resistance (Tipton et al., 2018).

Initially, survival of *A. baumannii* ATCC 17978 WT and acapsular variants in the presence of hen's egg white derived lysozyme (HEWL) was assessed (Section 2.15). Previous studies have shown bactericidal effects of HEWL on Gram-negative bacteria at concentrations between 1 µg- 2.5 mg/ mL (Deckers et al., 2008, Bao et al., 2018). In the case of *A. baumannii*, a recent study on lysozyme resistance of the *A. baumannii* strain ATCC 19606 found a concentration of 1 mg/ mL of HEWL to be sufficient for bacterial killing (Kamoshida et al., 2020). Interestingly, HEWL was ineffective at killing the WT and acapsular ATCC 17978 strains, even at high concentrations up to 25 mg/ mL (data not shown). The disparity between HEWL resistance of the *A. baumannii* ATCC 17978 and ATCC 19606 strains suggests resistance to HEWL in *A. baumannii* is strain specific. Interestingly, ATCC 19606 showed high levels of resistance to human lysozyme, though not as high as ATCC 17978 (Section 3.2.4). Additionally, HEWL belongs to the same c-type class of lysozyme as human derived, and has been shown to elicit peptidoglycan independent activity in pore formation in the cell membranes of *P. aeruginosa* and *E. coli* (Deckers et al., 2008). Due to the lack of activity using HEWL, assays were repeated with human-derived lysozyme (Section 2.15).

After incubation for one hour in human lysozyme (Section 2.15), survival of all ATCC 17978 WT and acapsular strains decreased compared to the untreated control; no significant differences in survival were seen between the strains (Figure 6.2). Compared to the WT strain (3.4 X 10^5 CFU/ mL), viability of Δ*itrA2*, Δ*wzy*, and Δ*cps* cells were reduced by 21- (1.1 X 10^4 CFU/ mL), 39- (6.7 X 10^3 CFU/ mL) and 3-fold (1.1 X 10^5 CFU/ mL), respectively (Figure 6.2). Additionally, lysozyme resistance varied between the acapsular strains (Figure 6.2). These differences were deemed significant using an unpaired two-tailed Student t-test between the Δ*cps* strain and both the Δ*itrA2* and Δ*wzy* strains, but not between the Δ*itrA2* and Δ*wzy* strains (Figure 6.2). Complementation of Δ*itrA2* and Δ*wzy* with the WT *itrA2* and *wzy* genes, respectively, resulted in partial restoration of lysozyme resistance (Figure 6.3).

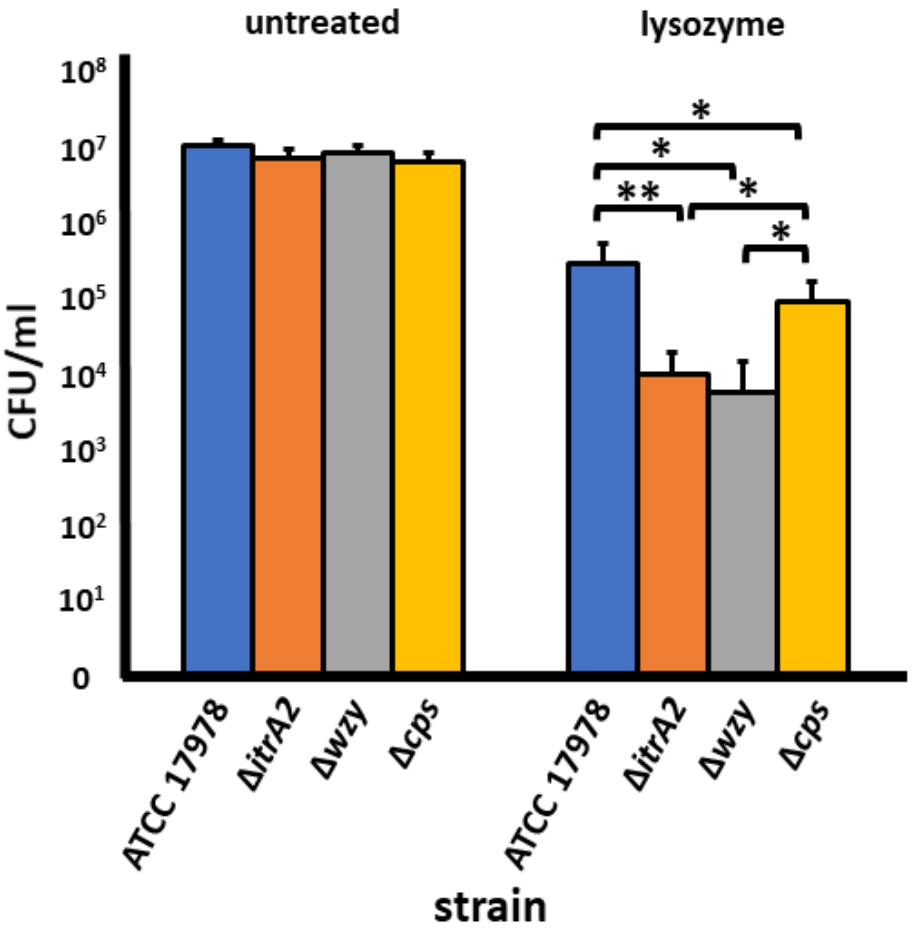

Figure 6.2. Viability of *A. baumannii* ATCC 17978 WT and acapsular variants after treatment with human lysozyme. Strains were grown in MH broth at 37ºC shaking until reaching an OD_{600} of 0.6 prior to incubation with 1 mg/ mL human lysozyme for one hr at 37ºC with gentle shaking. Ten-fold serial dilutions of bacterial samples were plated on LB agar and incubated ON at 37ºC and enumerated. Data represent the average of at least three independent replicates. Error bars represent the standard deviation. Statistical significance was determined using an unpaired two-tailed Student t-test (*= P <0.05 and **= P <0.01).

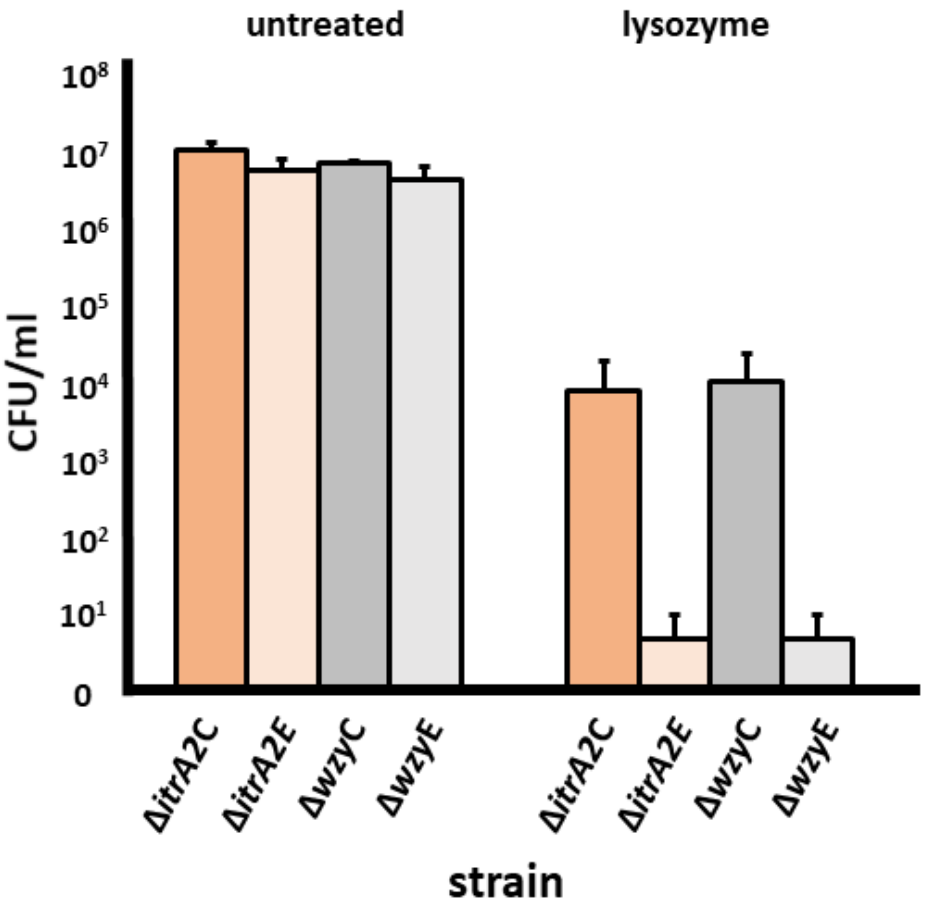

Figure 6.3. Viability of complemented *A. baumannii* ATCC 17978 Δ*itrA2* and Δ*wzy* after treatment with human lysozyme. Strains were grown in MH broth at 37°C shaking until reaching an OD_{600} of 0.6 prior to incubation with 1 mg/ mL human lysozyme for one hr at 37°C with gentle shaking. Serial dilutions of bacterial samples were then plated on LB agar and incubated ON at 37°C and enumerated. Strains are represented by; Δ*itrA2* complemented with the WT *itrA2* gene (Δ*itrA2*C), Δ*itrA2* containing the empty pWH1266 vector (Δ*itrA2*E), Δ*wzy* complemented with the WT *wzy* gene (Δ*wzy*C), Δ*wzy* containing the empty pWH1266 vector (Δ*wzy*E). Data represent at least three independent replicates; error bars represent the standard deviation. No statistical significance was found using an unpaired two-tailed Student t-test.

Although an obvious difference was seen between the complemented Δ*wzy* and Δ*itrA2* and the empty control strains it was not found to be statistically significant, this may be due to the variability between isolates (Figure 6.3). For example, the range for Δ*itr*A2C was between 10^2 CFU/mL and 2.6 x 10^4 CFU/mL

The increased sensitivity of acapsular strains compared to its parent was expected, though the large difference between Δ*cps* and Δ*itrA2* was not, as both mutants affect the initial stages of capsule synthesis and thus should have similar resistance profiles (Section 4.2.3). Furthermore, a difference in lysozyme resistance was expected between the Δ*wzy* and Δ*itrA2*, as deletion of *wzy* resulted in cell structure abnormalities whereas the Δ*itrA2* cells are more similar to the WT morphology (Figure 4.12). Additionally, the Δ*wzy* mutant is thought to have a perturbation in peptidoglycan synthesis which may affect Δ*wzy* differentially to the other acapsular mutants assessed (Section 4.2.5.5). Overall, the reduction in lysozyme resistance seen in all the acapsular mutants corroborate results of a previous study which showed reduced lysozyme resistance in acapsular *A. baumannii* AB5075 (Tipton et al., 2018).

6.2.3 Capsule is essential for serum resistance of *A. baumannii*

Activation of the complement system upon infection results in a coordinated response by complement proteins. This 'complement cascade' leads to opsonisation of pathogens, which targets them for degradation by phagocytes as well as direct cell lysis via the formation of pores in the bacterial membrane (Sarma and Ward, 2011). Bacterial pathogens, including *A. baumannii*, have evolved mechanisms to resist killing by serum complement such as the production of complement inactivation or inhibiting proteins (King et al., 2009, Koenigs et al., 2016), lipid asymmetry pathways (Sanchez-Larrayoz et al., 2017) and capsule production (Russo et al., 2010, Geisinger and Isberg, 2015, Niu et al., 2020).

Capsule production is essential for survival of *A. baumannii* within human serum, primarily as it protects cells from complement-directed cell lysis (Section 1.3.4). Several studies have shown acapsular *A. baumannii* to be completely sensitive to complement-mediated killing (Niu et al., 2020, Russo et al., 2010, Geisinger and Isberg, 2015). In this study, complement resistance was assessed for the WT and acapsular

variants of the *A. baumannii* strains 04117201 and ATCC 17978 as well as the complemented strains of the ATCC 17978 acapsular mutants.

6.2.3.1 *Serum resistance of 04117201 is mediated by the production of capsule*

Serum resistance of *A. baumannii* 04117201 and the acapsular 04117201Δ*wzy* variant was determined by survival of bacterial cells exposed to 40% guinea pig serum for two hours (Section 2.14). Compared to the WT 04117201 strain, a 6-log reduction in viability was seen in the acapsular Δ*wzy* strain (Figure 6.4). To confirm this finding, bacterial survival was compared to a heat-inactivated complement control (Section 2.14). Compared to the control, 04117201 WT survival in serum was approximately 45%, whereas survival of the acapsular Δ*wzy* strain was less than 0.001% (Figure 6.4a). Because of the extremely low resistance of 04117201Δ*wzy*, survival in a range of guinea pig serum concentrations was investigated (Figure 6.4b). A reduction in Δ*wzy* cell viability by at least 10-fold was seen in serum concentrations as low as 0.12%, highlighting the extreme sensitivity of the acapsular 04117201 strain to serum (Figure 6.4b). Capsule production is essential for survival of ATCC 17978 in human serum.

Human-derived serum was used in the survival assays of ATCC 17978 WT and acapsular variants to better mimic the response seen in the human host. Methodologies used were the same as that used for the *A. baumannii* strain 04117201 assay employing guinea pig serum (Section 2.14). Briefly, bacterial aliquots were incubated in 40% human serum for two hours, 10-fold serial dilutions were plated onto LB agar and incubated ON for enumeration and comparison to the heat-inactivated serum control (Section 2.14). Prior to changing to human serum, the resistance of ATCC 17978 WT and Δ*itrA2* strains to guinea pig serum was determined. The WT strain displayed a survival rate of 65% compared to the inactivated control whereas the resistance of Δ*itrA2* dropped to approximately 2% (data not shown). When the WT *itrA2* gene was reintroduced into Δ*itrA2* a partial restoration of 35% resistance was seen (data not shown).

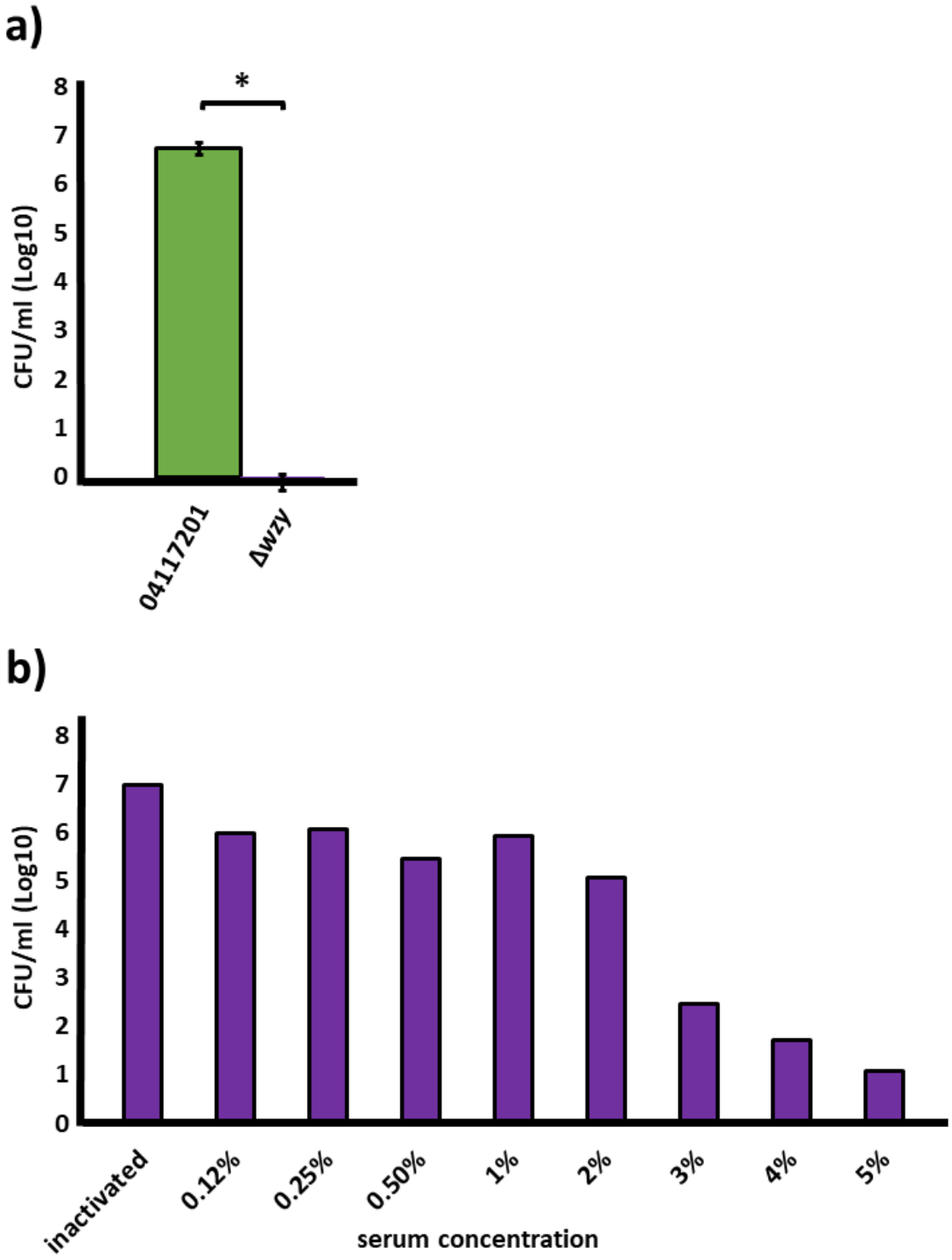

Figure 6.4 Survival of 04117201 WT and Δ*wzy* in 40% guineapig serum. Strains were grown to an OD_{600} of 0.6 and incubated with guinea pig serum for 2 hrs slowly shaking at 37^{o}C. a) WT 04117201 and Δ*wzy* incubated in 40% serum, b) Δ*wzy* incubated in a range of serum concentrations. Statistical significance was determined using an unpaired two-tailed Student t-test (*= P <0.05).

As expected, survival in human serum was drastically reduced for all acapsular ATCC 17978 variants compared to the WT strain, with a reduction of cell viability of >3-log for all acapsular mutants (Figure 6.5a). Survival in human serum compared to survival in inactivated serum was 17% for the WT ATCC 17978, <0.001% for the Δ*itrA2* and <0.01% for Δ*cps* and Δ*wzy* (Figure 6.5a). Although a statistically significant difference was seen between the Δ*itrA2* and Δ*cps* strains ($p = 0.02$), survival rates of both strains were extremely low and thus both strains would be incapable of surviving within a host organism(Sanchez-Larrayoz et al., 2017) (Figure 6.5a). Upon complementation with the WT *itrA2* and *wzy* genes in the Δ*itrA2* and Δ*wzy* variants, respectively, survival in human serum returned to WT levels when compared to the empty vector control (Figure 6.5b).

The extreme reduction in serum resistance seen in the acapsular variants of 04117201 and ATCC 17978 mirror the results of previous studies on capsule-deficient *A. baumannii*. One study found inactivation of genes encoding the capsule export proteins Wza and Wzc in the *A. baumannii* strain 307-0294, resulted in a 1% and 0% survival in human serum, respectively, compared to 100% for the WT strain (Russo et al., 2010). A recent study investigating the role of capsule in virulence of an MDR isolate, SKLX024256, reported serum survival of a Δ*wza* mutant to be greatly diminished compared to the WT strain, with survival rates of 2% and 40%, respectively (Niu et al., 2020). Lastly, a study by Geisinger et al reported 0% survival in 30% rabbit serum for an Δ*itrA* mutant in ATCC 17978 (Geisinger and Isberg, 2015). Interestingly, survival of the WT ATCC 17978 in rabbit serum was only approximately 1% when compared to the heat-inactivated control (Geisinger and Isberg, 2015). Thus, survival of ATCC 17978 in rabbit serum was far lower than we reported for human (17%) and guinea pig (65%) serum. This inconsistency demonstrates that the source of biological products for *in vitro* virulence assays, such as serum, should be of human origin where possible to best model the human host.

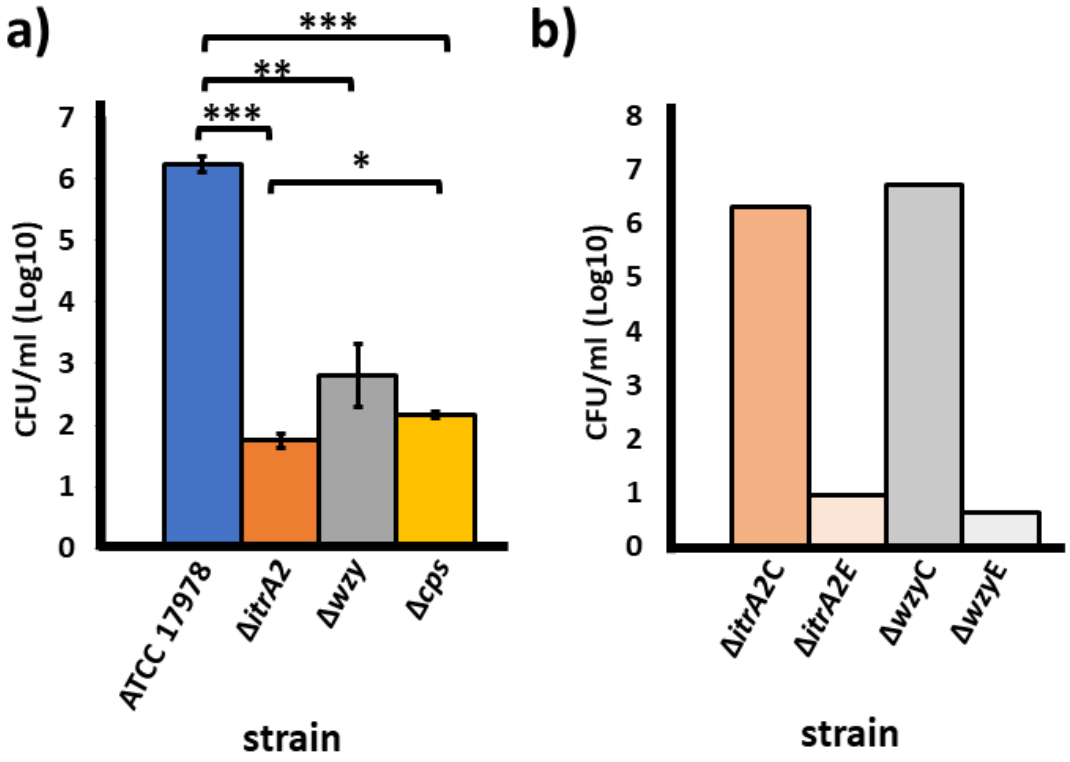

Figure 6.5 Survival of ATCC 17978 WT and acapsular mutants in human serum. Strains were grown to an OD_{600} of 0.6 and incubated with 40% human serum for 2 hrs slowly shaking at 37^{o}C. Survival in human serum expressed as log10 CFU/ mL. a) WT ATCC 17978 and acapsular mutants incubated in 40% serum. Data represent the average of three replicates, error bars represent standard error. Statistical significance was determined using an unpaired two-tailed Student t-test (*= P <0.05, **= P <0.01, ***=P<0.001). b) Strains represented by; Δ*itrA2* complemented with the WT *itrA2* gene (Δ*itrA2*C), Δ*itrA2* containing the empty pWH1266 vector (Δ*itrA2*E), Δ*wzy* complemented with the WT *wzy* gene (Δ*wzy*C), Δ*wzy* containing the empty pWH1266 vector (Δ*wzy*E), data represent the average of two independent replicates.

6.2.4 Assessment of the role capsule plays in adherence of *A. baumannii* to A549 human type 2 pneumocytes

Adherence of *A. baumannii* to host tissue is an essential step in colonisation and subsequent infection of the human host. Previous studies have shown that *A. baumannii* isolates are capable of adhering to a range of host tissues, though epithelial cells derived from the respiratory tract seem to be more susceptible (Choi et al., 2008). Additionally, the ability to adhere to eukaryotic cells differs substantially between *A. baumannii* strains (Eijkelkamp et al., 2011b). In this study, the adherence capabilities of *A. baumannii* WT and acapsular strains to A549 human type 2 pneumocytes was investigated (Section 2.21, Table 2.2). The A549 pneumocyte cell line was chosen as it mimics colonisation of the lung, a common site of *A. baumannii* infection (Section 1.1.3). Furthermore, the A549 cell line has previously been used as an infection model for a number of respiratory pathogens including *A. baumannii* (Eijkelkamp et al., 2011b). It was hypothesised that removal of capsule would result in increased adherence to A549 pneumocytes due to increased exposure of surface proteins; such as OmpA and biofilm associated protein (BAP), identified as important for *A. baumannii* adhesion to host tissues (Choi et al., 2008, Brossard and Campagnari, 2012, Gaddy et al., 2009). In addition, the drastic shift in hydrophobicity seen in the acapsular ATCC 17978 strains may affect interactions between the cell surface interface between bacterium and host (Section 5.2.2). Furthermore, the acapsular variants of both ATCC 17978 and 04117201 show higher levels of biofilm production, which may influence adherence to eukaryotic cells (Section 5.2.2) (Ryu et al., 2017).

6.2.4.1 *Adherence of 04117201 WT and acapsular Δwzy to A549 pneumocytes*

Adherence assays were undertaken to assess adherence of 04117201 WT and Δ*wzy* to A549 pneumocytes (Section 2.21, Section 2.2). For each adherence assay, a multiplicity of infection (MOI) of approximately 100:1 bacterial to eukaryotic cells was aimed for based on previous studies (Brossard and Campagnari, 2012, Choi et al., 2008). This is because high bacterial loads can lead to cytotoxicity and destruction of tissue culture monolayers cells, indicated by tissue cells sloughing off the culture plate surface (Krzymińska et al., 2012, Lee et al., 2001).The actual MOI for adherence assays was slightly higher than optimal with a range of 120 to 230 bacterial cells per A549 cell

(data not shown). Although the inoculum of bacterial cells was high, there was no indication of reduced A549 viability during the experiments. The acapsular 04117201 Δ*wzy* strain showed an increased adherence of approximately 1.5-fold compared to its parent, though this difference was not deemed to be statistically significant (P=0.056) using an unpaired two-tailed Student t-test. (Figure 6.6).

6.2.4.2 *Removal of capsule influences A. baumannii ATCC 17978 adherence to, and invasion of A549 pneumocytes*

The adherence of ATCC 17978 WT and acapsular variants to A549 pneumocytes was assessed (Section 2.21). Interestingly, compared to the 04117201 WT and acapsular strains (Section 6.2.4.1), all ATCC 17978 strains displayed markedly lower adherence to A549 cells (Figures 6.6 and 6.7). This may be due to the higher starting concentration of the 04117201 derived strains, which had an initial average inoculum of 2.5 x 10^7 compared to that of ATCC 17978 which had an initial inoculum of 9.5 x 10^6. Despite this, 80% of the initial inoculum of 04117201 adhered to the A549 cells whereas only 0.29% of the ATCC 17978 strain adhered. This supports a previous study identifying that strains of *A. baumannii* differ greatly in their ability to adhere to A549 pneumocytes (Eijkelkamp et al., 2011b).

As expected, both the Δ*itrA2* and Δ*wzy* variants showed increased adherence to A549 cells compared to the WT ATCC 17978 strain, displaying a 3.1- and 2.4-fold increase in adherence, respectively (Figure 6.7a). Despite this, differences observed were not deemed statistically significant, most likely due to inconsistent results between replicates which resulted in wide error margins (Figure 6.7a). Unfortunately, despite attempts to control factors including the bacterial inoculum, consistency of pneumocyte monolayers, timing, and media composition, the results remained inconsistent between replicates. The Δ*cps* strain was not included in this assay as it had not yet been generated when the assay was performed.

It was previously demonstrated that the Δ*wzy* strain grows slower in the nutrient rich MH media than the WT, Δ*itrA2,* and Δ*cps* ATCC 17978 strains (Section 5.2.1). As the difference in growth rate may skew data of the adherence assays all strains were grown in A549 growth medium in parallel with the adherence assays.

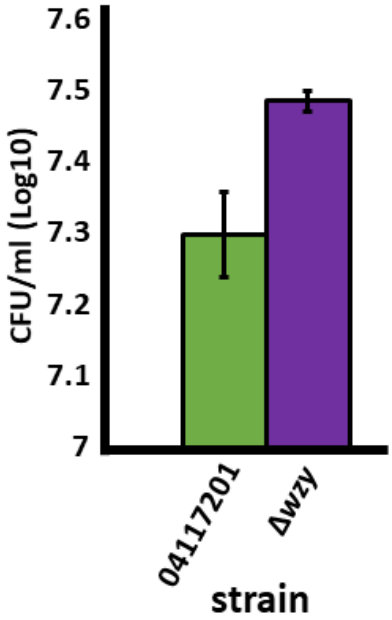

Figure 6.6 Adherence of 04117201 WT and Δ*wzy* mutant to A549 pneumocytes. Strains were incubated with A549 pneumocytes for 4 hrs at 37ºC before washing and enumeration by a plate dilution method. The number of adherent bacterial cells is expressed as the log10 CFU/ mL. Data represent the average of three independent replicates. No statistical significance was found using an unpaired two-tailed Student t-test.

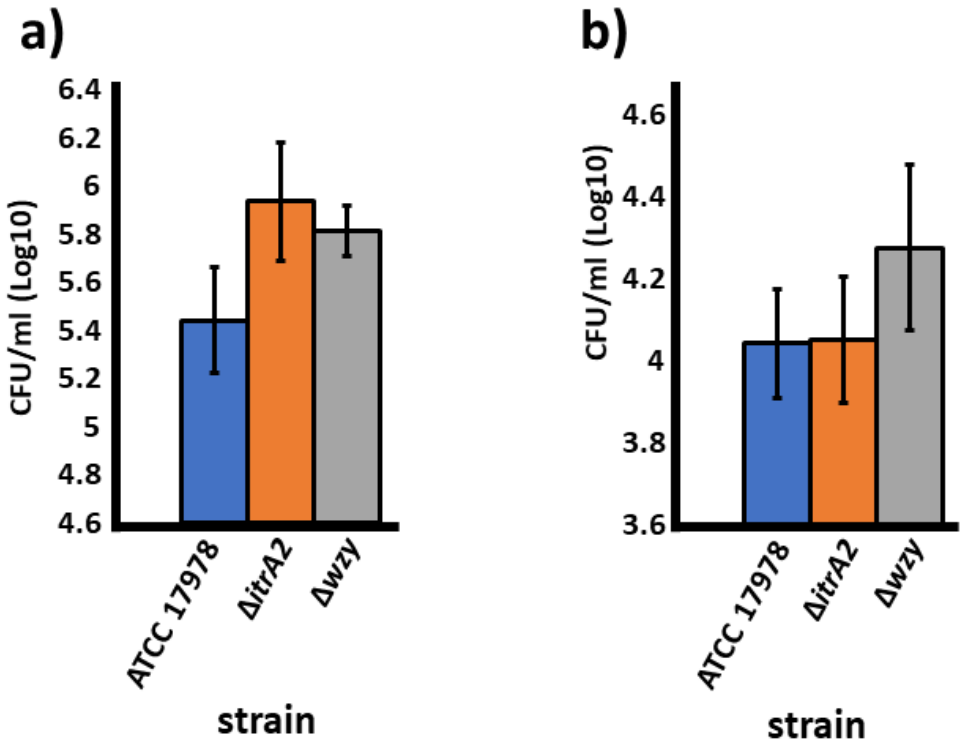

Figure 6.7 Adherence of ATCC 7978 WT and acapsular mutants to A549 pneumocytes. a) adherence to A549 pneumocytes. Strains were incubated with pneumocytes for 4 hrs before washing and enumeration by plate dilution method. b) invasion of A549 pneumocytes. Strains were incubated with pneumocytes for 4 hrs before treatment with 12.5 µg/ mL gentamicin for 45 min. Pneumocytes were then lysed with trypsin and bacteria enumerated by plate dilution method. The number of adherent or invading bacterial cells is expressed as the log10 CFU/ mL. Data represent the average of three independent replicates. No statistical significance was found using an unpaired two-tailed Student t-test.

Only a small difference in growth was seen between the *A. baumannii* WT and acapsular variants after 4 hrs incubation in DMEM (data not shown). All strains exhibited a 2- to 2.4-fold increase in CFU/ well, suggesting growth rates were similar between strains and thus not likely to influence adherence results (data not shown).

It was also of note that small colony variants were often isolated on the Δ*wzy* enumeration plates used to determine adherence CFU/ well. When these colonies were re-streaked onto solid medium the normal colonies (approximately 1.5-2 mm diameter) resulted in only normal colonies whereas punctiform colonies gave rise to both normal and punctiform subtypes (data not shown). Whether or not this phenotype affected adherence capabilities remains to be investigated but may represent a response of Δ*wzy* to stressful conditions.

Adaptions were made to the methodology of the adherence assays as pneumocytes had a tendency of sloughing off the plate during the washing process (Section 2.21). Initially, after co-incubation of pneumocytes and bacteria, the DMEM medium was removed and replaced with 1 mL of PBS (Section 2.21, Table 2.4). All wells were then washed three times with PBS prior to lysis of pneumocytes and plating of adherent bacteria. Because the washing procedure was thorough, it took almost 50 minutes to wash all 24 wells. This may have resulted in stress on the pneumocytes sitting in PBS and subsequent issues with sloughing cells. To circumvent this issue, the protocol was adjusted to wash one column (4 wells) of the 24 well plate at a time (Section 2.21). For the other wells, medium was removed and 200 µL of DMEM was added, as this may be more favourable for maintaining pneumocyte attachment than PBS (Table 2.4). As each column represented one replicate for each strain the new method would not significantly alter results gained.

In addition to adherence, the ability of WT and acapsular Δ*itrA2* and Δ*wzy* ATCC 17978 to invade A549 pneumocytes was assessed (Section 2.21). This was performed as per the adherence assay except after co-incubation of A549 cells with bacteria the medium was replaced with DMEM containing 12.5 µg/ mL gentamicin to kill all extracellular bacteria (Section 2.21). All three strains were capable of invading A549 epithelial cells, though the bacterial load was higher for Δ*wzy* compared to the WT and Δ*itrA2* ATCC 17978 strains (Figure 6.7b). This result was unexpected as a correlation between

increased adherence and increased invasion was predicted for both Δ*itrA2* and Δ*wzy* strains compared to the WT parent.

6.2.4.3 *Immune gene expression of pneumocytes challenged with A. baumannii ATCC 17978*

The pulmonary innate immune response is vital in preventing and rectifying primary pneumonia caused by *A. baumannii* (Section 1.3). Pulmonary epithelial cells secrete many immunoregulatory chemokines and cytokines in response to bacterial challenge. For example, secretion of the cytokines IL-6 and IL-8 are important for pulmonary clearance of *A. baumannii* as they recruit phagocytes to the site of infection (De Breij et al., 2010, March et al., 2010). Previous studies have found an increase in the production of certain cytokines in response to challenge with acapsular bacterial strains compared to their WT counterparts. For example, one study found A549 pneumocytes challenged with acapsular *K. pneumoniae* produced higher levels of IL-8 than pneumocytes challenged with the WT strain (Regueiro et al., 2006).

In this study, the immunoregulatory response of A549 pneumocytes to challenge with ATCC 17978 WT and acapsular mutants was assessed (Sections 2.21 and 2.7). The expression of two proinflammatory cytokines, IL-6 and IL-8, by naive pneumocytes and those challenged with ATCC 17978 WT and acapsular variants, Δ*wzy* and Δ*itrA2*, were determined (Sections 2.21 and 2.7). The RNA was extracted from pneumocytes after 4 hours co-incubation with *A. baumannii* ATCC 17978 and the two acapsular derivatives and naive pneumocytes as a negative control (Section 2.7.1). Th extracted RNA was reverse transcribed as per description in section 2.7. The complementary DNA (cDNA) then used as a template to amplify the genes of interest using RT PCR. In addition to IL-6 and IL-9 the housekeeping gene β-Actin was amplified as a control to normalise the results of the genes of interest between samples (Section 2.7, Table 2.6)(Vogel et al., 2012). Transcriptional differences were calculated using the $\Delta\Delta C_t$ method (Section 2.7.2). The RT PCR experiment included amplification of the β-Actin gene, which is constitutively expressed. The cycle threshold (C_t) of each experimental sample can then be compared to the C_t of the β-Actin gene to normalise the samples (Vogel et al., 2012). Preliminary experiments demonstrated that the pneumocytes elicited a strong proinflammatory response to all three bacterial strains (Figure 6.8).

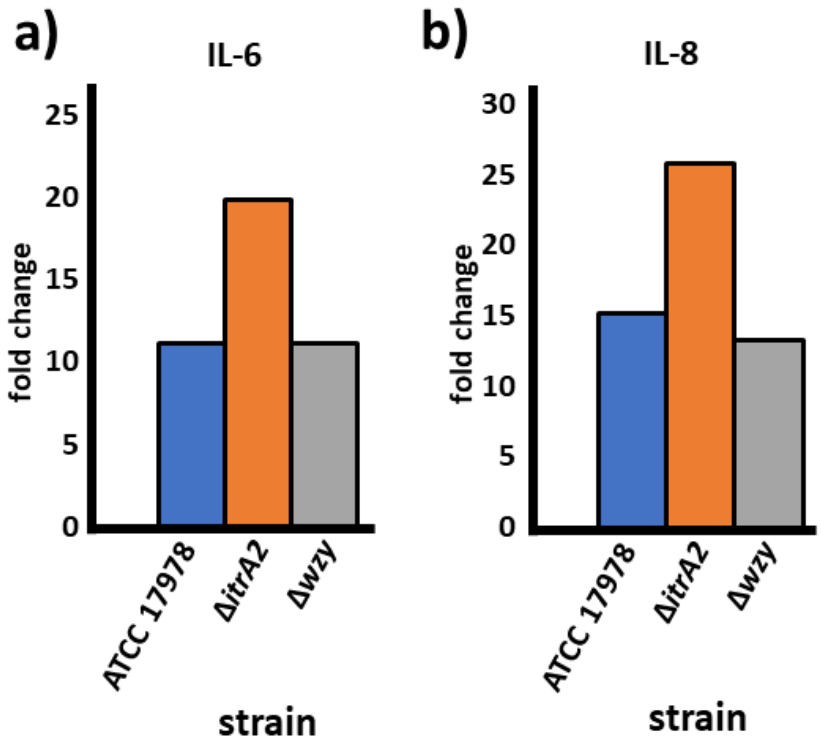

Figure 6.8 Expression of IL-6 and IL-8 by A549 pneumocytes in response to bacterial challenge. Total RNA was extracted from pneumocytes incubated with or without bacteria for 4 hrs at 37^{o}C. Expression of a) IL-6 and b) IL-8 of pneumocytes were determined by qRT-PCR. Fold changes were determined by comparing expression levels to naive pneumocytes. RNA was extracted from three independent replicates and pooled samples were run in quadruplicate. C_t values were normalised against β-actin expression.

Compared to naive A549 cells, pneumocytes showed an 11-fold increase in IL-6 gene expression when challenged with ATCC 17878 WT and Δ*wzy*, and a 20-fold increase when challenged with Δ*itrA2*. A similar trend was seen for IL-8 with a 13-fold, 15-fold and 26-fold increase in expression by pneumocytes when challenged with WT, Δ*wzy* and Δ*itrA2*, respectively (Figure 6.8). These results suggest that the Δ*itrA2* strain may elicit a stronger immune response compared to the WT and Δ*wzy* strains. As the Δ*itrA2* strain has inhibited protein glycosylation, this may account for the increased immunogenicity as un-glycosylated proteins may be more readily identified by the immune system and thus result in an enhanced immune response. Ultimately,further replicates would be needed to confirm this result. Replicates were not performed due to time constraints and limited resources available.

6.2.1 Capsule production may affect phagocytosis of *A. baumannii* by macrophages

The ability to evade uptake and resist lysis by macrophages is a key determinant of bacterial survival within the host and plays an important role in *A. baumannii* infections (Section 1.3.1). For example, a study which infected mice intranasally with *A. baumannii* showed macrophages to be the major immune cell type present in the airway 2-4 hrs post-infection (Qiu et al., 2012).

To assess whether capsule protects *A. baumannii* from macrophage phagocytosis, murine-derived RAW 264.7 macrophages were challenged with the WT and acapsular variants of 04117201 and ATCC 17978. In addition, phagocytosis of ATCC 17978 WT and acapsular mutants by human-derived macrophages including the U937 immortal monocyte cell line and human MDMs were assessed (Table 2.2, Section 2.22).

6.2.1.1 *Phagocytosis and intracellular survival of A. baumannii within murine RAW 264.7 macrophages*

Macrophage phagocytosis and bacterial intracellular survival of ATCC 17978 WT, 04117201 WT and 04117201Δ*wzy* strains was assessed using RAW 264.7 murine macrophages. Adherent monolayers of RAW 264.7 cells were challenged with approximately 10^6 bacteria per well, a MOI of 2:1 macrophage: bacteria, for 45 min before treatment with amikacin to kill extracellular bacteria (Section 2.22.1).

Macrophages were then lysed, and intracellular bacteria enumerated at various time points post amikacin treatment (Figure 6.9). At 45 min post amikacin treatment approximately 2-fold more 04117201 WT ($1.4x\ 10^5$) cells were recovered compared to ATCC 17978 WT ($7.7x\ 10^4$) (P=<0.01) (Figure 6.9).

The 04117201Δ*wzy* strain also showed significantly higher levels of recovered bacteria compared to ATCC 17978, though this was not deemed statistically significant (Figure 6.9). Intra-macrophage bacterial counts were taken at time points up to 315 min post amikacin treatment to ascertain intracellular survival (Section 2.22.1). Both 04117201 WT and acapsular variant were capable of growth within macrophages (Figure 6.9). The 04117201 WT and acapsular variant showed an increase in viable count of approximately 3-fold over the 315 min incubation, whereas intra-macrophage survival of ATCC 17978 WT reduced by 5.8-fold (Figure 6.9). Intra-macrophage survival of the 04117201Δ*wzy* strain was very similar to that of the 04117201 WT strain, suggesting capsule is not important for intra-macrophage survival of 04117201.

In some studies, macrophages are activated with a *E. coli* LPS prior to phagocytosis assays to stimulate a more robust immune response (Chen et al., 2018, Lee et al., 2017b). To test whether the addition of *E. coli* LPS affected bacterial uptake and lysis by RAW 264.7 macrophages, assays including *E. coli* LPS were performed in parallel with an untreated control. No differences between the LPS treated and non LPS treated RAW 264.7 macrophages were identified (Figure 6.10).

6.2.1.1 *Macrophage phagocytosis of ATCC 17978 acapsular variants by human derived macrophages*

The U937 immortal monocyte cell line was initially chosen for macrophage phagocytosis assays of ATCC 17978 WT and acapsular variants (Table 2.3). Despite troubleshooting measures employed, no useable data were gathered from the U937 assays (data not shown). For the first attempt the U937 cells, cultured in RPMI medium (Section 2.2), adhered onto the wells of a 24 well plate by culturing in the presence of 10 mM PMA for 24-48 hrs (Section 2.22.2). Although differentiation and adherence of U937 cells resulted in confluence, during the washing steps of the assay approximately 50% of cells sloughed off the plate surface. As patchy coverage can lead to inaccurate results this attempt was abandoned.

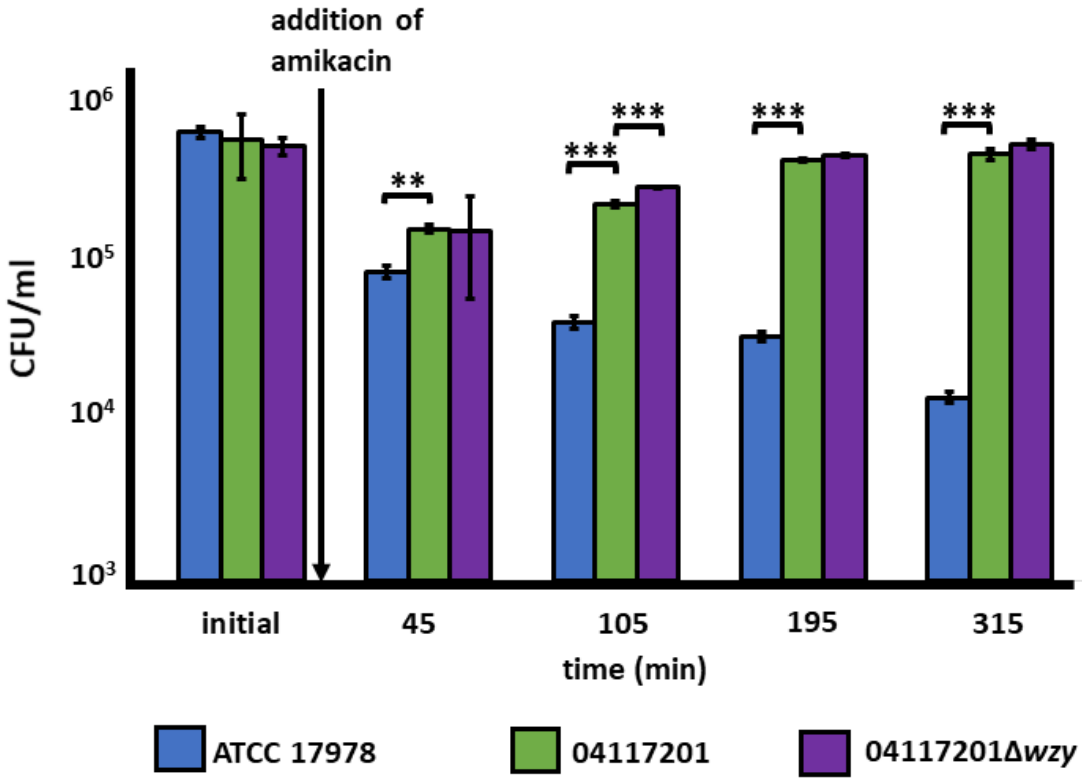

Figure 6.9 survival of *A. baumannii* ATCC 17978 WT, 04117201 WT and 04117201Δ*wzy* within RAW 264.7 macrophages. Macrophages were inoculated with approximately 10^6 of each bacterial strain and incubated at 37^{o}C for 1 hr before the addition of 25 µg/ mL amikacin to kill all bacterial cells not taken up by macrophages. Macrophages were lysed, and bacteria enumerated by plate dilution method at given time points. Assays were completed in triplicate. Error bars represent standard deviation. Statistical significance was determined using an unpaired two-tailed Student t-test (**= P <0.01 and ***= P <0.001).

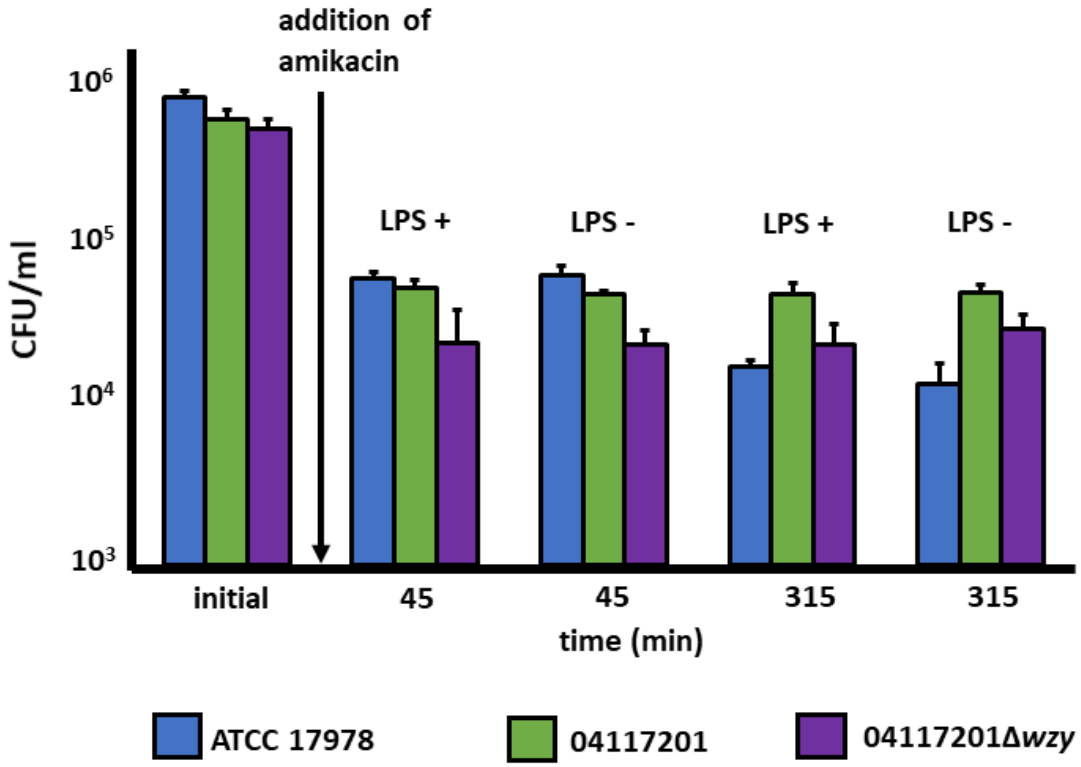

Figure 6.10 survival of *A. baumannii* ATCC 17978, 04117201 WT and 04117201Δ*wzy* within RAW 264.7 macrophages with and without pre-treatment with LPS. Macrophages were stimulated with 10 ng/ mL *E. coli* LPS 24 hrs prior to incubation with bacteria (LPS +). Macrophage monolayers were inoculated with approximately 10^6 of each bacterial strain and incubated at 37^{o}C for 1 hr before the addition of amikacin to kill all bacterial cells not taken up by macrophages. Macrophages were lysed and bacteria enumerated by plate dilution method at given time points. Assays were completed in triplicate. Error bars represent standard deviation.

For the subsequent assay, U937 monocytes were grown in RPMI medium and differentiated using a lower concentration of PMA, which does not stimulate adherence, and the assay was performed in suspension. Differentiated U937 cells were visualised by microscopy, with trypan blue staining to enumerate live versus dead cells, and resuspended in RPMI media to a density of 5 X 10^6 live cells per sample (Section 2.22.2).

Macrophage suspensions were then challenged with ATCC 17978 and Δ*itrA2* cells at a MOI of 10:1 bacterial to macrophage cells. Only a small number of the bacterial inoculum was recovered from the phagocytosis assay, indicating a higher MOI was required (data not shown). Further attempts to sub-culture U937 cells proved unsuccessful; attempts to identify the cause of this included changing the media used to grow the cells and testing for mycoplasma contamination using RT-PCR (data not shown).

To circumvent the need to routinely subculture monocyte cell lines, a method involving the isolation of MDMs was trialled. Human MDMs were isolated from human blood buffy coats and processed as per Section 2.20. Each respective well of MDMs was inoculated with a MOI of 5:1 bacteria to macrophages and incubated for 1 hr before the addition of 16 µg/ mL gentamicin to kill extracellular bacteria (Section 2.22.3). The MDMs were harvested and lysed one hour after the addition of gentamicin and intracellular bacteria enumerated (Figure 6.11). Both the Δ*itrA2* and Δ*cps* acapsular variants were more readily phagocytised compared to the ATCC 17978 WT strain, with an increase of 3.5- and 4.9-fold intracellular bacteria respectively (P= <0.05). The ATCC 17978 WT and Δ*wzy* variant showed similar levels of phagocyte uptake (Figure 6.11). As the initial inoculum of Δ*wzy* (~8 X 10^4 cells/well) was significantly lower than the WT, Δ*itrA2*, and Δ*cps* strains (~2 X 10^5 cells/well).

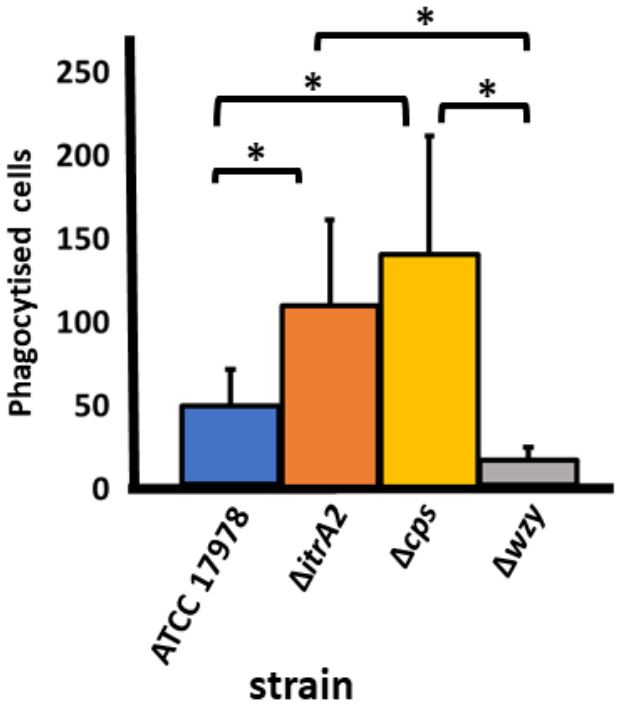

Figure 6.11 Phagocytosis by human monocyte derived macrophages. Macrophages were challenged with a MOI of 5:1 bacterial to macrophage cells. Assays were performed in triplicate. Error bars represent standard deviation. Statistical significance was determined using an unpaired two-tailed Student t-test (*= P <0.05 and **= P <0.01).

6.1 Conclusions

In this chapter it was clearly demonstrated that capsule is involved in modulating the bacterium's response to several host innate immune defences. It is important to note that interplay between the host and microbe *in vivo* is extremely complex as the immune response involves a range of cells and secreted molecules, thus the studies conducted provide only a snapshot of potential interactions affected by the production of capsule. Due to the high susceptibility of the acapsular mutants to a range of innate defences, particularly serum and lysozyme, it is therefore likely that these acapsular variants would be quickly cleared from any animal model and therefore assessing their pathogenicity in a murine model would likely be futile.

Generally, all acapsular variants were highly sensitive to both human complement and human lysozyme, showing significant reductions in viability after incubation with these compounds compared to their parental strains. Interestingly, differences were seen between the acapsular variants of ATCC 17978 when subjected to a variety of assays replicating the host immunological response. For instance, the ATCC 17978 Δ*wzy* strain was particularly susceptible to iron limitation, whereas growth of Δ*itrA2* and Δ*cps* was similar to the WT strain under iron-limiting conditions. Furthermore, all three acapsular strains of ATCC 17978 showed a decrease in lysozyme resistance compared to the WT, but to varying degrees.

Further studies involving eukaryotic tissue culture are needed to verify the differences seen between WT and acapsular *A. baumannii* cells regarding adherence to eukaryotic cells and phagocytosis by macrophages seen in this study. Although increased adherence to eukaryotic cells was seen for the acapsular *A. baumannii* strains compared to their respective WT parents, results were not deemed statistically significant. Similarly, an increase in phagocytosis of acapsular strains by macrophages was seen. A more thorough investigation of the interactions between eukaryotic host cells and acapsular *A. baumannii* may provide a better insight into the role capsule pays in host cell invasion and immune evasion of this pathogen.

7 DISCUSSION

Infections caused by *A. baumannii* are a serious public health issue as this bacterium thrives in the nosocomial environment and can resist most commonly used antimicrobials. As no single attribute can account for its clinical success, this survival termed ‘persist and resist’ has been used to describe the pathogenic strategy of *A. baumannii* (Harding et al., 2017, Gordon and Wareham, 2010, Jawad et al., 1998). Despite being referred to as an opportunistic or conditional pathogen, the high rates of antimicrobial resistance and mortality of *A. baumannii* infections has led to this microbe in being named a top priority on the WHO list for the development of novel antimicrobials (WHO, 2017).

The presence of capsular polysaccharide is most definitely a pivotal factor in the persist and resist survival tactic used by *A. baumannii* (Tipton et al., 2018). Capsule provides a protective barrier against harsh environmental conditions including desiccation, and prevents phagocytosis and complement killing during infection (Tipton et al., 2018).

In the present study, adaption to changing environmental conditions, such as antimicrobial challenge, acid stress, and survival in human complement was assessed for a variety of *A. baumannii* strains representing different K types was assessed (Section 3). Additionally, the ability to adapt to a number of stressors was evaluated for four acapsular variants were generated in the *A. baumannii* strain ATCC 17978 (Sections 4 to 6). Lastly, this study investigated cloning techniques for making capsule-swapped mutants (Section 4).

During the course of this study advances in the understanding of the role of capsules in *A. baumannii* virulence has been elucidated (Hu et al., 2020, Tipton et al., 2018, Talyansky et al., 2021, Niu et al., 2020). In this section the results obtained during this study will be analysed in light of the current status of research on the capsule of *A. baumannii*. This will include what has been uncovered and how it fits into the big picture of *A. baumannii* research; future studies will also be discussed.

7.1 Capsule structure and *A. baumannii* virulence

For many bacterial species capsule type is an important determinant of virulence potential (Sections 1.6, 1.7, and 1.8). For instance, 95% of *H. influenzae* strains which cause invasive disease possess type B capsule (Preston and Apicella, 1999), certain *wzi* subtypes have been found to correlate to higher virulence in *K. pneumoniae* (Diago-Navarro et al., 2014), and specific K types of *E. coli* are predominant in virulent strains (Cross, 1990). In addition, bacteria with certain capsule types are often isolated from specific infection sites and thus associated with different disease states. For example, in pneumococcal infections, certain serotypes are consistently isolated from meningitis cases whereas others are correlated to pneumonia outbreaks (Hausdorff et al., 2000a, Hausdorff et al., 2000b, Hausdorff et al., 2005).

Determining the impact of capsule type on virulence is clinically relevant as it can help identify targets for vaccine and treatment development. For instance, the 23 most virulent of the over 90 structurally distinct capsule types of *S. pneumoniae* go to make up the highly successful multivalent pneumococcal vaccine (Kim et al., 2017) . Moreover, novel antimicrobial treatments could be developed for specific capsule types, for example the incorporation of non-2-ulosonic acids in capsule structures has been correlated with enhanced virulence (Kao et al., 2016, Hitchen et al., 2010).

7.1.1 Capsule structure influences *A. baumannii* virulence in ATCC 17978

Evidence is emerging that the structure of capsule is important for *A. baumannii* virulence (Talyansky et al., 2021). In Section 3 of this thesis, the pathogenic potential of a variety of *A. baumannii* strains was analysed (Section 3.2) These strains varied significantly in their ability to survive under a number of environmental stressors, though this could not be attributed solely on capsule type as many other factors influence survival (Section 1.2, 3.2). To ascertain the role of capsule in virulence isogenic strains displaying various capsule structures are required. A recent study found removing a side chain from the capsule structure of ATCC 17978 (K3) increases virulence (Talyansky et al., 2021). By comparing *A. baumannii* strains with and without

a natural transposon interruption of a specific glycosytransfersase gene which adds a second side chain to the K3 capsule type (Gtr6), authors identified a correlation between the presence of this side chain and attenuated virulence (Talyansky et al., 2021). To verify their findings, isogenic strains with *gtr6* removed (*gtr6*-) were generated in the *A. baumannii* strain ATCC 17978. The capsule structure of this *gtr6*- mutant lacked a second side chain and showed increased virulence in a murine model (Talyansky et al., 2021). The authors further identified increased virulence was associated with a reduction in macrophage phagocytosis, which is mediated by the interaction of the macrophage surface receptor CR3 and complement opsonised bacteria (Talyansky et al., 2021). In this thesis and previous studies, complement resistance was found to be exponentially higher in the encapsulated WT strains compared to the acapsular counterparts (Section 6.2.3) (Russo et al., 2010, Geisinger and Isberg, 2015, Singh et al., 2018). In the study by Talyansky *et al* the WT ATCC 17978 strain levels of complement deposition were found to be approximately 45%, whereas levels of complement deposition for the *gtr*- strain were undetected, and in an acapsular variant were >95% (Talyansky et al., 2021). It would be interesting to see whether the absence of the second branch in the capsule structure of ATCC 17978 leads to evasion of other host immune modulators and antimicrobials such as lysozyme and β-defensin (Figure 1.3).

Furthermore, studies into the role of the side chain in resistance to antibiotics such as colistin, which is known to be modified by the presence of capsule, would greatly enhance our understanding of the role capsule type plays in *A. baumannii* antimicrobial resistance. However, a downfall of the study comparing *gtr6*+ and *gtr6*- strains may be that they did not look at the role of capsule structure in a pulmonary model of infection, despite this being a major route of infection. Future *in vivo* studies using a pulmonary infection model may elucidate whether other immune factors found in pulmonary secretions are enough to thwart the infection before sepsis occurs (Talyansky et al., 2021).

Section 3 of this thesis explores capsule related phenotypes of *A. baumannii* strains representing varied capsule structures (Section 3). In light of the Talyansky experiments

additional *A. baumannii* strains with unbranched capsule types could have been selected and compared to single and double branched capsule types to see if there was any correlation between complexity of capsule type and virulence (Talyansky et al., 2021). The stains analysed in Section 3 showed no correlation between the number of capsule side chains and virulence. For example, the non-branched KL1 strains 307-0294 and A1 showed low and high resistance to complement, respectively (Section 3.2.5). Some of the K types assessed which have at least one side chain, such as KL12 and KL9, showed high levels of complement resistance (Section 3.2.5). Together this suggests complement resistance is multifactorial and not determined exclusively on capsule type. Furthermore, studies have identified a direct correlation between the amount of capsule produced and virulence (Chin et al., 2018, Tipton et al., 2018, Tipton et al., 2015) (Section 1.9). Levels of capsule produced by the various *A. baumannii* strains was not assessed in this thesis but may confound any differences seen between the various strains representing various capsule types (Section 3.2). Interestingly, a previous study by Geisinger and Isberg identified an increase in capsule production in *A. baumannii* when challenged with antimicrobials (Geisinger and Isberg, 2015) (Section 1.7). A quantitative relationship between the amount of capsule expressed on the cell surface and virulence has also been identified in *E. coli* and *K. pneumoniae* (Cross, 1990, Vermeulen et al., 1988). In the case of *E. coli* K1 capsule, low levels of capsule production reduced serum resistance substantially, and in *K. pneumoniae* decreased capsule expression leads to impaired colonisation of the urinary tract in mice (Struve and Krogfelt, 2003, Vermeulen et al., 1988). Additionally, an early study in pneumococcus revealed slightly increased virulence in mice when capsule levels were increased (MacLeod and Krauss, 1950).

Phase variation has been identified in multiple *A. baumannii* strains from a variety of multi-locus phenotypes (Ahmad et al., 2019). One study found the A. baumannii strain AB5075 (K25) has been associated with alterations in capsule production, as highly virulent opaque variants produce a capsule layer with twice the thickness of their translucent counterparts (Chin et al., 2018). This transition from translucent to opaque also dramatically increased the pathogenic potential of *A. baumannii* AB5075. Resistance to common hospital disinfectants and a subset of aminoglycoside antibiotics

were also increased (Tipton et al., 2015, Chin et al., 2018) and opaque variants were more resistant to human lysozyme, the cathelicidin-related antimicrobial peptide LL37 and hydrogen peroxide compared to translucent colonies (Chin et al., 2018). Furthermore, opaque isolates had an increased tolerance to desiccated conditions and out-competed translucent counterparts in a mouse infection model (Chin et al., 2018). Together, these studies suggest a relationship between virulence potential and capsule structure as well as the quantity of capsule produced.

7.1.2 Implications of *A. baumannii* capsule type for development of vaccines and treatments for *A. baumannii* infections

A 2013 study by Russo and colleagues outlined the potential for an *A. baumannii* capsule serotype as a target for passive immunisation, providing proof-of-concept for the development of capsule targeted therapies in *A. baumannii*. The authors found antibodies generated against the K1 capsule of *A. baumannii* strain AB307-0294 to be protective against infection in a mouse model. The efficacy of using K1 capsule antibodies against other *A. baumannii* strains was promising as 13% of the 100 clinical *A. baumannii* isolates tested in this study were reactive (Russo et al., 2013). A more recent study found capsule induced antibodies to offer 55% protection against a range of clinical *A. baumannii* strains (Yang et al., 2017). These studies indicate a polyvalent vaccine incorporating clinically relevant capsular types may protect vulnerable populations against *A. baumannii* infection (Section 1.10) (Russo et al., 2013). The use of anti-capsule phage therapy has also been explored to combat topical infections with *A. baumannii*. For example, a study recently demonstrated incorporation of anti-capsule *A. baumannii* phage in burn wound dressings improves outcomes in a porcine model; furthermore, these bacteriophage were shown to be stable in the presence of other antimicrobial impregnated dressings (Altamirano et al., 2020)

The addition of new K types to the repertoire of *A. baumannii* has been exponential, in line with increased WGS availability and data mining software development. For example a the development of an online reference database, *Kaptive*, which includes 92 distinct *A. baumannii* K loci, provides a standardised library of K loci and a tool for *in silico* typing of *A. baumannii* based on capsule sequences (Wyres et al., 2020). .

Evolutionarily, it makes sense for pathogens like *A. baumannii* to diversify its surface structures like capsule to evade adaptive immune responses. As we identify more K types, better analysis of the determinants of capsule structure and their role in virulence can be obtained. For example, whether certain residues such as non-2-ulosonic acid increase virulence, or whether the number of side chains affects the immune response to *A. baumannii* during infection.

7.2 Implications of removing specific capsule related genes

7.2.1 Generation of acapsular mutants

Most studies, including this one, generate gene deletion mutants in *A. baumannii* using homologous recombination of the chromosomal region of interest with a resistance marker flanked by homology regions on either one or both sides (Sections 4.2.2 and 4.2.5). The donor source of DNA then undergoes recombination with homologous regions on the bacterial chromosome (Tucker et al., 2014, Hoang et al., 1998, Aranda et al., 2010) (Section 2.5). This allows for incorporation of the resistance cassette and removal of the target gene (Section 2.5). Initially in this study, a resistance marker flanked by sequences homologous to the desired chromosomal target were incorporated into a non-replicating suicide delivery vector/plasmid to construct acapsular mutants (Hoang et al., 1998, Aranda et al., 2010) (Section 4.2.5). During this study, a paper was published outlining an alternative method which uses a linear PCR fragment which encodes a resistance gene flanked by chromosomal regions of the gene of interest to generate mutants (Tucker et al., 2014). This novel method was subsequently adopted as using linear DNA circumvented complicated and time-consuming cloning steps required when a plasmid vector is used (Tucker et al., 2014). This method was used for the successful generation of all three acapsular mutants in the *A. baumannii* strain ATCC 17978 (Section 4.2.5) (Tucker et al., 2014).

7.2.2 Selection of gene targets

The choice of gene targets for making acapsular *A. baumannii* variants is important as deletion of certain genes can have downstream or off-target effects. For example, deletion of *itrA2* can lead to a loss of capsule production and protein glycosylation as

this gene is used in both pathways (Section 4.2.5, Figures 1.2, 4.10 and 4.11). Understanding how mutations effect off-target processes is important for the interpretation of results and demonstrates the importance of complementing deletion mutants to ensure phenotypes seen are due to the target mutation and not compensatory mutations (Jorgenson and Young, 2016).

In this study three capsule deficient mutants, Δ*wzy*, Δ*itrA2*, and Δ*cps* were constructed in ATCC 17978 (KL3), and one capsule deficient mutant, Δ*wzy*, was generated in 04117201 (KL2) (Sections 4.2 and 4.5). The generation of Δ*wzy* in ATCC 17978 led to unanticipated downstream effects, such as compensatory mutations, and the generation of Δ*itrA2* and Δ*cps* resulted in the obstruction of protein glycosylation in ATCC 17978 (Section 4.2.5,). In this study many of the Δ*wzy* mutants constructed displayed a loss of protein glycosylation even though removing Δ*wzy* should leave that pathway intact (Figure 1.2). The Δ*cps* strain made in this study did not remove all capsule genes, just those required to construct a capsule swapped variant in ATCC 17978 (Figure 4.7). Concurrent to this study, a colleague constructed a capsule deficient strain of ATCC 17978 which removed all capsule loci genes which are located between *fkpA* and *lldp* in ATCC 17978 (Figure 1.3a). Interestingly, the responses to stress assays varied between the Δ*cps* created in this study and the Δ*cps* generated by a colleague (Cox, 2018). For example, the Δ*cps* variant, which removed the whole capsule loci was more susceptible to a range of antimicrobials including lysozyme, chlorhexidine, and benzalkonium, compared to the Δ*cps* generated in this study (Cox, 2018).

Complementation of the acapsular KL2 04117201 Δ*wzy* strain generated here was hindered due to the lack of finding suitable resistance markers. In this study, the generation of acapsular mutants required the insertion of a resistance marker to aid in selection (Aranda et al., 2010) (Section 4.2.4). As many *A. baumannii* strains, such as 04117201, are resistant to multiple antibiotics, the generation of markerless mutants would be useful for manipulating strains. This has previously been done by other research groups (Amin et al., 2013), and was explored by colleagues in my lab (Felise Adams, personal communication). Due to time constraints, the generation of markerless acapsular variants was not undertaken in this study. Additionally, the use of alternative

selection methods such as colour selection, or the incorporation of genes encoding fluorescence, may help circumvent selection issues such as those seen in complementing the Δ*wzy* strain in 04117201 (Godeux et al., 2018, Gallagher, 2019, Gallagher et al., 2015).

7.2.3 Generation of acapsular mutants and subsequent effects on colony morphology

Three acapsular mutants were generated in *A. baumannii* ATCC 17978 by removing the *wzy* polymerase gene, the *itrA2* initial transferase gene, and the multigene region of the K loci spanning from *gna* to *galU* (Δ*cps*) (Figure 4.7). In other studies, bacterial acapsular mutants exhibited a rough colony morphology with irregular edges (Morona et al., 2003, Jung et al., 2013). In this thesis, colonies of all three mutants were smaller and less viscous than the WT parental strain but did not display irregular edges (Figure 5.1). Complementation of Δ*wzy* and Δ*itrA2* strains with the respective WT gene did not fully restore growth (Figure 5.3). In this study, we were unable to complement the Δ*cps* strain due to issues cloning large fragments of DNA (Section 7.3).

The construction of Δ*wzy* in ATCC 17978 proved especially difficult (Section 4.2.5). This is consistent with other studies attempting to make mutants in genes required for capsule synthesis downstream of *itrA2* (Figure 1.2). For example, repeated attempts were needed by Geisinger *et al* to isolate a Δ*wzc* ATCC 17978 derivative (Geisinger and Isberg, 2015). Furthermore, the authors found these strains often required second-site mutations to remain viable. Growth of the Δ*wzc* strain lagged compared to the WT strain in standard growth media, this was also seen in this current study for Δ*wzy* (Section 4.2.5) (Geisinger and Isberg, 2015). Similar to this thesis, complementation of Δ*wzc* with the WT *wzc* gene did not restore growth to WT levels (Geisinger and Isberg, 2015). Interestingly, Geisinger *et al* also found a point mutation in the histidine kinase associated with the BfmRS TCS (*bfmS*), in a complemented Δ*wzc* isolate, showing that off target compensatory mutations are not limited to the capsule operon but may affect other gene regions (Section 1.9.1) (Geisinger and Isberg, 2015). This *bfmRS* mutation led to a highly mucoid phenotype, previous studies have shown *bfmRS* to be involved in complement resistance, biofilm production and OM stability (Liou et al., 2014) (Section

1.9.1).

Although the Δ*wzy* mutant was able to be partially restored to functionality in this thesis by complementation with the WT gene (Section 4.2.5), it is not known whether the Δ*wzy* strain constructed in this study had any point mutations in other genes such as global regulators. To determine this the WGS of this strain is required. In this study larger more mucoid colonies were often identified when grown on solid media (Figure 5.1). These may represent isolates with similar mutations seen by Geisinger and Isberg (Geisinger and Isberg, 2015). Interestingly, isolation and re-plating of these mucoid colonies did not result in mucoid progeny, suggesting a transient reason rather than a permanent point mutation (data not shown). In the Δ*wzy* isolate, complementation with the WT *wzy* gene partially restored WT phenotypes (Sections 5 and 6).

7.2.4 Removal of capsule related genes leads to changes in cell morphology in *A. baumannii*

When viewed under a compound microscope, the cellular morphology for both the Δ*itrA2* and Δ*cps* variants appeared enlarged and swollen compared to the WT progenitor strain (Figure 4.12a). This morphology has been previously reported in an Δ*itrA2* mutant generated in *A. baumannii* (Geisinger and Isberg, 2015). Furthermore, acapsular mutants in the closely related bacterium *P. aeruginosa* resulted in cells 7-9% larger than the WT and a deviation from the typical rod shaped morphology (Jorgenson et al., 2016, Burrows and Lam, 1999). Similarly, the removal of *wzy* in *A. baumannii* ATCC 17978 resulted in district morphological differences in cell shape compared to the WT strain (Figure 4.12a). The Δ*wzy* cells appeared elongated and formed a chain like structures (Figure 4.12a). Interestingly, a similar cellular morphology was seen for a Δ*wzc* mutant generated in *A. baumannii* (Geisinger and Isberg, 2015). This elongated morphology has also been shown in many previous studies where mutations affect one or more of the pathways reliant on the Und-P lipid carrier (Tatar et al., 2007, Bhavsar et al., 2001, Mao et al., 2001, Mao et al., 2006). Furthermore, some studies have identified that removing genes for processes needing Und-P are lethal in the absence of secondary mutations (Xayarath and Yother, 2007, Burrows and Lam, 1999, Jorgenson et al., 2016). The presence of a secondary mutation is not however always the case. For

example, previous *A. baumannii* studies have been able to complement mutations which influence Und-P dependant pathways (Niu et al., 2020, Geisinger and Isberg, 2015). When complemented with the WT *wzy* gene, the Δ*wzy* cells showed reversion to the normal Acinetobacter morphology coccobacillus, but cells were still enlarged compared to the WT (Figure 4.12a). Complemented Δ*itr* were closer to WT size and shape compared to cells carrying the empty vector used for supplying the WT *itr* gene which showed enlarged, bloated cells (Figure 4.12a). Further studies, such as WGS and transcriptome analyses, may determine what off target gene/s are mutated as well as changes in gene regulation which may compensate for deleterious effects of capsule knockouts.

7.2.5 Removal of capsule related genes affects other Und-P reliant pathways

Und-P is a lipid carrier essential for the synthesis of many cellular carbohydrates including CA, O-antigen, core polysaccharide and capsule (Jorgenson et al., 2016, Jorgenson and Young, 2016, Tatar et al., 2007, Richie et al., 2018). It is also essential in the formation of peptidoglycan, which plays a vital role in cell elongation and maintenance of cell shape (Jorgenson et al., 2016). Bacteria possess a limited pool of Und-P thus, accumulation of dead-end intermediates sequester available Und-P resulting in the unavailability of this essential lipid carrier for peptidoglycan synthesis (Jorgenson et al., 2016). Growth defects and morphological changes in cell shape seen in the acapsular mutants may be due to accumulation of Und-P linked intermediates (Jorgenson et al., 2016, Jorgenson and Young, 2016, Ranjit and Young, 2016).

The most likely cause of the extreme variation of the Δ*wzy* mutants compared to the WT is the disruption of peptidoglycan synthesis, and thus a defective membrane envelope (Jorgenson et al., 2016). Previous studies in *E. coli* have shown the removal of genes encoding proteins involved in CA synthesis, which uses the same Wzy-dependant synthesis pathway as *A. baumannii* capsule, lead to elongated filamentous cells which were prone to lysis (Jorgenson et al., 2016, Jorgenson and Young, 2016). Furthermore, deletions upstream of the initial transferase step of O-antigen synthesis do not accumulate Und-P, thus it is free to be used for other Und-P associated pathways

(Jorgenson et al., 2016). It is hypothesized that this elongation of cells may be due to the lack of continuous uniform peptidoglycan, which affects cell division (Jorgenson et al., 2016). Furthermore, Und-P accumulation results in bulges in the periplasmic space in *E. coli* (Ranjit and Young, 2016). The gross deformities seen in mutants which affect Und-P recycling result in changes in cell size and shape weaken the OM and thus make the bacterium more susceptible to a variety of stressors.

7.2.6 Variation between the acapsular mutants

Interestingly, many differences in the response to environmental stressors were seen between the various acapsular mutants generated in this study. For example, the Δ*itrA2* and Δ*cps* derivatives were sensitive to low pH stress, whereas the Δ*wzy* strain showed near WT level resistance to low pH stress (Section 5.2.3). Conversely, the Δ*itrA2* and Δ*cps* mutants showed similar levels of resistance to osmotic stress as the WT but Δ*wzy* cells were slightly more susceptible (Section 5.2.4). Differences were also seen between the acapsular mutants in response to various host protective factors including iron limitation (Section 6.2.1), lysozyme (Section 6.2.2), survival in human serum (Section 6.2.3), and phagocytosis by human monocyte derived macrophages (Section 6.2.5). These inconsistencies between acapsular strains highlights the need for more studies comparing various capsule related gene knock-outs.

7.3 Cloning the capsule loci and the difficulties working with large DNA segments

Several methods were employed in attempts to generate capsule swapped mutants in *A. baumannii* (Section 4.2.6). An essential part of this was working with large segments of DNA, as the capsule region needs to be reintroduced into acapsular strains to achieve a capsule swap. The K loci of the two *A. baumannii* strains used in this study, 04117201 and ATCC 17978, are approximately 23 and 20 kb, respectively (Section 4.2.6). Methods employed to generate capsule-swapped mutants include the incorporation of the K loci into a plasmid vector, recombineering methods similar to those used to make the acapsular mutants (Section 4.6.2), and employing a yeast cloning system (Section 4.2.7).

The most promising method for the cloning of the K loci was the employment of an OAP system that was published by Liu et al in 2017. In this study, the authors used the recombination DNA repair pathway of *S. cerevisiae* to simultaneously clone several DNA segments of the *E. coli* O-antigen into a shuttle vector (Liu et al., 2017). These constructs were then used to create *wzx*-swapped mutants to identify substrate preferences for this inner membrane protein (Liu et al., 2017). In a later study, the authors adopted this same system to generate capsule swapped mutants in *E. coli* (Liu and Reeves, 2019). This study showed that direct comparison of the influence of O-antigen type can be achieved using the OAP (Liu and Reeves, 2019). This was demonstrated with a number of different capsule operons, showing that swapping the capsule type can easily be modified using a wide variety of donor DNA from multiple *E. coli* strains (Liu and Reeves, 2019).

The colleagues who developed the OAP provided their detailed methodology and vectors. These were then used as the basis for establishing a method for generation of capsule swapped *A. baumannii* (Section 4.2.7) strains. Modification of the vector used in the OAP was needed to allow for replication in *A. baumannii*. The OAP vector, pPR2274, required the incorporation of an *A. baumannii* specific origin of replication (*ori*) (Section 4.2.7). By cloning the *ori* from the pWH1266 *A. baumannii* shuttle vector, used for the complementation of acapsular mutants generated in this study, the modified pPR2274 plasmid would be able to replicate in *A. baumannii*. Initially, this modification proved unsuccessful. This may have been because the pWH1266 plasmid encodes a toxin/antitoxin system which may have impaired the growth of isolates incorporating the required plasmid construct (Section 4.2.7). Concurrently, a colleague in our research group was able to successfully clone the pWH1266 *ori* into the pPR2274 vector using a more selective region of the pWH1266 plasmid (Cox, 2018). Furthermore, the modified pPR2274 was capable of replication within *A. baumannii* ATCC 17978. Due to time constraints, the generation capsule swapped mutants using this OAP was not completed. Future work in this area involves refinement of this protocol and undertaking the next step in the OAP process which involves amplifying overlapping regions of the KL2 region of *A. baumannii* 04117201 by PCR and incorporating them into the pPR2274 + pWH1266 ori construct (Section 4.2.7). The

resulting plasmid can then be introduced into the acapsular *A. baumannii* ATCC 17978 (KL3) variant to undergo homologous recombination, thus generating an isogenic ATCC 17978 capsule swapped mutant (Section 4.2.7).

In light of the successful generation of O-antigen mutants in *E. coli*, as well as the successful replication of pPR2274 + pWH1266 ori construct in *A. baumannii* suggests using the OAP to generate a number of capsule swapped mutants in *A. baumannii* is very much feasible (Liu and Reeves, 2019). Additionally, this method may be useful for the manipulation of large gene regions within the *A. baumannii* chromosome.

7.4 Conclusions

Overall, this thesis has demonstrated that capsule is important for the survival of *A. baumannii* under various stressful conditions, both in the hospital environment and within the host during infection. Comparison of cells with mutations that interrupt different stages of the capsule biosynthesis pathway showed the selection of target gene/s for inactivation or removal influences the outcome of subsequent virulence assays (Section 4.2). Importantly, this study is the first to successfully generate a Δ*wzy* mutant in *A. baumannii*, which allows for the comparison between a mutant with only capsule production affected and mutants with capsule plus protein glycosylation affected (Section 4.2). Generally, removal of capsule associated genes resulted in increased hydrophobicity and adherence to plastics and human tissue culture (Sections 5 and 6). Additionally, the acapsular strains showed higher susceptibility to antimicrobial compounds including ethanol, lysozyme, and complement; and reduced growth under iron limiting conditions (Sections 5 and 6).

The extraordinary ability of *A. baumannii* to survive in a range of hostile environments is definitely concerning and poses a substantial risk to public health, especially for our most vulnerable populations in the acute hospital setting. Increasing our understanding of the mechanisms behind this bacterium's persistence in is vital to the development of appropriate treatments against this problematic pathogen.

8 APPENDICES

8.1 Abbreviations

A

ABC; ATP-binding cassette

Aci5Ac7Ac 5,7-di-*N*-acetylacinetaminic acid

AGRF; Australian Genome Research Facility

AM; alveolar macrophage

Amp; ampicillin

Amp100; 100 µg/ml Amp

Amk; amikacin

ANOVA; analysis of variance

APS; ammonium persulfate

ATCC; American type culture collection

ATP: adenosine triphosphate

AVR; ATCC 17978 capsule variable region

B

BAP; biofilm associated protein

Blast; Basic logical alignment search tool

Bp; base pairs

BSA; bovine serum albumin

C

C; Celsius

CA; colanic acid

$CaCl_2$; calcium chloride

CAMPs; cationic antimicrobial peptides

cDNA; copy DNA

CFU; colony forming units

Cm; chloramphenicol

cm; centimetre

COH; carbohydrate

CPS; capsular polysaccharide

CRAB; carbapenem resistant *A. baumannii*

ct; cycle threshold

D

Da; daltons

DFR; downstream flanking region

D-FucpNAc; N-acetyl-D-fucosaminic acid

D-GalpNAcA; N-acetyl-D-galactosaminuronic acid

dH_2O; deionised water

DIP; 2,2’ dipyridyl

DMEM Dulbecco’s Modified Eagle Media

DMSO; dimethyl sulphoxide

DNA; deoxyribose nucleic acid

D-QuipNAc; N-acetyl-D-quinovosaminic acid

D-QuipNAc4NAc; 2,4-diacetamido-2,4,6-trideoxy-D-glucopyranose (N,N'-diacetyl-bacillosamine)

E

EDTA; ethylenediaminetetra-acetic acid

Ery; erythromycin

ery^R; erythromycin resistance cartridge

Ery12; 12µg/ml erythromycin

ETOH; ethanol

F

FCS; foetal calf serum

FUR; Ferric Uptake Regulator

G

g; grams

GT; glycosyl transferases

Gent; gentamicin

H

HβD; human β-defensin

HBBS; Hanks Balanced Salt Solution

HEPES; N-2-hydroxyethylpiperazine-N-2-ethane sulfonic acid

HEWL; hen's egg white derived lysozyme

HI; hydrophobicity index

H-NS; histone-like nucleoid structuring protein

hr; hour

H_2O_2; hydrogen peroxide

H_5IO_6; periodic acid

I

IC; international clones

IFN- interferon

IL; interleukin

OC; outer core

IPTG; isopropyl-β-D-galactopyranoside

IT; initial transferase

K

K; capsule

kb; kilobase

KEGG; Kyoto encyclopaedia of genes and genomes

KH_2PO_4;

KL; capsule loci

K unit; capsule unit

kV

L

L; litre

LB; Lysogeny Broth

LiAc; lithium acetate

LOS; lipooligosaccharide

LPS; lipopolysaccharide

M

Mab; monoclonal antibodies

MDM; monocyte derived macrophages

MDR; multidrug resistance

mg; milligram

MgCl2; magnesium chloride

$MgSO_4$; magnesium sulphate

MH; Mueller Hinton

MIC; minimal inhibitory concentration

min; minute

MIP; macrophage inflammatory protein

ml; millilitres

mM; millimolar

MOPS;

MOI; multiplicity of infection

N

Na; sodium

NaCl; sodium chloride

$Na_2.PO_4$; sodium phosphate

$Na_2S_2O_5$;

NCBI; national centre for biotechnology

NETs; neutrophil extracellular traps

ng; nanogram

NH_4Cl;

NK; natural killer

nm; nanometers

NMR;

NO; nitric oxide

NOD; Nucleotide-binding oligomerisation domain

NOL; nested over-lap

NVR; 04117201 variable region

O

OAP; Operon Assembly Protocol

OAV; operon assembly vector

OD; optical density

OD_{600} OD at 600 nm

OM; outer membrane

OMP; outer membrane protein

ON; overnight

O-OTase; oligosaccharyltransferase

ORF; open reading frame

P

PAGE; polyacrylamide gel electrophoresis

PAMPS; pathogen associated molecular patterns

PAS; Periodic acid-Schiff

PBS; Phosphate buffered saline

PCR; polymerase chain reaction

PEG;

PMA; Phorbol 12-myristate 13-acetate

pmol; picomole

PNAG; poly-N-acetyl glucosamine

PO_4;

PRR; pattern recognition receptors

Psep5Ac7Ac; 5,7-diacetamido-3,5,7,9-tetradeoxy-L-glycero-L-manno-non-2-ulosonic (pseudaminic) acid

Psi; per square inch

PUM; potassium urea magnesium

Q

qPCR; quantitative reverse transcription PCR

R

^{R}; Resistance

RAST; rapid annotation using subsystem technology

RH; Relative humidity

RNA; ribonucleic acid

RND; Resistance-Nodulation-Cell Division Type efflux pump

ROS; reactive oxygen species

Rpm; revolutions per minute

RPMI; Roswell Park Memorial Institute

RT room temperature

RT-qPCR; reverse transcription qualitative PCR

S

SD; Sabouraud dextrose

SDS; sodium dodecyl sulfate

SDS-PAGE; sodium dodecyl sulfate polyacrylamide gel electrophoresis

Sec; second

SEM; scanning electron microscopy

Strep; streptomycin

$Strep^R$; streptomycin resistance

ST; sequence type

T

TAE;

TCS; two component signal transduction system

TE;

Tel; potassium tellurite

Tet; tetracycline

Tet12; 12µg/ml tetracycline

TFB; transformation buffer

TLR: toll like receptor

^{TM}; trademark

TMED; N, N, N′, N′-tetramethylethylenediamine

Tn; transposon

TNF: tumour necrosis factor

TVC; total viable counts

U

U; Weiss Units

UFR; upstream flanking region

µg; micrograms

Und-p; undecaprenyl pyrophosphate

Ura; uracil

V

V; Volts

v; volume

W

WCL; whole cell lysate

WGS; whole genome sequencing

WHO; World Health Organisation

WT; wild-type

w/v; weight per volume

X

X; times

xg; times earth’s gravitational force

X-gal; 5-bromo-4-chloro-3-indoyl-β-D-galacto-pyranoside

Y

YPD; Yeast Extract–Peptone–Dextrose

Z

ZUR; zinc uptake regulator

Δ; delta

B; beta

µM; micromolar

µL; microliter

µg; microgram

^{o}C; degrees Celsius

/; per

-; minus

+; plus

Ω;

µF;

%; percent

$\Delta\Delta C_t$;

~; approximately

>; more than

=; equals

8.2 Publications

MINIREVIEW

Diversity and function of capsular polysaccharide in *Acinetobacter baumannii*

Jennifer Singh[1], Felise G Adams[1] Melissa H Brown[1*]

[1]College of Science and Engineering, Flinders University, Bedford Park, SA, Australia

***Correspondence:**

Corresponding Author

melissa.brown@flinders.edu.au

Keywords: *Acinetobacter*, capsule, polysaccharide, virulence factor, persistence

Running title: *Acinetobacter baumannii* capsule

ABSTRACT

The Gram-negative opportunistic bacterium *Acinetobacter baumannii* is a significant cause of hospital-borne infections worldwide. Alarmingly, the rapid development of antimicrobial resistance coupled with the remarkable ability of isolates to persist on surfaces for extended periods of time has led to infiltration of *A. baumannii* into our healthcare environments. A major virulence determinant of *A. baumannii* is the presence of a capsule that surrounds the bacterial surface. This capsule is comprised of tightly packed repeating polysaccharide units which forms a barrier around the bacterial cell wall, providing protection from environmental pressures including desiccation and disinfection regimes as well as host immune responses such as serum complement. Additionally, capsule has been shown to confer resistance to a range of clinically relevant antimicrobial compounds. Distressingly, treatment options for *A. baumannii* infections are becoming increasingly limited, and the urgency to develop effective infection control strategies and therapies to combat infections is apparent. An increased understanding of the contribution of capsule to the pathobiology of *A. baumannii* is required to determine its feasibility as a target for new strategies to combat drug resistant infections. Significant variation in capsular polysaccharide structures between *A. baumannii* isolates has been identified, with over 100 distinct capsule types, incorporating a vast variety of sugars. This review examines the studies undertaken to elucidate capsule diversity and advance our understanding of the role of capsule in *A. baumannii* pathogenesis.

Introduction

Nosocomial infections caused by multidrug resistant *Acinetobacter baumannii* are becoming increasingly common worldwide, especially in the intensive care setting (Wieland et al., 2018). The success of this bacterium is facilitated by its ability to survive in a variety of environments compounded by its rapid ability to acquire multidrug resistance. Surface carbohydrates play key roles in the overall fitness and virulence of *A. baumannii* (Geisinger and Isberg, 2015, Lees-Miller et al., 2013, Weber et al., 2016). *A. baumannii* produces high molecular weight capsular polysaccharide (CPS) which surrounds the outer membrane (Figure 1) (Russo et al., 2010). Comprised

of tightly packed repeating oligosaccharide subunits (K units), CPS forms a discrete layer on the bacterial surface providing protection from diverse environmental conditions, assisting in evasion of host immune defences, and increasing resistance to a number of antimicrobial compounds (Geisinger and Isberg, 2015, Russo et al., 2010, Iwashkiw et al., 2012).

In *A. baumannii*, capsule assembly and export occurs via a Wzy-dependent pathway (Kenyon and Hall, 2013, Hu et al., 2013, Willis and Whitfield, 2013, Woodward and Naismith, 2016) (Figure 1). Typically consisting of 4-6 sugars, the K unit is assembled on the lipid carrier molecule undecaprenyl pyrophosphate (Und-P) which provides a scaffold for the growing sugar chain (Whitfield, 2006). The first sugar in the K unit is recruited by an inner membrane (IM)-bound initial transferase (Itr), followed by the sequential addition of sugars to the growing K unit by specific glycosyl transferase (Gtr) enzymes (Figure 1) (Woodward and Naismith, 2016). Each K unit is then transferred to the periplasmic side of the IM by the Wzx translocase and polymerised by Wzy, which transfers the growing polysaccharide chain from one Und-P carrier to the next incoming subunit (Figure 1) (Collins et al., 2007). After the CPS polymer is synthesised, it is transported to the cell surface via a highly co-ordinated process involving the interaction of three proteins; Wza, Wzb and Wzc, that comprise the export machinery (Figure 1). CPS synthesis represents one arm of a bifurcated pathway, as these K units are also used to decorate certain surface proteins via *O*-linked protein glycosylation (Lees-Miller et al., 2013). In this case, single K units are transferred to recipient proteins by the *O*-oligosaccharyltransferase PglL (Figure 1) (Iwashkiw et al., 2012). In *A. baumannii*, protein glycosylation contributes to biofilm formation by enhancing initial attachment and maturation of biofilms, and pathogenicity as demonstrated in a number of animal infection models (Iwashkiw et al., 2012, Harding et al., 2015, Scott et al., 2014). Biofilm is a growth state in which bacterial communities are enclosed within an exopolysaccharide matrix and has been shown to play a significant role in *A. baumannii* persistence and resistance.

Other surface carbohydrates known to influence pathogenicity of *A. baumannii* include lipooligosaccharide (LOS) and the exopolysaccharide poly-β-(1-6)-*N*-

acetylglucosamine (PNAG) (Preston et al., 1996, Weber et al., 2016). PNAG forms the cohesive "glue" of biofilms and constitutes a substantial proportion of biofilms (Choi et al., 2009, Longo et al., 2014). Unlike most Gram-negative bacteria, *A. baumannii* does not produce traditional lipopolysaccharide, but instead a similar surface glyco-conjugate, LOS, comprised of a lipid A core that lacks O-antigen (Kenyon and Hall, 2013, Kenyon et al., 2014b). Loss of LOS production in *A. baumannii* decreases stability of the outer membrane leading to reduced fitness (Moffatt et al., 2010, Beceiro et al., 2014).

Although many carbohydrate moieties influence pathogenicity, it can be argued that CPS is a predominant virulence factor of *A. baumannii*. This review aims to consolidate what is known about *A. baumannii* capsule including selected structures, biosynthesis and gene organisation, the role of CPS in virulence, and the potential for CPS as a target for future vaccine and drug development.

Genetic organisation of K loci

As the complete genomes of more *A. baumannii* isolates become available, the true diversity of capsule structures present within this bacterium is becoming apparent. To date, over 100 unique capsule loci (KL) have been identified in *A. baumannii* (Figure 2A) (Shashkov et al., 2017). These regions typically range from 20 to 35 kb in size. Analysis of the genes directing CPS synthesis in ten complete *A. baumannii* genomes originally resulted in the designation of nine capsule types, KL1-KL9, which became the basis for a universal typing scheme for these loci (Kenyon and Hall, 2013). The chromosomal location of the K locus, between the *fkpA* and *lldP* genes, is highly conserved between *A. baumannii* strains and contains those genes required for the biosynthesis and export specific to each CPS type (Figure 2) (Kenyon and Hall, 2013, Hu et al., 2013). An exception to this rule are *A. baumannii* strains possessing KL19 and KL39 regions, where the gene encoding the Wzy polymerase, *wzy*, is found on a small genetic island elsewhere on the chromosome (Kenyon et al., 2016a). Additionally, the genes required for some of the common sugars seen in CPS are found elsewhere. All K loci show a similar genetic configuration, a highly variable cluster of synthesis and transferase genes required for the biosynthesis of unique KL-type complex sugars,

flanked on one side by the highly conserved CPS export genes, and on the other side by a set of genes encoding conserved simple sugars and precursors (Figure 2A). The *wzx* and *wzy* genes required for repeat-unit processing are highly variable between K loci (Figure 2A, light blue), indicating specificity for particular K unit structures and, in general, the order of *gtr* determinants, encoding specific glycosyltransferases within the KL regions, inversely corresponds with the order of action.

The variable region of some KL gene clusters, such as KL37 and KL14, lack genes for complex sugar synthesis, as they only contain simple sugars in their K units (Kenyon et al., 2015a, Arbatsky et al., 2015). Also adding to their diversity, several KL regions contain redundant genes which are not required for the synthesis of the final K unit. For example KL8 and KL9 contain two *itr* genes (Kenyon and Hall, 2013) and KL37 has the *pgt1* phosphoglyceroltransferase, but no corresponding phosphoglycerol residue in the determined structure (Arbatsky et al., 2015). Furthermore, in KL93, two insertion sequence elements (IS*Aba26* and IS*Aba22*) interrupt the *pgt1* determinant (Figure 2) (Kasimova et al., 2017). The genes required for specific sugar biosynthesis will not be discussed as these pathways have been covered previously and are beyond the scope of this review (Hu et al., 2013, Kenyon and Hall, 2013). Additionally, other genes located within the KL encode products predicted to be involved in acetylation or acylation modification of specific glycans (Figure 2A, pink). Although examination of the K loci can reveal a lot about K unit structures, chemical analysis and biochemical testing is required to determine exact structures and identify specific linkages between repeat sugars.

CPS structures

The earliest studies on CPS serotyping of *A. baumannii* were driven by the need to develop a method to discriminate *A. baumannii* isolates from other *Acinetobacter* species, as phenotypic analysis was burdened with ambiguity and misidentification (Traub, 1989). As described above, there is phenomenal diversity seen in *A. baumannii* CPS biosynthesis gene clusters, which translates into the diversity seen in K unit structure (Kenyon and Hall, 2013, Hu et al., 2013). Collectively, over 40 diverse *A. baumannii* K unit structures have been elucidated thus far using NMR spectroscopy and

chemical analysis. K unit structures differ in sugar composition. They may include derivatives of common UDP-linked sugars such as glucose, galactose and glucuronic acid or rare and atypical sugars such as non-2-ulosonic acids. Structures vary in length and may consist of only two residues, as seen for K53 type CPS (Shashkov et al., 2018), or up to five or six monosaccharides, such as that seen in K37 (Figure 2B) (Arbatsky et al., 2015). Structures also differ in the linkages both within and between K units resulting in the production of K units that are linear or involve side branches, as seen in K1 and K93, respectively (Figure 2B) (Kenyon et al., 2016a, Kasimova et al., 2017). Differences in the location of specific glycosidic bonds and *O*-acetylation patterns of various oligosaccharides within a structure also contribute to K unit diversity.

Variation between K unit structures may be subtle, for example, K12 and K13 differ only by the linkage of two glycans, which requires the use of an alternate Wzy polymerase; accordingly, the K loci of both strains are identical except for the *wzy* gene (Figure 2). Alternatively the variation may be striking, such as the incorporation of rare sugars including pseudaminic, legionaminic or acinetaminic acid derivatives as seen in K2/6, K49, and K12/13 structures, respectively (Figure 2) (Kasimova et al., 2018, Kenyon et al., 2014a, Vinogradov et al., 2014, Kenyon et al., 2015a). Interestingly, acinetaminic acid derivatives have only been identified in *A. baumannii* and are found nowhere else in nature (Kenyon et al., 2017b). Additionally, some K units incorporate unique derivatives of specific glycans, for instance the pseudaminic acid of K93 is acetylated with a (*R*)-3-hydroxybutanoyl group (Kasimova et al., 2017), whereas in K2 and K6 the pseudaminic acid is non-acetylated (Figure 2). Furthermore, the structure of K4 is unique as it contains only aminosugars, D-Qui*p*NAc, and one terminal *N*-acetyl-D-galactosamine (D-Gal*p*NAcA) branch which is capped with a pyruvyl group, a rare motif and the first to be described in *Acinetobacter* (Figure 2A, black) (Kenyon et al., 2016b). As the number of K unit structures elucidated increases, so does the confidence to infer the K unit structure from analysis of the biosynthesis clusters positioned in the *A. baumannii* KL. However, although informative, an understanding of the role CPS plays in pathogenesis is important to apply this knowledge to improving outcomes of *A. baumannii* infections.

Role in virulence, antimicrobial resistance, and persistence

It is beyond doubt that the presence of CPS is essential for *A. baumannii* pathogenicity. Not only is it necessary for evasion of host immune defences (Russo et al., 2010, Geisinger and Isberg, 2015), but it is important for resistance to antimicrobial compounds and survival in adverse environments (Luke et al., 2010, Russo et al., 2010, Geisinger and Isberg, 2015). CPS mediates immune evasion in many *A. baumannii* strains by limiting interactions between immunogenic surface structures of the bacteria and host defences (Preston et al., 1996, Wu et al., 2009, Wang-Lin et al., 2017, Russo et al., 2010, Umland et al., 2012, Lees-Miller et al., 2013, Geisinger and Isberg, 2015). The abolition of capsule in multiple different *A. baumannii* strains has shown reduced survival in human serum and acites fluid, and attenuation in rat and murine infection models (Russo et al., 2010, Umland et al., 2012, Lees-Miller et al., 2013, Sanchez-Larrayoz et al., 2017). Furthermore, the up-regulation of capsule production in the commonly utilised *A. baumannii* strain ATCC 17978 (K3 CPS type) increased serum resistance and virulence in a mouse infection model (Geisinger and Isberg, 2015). Moreover, novel antimicrobial treatments could be developed for specific CPS types, for example those containing pseudaminic acid, as its presence has been correlated with enhanced virulence (Kao et al., 2016, Hitchen et al., 2010).

Besides protection from host defences, in *A. baumannii* CPS production increases resistance to a range of antimicrobial compounds, including those used for disinfection in clinical settings (Chen et al., 2017, Geisinger and Isberg, 2015, Tipton et al., 2015). Furthermore, growth of *A. baumannii* in sub-inhibitory levels of antimicrobials influences CPS production. For example, exposure to the antibiotics chloramphenicol or erythromycin led to enhanced capsule synthesis in ATCC 17978 (Geisinger and Isberg, 2015) and meropenem exposure selected for mutations leading to a loss in CPS production in the isolate 37662 (Chen et al., 2017). Studies conducted on a broader range of *A. baumannii* strains are required to identify if the protection against antimicrobials afforded by CPS is strain specific, capsule-type specific, or universal.

The ability of *A. baumannii* to persist in the clinical environment has undoubtedly enhanced colonisation and infections in susceptible patients. *A. baumannii* is capable of

surviving for months on hospital surfaces such as bed rails, furniture and medical devices, providing a reservoir that is often the source of transmission and infection (Wendt et al., 1997, Gayoso et al., 2013). The remarkable desiccation tolerance of *A. baumannii* is thought to be due to a 'bust or boom' strategy, where a persistent subpopulation of cells survive at the expense of dying cells; CPS enhances desiccation tolerance by providing a physical barrier facilitating water retention (Roberts, 1996, Webster et al., 2000, Gayoso et al., 2013, Bravo et al., 2016). Furthermore, in two close relatives of *A. baumannii*, *Acinetobacter calcoaceticus* and *Acinetobacter baylyi*, production of exopolysaccharide and/or CPS has been shown to promote desiccation survival (Roberson and Firestone, 1992, Ophir and Gutnick, 1994). In addition to influencing resistance to desiccation, CPS has been associated with other virulence traits including motility (Huang et al., 2014, McQueary et al., 2012) and the production of biofilm (Umland et al., 2012, Lees-Miller et al., 2013), thus cementing its role as a pathogenic factor.

Recent studies have linked the phase-variable phenotype of *A. baumannii* AB5075 (K25 CPS type) with alterations in CPS production, as highly virulent opaque variants produce a CPS layer with twice the thickness of their translucent counterparts (Chin et al., 2018). This transition from translucent to opaque also dramatically increased the pathogenic potential of *A. baumannii* AB5075. Resistance to common hospital disinfectants and a subset of aminoglycoside antibiotics were also increased (Tipton et al., 2015, Chin et al., 2018) and opaque variants were also more resistant to human lysozyme, the cathelicidin-related antimicrobial peptide LL37 and hydrogen peroxide compared to translucent colonies (Chin et al., 2018). Furthermore, opaque isolates had an increased tolerance to desiccated conditions and out-competed translucent counterparts in a mouse infection model (Chin et al., 2018). However, as multiple factors are involved in phase variation, further studies are required to determine the exact contribution of CPS production to the more virulent opaque phenotype.

Regulation of CPS production

Environmental cues, such as temperature, osmotic pressure and changes in metabolite and ion availability can influence bacterial CPS production (Hagiwara et al., 2003,

Mouslim et al., 2004, Lai et al., 2003, Willenborg et al., 2011). It is unsurprising that few regulatory mechanisms have been identified for CPS production as CPS levels are commonly regulated post-translationally through the phosphorylation of CPS export machinery (Whitfield and Paiment, 2003, Chiang et al., 2017). In *A. baumannii*, only two regulators of capsule production have thus far been identified; BfmRS and OmpR-EnvZ, both two component signal transduction systems which play multiple regulatory roles involved in envelope biogenesis (Tipton and Rather, 2017, Geisinger and Isberg, 2015, Geisinger et al., 2018). When subjected to antibiotic pressure, *A. baumannii* ATCC 17978 *cps* expression was increased in a BfmRS-dependent manner (Geisinger and Isberg, 2015). Phase variation, and thus potentially CPS production, is highly regulated by the OmpR-EnvZ system in *A. baumannii* AB5075, as mutations in either OmpR or EnvZ resulted in a significant increase in opaque to translucent switching frequency (Tipton and Rather, 2017). Although transition from translucent to opaque results in a two-fold increase in capsule thickness, transcriptomic analyses have not identified any differences in expression levels of KL genes between the two phases.

CPS as a target for the development of vaccines and treatments against *A. baumannii*

Antibiotic (specifically cabapenem) resistant *A. baumannii* are classified a World Health Organisation Priority 1 Critical organism for the development of new antimicrobials (WHO, 2017). Although there are no non-antibiotic treatments or vaccines licensed for *A. baumannii* at present, there is an increased interest in their development and preliminary studies look promising. Surface exposure and prevalence in pathogenic strains of *A. baumannii* makes CPS an ideal target for both antimicrobial treatments and vaccines (Russo et al., 2013). These include the development of antibody-based therapies such as prophylactic vaccines, passive immunisation, and phage therapy (García-Quintanilla et al., 2013).

Several studies have shown the efficacy of passive immunisation in mice using a CPS-specific antibody, which is protective against bacterial challenge with 13-55% of clinical *A. baumannii* isolates (Russo et al., 2013, Yang et al., 2017, Lee et al., 2018). Additionally, inoculation with conjugate vaccines incorporating CPS glycans attached to a protein carrier elicit better immune protection than purified CPS against a diverse

range of *A. baumannii* strains (Yang et al., 2017).

Interest in phage therapy to treat bacterial infections has increased in recent years in response to the current crisis of rising antimicrobial resistance. Phage therapy is attractive as a potential treatment avenue for multidrug resistant *A. baumannii* infections. For example, a phage encoding a CPS depolymerase was found to degrade the CPS of approximately 10% of clinical multidrug resistant *A. baumannii* tested (Hernandez-Morales et al., 2018). Although the host range of this phage is limited, it could be incorporated as part of a phage cocktail to maximise effectiveness or target specific outbreaks (Hernandez-Morales 2018). A phage which selectively cleaves the linkage of *A. baumannii* CPS at a pseudaminic acid branch may be valuable for phage therapy, or to efficiently manufacture purified CPS for vaccine and antibody development (Lee et al., 2018). Phage targeting *A. baumannii* were recently shown to be stable when impregnated in burn wound care products under a range of conditions including in the presence of antimicrobials (Merabishvili et al., 2017). However, as the majority of studies investigating *A. baumannii* CPS are usually confined to a particular *A. baumannii* strain, it is not known if these findings translate to all *A. baumannii* isolates or if they are strain or capsule type specific. Understanding what roles capsule plays in multiple strains is paramount in identifying CPS types which represent the best targets for new vaccines, or whether the development of antimicrobials targeting capsule biosynthesis pathway is indeed even feasible.

Concluding remarks

Although capsule represents an important virulence trait of *A. baumannii* there are limited data available on the role different CPS types play in causing disease. To develop effective vaccines and therapies targeting CPS, we must first gain a comprehensive understanding towards the mechanisms behind its synthesis and expression, alongside the advantages that capsule conveys to the host bacteria. This research needs to be addressed in the context of the extreme variation of CPS serotypes found in *A. baumannii*, to ensure potential interventions work against strains producing diverse CPS structures. Further studies on CPS are required to provide a platform for the development of preventative measures and treatments against this increasingly

persistent and deadly human pathogen.

Conflict of interests

The authors declare that the research was conducted in the absence of any commercial or financial relationships that could be construed as a potential conflict of interest.

Author contributions

JS wrote the first draft. MB provided academic input and critical revision of the article. FA produced genome alignments and provided critical revision of the manuscript. All authors approved the final version.

Acknowledgements

This work was supported by a Flinders Medical Research Foundation Grant to MHB. FGA was supported by AJ and IM Naylon and Playford Trust Ph.D. Scholarships. JS was supported by a AJ and IM Naylon scholarship and FA by AJ and IM Naylon and Playford Trust Ph.D. Scholarships.

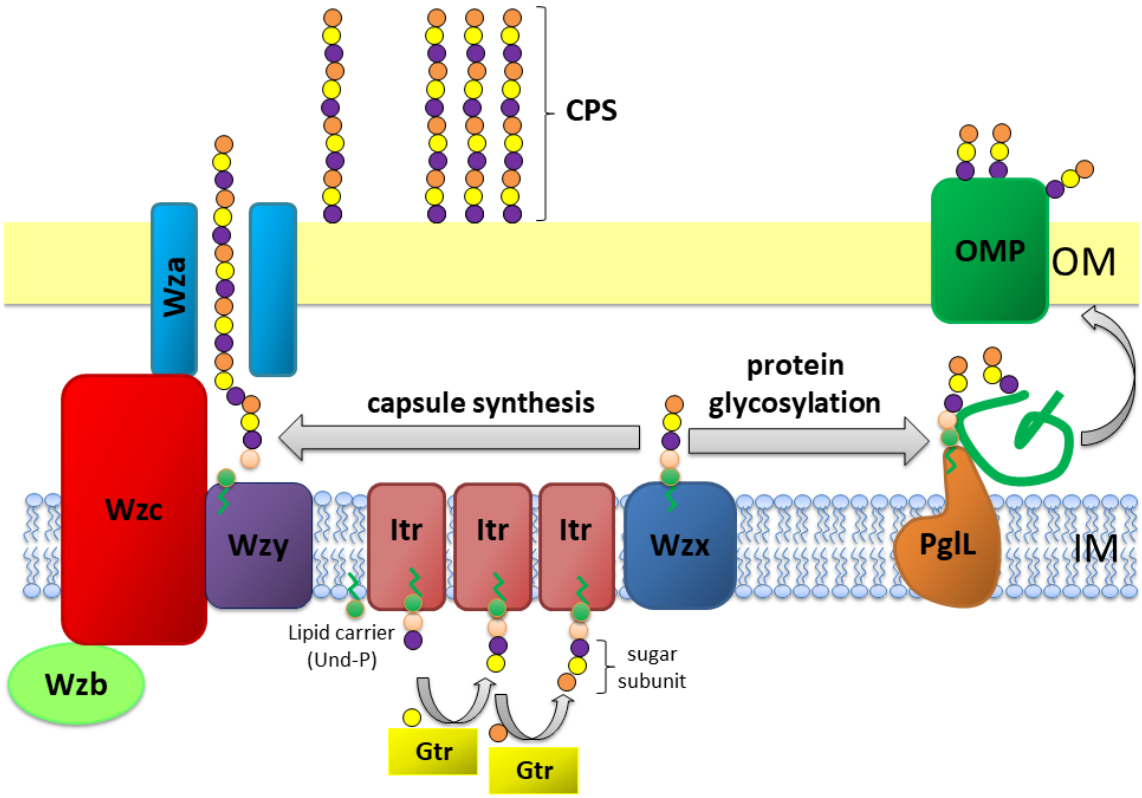

Figure 1: Schematic representation of capsule polysaccharide assembly and export in *A. baumannii*. Synthesis begins with the initial transferase (Itr; maroon) located in the inner membrane (IM) transferring the first sugar of the repeating unit to a lipid carrier (Und-P; green circle). Subsequent sugars are then added to the growing unit by specific glycosyltransferases (Gtr; yellow) on the cytosolic side of the inner membrane. The capsule subunit (K unit) is then transferred to the periplasm via the integral membrane protein Wzx (dark blue). The sugar subunits are polymerised by the Wzy protein (purple) and the Wza/Wzb/Wzc complex (cyan, lime, red) coordinates high level polymerisation and export of the growing chain, moving them to the outer membrane (OM). For glycosylation, PglL (orange) links the K units onto selected outer membrane proteins (OMP; dark green).

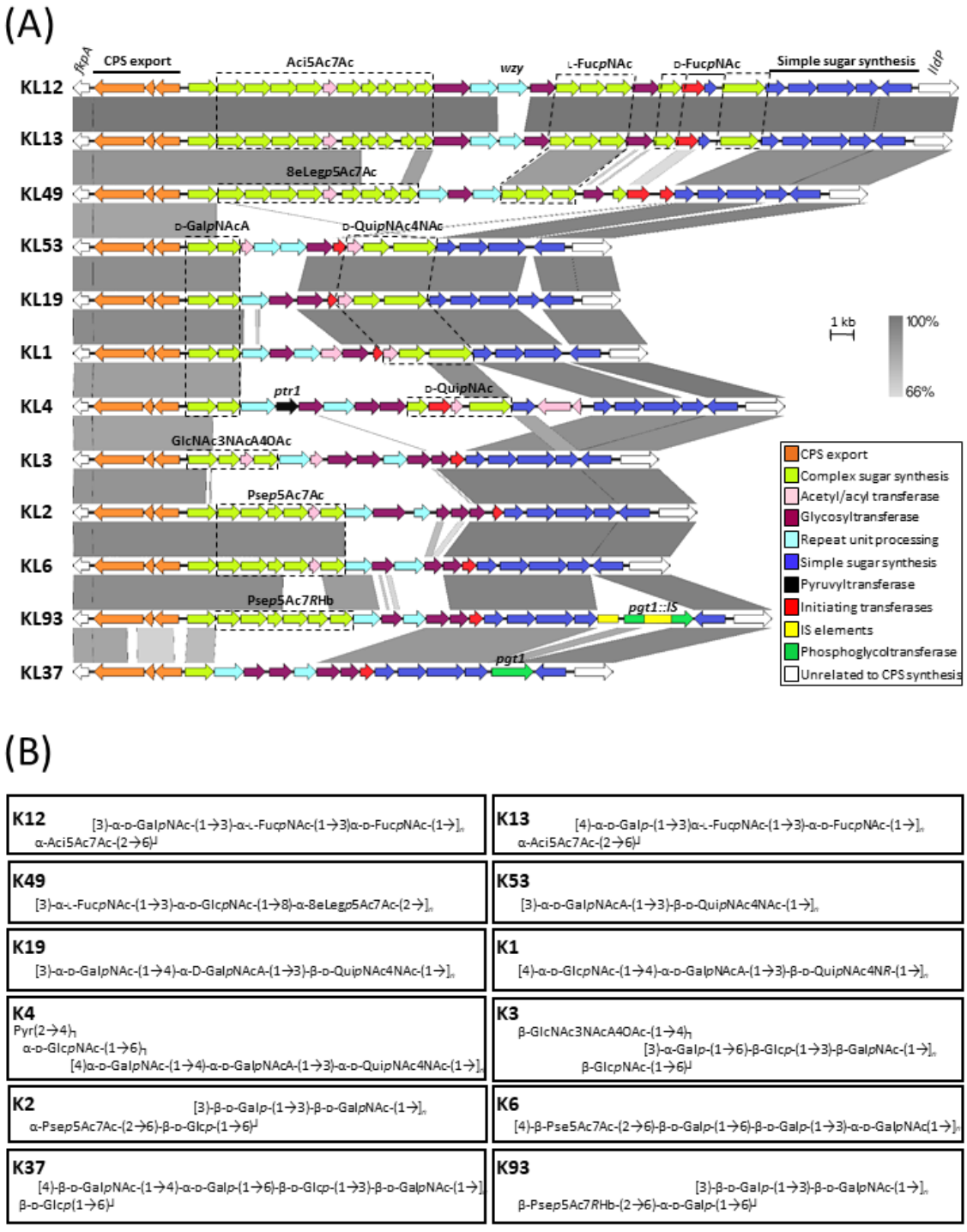

Figure 2: Comparison of representative *A. baumannii* CPS biosynthesis gene clusters and corresponding structures. **(A)** Nucleotide sequences representing different KL regions focusing on genes between *fkpA* and *lldP* were obtained from the NCBI database and aligned using the Easyfig 2.2.2 tool (Sullivan et al., 2011). Genes are

depicted by arrows and indicate direction of transcription whilst IS elements are represented by square boxes. Colour scheme is based on homology to the putative function of gene products and are outlined in the key. Nucleotide sequence homology shared between regions is represented by colour gradient. Figure is drawn to scale. Gene modules for sugar synthesis of interest are indicated, where Aci5Ac7Ac represents genes involved in the production of 5,7-di-*N*-acetylacinetaminic acid; L-Fuc*p*NAc, *N*-acetyl-L-fucosaminic acid; D-Fuc*p*NAc, *N*-acetyl-D-fucosaminic acid; 8eLeg*p*5Ac7Ac, 5,7-diacetamido-3,5,7,9-tetradeoxy-L-*glycero*-D-*galacto*-non-2-ulopyranosonic (di-*N*-acetyl-8-epilegionaminic) acid; D-Gal*p*NAcA, *N*-acetyl-D-galactosaminuronic acid; D-Qui*p*NAc4NAc, 2,4-diacetamido-2,4,6-trideoxy-D-glucopyranose (*N*,*N*'-diacetyl-bacillosamine); D-Qui*p*NAc, *N*-acetyl-D-quinovosaminic acid; GlcNAc3NAcA4OAc, 2,3-diacetamido-2,3-dideoxy-α-D-glucuronic acid with an additional O-acetyl group; Pse*p*5Ac7Ac, 5,7-diacetamido-3,5,7,9-tetradeoxy-L-*glycero*-L-*manno*-non-2-ulosonic (pseudaminic) acid and Pse*p*5Ac7*R*Hb, 5-acetamido-3,5,7,9-tetradeoxy-7-(3-hydroxybutanoylamino)-L-*glycero*-L-*manno*-non-2-ulosonic acid. Genes of interest are labelled above corresponding gene, see text for further details. Genbank accession numbers for sequences used in gene alignment are as follows; KL12, JN107991.2 (38.5 kb region; base position range 2332-40832); KL13, MF522810.1 (38.2 kb region); KL49, KT359616.1 (34.5 kb region); KL53, MH190222.1 (23.4 kb region); KL19, KU165787.1 (23.8 kb); KL1, CP001172.1 (24.9 kb; base position range 366401 to 3691388); KL4, JN409449.3 (30.9 kb; base position range 2375 to 33327); KL3, CP012004.1, (25.4 kb; base position range 3762660-3788118); KL2, CP000863.1 (27.1 kb; base position range 77125-104246); KL6, KF130871.1 (25.5 kb); KL93, CP021345.1 30.3 kb (base position range 3338210-3368604) and KL37 KX712115.1 (23.4 kb).

(B) Capsule structures corresponding to KL gene regions in (A) are shown. Percentage of O-acetylation of specific glycans from K53, K19, K1 are not represented in structural configurations (Shashkov et al., 2018, Kenyon et al., 2016a)

9 REFERENCES

ABDOLLAHI, S., RASOOLI, I. & GARGARI, S. L. M. 2018. The role of TonB-dependent copper receptor in virulence of *Acinetobacter baumannii*. *Infection, Genetics and Evolution,* 60**,** 181-190.

ACTIS, L. A., TOLMASKY, M., CROSA, L. & CROSA, J. 1993. Effect of iron-limiting conditions on growth of clinical isolates of *Acinetobacter baumannii*. *Journal of Clinical Microbiology,* 31**,** 2812-2815.

AHMAD, I., KARAH, N., NADEEM, A., WAI, S. N. & UHLIN, B. E. 2019. Analysis of colony phase variation switch in Acinetobacter baumannii clinical isolates. *PloS one,* 14**,** e0210082.

AJIBOYE, T., SKIEBE, E. & WILHARM, G. 2018. Contributions of ferric uptake regulator Fur to the sensitivity and oxidative response of *Acinetobacter baumannii* to antibiotics. *Microbial Pathogenesis,* 119**,** 35-41.

AKINBI, H. T., EPAUD, R., BHATT, H. & WEAVER, T. E. 2000. Bacterial killing is enhanced by expression of lysozyme in the lungs of transgenic mice. *The Journal of Immunology,* 165**,** 5760-5766.

AL ATROUNI, A., JOLY-GUILLOU, M.-L., HAMZE, M. & KEMPF, M. 2016. Reservoirs of non-*baumannii Acinetobacter* species. *Frontiers in Microbiology,* 7**,** 49.

ALTAMIRANO, F. L. G., FORSYTH, J. H., PATWA, R., KOSTOULIAS, X., TRIM, M., SUBEDI, D., ARCHER, S., MORRIS, F. C., OLIVEIRA, C. & KIELTY, L. 2020. Bacteriophages targeting *Acinetobacter baumannii* capsule induce antimicrobial resensitization. *bioRxiv*.

ALTSCHUL, S. F., GISH, W., MILLER, W., MYERS, E. W. & LIPMAN, D. J. 1990. Basic local alignment search tool. *Journal of Molecular Biology,* 215**,** 403-10.

AMERA, G. M., KHAN, R. J., PATHAK, A., JHA, R. K., MUTHUKUMARAN, J. & SINGH, A. K. 2020. Computer aided ligand based screening for identification of promising molecules against enzymes involved in peptidoglycan biosynthetic pathway from *Acinetobacter baumannii*. *Microbial Pathogenesis***,** 104205.

AMIN, I. M., RICHMOND, G. E., SEN, P., KOH, T. H., PIDDOCK, L. J. & CHUA, K. L. 2013. A method for generating marker-less gene deletions in multidrug-resistant *Acinetobacter baumannii*. *BMC Microbiology,* 13**,** 158.

ANTUNES, L. C., IMPERI, F., CARATTOLI, A. & VISCA, P. 2011. Deciphering the multifactorial nature of *Acinetobacter baumannii* pathogenicity. *PloS One,* 6**,** e22674.

ARAKAWA, Y. 1994. Genomic organization and regulation of cps cluster that is involved in synthesis of capsular polysaccharide as a virulence factor of *Klebsiella pneumoniae*. *Nihon Saikingaku Zasshi,* 49**,** 455-63.

ARANDA, J., BARDINA, C., BECEIRO, A., RUMBO, S., CABRAL, M. P., BARBÉ, J. &

BOU, G. 2011. *Acinetobacter baumannii* RecA protein in repair of DNA damage, antimicrobial resistance, general stress response, and virulence. *Journal of Bacteriology,* 193**,** 3740-3747.

ARANDA, J., POZA, M., PARDO, B. G., RUMBO, S., RUMBO, C., PARREIRA, J. R., RODRÍGUEZ-VELO, P. & BOU, G. 2010. A rapid and simple method for constructing stable mutants of *Acinetobacter baumannii*. *BMC Microbiology,* 10**,** 279.

ARBATSKY, N. P., SHNEIDER, M. M., KENYON, J. J., SHASHKOV, A. S., POPOVA, A. V., MIROSHNIKOV, K. A., VOLOZHANTSEV, N. V. & KNIREL, Y. A. 2015. Structure of the neutral capsular polysaccharide of *Acinetobacter baumannii* NIPH146 that carries the KL37 capsule gene cluster. *Carbohydrate Research,* 413**,** 12-15.

ARROYO, L. A., HERRERA, C. M., FERNANDEZ, L., HANKINS, J. V., TRENT, M. S. & HANCOCK, R. E. 2011. The *pmr*CAB operon mediates polymyxin resistance in *Acinetobacter baumannii* ATCC 17978 and clinical isolates through phosphoethanolamine modification of Lipid A. *Antimicrobial agents and chemotherapy***,** AAC. 00256-11.

AUSTRIAN, R. 2011. Bacterial polysaccharide vaccines. *History of Vaccine Development.* Springer.

AYOUB MOUBARECK, C. & HAMMOUDI HALAT, D. 2020. Insights into *Acinetobacter baumannii*: A Review of Microbiological, Virulence, and Resistance Traits in a Threatening Nosocomial Pathogen. *Antibiotics,* 9**,** 119.

BADAVE, G. K. & KULKARNI, D. 2015. Biofilm producing multidrug resistant *Acinetobacter baumannii*: an emerging challenge. *Journal of Clinical Diagnostic Research*

9**,** DC08.

BAO, Y., ZHANG, H., HUANG, X., MA, J., LOGUE, C. M., NOLAN, L. K. & LI, G. 2018. O-specific polysaccharide confers lysozyme resistance to extraintestinal pathogenic *Escherichia coli*. *Virulence*.

BARBE, V., VALLENET, D., FONKNECHTEN, N., KREIMEYER, A., OZTAS, S., LABARRE, L., CRUVEILLER, S., ROBERT, C., DUPRAT, S. & WINCKER, P. 2004. Unique features revealed by the genome sequence of *Acinetobacter sp*. ADP1, a versatile and naturally transformation competent bacterium. *Nucleic Acids Research,* 32**,** 5766-5779.

BECEIRO, A., LLOBET, E., ARANDA, J., BENGOECHEA, J. A., DOUMITH, M., HORNSEY, M., DHANJI, H., CHART, H., BOU, G. & LIVERMORE, D. M. 2011. Phosphoethanolamine modification of lipid A in colistin-resistant variants of *Acinetobacter baumannii* mediated by the pmrAB two-component regulatory system. *Antimicrobial Agents and Chemotherapy,* 55**,** 3370-3379.

BECEIRO, A., MORENO, A., FERNÁNDEZ, N., VALLEJO, J. A., ARANDA, J., ADLER, B., HARPER, M., BOYCE, J. D. & BOU, G. 2014. Biological cost of different mechanisms of colistin resistance and their impact on virulence in *Acinetobacter baumannii*. *Antimicrobial Agents and Chemotherapy,* 58**,** 518-526.

BENTANCOR, L. V., O'MALLEY, J. M., BOZKURT-GUZEL, C., PIER, G. B. & MAIRA-LITRÁN, T. 2012. Poly-N-acetyl-β-(1-6)-glucosamine is a target for protective immunity against *Acinetobacter baumannii* infections. *Infection and Immunity,* 80**,** 651-656.

BENZ, I. & SCHMIDT, M. A. 2002. Never say never again: protein glycosylation in

pathogenic bacteria. *Molecular Microbiology,* 45**,** 267-276.

BERLAU, J., AUCKEN, H., MALNICK, H. & PITT, T. 1999. Distribution of *Acinetobacter* species on skin of healthy humans. *European Journal of Clinical Microbiology and Infectious Diseases,* 18**,** 179-183.

BHARGAVA, N., SHARMA, P. & CAPALASH, N. 2014. Pyocyanin stimulates quorum sensing-mediated tolerance to oxidative stress and increases persister cell populations in *Acinetobacter baumannii*. *Infection and Immunity,* 82**,** 3417-3425.

BHAVSAR, A. P., BEVERIDGE, T. J. & BROWN, E. D. 2001. Precise deletion of tagD and controlled depletion of its product, Glycerol 3-Phosphate Cytidylyltransferase, leads to irregular morphology and lysis of *Bacillus subtilis* grown at physiological temperature. *Journal of Bacteriology,* 183**,** 6688-6693.

BIST, P., DIKSHIT, N., KOH, T. H., MORTELLARO, A., TAN, T. T. & SUKUMARAN, B. 2014. The Nod1, Nod2, and Rip2 axis contributes to host immune defense against intracellular *Acinetobacter baumannii* infection. *Infection and immunity,* 82**,** 1112-1122.

BLANCO, N., HARRIS, A. D., ROCK, C., JOHNSON, J. K., PINELES, L., BONOMO, R. A., SRINIVASAN, A., PETTIGREW, M. M. & THOM, K. A. J. 2018. Risk factors and outcomes associated with multidrug-resistant *Acinetobacter baumannii* upon intensive care unit admission. *Antimicrobial Agents and Chemotherapy,* 62**,** e01631-17.

BOLL, E. J., FRIMODT-MØLLER, J., OLESEN, B., KROGFELT, K. A. & STRUVE, C. 2016a. Heat resistance in extended-spectrum beta-lactamase-producing *Escherichia coli* may favor environmental survival in a hospital setting. *Research in Microbiology,* 167**,** 345-349.

BOLL, E. J., MARTI, R., HASMAN, H., OVERBALLE-PETERSEN, S., STEGGER, M., NG, K., KNØCHEL, S., KROGFELT, K. A., HUMMERJOHANN, J. & STRUVE, C. 2017. Turn Up the Heat—Food and Clinical *Escherichia coli* Isolates Feature Two Transferrable Loci of Heat Resistance. *Frontiers in Microbiology,* 8.

BOLL, J. M., CROFTS, A. A., PETERS, K., CATTOIR, V., VOLLMER, W., DAVIES, B. W. & TRENT, M. S. 2016b. A penicillin-binding protein inhibits selection of colistin-resistant, lipooligosaccharide-deficient *Acinetobacter baumannii*. *Proceedings of the National Academy of Sciences,* 113**,** E6228-E6237.

BOLL, J. M., TUCKER, A. T., KLEIN, D. R., BELTRAN, A. M., BRODBELT, J. S., DAVIES, B. W. & TRENT, M. S. 2015. Reinforcing lipid A acylation on the cell surface of *Acinetobacter baumannii* promotes cationic antimicrobial peptide resistance and desiccation survival. *MBio,* 6**,** e00478-15.

BOU, G. & MARTÍNEZ-BELTRÁN, J. 2000. Cloning, nucleotide sequencing, and analysis of the gene encoding an AmpC β-lactamase in *Acinetobacter baumannii*. *Antimicrobial Agents and Chemotherapy,* 44**,** 428-432.

BOUJAAFAR, N., FRENEY, J., BOUVET, P. & JEDDI, M. 1990. Cell surface hydrophobicity of 88 clinical strains of *Acinetobacter baumannii*. *Research in Microbiology,* 141**,** 477-482.

BOUVET, P. J. & GRIMONT, P. A. 1986. Taxonomy of the genus *Acinetobacter* with the recognition of *Acinetobacter baumannii sp.* nov., *Acinetobacter haemolyticus sp*. nov., *Acinetobacter johnsonii sp.* nov., and *Acinetobacter junii sp*. nov. and emended descriptions of *Acinetobacter calcoaceticus* and *Acinetobacter lwoffii*. *International Journal of Systematic and*

Evolutionary Microbiology, 36**,** 228-240.

BRAVO, Z., ORRUÑO, M., PARADA, C., KABERDIN, V., BARCINA, I. & ARANA, I. 2016. The long-term survival of *Acinetobacter baumannii* ATCC 19606^{T} under nutrient-deprived conditions does not require the entry into the viable but non-culturable state. *Archives of Microbiology,* 198**,** 399-407.

BREAKWELL, D. P., MOYES, R. B. & REYNOLDS, J. 2009. Differential staining of bacteria: capsule stain. *Current Protocols in Microbiology,* 15**,** A. 3I. 1-A. 3I. 4.

BREISCH, J. & AVERHOFF, B. 2020. Identification of osmo-dependent and osmo-independent betaine-choline-carnitine transporters in *Acinetobacter baumannii*: role in osmostress protection and metabolic adaptation. *Environmental Microbiology*.

BRIMACOMBE, C. A., STEVENS, A., JUN, D., MERCER, R., LANG, A. S. & BEATTY, J. T. 2013. Quorum-sensing regulation of a capsular polysaccharide receptor for the *Rhodobacter capsulatus* gene transfer agent (RcGTA). *Molecular Microbiology,* 87**,** 802-817.

BROSSARD, K. A. & CAMPAGNARI, A. A. 2012. The *Acinetobacter baumannii* biofilm-associated protein plays a role in adherence to human epithelial cells. *Infection and Immunity,* 80**,** 228-233.

BRUHN, K. W., PANTAPALANGKOOR, P., NIELSEN, T., TAN, B., JUNUS, J., HUJER, K. M., WRIGHT, M. S., BONOMO, R. A., ADAMS, M. D. & CHEN, W. 2015. Host fate is rapidly determined by innate effector-microbial interactions during *Acinetobacter baumannii* bacteremia. *The Journal of Infectious Diseases,* 211**,** 1296-1305.

BUCKLES, E. L., WANG, X., LANE, M. C., LOCKATELL, C. V., JOHNSON, D. E., RASKO, D. A., MOBLEY, H. L. & DONNENBERG, M. S. 2009. Role of the K2 capsule in *Escherichia coli* urinary tract infection and serum resistance. *Journal of Infectious Diseases,* 199**,** 1689-1697.

BURNS, S. M. & HULL, S. I. 1999. Loss of resistance to ingestion and phagocytic killing by O− and K− mutants of a uropathogenic *Escherichia coli* O75: K5 strain. *Infection and immunity,* 67**,** 3757-3762.

BURROWS, L. L. & LAM, J. S. 1999. Effect of wzx (rfbX) mutations on A-band and B-band lipopolysaccharide biosynthesis in *Pseudomonas aeruginosa* O5. *Journal of Bacteriology,* 181**,** 973-980.

CAGATAY, T. I. & HICKFORD, J. G. 2008. Glycosylation of type-IV fimbriae of *Dichelobacter nodosus*. *Veterinary Microbiology,* 126**,** 160-167.

CAMARENA, L., BRUNO, V., EUSKIRCHEN, G., POGGIO, S. & SNYDER, M. 2010. Molecular mechanisms of ethanol-induced pathogenesis revealed by RNA-sequencing. *PLoS Pathogens,* 6**,** e1000834.

CAMPAGNARI, A. A., SPINOLA, S. M., LESSE, A. J., KWAIK, Y. A., MANDRELL, R. E. & APICELLA, M. A. 1990. Lipooligosaccharide epitopes shared among gram-negative non-enteric mucosal pathogens. *Microbial Pathogenesis,* 8**,** 353-362.

CAMPOS, M. A., VARGAS, M. A., REGUEIRO, V., LLOMPART, C. M., ALBERTÍ, S. & BENGOECHEA, J. A. 2004. Capsule polysaccharide mediates bacterial resistance to antimicrobial peptides. *Infection and Immunity,* 72**,** 7107-7114.

CARRETERO-LEDESMA, M., GARCÍA-QUINTANILLA, M., MARTÍN-PEÑA, R., PULIDO, M. R., PACHÓN, J. & MCCONNELL, M. J. 2018. Phenotypic changes associated with Colistin resistance due to Lipopolysaccharide loss in *Acinetobacter baumannii*. *Virulence,* 9**,** 930-942.

CENDRERO, J. A. C., SOLÉ-VIOLÁN, J., BENITEZ, A. B., CATALÁN, J. N., FERNÁNDEZ, J. A., SANTANA, P. S. & DE CASTRO, F. R. 1999. Role of different routes of tracheal colonization in the development of pneumonia in patients receiving mechanical ventilation. *Chest,* 116**,** 462-470.

CHAPARTEGUI-GONZÁLEZ, I., LÁZARO-DÍEZ, M., BRAVO, Z., NAVAS, J., ICARDO, J. M. & RAMOS-VIVAS, J. 2018. *Acinetobacter baumannii* maintains its virulence after long-time starvation. *PLoS One,* 13**,** e0201961.

CHEN, Q., LI, X., ZHOU, H., JIANG, Y., CHEN, Y., HUA, X. & YU, Y. 2013. Decreased susceptibility to tigecycline in *Acinetobacter baumannii* mediated by a mutation in *trm* encoding SAM-dependent methyltransferase. *Journal of Antimicrobial Chemotherapy,* 69**,** 72-76.

CHEN, S., LU, Z., WANG, F. & WANG, Y. 2018. Cathelicidin-WA polarizes *E. coli* K88-induced M1 macrophage to M2-like macrophage in RAW264. 7 cells. *International Immunopharmacology,* 54**,** 52-59.

CHEN, W. 2020. Host innate immune responses to Acinetobacter baumannii infection. *Frontiers in Cellular and Infection Microbiology,* 10.

CHEN, X., MENG, X., GAO, Q., ZHANG, G., GU, H. & GUO, X. 2017. Meropenem selection induced overproduction of the intrinsic carbapenemase as well as phenotype divergence in *Acinetobacter baumannii*. *International Journal of Antimicrobial Agents,* 50**,** 419-426.

CHENG, H., CHEN, Y., WU, C., CHANG, H., LAI, Y. & PENG, H. 2010. RmpA regulation of capsular polysaccharide biosynthesis in *Klebsiella pneumoniae* CG43. *Journal of Bacteriology,* 192**,** 3144-3158.

CHIANG, S.-R., JUNG, F., TANG, H.-J., CHEN, C.-H., CHEN, C.-C., CHOU, H.-Y. & CHUANG, Y.-C. 2017. Desiccation and ethanol resistances of multidrug resistant *Acinetobacter baumannii* embedded in biofilm: The favorable antiseptic efficacy of combination chlorhexidine gluconate and ethanol. *Journal of Microbiology, Immunology and Infection*.

CHIN, C.-Y., GREGG, K. A., NAPIER, B. A., ERNST, R. K. & WEISS, D. S. 2015. A PmrB-regulated deacetylase required for lipid A modification and polymyxin resistance in *Acinetobacter baumannii*. *Antimicrobial Agents and Chemotherapy,* 59**,** 7911-7914.

CHIN, C. Y., TIPTON, K. A., FAROKHYFAR, M., BURD, E. M., WEISS, D. S. & RATHER, P. N. 2018. A high-frequency phenotypic switch links bacterial virulence and environmental survival in *Acinetobacter baumannii*. *Nature Microbiology,* 3**,** 563-569.

CHOI, A. H., SLAMTI, L., AVCI, F. Y., PIER, G. B. & MAIRA-LITRÁN, T. 2009. The *pgaABCD* locus of *Acinetobacter baumannii* encodes the production of poly-β-1-6-*N*-acetylglucosamine, which is critical for biofilm formation. *Journal of Bacteriology,* 191**,** 5953-5963.

CHOI, C. H., LEE, J. S., LEE, Y. C., PARK, T. I. & LEE, J. C. 2008. *Acinetobacter baumannii*

invades epithelial cells and outer membrane protein A mediates interactions with epithelial cells. *BMC Microbiology,* 8**,** 216.

CHUSRI, S., CHONGSUVIVATWONG, V., SILPAPOJAKUL, K., SINGKHAMANAN, K., HORTIWAKUL, T., CHARERNMAK, B. & DOI, Y. 2019. Clinical characteristics and outcomes of community and hospital-acquired *Acinetobacter baumannii* bacteremia. *Journal of Microbiology, Immunology and Infection,* 52**,** 796-806.

COLLINS, R. F., BEIS, K., DONG, C., BOTTING, C. H., MCDONNELL, C., FORD, R. C., CLARKE, B. R., WHITFIELD, C. & NAISMITH, J. H. 2007. The 3D structure of a periplasm-spanning platform required for assembly of group 1 capsular polysaccharides in *Escherichia coli*. *Proceedings of the National Academy of Sciences,* 104**,** 2390-2395.

COLQUHOUN, J. M. & RATHER, P. N. 2020. Insights into mechanisms of biofilm formation in *Acinetobacter baumannii* and implications for uropathogenesis. *Frontiers in Cellular and Infection Microbiology,* 10**,** 253.

CORBETT, D., HUDSON, T. & ROBERTS, I. S. 2010. Bacterial polysaccharide capsules. *Prokaryotic Cell Wall Compounds.* Springer.

CORTÉS, G., BORRELL, N., DE ASTORZA, B., GÓMEZ, C., SAULEDA, J. & ALBERTÍ, S. 2002. Molecular analysis of the contribution of the capsular polysaccharide and the lipopolysaccharide O side chain to the virulence of *Klebsiella pneumoniae* in a murine model of pneumonia. *Infection and Immunity,* 70**,** 2583-2590.

COSTA, G. F. D. M., TOGNIM, M. C. B., CARDOSO, C. L., CARRARA-MARRONE, F. E. & GARCIA, L. B. 2006. Preliminary evaluation of adherence on abiotic and cellular surfaces of *Acinetobacter baumannii* strains isolated from catheter tips. *Brazilian Journal of Infectious Diseases,* 10**,** 346-351.

COX, M. 2018. Capsule in *Acinetobacter baumannii*. *In:* FLINDERS UNIVERSITY, C. O. S. A. E. (ed.).

CRÉPIN, S., OTTOSEN, E. N., CHANDLER, C. E., SINTSOVA, A., ERNST, R. K. & MOBLEY, H. L. 2020. The UDP-GalNAcA biosynthesis genes *gna-gne*2 are required to maintain cell envelope integrity and in vivo fitness in multi-drug resistant *Acinetobacter baumannii*. *Molecular Microbiology,* 113**,** 153-172.

CROSS, A. 1990. The biologic significance of bacterial encapsulation. *Bacterial Capsules.* Springer.

CUESTA, G., SUAREZ, N., BESSIO, M. I., FERREIRA, F. & MASSALDI, H. 2003. Quantitative determination of pneumococcal capsular polysaccharide serotype 14 using a modification of phenol–sulfuric acid method. *Journal of Microbiological Methods,* 52**,** 69-73.

DAHDOUH, E., ORGAZ, B., GÓMEZ-GIL, R., MINGORANCE, J., DAOUD, Z., SUAREZ, M. & SAN JOSE, C. 2016. Patterns of biofilm structure and formation kinetics among *Acinetobacter baumannii* clinical isolates with different antibiotic resistance profiles. *MedChemComm,* 7**,** 157-163.

DAI, M., PAN, P., LI, H., LIU, S., ZHANG, L., SONG, C., LI, Y., LI, Q., MAO, Z. & LONG, Y. 2018. The antimicrobial cathelicidin peptide hlF (1-11) attenuates alveolar macrophage pyroptosis induced by *Acinetobacter baumannii* in vivo. *Experimental Cell Research,* 364**,** 95-103.

DAI, T., TEGOS, G. P., LU, Z., HUANG, L., ZHIYENTAYEV, T., FRANKLIN, M. J., BAER, D. G. & HAMBLIN, M. R. 2009. Photodynamic therapy for *Acinetobacter baumannii* burn infections in mice. *Antimicrobial Agents and Chemotherapy,* 53**,** 3929-3934.

DAJANI, R., ZHANG, Y., TAFT, P. J., TRAVIS, S. M., STARNER, T. D., OLSEN, A., ZABNER, J., WELSH, M. J. & ENGELHARDT, J. F. 2005. Lysozyme secretion by submucosal glands protects the airway from bacterial infection. *American Journal of Respiratory Cell and Molecular Biology,* 32**,** 548-552.

DAVIS, J. S., MCMILLAN, M., SWAMINATHAN, A., KELLY, J. A., PIERA, K. E., BAIRD, R. W., CURRIE, B. J. & ANSTEY, N. M. J. C. 2014. A 16-year prospective study of community-onset bacteremic *Acinetobacter* pneumonia: low mortality with appropriate initial empirical antibiotic protocols. *Chest,* 146**,** 1038-1045.

DE BREIJ, A., DIJKSHOORN, L., LAGENDIJK, E., VAN DER MEER, J., KOSTER, A., BLOEMBERG, G., WOLTERBEEK, R., VAN DEN BROEK, P. & NIBBERING, P. 2010. Do biofilm formation and interactions with human cells explain the clinical success of *Acinetobacter baumannii*? *PLoS One,* 5**,** e10732.

DE BREIJ, A., EVEILLARD, M., DIJKSHOORN, L., VAN DEN BROEK, P. J., NIBBERING, P. H. & JOLY-GUILLOU, M.-L. 2012. Differences in *Acinetobacter baumannii* strains and host innate immune response determine morbidity and mortality in experimental pneumonia. *PLoS One,* 7**,** e30673.

DE CASTRO, C., PARRILLI, M., HOLST, O. & MOLINARO, A. 2010. Microbe-associated molecular patterns in innate immunity: Extraction and chemical analysis of Gram-negative bacterial lipopolysaccharides. *Methods in Enzymology.* Elsevier.

DECKERS, D., VANLINT, D., CALLEWAERT, L., AERTSEN, A. & MICHIELS, C. W. 2008. Role of the lysozyme inhibitor Ivy in growth or survival of *Escherichia coli* and *Pseudomonas aeruginosa* bacteria in hen egg white and in human saliva and breast milk. *Applied and Environmental Microbiology,* 74**,** 4434-4439.

DEXTER, C., MURRAY, G. L., PAULSEN, I. T. & PELEG, A. Y. 2015. Community-acquired *Acinetobacter baumannii*: clinical characteristics, epidemiology and pathogenesis. *Expert Review of Anti-infective Therapy,* 13**,** 567-573.

DIAGO-NAVARRO, E., CHEN, L., PASSET, V., BURACK, S., ULACIA-HERNANDO, A., KODIYANPLAKKAL, R., LEVI, M., BRISSE, S., KREISWIRTH, B. & FRIES, B. 2014. Carbapenem-Resistant *Klebsiella pneumoniae* exhibit variability in capsular polysaccharide and capsule associated virulence traits. *Journal of Infectious Diseases***,** 157.

DIJKSHOORN, L., NEMEC, A. & SEIFERT, H. 2007. An increasing threat in hospitals: multidrug-resistant *Acinetobacter baumannii*. *Nature Reviews Microbiology,* 5**,** 939.

DIJKSHOORN, L. & VAN DER TOORN, J. 1992. Acinetobacter species: which do we mean? *Clinical Infectious Diseases,* 15**,** 748-749.

DIKSHIT, N., KALE, S., KHAMENEH, H., BALAMURALIDHAR, V., TANG, C., KUMAR, P., LIM, T., TAN, T., KWA, A. & MORTELLARO, A. 2018. NLRP3 inflammasome pathway has a critical role in the host immunity against clinically relevant *Acinetobacter baumannii* pulmonary infection. *Mucosal Immunology,* 11**,** 257-272.

DONG, C., BEIS, K., NESPER, J., BRUNKAN, A. L., CLARKE, B. R., WHITFIELD, C. &

NAISMITH, J. H. 2006. The structure of Wza, the translocon for group 1 capsular polysaccharides in *Escherichia coli*, identifies a new class of outer membrane protein. *Nature,* 444**,** 226.

DORSEY, C. W., BEGLIN, M. S. & ACTIS, L. A. 2003. Detection and analysis of iron uptake components expressed by *Acinetobacter baumannii* clinical isolates. *Journal of Clinical Microbiology,* 41**,** 4188-4193.

DRAGO-SERRANO, M. E., DE LA GARZA-AMAYA, M., LUNA, J. S. & CAMPOS-RODRÍGUEZ, R. 2012. Lactoferrin-lipopolysaccharide (LPS) binding as key to antibacterial and antiendotoxic effects. *International Immunopharmacology,* 12**,** 1-9.

EBERHARDT, A., HOYLAND, C. N., VOLLMER, D., BISLE, S., CLEVERLEY, R. M., JOHNSBORG, O., HÅVARSTEIN, L. S., LEWIS, R. J. & VOLLMER, W. 2012. Attachment of capsular polysaccharide to the cell wall in *Streptococcus pneumoniae*. *Microbial drug resistance,* 18**,** 240-255.

EICHLER, J. & KOOMEY, M. 2017. Sweet new roles for protein glycosylation in prokaryotes. *Trends in Microbiology,* 25**,** 662-672.

EIJKELKAMP, B. 2012. Factors contributing to the success of *Acinetobacter baumannii* as a human pathogen. *In:* FLINDERS UNIVERSITY, S. O. B. S. (ed.).

EIJKELKAMP, B. A., HASSAN, K. A., PAULSEN, I. T. & BROWN, M. H. 2011a. Investigation of the human pathogen *Acinetobacter baumannii* under iron limiting conditions. *BMC Genomics,* 12**,** 126.

EIJKELKAMP, B. A., STROEHER, U. H., HASSAN, K. A., ELBOURNE, L. D., PAULSEN, I. T. & BROWN, M. H. 2013. H-NS plays a role in expression of *Acinetobacter baumannii* virulence features. *Infection and Immunity,* 81**,** 2574-2583.

EIJKELKAMP, B. A., STROEHER, U. H., HASSAN, K. A., PAULSEN, I. T. & BROWN, M. H. 2014. Comparative analysis of surface-exposed virulence factors of *Acinetobacter baumannii*. *BMC Genomics,* 15**,** 1020.

EIJKELKAMP, B. A., STROEHER, U. H., HASSAN, K. A., PAULSEN, I. T., BROWN, M. H. & LO, R. 2011b. Adherence and motility characteristics of clinical *Acinetobacter baumannii* isolates. *FEMS Microbiology Letters,* 323**,** 44-51.

ELLISON 3RD, R. & GIEHL, T. J. 1991. Killing of Gram-negative bacteria by lactoferrin and lysozyme. *Journal of Clinical Investigation,* 88**,** 1080.

ERRIDGE, C., MONCAYO-NIETO, O. L., MORGAN, R., YOUNG, M. & POXTON, I. R. 2007. *Acinetobacter baumannii* lipopolysaccharides are potent stimulators of human monocyte activation via Toll-like receptor 4 signalling. *Journal of Medical Microbiology,* 56**,** 165-171.

ESPINAL, P., MARTI, S. & VILA, J. 2012. Effect of biofilm formation on the survival of *Acinetobacter baumannii* on dry surfaces. *Journal of Hospital Infection,* 80**,** 56-60.

FARNAUD, S. & EVANS, R. W. 2003. Lactoferrin—a multifunctional protein with antimicrobial properties. *Molecular Immunology,* 40**,** 395-405.

FARROW III, J. M., WELLS, G. & PESCI, E. C. 2018. Desiccation tolerance in Acinetobacter baumannii is mediated by the two-component response regulator BfmR. *PLoS One,* 13**,**

e0205638.

FATTAHIAN, Y., RASOOLI, I., MOUSAVI GARGARI, S. L., RAHBAR, M. R., DARVISH ALIPOUR ASTANEH, S. & AMANI, J. 2011. Protection against *Acinetobacter baumannii* infection via its functional deprivation of biofilm associated protein (Bap). *Microbial Pathogenesis,* 51**,** 402-406.

FAVRE-BONTE, S., JOLY, B. & FORESTIER, C. 1999. Consequences of reduction of *Klebsiella pneumoniae* capsule expression on interactions of this bacterium with epithelial cells. *Infection and Immunity,* 67**,** 554-561.

FENG, X., SAMBANTHAMOORTHY, K., PALYS, T. & PARANAVITANA, C. 2013. The human antimicrobial peptide LL-37 and its fragments possess both antimicrobial and antibiofilm activities against multidrug-resistant *Acinetobacter baumannii*. *Peptides,* 49**,** 131-137.

FENG, Z., JIA, X., ADAMS, M. D., GHOSH, S. K., BONOMO, R. A. & WEINBERG, A. 2014. Epithelial innate immune response to *Acinetobacter baumannii* challenge. *Infection and Immunity,* 82**,** 4458-4465.

FERNÁNDEZ-CUENCA, F., TOMÁS, M., CABALLERO-MOYANO, F.-J., BOU, G., MARTÍNEZ-MARTÍNEZ, L., VILA, J., PACHÓN, J., CISNEROS, J.-M., RODRÍGUEZ-BAÑO, J. & PASCUAL, Á. 2015. Reduced susceptibility to biocides in *Acinetobacter baumannii*: association with resistance to antimicrobials, epidemiological behaviour, biological cost and effect on the expression of genes encoding porins and efflux pumps. *Journal of Antimicrobial Chemotherapy,* 70**,** 3222-3229.

FITZPATRICK, M. A., OZER, E. A. & HAUSER, A. R. 2016. Utility of whole-genome sequencing in characterizing *Acinetobacter* epidemiology and analyzing hospital outbreaks. *Journal of Clinical Microbiology,* 54**,** 593-612.

FOURNIER, P. E., RICHET, H. & WEINSTEIN, R. A. 2006. The epidemiology and control of *Acinetobacter baumannii* in health care facilities. *Clinical Infectious Diseases,* 42**,** 692-699.

FRANK, M. M., JOINER, K. & HAMMER, C. 1987. The function of antibody and complement in the lysis of bacteria. *Review of Infectious Diseases,* 9**,** S537-S545.

FUNAHASHI, T., TANABE, T., MIHARA, K., MIYAMOTO, K., TSUJIBO, H. & YAMAMOTO, S. 2012. Identification and characterization of an outer membrane receptor gene in *Acinetobacter baumannii* required for utilization of desferricoprogen, rhodotorulic acid, and desferrioxamine B as xenosiderophores. *Biological and Pharmaceutical Bulletin,* 35**,** 753-760.

FUNG, C.-P., CHANG, F.-Y., LIN, J.-C., HO, D. M.-T., CHEN, C.-T., CHEN, J.-H., YEH, K.-M., CHEN, T.-L., LIN, Y.-T. & SIU, L. K. 2011. Immune response and pathophysiological features of *Klebsiella pneumoniae* liver abscesses in an animal model. *Laboratory Investigation,* 91**,** 1029-1039.

GADDY, J. A. & ACTIS, L. A. 2009. Regulation of *Acinetobacter baumannii* biofilm formation. *Future Microbiology,* 4.

GADDY, J. A., ARIVETT, B. A., MCCONNELL, M. J., LÓPEZ-ROJAS, R., PACHÓN, J. & ACTIS, L. A. 2012. Role of acinetobactin-mediated iron acquisition functions in the interaction of *Acinetobacter baumannii* ATCC 19606T with human lung epithelial cells, *Galleria mellonella* caterpillars and mice. *Infection and Immunity*

80**,** 1015-1024.

GADDY, J. A., TOMARAS, A. P. & ACTIS, L. A. 2009. The *Acinetobacter baumannii* 19606 OmpA protein plays a role in biofilm formation on abiotic surfaces and in the interaction of this pathogen with eukaryotic cells. *Infection and Immunity,* 77**,** 3150-3160.

GALLAGHER, L. A. 2019. Methods for Tn-Seq analysis in *Acinetobacter baumannii*. *Acinetobacter baumannii*. Humana Press, New York, NY.

GALLAGHER, L. A., RAMAGE, E., WEISS, E. J., RADEY, M., HAYDEN, H. S., HELD, K. G., HUSE, H. K., ZURAWSKI, D. V., BRITTNACHER, M. J. & MANOIL, C. 2015. Resources for genetic and genomic analysis of emerging pathogen *Acinetobacter baumannii*. *Journal of Bacteriology,* 197**,** 2027-2035.

GARCÍA-PATIÑO, M. G., GARCÍA-CONTRERAS, R. & LICONA-LIMÓN, P. 2017. The immune response against *Acinetobacter baumannii*, an emerging pathogen in nosocomial infections. *Frontiers in Immunology,* 8.

GARCÍA-QUINTANILLA, M., PULIDO, M. R., LÓPEZ-ROJAS, R., PACHÓN, J. & MCCONNELL, M. J. 2013. Emerging therapies for multidrug resistant *Acinetobacter baumannii*. *Trends in Microbiology,* 21**,** 157-163.

GARCÍA-QUINTANILLA, M., PULIDO, M. R., MORENO-MARTÍNEZ, P., MARTÍN-PEÑA, R., LÓPEZ-ROJAS, R., PACHÓN, J. & MCCONNELL, M. J. 2014. Activity of host antimicrobials against multidrug-resistant *Acinetobacter baumannii* acquiring colistin resistance through loss of lipopolysaccharide. *Antimicrobial Agents and Chemotherapy,* 58**,** 2972-2975.

GARCÍA, A., SOLAR, H., GONZÁLEZ, C. & ZEMELMAN, R. 2000. Effect of EDTA on the resistance of clinical isolates of *Acinetobacter baumannii* to the bactericidal activity of normal human serum. *Journal of Medical Microbiology,* 49**,** 1047-1050.

GARNACHO-MONTERO, J. & AMAYA-VILLAR, R. 2010. Multiresistant *Acinetobacter baumannii* infections: epidemiology and management. *Current Opinion in Infectious Diseases,* 23**,** 332-339.

GARNACHO-MONTERO, J., ORTIZ-LEYBA, C., FERNÁNDEZ-HINOJOSA, E., ALDABÓ-PALLÁS, T., CAYUELA, A., MARQUEZ-VÁCARO, J. A., GARCIA-CURIEL, A. & JIMÉNEZ-JIMÉNEZ, F. 2005. *Acinetobacter baumannii* ventilator-associated pneumonia: epidemiological and clinical findings. *Intensive Care Medicine,* 31**,** 649-655.

GARUFI, G., WANG, Y.-T., OH, S.-Y., MAIER, H., MISSIAKAS, D. M. & SCHNEEWIND, O. 2012. Sortase-conjugation generates a capsule vaccine that protects guinea pigs against *Bacillus anthracis*. *Vaccine,* 30**,** 3435-3444.

GAYOSO, C. M., MATEOS, J. S., MÉNDEZ, J. A., FERNÁNDEZ-PUENTE, P., RUMBO, C., TOMÁS, M., MARTÍNEZ DE ILARDUYA, O. S. & BOU, G. N. 2013. Molecular mechanisms involved in the response to desiccation stress and persistence in *Acinetobacter baumannii*. *Journal of Proteome Research,* 13**,** 460-476.

GEISINGER, E., HUO, W., HERNANDEZ-BIRD, J. & ISBERG, R. R. 2019. *Acinetobacter baumannii*: Envelope Determinants That Control Drug Resistance, Virulence, and Surface Variability. *Annual Review of Microbiology,* 73.

GEISINGER, E. & ISBERG, R. R. 2015. Antibiotic modulation of capsular exopolysaccharide

and virulence in *Acinetobacter baumannii*. *PLoS Pathogens,* 11**,** e1004691.

GEISINGER, E., MORTMAN, N. J., VARGAS-CUEBAS, G., TAI, A. K. & ISBERG, R. R. 2018. A global regulatory system links virulence and antibiotic resistance to envelope homeostasis in *Acinetobacter baumannii*. *PLoS Pathogens,* 14**,** e1007030.

GIAMARELLOU, H., ANTONIADOU, A. & KANELLAKOPOULOU, K. 2008. *Acinetobacter baumannii*: a universal threat to public health? *International Journal of Antimicrobial Agents,* 32**,** 106-119.

GIARD, D. J., AARONSON, S. A., TODARO, G. J., ARNSTEIN, P., KERSEY, J. H., DOSIK, H. & PARKS, W. P. 1973. In vitro cultivation of human tumors: establishment of cell lines derived from a series of solid tumors. *Journal of the National Cancer Institute,* 51**,** 1417-1423.

GIL-PEROTIN, S., RAMIREZ, P., MARTI, V., SAHUQUILLO, J. M., GONZALEZ, E., CALLEJA, I., MENENDEZ, R. & BONASTRE, J. 2012. Implications of endotracheal tube biofilm in ventilator-associated pneumonia response: a state of concept. *Critical Care,* 16**,** R93.

GILES, S. K., STROEHER, U. H., EIJKELKAMP, B. A. & BROWN, M. H. 2015. Identification of genes essential for pellicle formation in *Acinetobacter baumannii*. *BMC Microbiology,* 15**,** 116.

GODEUX, A.-S., LUPO, A., HAENNI, M., GUETTE-MARQUET, S., WILHARM, G., LAABERKI, M.-H. & CHARPENTIER, X. 2018. Fluorescence-based detection of natural transformation in drug-resistant *Acinetobacter baumannii*. *Journal of Bacteriology,* 200**,** e00181-18.

GOGOU, V., POURNARAS, S., GIANNOULI, M., VOULGARI, E., PIPERAKI, E.-T., ZARRILLI, R. & TSAKRIS, A. 2011. Evolution of multidrug-resistant *Acinetobacter baumannii* clonal lineages: a 10 year study in Greece (2000–09). *Journal of Antimicrobial Chemotherapy,* 66**,** 2767-2772.

GORDON, N. C. & WAREHAM, D. W. 2010. Multidrug-resistant *Acinetobacter baumannii*: mechanisms of virulence and resistance. *International Journal of Antimicrobial Agents,* 35**,** 219-226.

GORDON, S. & READ, R. 2002. Macrophage defences against respiratory tract infections: The immunology of childhood respiratory infections. *British Medical Bulletin,* 61**,** 45-61.

GUPTA, V., DATTA, P. & CHANDER, J. 2006. Prevalence of metallo-β lactamase (MBL) producing *Pseudomonas spp.* and *Acinetobacter spp.* in a tertiary care hospital in India. *Journal of Infection,* 52**,** 311-314.

HAGIWARA, D., SUGIURA, M., OSHIMA, T., MORI, H., AIBA, H., YAMASHINO, T. & MIZUNO, T. 2003. Genome-wide analyses revealing a signaling network of the RcsC-YojN-RcsB phosphorelay system in *Escherichia coli*. *Journal of Bacteriology,* 185**,** 5735-5746.

HAMIDIAN, M. & HALL, R. M. 2013. pACICU2 is a conjugative plasmid of *Acinetobacter* carrying the aminoglycoside resistance transposon Tn aphA6. *Journal of Antimicrobial Chemotherapy,* 69**,** 1146-1148.

HAN, S., WU, W., WANG, X., XU, J. & HAN, L. 2016. Extensively drug-resistant *Acinetobacter baumannii* outbreak cross-transmitted in an intensive care unit and respiratory intensive care unit. *American Journal of Infection Control,* 44**,** 1280-1284.

HANAHAN, D. 1983. Studies on transformation of *Escherichia coli* with plasmids. *Journal of Molecular Biology,* 166**,** 557-580.

HARDING, C. M., HENNON, S. W. & FELDMAN, M. F. 2017. Uncovering the mechanisms of *Acinetobacter baumannii* virulence. *Nature Reviews Microbiology*.

HARDING, C. M., NASR, M. A., KINSELLA, R. L., SCOTT, N. E., FOSTER, L. J., WEBER, B. S., FIESTER, S. E., ACTIS, L. A., TRACY, E. N. & MUNSON, R. S. 2015. *Acinetobacter* strains carry two functional oligosaccharyltransferases, one devoted exclusively to type IV pilin, and the other one dedicated to *O*-glycosylation of multiple proteins. *Molecular Microbiology,* 96**,** 1023-1041.

HARSHEY, R. M. 2003. Bacterial motility on a surface: many ways to a common goal. *Annual Reviews in Microbiology,* 57**,** 249-273.

HASSAN, K. A., PEDERICK, V. G., ELBOURNE, L. D., PAULSEN, I. T., PATON, J. C., MCDEVITT, C. A. & EIJKELKAMP, B. A. 2017. Zinc stress induces copper depletion in *Acinetobacter baumannii*. *BMC Microbiology,* 17**,** 59.

HAUSDORFF, W. P., BRYANT, J., KLOEK, C., PARADISO, P. R. & SIBER, G. R. 2000a. The contribution of specific *pneumococcal* serogroups to different disease manifestations: implications for conjugate vaccine formulation and use, part II. *Clinical Infectious Diseases,* 30**,** 122-140.

HAUSDORFF, W. P., BRYANT, J., PARADISO, P. R. & SIBER, G. R. 2000b. Which *pneumococcal* serogroups cause the most invasive disease: implications for conjugate vaccine formulation and use, part I. *Clinical Infectious Diseases,* 30**,** 100-121.

HAUSDORFF, W. P., FEIKIN, D. R. & KLUGMAN, K. P. 2005. Epidemiological differences among *pneumococcal* serotypes. *The Lancet Infectious Diseases,* 5**,** 83-93.

HE, C., XIE, Y., FAN, H., KANG, M., TAO, C., ZHANG, R., HU, Y., CHEN, Z. & WANG, L. J. 2011. Spread of imipenem-resistant *Acinetobacter baumannii* of European clone II in Western China. *International Journal of Antimicrobial Agents,* 38**,** 257-260.

HEATH, C. H., ORRELL, T. C., LEE, R. C., PEARMAN, J. W., MCCULLOUGH, C. & CHRISTIANSEN, K. J. 2003. A review of the Royal Perth Hospital Bali experience: an infection control perspective. *Healthcare Infection,* 8**,** 43-54.

HEIDRICH, C., URSINUS, A., BERGER, J., SCHWARZ, H. & HÖLTJE, J.-V. 2002. Effects of multiple deletions of murein hydrolases on viability, septum cleavage, and sensitivity to large toxic molecules in *Escherichia coli*. *Journal of Bacteriology,* 184**,** 6093-6099.

HEINDORF, M., KADARI, M., HEIDER, C., SKIEBE, E. & WILHARM, G. 2014. Impact of *Acinetobacter baumannii* superoxide dismutase on motility, virulence, oxidative stress resistance and susceptibility to antibiotics. *PloS One,* 9.

HENRY, R., VITHANAGE, N., HARRISON, P., SEEMANN, T., COUTTS, S., MOFFATT, J. H., NATION, R. L., LI, J., HARPER, M. & ADLER, B. 2011. Colistin-resistant, lipopolysaccharide-deficient *Acinetobacter baumannii* responds to lipopolysaccharide loss through increased expression of genes involved in the synthesis and transport of lipoproteins, phospholipids and poly-β-1, 6-N-acetylglucosamine. *Antimicrobial Agents and Chemotherapy***,** AAC. 05191-11.

HERNANDEZ-MORALES, A., LESSOR, L., WOOD, T., MIGL, D., MIJALIS, E., CAHILL, J., RUSSELL, W., YOUNG, R. & GILL, J. 2018. Genomic and biochemical characterization of *Acinetobacter* podophage petty reveals a novel lysis mechanism and tail-associated depolymerase activity. *Journal of Virology,* 92**,** e01064-17.

HIDRON, A. I., EDWARDS, J. R., PATEL, J., HORAN, T. C., SIEVERT, D. M., POLLOCK, D. A. & FRIDKIN, S. K. 2008. Antimicrobial-resistant pathogens associated with healthcare-associated infections: annual summary of data reported to the National Healthcare Safety Network at the Centers for Disease Control and Prevention, 2006–2007. *Infection Control Hospital Epidemiology,* 29**,** 996-1011.

HIGGINS, P. G., DAMMHAYN, C., HACKEL, M. & SEIFERT, H. 2010. Global spread of carbapenem-resistant *Acinetobacter baumannii*. *Journal of Antimicrobial Chemotherapy,* 65**,** 233-238.

HIGGINS, P. G., PRIOR, K., HARMSEN, D. & SEIFERT, H. 2017. Development and evaluation of a core genome multilocus typing scheme for whole-genome sequence-based typing of *Acinetobacter baumannii*. *PloS One,* 12**,** e0179228.

HITCHEN, P., BRZOSTEK, J., PANICO, M., BUTLER, J. A., MORRIS, H. R., DELL, A. & LINTON, D. 2010. Modification of the *Campylobacter jejuni* flagellin glycan by the product of the Cj1295 homopolymeric-tract-containing gene. *Microbiology,* 156**,** 1953-1962.

HOANG, T. T., KARKHOFF-SCHWEIZER, R. R., KUTCHMA, A. J. & SCHWEIZER, H. P. 1998. A broad-host-range Flp- FRT recombination system for site-specific excision of chromosomally-located DNA sequences: application for isolation of unmarked *Pseudomonas aeruginosa* mutants. *Gene,* 212**,** 77-86.

HØIBY, N., CIOFU, O., JOHANSEN, H. K., SONG, Z.-J., MOSER, C., JENSEN, P. Ø., MOLIN, S., GIVSKOV, M., TOLKER-NIELSEN, T. & BJARNSHOLT, T. 2011. The clinical impact of bacterial biofilms. *International Journal of Oral Science,* 3**,** 55.

HOOD, M. I., MORTENSEN, B. L., MOORE, J. L., ZHANG, Y., KEHL-FIE, T. E., SUGITANI, N., CHAZIN, W. J., CAPRIOLI, R. M. & SKAAR, E. P. 2012. Identification of an *Acinetobacter baumannii* zinc acquisition system that facilitates resistance to calprotectin-mediated zinc sequestration. *PLoS Pathogens,* 8**,** e1003068.

HOWARD, A., O'DONOGHUE, M., FEENEY, A. & SLEATOR, R. D. 2012. *Acinetobacter baumannii*: an emerging opportunistic pathogen. *Virulence,* 3**,** 243-250.

HSU, C.-R., LIN, T.-L., PAN, Y.-J., HSIEH, P.-F. & WANG, J.-T. 2013. Isolation of a Bacteriophage Specific for a New Capsular Type of *Klebsiella pneumoniae* and Characterization of Its Polysaccharide Depolymerase. *PloS One,* 8**,** e70092.

HU, D., LIU, B., DIJKSHOORN, L., WANG, L. & REEVES, P. R. 2013. Diversity in the major polysaccharide antigen of *Acinetobacter baumannii* assessed by DNA sequencing, and development of a molecular serotyping scheme. *PloS One,* 8**,** e70329.

HU, L., SHI, Y., XU, Q., ZHANG, L., HE, J., JIANG, Y., LIU, L., LEPTIHN, S., YU, Y. & HUA, X. 2020. Capsule thickness, not biofilm formation, gives rise to mucoid *Acinetobacter baumannii* phenotypes that are more prevalent in long-term infections: a study of clinical isolates from a hospital in china. *Infection and Drug Resistance,* 13**,** 99.

HU, S., YU, Y., WU, X., XIA, X., XIAO, X. & WU, H. 2017. Comparative proteomic analysis

of *Cronobacter sakazakii* by iTRAQ provides insights into response to desiccation. *Food Research International,* 100**,** 631-639.

HUANG, T.-W., LAM, I., CHANG, H.-Y., TSAI, S.-F., PALSSON, B. O. & CHARUSANTI, P. 2014. Capsule deletion via a lamda-Red knockout system perturbs biofilm formation and fimbriae expression in *Klebsiella pneumoniae* MGH 78578. *BMC Research Notes,* 7**,** 13.

HUGHES, R. B. & SMITH, A. C. 2007. Capsule stain protocols.

HUNGER, M., SCHMUCKER, R., KISHAN, V. & HILLEN, W. 1990. Analysis and nucleotide sequence of an origin of DNA replication in *Acinetobacter calcoaceticus* and its use for *Escherichia coli* shuttle plasmids. *Gene,* 87**,** 45-51.

HYAMS, C., YUSTE, J., BAX, K., CAMBERLEIN, E., WEISER, J. N. & BROWN, J. S. 2010. *Streptococcus pneumoniae* resistance to complement-mediated immunity is dependent on the capsular serotype. *Infection and Immunity,* 78**,** 716-725.

IACONO, M., VILLA, L., FORTINI, D., BORDONI, R., IMPERI, F., BONNAL, R. J., SICHERITZ-PONTEN, T., DE BELLIS, G., VISCA, P. & CASSONE, A. 2008. Whole-genome pyrosequencing of an epidemic multidrug-resistant *Acinetobacter baumannii* strain belonging to the European clone II group. *Antimicrobial Agents and Chemotherapy,* 52**,** 2616-2625.

ISLER, B., DOI, Y., BONOMO, R. A. & PATERSON, D. L. 2019. New treatment options against carbapenem-resistant *Acinetobacter baumannii* infections. *Antimicrobial Agents and Chemotherapy,* 63**,** e01110-18.

IWASHKIW, J. A., SEPER, A., WEBER, B. S., SCOTT, N. E., VINOGRADOV, E., STRATILO, C., REIZ, B., CORDWELL, S. J., WHITTAL, R. & SCHILD, S. 2012. Identification of a general O-linked protein glycosylation system in *Acinetobacter baumannii* and its role in virulence and biofilm formation. *PLoS Pathogens,* 8**,** e1002758.

JAMES, J. & SWANSON, J. 1977. The capsule of the gonococcus. *The Journal of Experimental Medicine,* 145**,** 1082-1086.

JAŚKIEWICZ, M., NEUBAUER, D., KAZOR, K., BARTOSZEWSKA, S. & KAMYSZ, W. 2019. Antimicrobial activity of selected antimicrobial peptides against planktonic culture and biofilm of *Acinetobacter baumannii*. *Probiotics and Antimicrobial Proteins,* 11**,** 317-324.

JAWAD, A., SEIFERT, H., SNELLING, A., HERITAGE, J. & HAWKEY, P. 1998. Survival of *Acinetobacter baumannii* on dry surfaces: comparison of outbreak and sporadic isolates. *Journal of Clinical Microbiology,* 36**,** 1938-1941.

JENNINGS, H. 1990. Capsular polysaccharides as vaccine candidates. *Bacterial Capsules.* Springer.

JOLY-GUILLOU, M. L. 2005. Clinical impact and pathogenicity of *Acinetobacter*. *Clinical Microbiology and Infection,* 11**,** 868-873.

JORGENSON, M. A., KANNAN, S., LAUBACHER, M. E. & YOUNG, K. D. 2016. Dead-end intermediates in the enterobacterial common antigen pathway induce morphological defects in *Escherichia coli* by competing for undecaprenyl phosphate. *Molecular Microbiology,* 100**,** 1-14.

JORGENSON, M. A. & YOUNG, K. D. 2016. Interrupting biosynthesis of O antigen or the

lipopolysaccharide core produces morphological defects in *Escherichia coli* by sequestering undecaprenyl phosphate. *Journal of Bacteriology,* 198**,** 3070-3079.

JUNG, S.-G., JANG, J.-H., KIM, A.-Y., LIM, M.-C., KIM, B., LEE, J. & KIM, Y.-R. 2013. Removal of pathogenic factors from 2, 3-butanediol-producing *Klebsiella* species by inactivating virulence-related wabG gene. *Applied Microbiology and Biotechnology,* 97**,** 1997-2007.

KABHA, K., NISSIMOV, L., ATHAMNA, A., KEISARI, Y., PAROLIS, H., PAROLIS, L., GRUE, R. M., SCHLEPPER-SCHAFER, J., EZEKOWITZ, A. & OHMAN, D. E. 1995. Relationships among capsular structure, phagocytosis, and mouse virulence in *Klebsiella pneumoniae*. *Infection and Immunity,* 63**,** 847-852.

KAKUTA, N., NAKANO, R., NAKANO, A., SUZUKI, Y., TANOUCHI, A., MASUI, T., HORIUCHI, S., ENDO, S., KAKUTA, R. & ONO, Y. 2020. A Novel Mismatched PCR-Restriction Fragment Length Polymorphism Assay for Rapid Detection of *gyrA* and *parC* Mutations Associated With Fluoroquinolone Resistance in *Acinetobacter baumannii*. *Annals of Laboratory Medicine,* 40**,** 27-32.

KAMOSHIDA, G., AKAJI, T., TAKEMOTO, N., SUZUKI, Y., SATO, Y., KAI, D., HIBINO, T., YAMAGUCHI, D., KIKUCHI-UEDA, T. & NISHIDA, S. 2020. Lipopolysaccharide-deficient *Acinetobacter baumannii* due to colistin resistance Is killed by neutrophil-produced lysozyme. *Frontiers in Microbiology,* 11**,** 573.

KAMOSHIDA, G., KIKUCHI-UEDA, T., NISHIDA, S., TANSHO-NAGAKAWA, S., UBAGAI, T. & ONO, Y. 2018. Pathogenic bacterium *Acinetobacter baumannii* inhibits the formation of neutrophil extracellular traps by suppressing neutrophil adhesion. *Frontiers in Immunology,* 9**,** 178.

KAMOSHIDA, G., KIKUCHI-UEDA, T., TANSHO-NAGAKAWA, S., NAKANO, R., NAKANO, A., KIKUCHI, H., UBAGAI, T. & ONO, Y. 2015. *Acinetobacter baumannii* escape from neutrophil extracellular traps (NETs). *Journal of Infection and Chemotherapy,* 21**,** 43-49.

KAMOSHIDA, G., TANSHO-NAGAKAWA, S., KIKUCHI-UEDA, T., NAKANO, R., HIKOSAKA, K., NISHIDA, S., UBAGAI, T., HIGASHI, S. & ONO, Y. 2016. A novel bacterial transport mechanism of *Acinetobacter baumannii* via activated human neutrophils through interleukin-8. *Journal of Leukocyte Biology,* 100**,** 1405-1412.

KAMPF, G. 2018. Ethanol. *Antiseptic Stewardship*. Springer.

KANEHISA, M. & GOTO, S. 2000. KEGG: kyoto encyclopedia of genes and genomes. *Nucleic Acids Research,* 28**,** 27-30.

KAO, C.-Y., SHEU, B.-S. & WU, J.-J. 2016. *Helicobacter pylori* infection: An overview of bacterial virulence factors and pathogenesis. *Biomedical Journal,* 39**,** 14-23.

KARIM, M., KHAN, W., FAROOQI, B. & MALIK, I. 1991. Bacterial isolates in neutropenic febrile patients. *Journal of Pakistan Medical Association,* 41**,** 35.

KASIMOVA, A., SHNEIDER, M., ARBATSKY, N., POPOVA, A., SHASHKOV, A., MIROSHNIKOV, K., BALAJI, V., BISWAS, I. & KNIREL, Y. A. 2017. Structure and gene cluster of the K93 capsular polysaccharide of *Acinetobacter baumannii* B11911 containing 5-*N*-Acetyl-7-*N*-[(R)-3-hydroxybutanoyl] pseudaminic acid. *Biochemistry* 4**,** 483-489.

KASIMOVA, A. A., CAHILL, S. M., SHPIRT, A. M., DUDNIK, A. G., SHNEIDER, M. M., POPOVA, A. V., SHELENKOV, A. A., MIKHAILOVA, Y. V., CHIZHOV, A. O. & KENYON, J. J. 2021. The K139 capsular polysaccharide produced by *Acinetobacter baumannii* MAR17-1041 belongs to a group of related structures including K14, K37 and K116. *International Journal of Biological Macromolecules*.

KASIMOVA, A. A., KENYON, J. J., ARBATSKY, N. P., SHASHKOV, A. S., POPOVA, A. V., SHNEIDER, M. M., KNIREL, Y. A. & HALL, R. M. 2018. *Acinetobacter baumannii* K20 and K21 capsular polysaccharide structures establish roles for UDP-glucose dehydrogenase Ugd2, pyruvyl transferase Ptr2 and two glycosyltransferases. *Glycobiology,* 28**,** 876-884.

KATOH, H., ASTHANA, R. & OHMORI, M. 2004. Gene expression in the cyanobacterium *Anabaena* sp. PCC7120 under desiccation. *Microbial Ecology,* 47**,** 164-174.

KEHL-FIE, T. E. & SKAAR, E. P. J. 2010. Nutritional immunity beyond iron: a role for manganese and zinc. *Current Opinion in Chemical Biology,* 14**,** 218-224.

KENYON, J. J. & HALL, R. M. 2013. Variation in the complex carbohydrate biosynthesis loci of *Acinetobacter baumannii* genomes. *PloS One,* 8**,** e62160.

KENYON, J. J., HALL, R. M. & DE CASTRO, C. 2015a. Structural determination of the K14 capsular polysaccharide from an ST25 *Acinetobacter baumannii* isolate, D46. *Carbohydrate Research,* 417**,** 52-56.

KENYON, J. J., KASIMOVA, A. A., NOTARO, A., ARBATSKY, N. P., SPECIALE, I., SHASHKOV, A. S., DE CASTRO, C., HALL, R. M. & KNIREL, Y. A. 2017a. *Acinetobacter baumannii* K13 and K73 capsular polysaccharides differ only in K-unit side branches of novel non-2-ulosonic acids: di-N-acetylated forms of either acinetaminic acid or 8-epiacinetaminic acid. *Carbohydrate Research,* 452**,** 149-155.

KENYON, J. J., MARZAIOLI, A., HALL, R. M. & DE CASTRO, C. 2014a. Structure of the K2 capsule associated with the KL2 gene cluster of *Acinetobacter baumannii*. *Glycobiology,* 24**,** 554-563.

KENYON, J. J., MARZAIOLI, A. M., HALL, R. M. & DE CASTRO, C. 2015b. Structure of the K6 capsular polysaccharide from *Acinetobacter baumannii* isolate RBH4. *Carbohydrate Research,* 409**,** 30-35.

KENYON, J. J., MARZAIOLI, A. M., HALL, R. M. & DE CASTRO, C. 2015c. Structure of the K12 capsule containing 5, 7-di-N-acetylacinetaminic acid from *Acinetobacter baumannii* isolate D36. *Glycobiology,* 25**,** 881-887.

KENYON, J. J., NIGRO, S. J. & HALL, R. M. 2014b. Variation in the OC locus of *Acinetobacter baumannii* genomes predicts extensive structural diversity in the lipooligosaccharide. *PLOS One,* 9**,** e107833.

KENYON, J. J., NOTARO, A., HSU, L. Y., DE CASTRO, C. & HALL, R. M. 2017b. 5, 7-Di-*N*-acetyl-8-epiacinetaminic acid: A new non-2-ulosonic acid found in the K73 capsule produced by an *Acinetobacter baumannii* isolate from Singapore. *Scientific Reports,* 7**,** 11357.

KENYON, J. J., SHNEIDER, M. M., SENCHENKOVA, S. N., SHASHKOV, A. S., SINIAGINA, M. N., MALANIN, S. Y., POPOVA, A. V., MIROSHNIKOV, K. A., HALL, R. M. & KNIREL, Y. A. 2016a. K19 capsular polysaccharide of *Acinetobacter baumannii* is produced via a Wzy polymerase encoded in a small genomic island rather than the KL19

capsule gene cluster. *Microbiology,* 162**,** 1479-1489.

KENYON, J. J., SPECIALE, I., HALL, R. M. & DE CASTRO, C. 2016b. Structure of repeating unit of the capsular polysaccharide from *Acinetobacter baumannii* D78 and assignment of the K4 gene cluster. *Carbohydrate Research,* 434**,** 12-17.

KIM, G.-L., SEON, S.-H. & RHEE, D.-K. 2017. Pneumonia and *Streptococcus pneumoniae* vaccine. *Archives of pharmacal research,* 40**,** 885-893.

KIM, S., VELA, A., CLOHISEY, S. M., ATHANASIADOU, S., KAISER, P., STEVENS, M. P. & VERVELDE, L. 2018. Host-specific differences in the response of cultured macrophages to *Campylobacter jejuni* capsule and O-methyl phosphoramidate mutants. *Veterinary Research,* 49**,** 3.

KIM, S. W., CHOI, C. H., MOON, D. C., JIN, J. S., LEE, J. H., SHIN, J. H., KIM, J. M., LEE, Y. C., SEOL, S. Y. & CHO, D. T. 2009. Serum resistance of *Acinetobacter baumannii* through the binding of factor H to outer membrane proteins. *FEMS Microbiology Letters,* 301**,** 224-231.

KING, L. B., PANGBURN, M. K. & MCDANIEL, L. S. 2013. Serine protease PKF of *Acinetobacter baumannii* results in serum resistance and suppression of biofilm formation. *The Journal of Infectious Diseases,* 207**,** 1128-1134.

KING, L. B., SWIATLO, E., SWIATLO, A. & MCDANIEL, L. S. 2009. Serum resistance and biofilm formation in clinical isolates of *Acinetobacter baumannii*. *FEMS Immunology & Medical Microbiology,* 55**,** 414-421.

KING, T., LUCCHINI, S., HINTON, J. C. & GOBIUS, K. 2010. Transcriptomic analysis of *Escherichia coli* O157: H7 and K-12 cultures exposed to inorganic and organic acids in stationary phase reveals acidulant-and strain-specific acid tolerance responses. *Applied and Environmental Microbiology,* 76**,** 6514-6528.

KNAPP, S., WIELAND, C. W., FLORQUIN, S., PANTOPHLET, R., DIJKSHOORN, L., TSHIMBALANGA, N., AKIRA, S. & VAN DER POLL, T. 2006. Differential roles of CD14 and Toll-like Receptors 4 and 2 in murine *Acinetobacter* pneumonia. *American Journal of Respiratory and Critical Care Medicine,* 173**,** 122-129.

KOENIGS, A., STAHL, J., AVERHOFF, B., GÖTTIG, S., WICHELHAUS, T. A., WALLICH, R., ZIPFEL, P. F. & KRAICZY, P. 2016. CipA of *Acinetobacter baumannii* is a novel plasminogen binding and complement inhibitory protein. *The Journal of Infectious Diseases,* 213**,** 1388-1399.

KONSTANTINIDIS, T., KAMBAS, K., MITSIOS, A., PANOPOULOU, M., TSIRONIDOU, V., DELLAPORTA, E., KOUKLAKIS, G., ARAMPATZIOGLOU, A., ANGELIDOU, I. & MITROULIS, I. 2016. Immunomodulatory role of clarithromycin in *Acinetobacter baumannii* infection via formation of neutrophil extracellular traps. *Antimicrobial Agents and Chemotherapy,* 60**,** 1040-1048.

KORNELSEN, V. & KUMAR, A. 2021. Update on Multidrug Resistance Efflux Pumps in Acinetobacter spp. *Antimicrobial Agents and Chemotherapy,* 65**,** e00514-21.

KRZYMIŃSKA, S., FRĄCKOWIAK, H. & KAZNOWSKI, A. 2012. *Acinetobacter calcoaceticus–baumannii* complex strains induce caspase-dependent and caspase-independent death of human epithelial cells. *Current Microbiology,* 65**,** 319-329.

KUOLEE, R., HARRIS, G., YAN, H., XU, H. H., CONLAN, W. J., PATEL, G. B. & CHEN, W. 2014. Intranasal immunization protects against *Acinetobacter baumannii*-associated pneumonia in mice. *Vaccine*.

KUZHIYIL, A., LEE, Y., SHIM, A. & XIONG, A. 2012. Osmotic stress induces kanamycin resistance in *Escherichia coli* B23 through increased capsule formation. *Journal of Exerimental Microbiology and Immunology,* 16**,** 5-10.

LAI, Y.-C., PENG, H.-L. & CHANG, H.-Y. 2003. RmpA2, an activator of capsule biosynthesis in *Klebsiella pneumoniae* CG43, regulates K2 *cps* gene expression at the transcriptional level. *Journal of Bacteriology,* 185**,** 788-800.

LÁZARO-DÍEZ, M., CHAPARTEGUI-GONZÁLEZ, I., REDONDO-SALVO, S., LEIGH, C., MERINO, D., SAN SEGUNDO, D., NAVAS, J., ICARDO, J. M., ACOSTA, F. & OCAMPO-SOSA, A. 2017. Human neutrophils phagocytose and kill *Acinetobacter baumannii* and *A. pittii*. *Scientific Reports,* 7**,** 1-11.

LE, N.-H., PETERS, K., ESPAILLAT, A., SHELDON, J. R., GRAY, J., VENANZIO, G. D., LOPEZ, J., DJAHANSCHIRI, B., MUELLER, E. A., HENNON, S. W., LEVIN, P. A., EBERSBERGER, I., SKAAR, E. P., CAVA, F., VOLLMER, W. & FELDMAN, M. F. 2020. Peptidoglycan editing provides immunity to *Acinetobacter baumannii* during bacterial warfare. *Science Advances,* 6**,** 2020.04.23.058008.

LEBRE, P. H., DE MAAYER, P. & COWAN, D. A. 2017. Xerotolerant bacteria: surviving through a dry spell. *Nature Reviews Microbiology,* 15**,** 285-296.

LEE, C.-R., LEE, J. H., PARK, M., PARK, K. S., BAE, I. K., KIM, Y. B., CHA, C.-J., JEONG, B. C. & LEE, S. H. 2017a. Biology of *Acinetobacter baumannii:* pathogenesis, antibiotic resistance mechanisms, and prospective treatment options. *Frontiers in Cellular and Infection Microbiology,* 7**,** 55.

LEE, H. W., KOH, Y., KIM, J., LEE, J. C., LEE, Y. C., SEOL, S. Y. & CHO, D. T. 2008. Capacity of multidrug-resistant clinical isolates of *Acinetobacter baumannii* to form biofilm and adhere to epithelial cell surfaces. *Clinical Microbiology and Infection,* 14**,** 49-54.

LEE, I.-M., YANG, F.-L., CHEN, T.-L., LIAO, K.-S., REN, C.-T., LIN, N.-T., CHANG, Y.-P., WU, C.-Y. & WU, S.-H. 2018. Pseudaminic acid on exopolysaccharide of *Acinetobacter baumannii* plays a critical role in phage-assisted preparation of glycoconjugate vaccine with high antigenicity. *Journal of the American Chemical Society,* 140**,** 8639-8643.

LEE, J.-Y., JEONG, M.-C., JEON, D., LEE, Y., LEE, W. C. & KIM, Y. 2017b. Structure-activity relationship-based screening of antibiotics against Gram-negative *Acinetobacter baumannii*. *Bioorganic & Medicinal Chemistry,* 25**,** 372-380.

LEE, J., OH, J., KIM, K., JEONG, Y., PARK, J. & CHO, J. 2001. Apoptotic cell death induced by *Acinetobacter baumannii* in epithelial cells through caspase-3 activation. *Apmis,* 109**,** 679-684.

LEE, J. C., KOERTEN, H., VAN DEN BROEK, P., BEEKHUIZEN, H., WOLTERBEEK, R., VAN DEN BARSELAAR, M., VAN DER REIJDEN, T., VAN DER MEER, J., VAN DE GEVEL, J. & DIJKSHOORN, L. 2006. Adherence of *Acinetobacter baumannii* strains to human bronchial epithelial cells. *Research in Microbiology,* 157**,** 360-366.

LEE, J. S., LEE, J. C., LEE, C.-M., JUNG, I. D., JEONG, Y.-I., SEONG, E.-Y., CHUNG, H.-Y.

& PARK, Y.-M. 2007. Outer membrane protein A of *Acinetobacter baumannii* induces differentiation of CD4+ T cells toward a Th1 polarizing phenotype through the activation of dendritic cells. *Biochemical Pharmacology,* 74**,** 86-97.

LEES-MILLER, R. G., IWASHKIW, J. A., SCOTT, N. E., SEPER, A., VINOGRADOV, E., SCHILD, S. & FELDMAN, M. F. 2013. A common pathway for *O*-linked protein-glycosylation and synthesis of capsule in *Acinetobacter baumannii*. *Molecular Microbiology,* 89**,** 816-830.

LEHMANN, M. H. 1998. Recombinant human granulocyte-macrophagecolony-stimulating factor triggers interleukin-10expression in the monocytic cell line U937. *Molecular Immunology,* 35**,** 479-485.

LEUNG, W.-S., CHU, C.-M., TSANG, K.-Y., LO, F.-H., LO, K.-F. & HO, P.-L. 2006. Fulminant community-acquired *Acinetobacter baumannii* pneumonia as a distinct clinical syndrome. *CHEST Journal,* 129**,** 102-109.

LEUS, I. V., WEEKS, J. W., BONIFAY, V., SMITH, L., RICHARDSON, S. & ZGURSKAYA, H. I. 2018. Substrate specificities and efflux efficiencies of RND efflux pumps of *Acinetobacter baumannii*. *Journal of Bacteriology,* 200.

LI, H., BHASKARA, A., MEGALIS, C. & TORTORELLO, M. L. 2012. Transcriptomic analysis of Salmonella desiccation resistance. *Foodborne Pathogens and Disease,* 9**,** 1143-1151.

LI, L., HASSAN, K. A., BROWN, M. H. & PAULSEN, I. T. 2016a. Rapid multiplexed phenotypic screening identifies drug resistance functions for three novel efflux pumps in *Acinetobacter baumannii*. *Journal of Antimicrobial Chemotherapy,* 71**,** 1223-1232.

LI, X., QUAN, J., YANG, Y., JI, J., LIU, L., FU, Y., HUA, X., CHEN, Y., PI, B. & JIANG, Y. 2016b. *abrp*, a new gene, confers reduced susceptibility to tetracycline, glycylcine, chloramphenicol and fosfomycin classes in *Acinetobacter baumannii*. *European Journal of Clinical Microbiology & Infectious Diseases,* 35**,** 1371-1375.

LI, Z.-T., ZHANG, R.-L., BI, X.-G., XU, L., FAN, M., XIE, D., XIAN, Y., WANG, Y., LI, X.-J. & WU, Z.-D. 2015. Outer membrane vesicles isolated from two clinical *Acinetobacter baumannii* strains exhibit different toxicity and proteome characteristics. *Microbial Pathogenesis,* 81**,** 46-52.

LIN, C.-T., WU, C.-C., CHEN, Y.-S., LAI, Y.-C., CHI, C., LIN, J.-C., CHEN, Y. & PENG, H.-L. 2011. Fur regulation of the capsular polysaccharide biosynthesis and iron-acquisition systems in *Klebsiella pneumoniae* CG43. *Microbiology,* 157**,** 419-429.

LIN, L., TAN, B., PANTAPALANGKOOR, P., HO, T., BAQUIR, B., TOMARAS, A., MONTGOMERY, J. I., BARBACCI, E. G., HUJER, K. & BONOMO, R. A. 2012. Inhibition of LpxC protects mice from resistant *Acinetobacter baumannii* by modulating inflammation and enhancing phagocytosis. *MBio,* 3.

LIN, M.-F., LIN, Y.-Y. & LAN, C.-Y. 2017. Contribution of EmrAB efflux pumps to colistin resistance in *Acinetobacter baumannii*. *Journal of Microbiology,* 55**,** 130-136.

LIN, S., WONG, W., FUNG, C., LIU, C. & LIU, C. 1998. *Acinetobacter calcoaceticus-baumannii* complex bacteremia: analysis of 82 cases. *Journal of Microbiology, Immunology, and Infection,* 31**,** 119-124.

LIOU, M.-L., SOO, P.-C., LING, S.-R., KUO, H.-Y., TANG, C. Y. & CHANG, K.-C. 2014. The sensor kinase BfmS mediates virulence in *Acinetobacter baumannii*. *Journal of Microbiology, Immunology and Infection,* 47**,** 275-281.

LIU, M. A., KENYON, J. J., LEE, J. & REEVES, P. R. 2017. Rapid customised operon assembly by yeast recombinational cloning. *Applied Microbiology and Biotechnology,* 101**,** 4569-4580.

LIU, M. A. & REEVES, P. R. 2019. Customizable Cloning of Whole Polysaccharide Gene Clusters by Yeast Homologous Recombination. *Bacterial Polysaccharides.* Springer.

LIU, Z., GARCÍA-DÍAZ, B., CATACCHIO, B., CHIANCONE, E. & VOGEL, H. J. 2015. Protecting Gram-negative bacterial cell envelopes from human lysozyme: Interactions with Ivy inhibitor proteins from *Escherichia coli* and *Pseudomonas aeruginosa*. *Biochimica et Biophysica Acta (BBA)-Biomembranes,* 1848**,** 3032-3046.

LIVAK, K. J. & SCHMITTGEN, T. D. 2001. Analysis of relative gene expression data using real-time quantitative PCR and the 2− ΔΔCT method. *Methods,* 25**,** 402-408.

LOB, S. H., HOBAN, D. J., SAHM, D. F. & BADAL, R. E. 2016. Regional differences and trends in antimicrobial susceptibility of *Acinetobacter baumannii*. *International Journal of Antimicrobial Agents,* 47**,** 317-323.

LOEHFELM, T. W., LUKE, N. R. & CAMPAGNARI, A. A. 2008. Identification and characterization of an *Acinetobacter baumannii* biofilm-associated protein. *Journal of Bacteriology,* 190**,** 1036-1044.

LONGO, F., VUOTTO, C. & DONELLI, G. 2014. Biofilm formation in *Acinetobacter baumannii*. *New Microbiology,* 37**,** 119-127.

LOPEZ, C., ARIVETT, B. A., ACTIS, L. A. & TOLMASKY, M. E. 2015. Inhibition of AAC (6′)-Ib-mediated resistance to amikacin in *Acinetobacter baumannii* by an antisense peptide-conjugated 2′, 4′-bridged nucleic acid-NC-DNA hybrid oligomer. *Antimicrobial Agents and Chemotherapy,* 59**,** 5798-5803.

LUCIDI, M., RUNCI, F., RAMPIONI, G., FRANGIPANI, E., LEONI, L. & VISCA, P. 2018. New shuttle vectors for gene cloning and expression in multidrug-resistant *Acinetobacter* species. *Antimicrobial Agents and Chemotherapy,* 62**,** e02480-17.

LUEBBERDING, S., KRUEGER, N. & KERSCHER, M. 2013. Skin physiology in men and women: in vivo evaluation of 300 people including TEWL, SC hydration, sebum content and skin surface pH. *International Journal of Cosmetic Science,* 35**,** 477-483.

LUKE, N. R., SAUBERAN, S. L., RUSSO, T. A., BEANAN, J. M., OLSON, R., LOEHFELM, T. W., COX, A. D., MICHAEL, F. S., VINOGRADOV, E. V. & CAMPAGNARI, A. A. 2010. Identification and characterization of a glycosyltransferase involved in *Acinetobacter baumannii* lipopolysaccharide core biosynthesis. *Infection and Immunity,* 78**,** 2017-2023.

LUO, G., LIN, L., IBRAHIM, A. S., BAQUIR, B., PANTAPALANGKOOR, P., BONOMO, R. A., DOI, Y., ADAMS, M. D., RUSSO, T. A. & SPELLBERG, B. 2012. Active and passive immunization protects against lethal, extreme drug resistant-*Acinetobacter baumannii* infection. *PloS One,* 7**,** e29446.

MACLEOD, C. M. & KRAUSS, M. R. 1950. Relation of virulence of *pneumococcal* strains for

mice to the quantity of capsular polysaccharide formed in vitro. *The Journal of Experimental Medicine,* 92**,** 1-9.

MACRITCHIE, D. M., BUELOW, D. R., PRICE, N. L. & RAIVIO, T. L. 2008. Two-component signaling and gram negative envelope stress response systems. *Bacterial Signal Transduction: Networks and Drug Targets.* Springer.

MANDAL, R. K. & KWON, Y. M. 2017. Global screening of *Salmonella enterica* serovar Typhimurium genes for desiccation survival. *Frontiers in Microbiology,* 8**,** 1723.

MAO, Y., DOYLE, M. & CHEN, J. 2006. Role of colanic acid exopolysaccharide in the survival of enterohaemorrhagic *Escherichia coli* O157: H7 in simulated gastrointestinal fluids. *Letters in Applied Microbiology,* 42**,** 642-647.

MAO, Y., DOYLE, M. P. & CHEN, J. 2001. Insertion mutagenesis of *wca* reduces acid and heat tolerance of enterohemorrhagic *Escherichia coli* O157: H7. *Journal of Bacteriology,* 183**,** 3811-3815.

MARCH, C., REGUEIRO, V., LLOBET, E., MORANTA, D., MOREY, P., GARMENDIA, J. & BENGOECHEA, J. A. 2010. Dissection of host cell signal transduction during *Acinetobacter baumannii*–triggered inflammatory response. *PLoS One,* 5**,** e10033.

MARIDIAN-BIOSCIENCE 2020. RANGER DNA polymenrase and mix. *In:* BIOSCIENCE, M. (ed.) *Maridian Bioscience.* Australia: Maridian Bioscience.

MARTÍN-ASPAS, A., GUERRERO-SÁNCHEZ, F. M., GARCÍA-COLCHERO, F., RODRÍGUEZ-ROCA, S. & GIRÓN-GONZÁLEZ, J.-A. 2018. Differential characteristics of *Acinetobacter baumannii* colonization and infection: risk factors, clinical picture, and mortality. *Infection Drug Resistance,* 11**,** 861.

MATHEE, K., CIOFU, O., STERNBERG, C., LINDUM, P. W., CAMPBELL, J. I., JENSEN, P., JOHNSEN, A. H., GIVSKOV, M., OHMAN, D. E. & SØREN, M. 1999. Mucoid conversion of *Pseudomonas aeruginosa* by hydrogen peroxide: a mechanism for virulence activation in the cystic fibrosis lung. *Microbiology,* 145**,** 1349-1357.

MAY, H. C., YU, J.-J., SHRIHARI, S., SESHU, J., KLOSE, K. E., CAP, A. P., CHAMBERS, J. P., GUENTZEL, M. N. & ARULANANDAM, B. P. 2019. Thioredoxin Modulates Cell Surface Hydrophobicity in *Acinetobacter baumannii*. *Frontiers in Microbiology,* 10.

MCCONNELL, M. J., DOMÍNGUEZ-HERRERA, J., SMANI, Y., LÓPEZ-ROJAS, R., DOCOBO-PÉREZ, F. & PACHÓN, J. 2011. Vaccination with outer membrane complexes elicits rapid protective immunity to multidrug-resistant *Acinetobacter baumannii*. *Infection and Immunity,* 79**,** 518-526.

MCCONNELL, M. J. & PACHÓN, J. 2010. Active and passive immunization against *Acinetobacter baumannii* using an inactivated whole cell vaccine. *Vaccine,* 29**,** 1-5.

MCDONALD, L. C., BANERJEE, S. N., JARVIS, W. R. & SYSTEM, N. N. I. S. 1999. Seasonal variation of *Acinetobacter* infections: 1987–1996. *Clinical Infectious Diseases,* 29**,** 1133-1137.

MCKIGHT, P. E. & NAJAB, J. 2010. Kruskal-wallis test. *The Corsini Encyclopedia of Psychology***,** 1-1.

MCQUEARY, C. N. & ACTIS, L. A. 2011. *Acinetobacter baumannii* biofilms: variations among strains and correlations with other cell properties. *The Journal of Microbiology,* 49**,** 243-250.

MCQUEARY, C. N., KIRKUP, B. C., SI, Y., BARLOW, M., ACTIS, L. A., CRAFT, D. W. & ZURAWSKI, D. V. 2012. Extracellular stress and lipopolysaccharide modulate *Acinetobacter baumannii* surface-associated motility. *The Journal of Microbiology,* 50**,** 434-443.

MERABISHVILI, M., MONSEREZ, R., VAN BELLEGHEM, J., ROSE, T., JENNES, S., DE VOS, D., VERBEKEN, G., VANEECHOUTTE, M. & PIRNAY, J.-P. 2017. Stability of bacteriophages in burn wound care products. *PloS One,* 12**,** e0182121.

METAN, G., ALP, E., AYGEN, B. & SUMERKAN, B. 2007. *Acinetobacter baumannii* meningitis in post-neurosurgical patients: clinical outcome and impact of carbapenem resistance. *Journal of Antimicrobial Chemotherapy,* 60**,** 197-199.

METZGAR, D., BACHER, J. M., PEZO, V., READER, J., DÖRING, V., SCHIMMEL, P., MARLIÈRE, P. & DE CRÉCY-LAGARD, V. 2004. *Acinetobacter sp.* ADP1: an ideal model organism for genetic analysis and genome engineering. *Nucleic Acids Research,* 32**,** 5780-5790.

MEUMANN, E. M., ANSTEY, N. M., CURRIE, B. J., PIERA, K. A., KENYON, J. J., HALL, R. M., DAVIS, J. S. & SAROVICH, D. S. 2019. Genomic epidemiology of severe community-onset *Acinetobacter baumannii* infection. *Microbial genomics,* 5.

MIHARA, K., TANABE, T., YAMAKAWA, Y., FUNAHASHI, T., NAKAO, H., NARIMATSU, S. & YAMAMOTO, S. 2004. Identification and transcriptional organization of a gene cluster involved in biosynthesis and transport of acinetobactin, a siderophore produced by *Acinetobacter baumannii* ATCC 19606T. *Journal of Microbiology,* 150**,** 2587-2597.

MIN, H. & COWMAN, M. K. 1986. Combined alcian blue and silver staining of glycosaminoglycans in polyacrylamide gels: application to electrophoretic analysis of molecular weight distribution. *Analytical Biochemistry,* 155**,** 275-285.

MOECK, G. S. & COULTON, J. W. 1998. TonB-dependent iron acquisition: mechanisms of siderophore-mediated active transport. *Molecular Microbiology,* 28**,** 675-681.

MOFFATT, J. H., HARPER, M., HARRISON, P., HALE, J. D., VINOGRADOV, E., SEEMANN, T., HENRY, R., CRANE, B., MICHAEL, F. S. & COX, A. D. 2010. Colistin resistance in *Acinetobacter baumannii* is mediated by complete loss of lipopolysaccharide production. *Antimicrobial Agents and Chemotherapy,* 54**,** 4971-4977.

MOFFATT, J. H., HARPER, M., MANSELL, A., CRANE, B., FITZSIMONS, T. C., NATION, R. L., LI, J., ADLER, B. & BOYCE, J. D. 2013. Lipopolysaccharide-deficient *Acinetobacter baumannii* shows altered signaling through host Toll-like receptors and increased susceptibility to the host antimicrobial peptide LL-37. *Infection and Immunity,* 81**,** 684-689.

MONTEIRO, M. A., BAQAR, S., HALL, E. R., CHEN, Y.-H., PORTER, C. K., BENTZEL, D. E., APPLEBEE, L. & GUERRY, P. 2009. Capsule polysaccharide conjugate vaccine against diarrheal disease caused by *Campylobacter jejuni*. *Infection and Immunity,* 77**,** 1128-1136.

MORONA, J. K., MORONA, R., MILLER, D. C. & PATON, J. C. 2003. Mutational analysis of the carboxy-terminal (YGX) 4 repeat domain of CpsD, an autophosphorylating tyrosine kinase required for capsule biosynthesis in *Streptococcus pneumoniae*. *Journal of Bacteriology,* 185**,** 3009-3019.

MORTENSEN, B. L., RATHI, S., CHAZIN, W. J. & SKAAR, E. P. 2014. *Acinetobacter baumannii* response to host-mediated zinc limitation requires the transcriptional regulator Zur. *Journal of Bacteriology,* 196**,** JB. 01650-14.

MORTENSEN, B. L. & SKAAR, E. P. 2013. The contribution of nutrient metal acquisition and metabolism to *Acinetobacter baumannii* survival within the host. *Frontiers in Cellular Infection and Immunity,* 3**,** 95.

MOSTOWY, R. J. & HOLT, K. E. 2018. Diversity-generating machines: genetics of bacterial sugar-coating. *Trends in Microbiology,* 26**,** 1008-1021.

MOUSLIM, C., DELGADO, M. & GROISMAN, E. A. 2004. Activation of the RcsC/YojN/RcsB phosphorelay system attenuates *Salmonella* virulence. *Molecular Microbiology,* 54**,** 386-395.

MOUSLIM, C. & GROISMAN, E. A. 2003. Control of the Salmonella ugd gene by three two-component regulatory systems. *Molecular microbiology,* 47**,** 335-344.

MUYRERS, J. P., ZHANG, Y. & STEWART, A. F. 2001. Techniques: recombinogenic engineering–new options for cloning and manipulating DNA. *Trends in biochemical sciences,* 26**,** 325-331.

NAPIER, B. A., BURD, E. M., SATOLA, S. W., CAGLE, S. M., RAY, S. M., MCGANN, P., POHL, J., LESHO, E. P. & WEISS, D. S. 2013. Clinical use of colistin induces cross-resistance to host antimicrobials in *Acinetobacter baumannii*. *MBio,* 4**,** e00021-13.

NEMEC, A., KRIZOVA, L., MAIXNEROVA, M., VAN DER REIJDEN, T. J., DESCHAGHT, P., PASSET, V., VANEECHOUTTE, M., BRISSE, S. & DIJKSHOORN, L. 2011. Genotypic and phenotypic characterization of the *Acinetobacter calcoaceticus–Acinetobacter baumannii* complex with the proposal of *Acinetobacter pittii sp*. nov.(formerly Acinetobacter genomic species 3) and *Acinetobacter nosocomialis sp.* nov.(formerly Acinetobacter genomic species 13TU). *Research in Microbiology,* 162**,** 393-404.

NESHANI, A., SEDIGHIAN, H., MIRHOSSEINI, S. A., GHAZVINI, K., ZARE, H. & JAHANGIRI, A. 2020. Antimicrobial peptides as a promising treatment option against *Acinetobacter baumannii* infections. *Microbial Pathogenesis,* 146**,** 104238.

NG, D. H., MARIMUTHU, K., LEE, J. J., KHONG, W. X., NG, O. T., ZHANG, W., POH, B. F., RAO, P., RAJ, M. D. R. & ANG, B. 2018. Environmental colonization and onward clonal transmission of carbapenem-resistant *Acinetobacter baumannii* (CRAB) in a medical intensive care unit: the case for environmental hygiene. *Antimicrobial Resistance & Infection Control,* 7**,** 1-8.

NIELSEN, S. S. 2010. Phenol-sulfuric acid method for total carbohydrates. *Food Analysis Laboratory Manual.* Springer.

NIGRO, S. J. & HALL, R. M. 2014. Amikacin resistance plasmids in extensively antibiotic-resistant GC2 *Acinetobacter baumannii* from two Australian hospitals. *Journal of Antimicrobial Chemotherapy,* 69**,** 3435-3437.

NIGRO, S. J., HOLT, K. E., PICKARD, D. & HALL, R. M. 2014. Carbapenem and amikacin resistance on a large conjugative *Acinetobacter baumannii* plasmid. *Journal of Antimicrobial Chemotherapy***,** dku486.

NIU, T., GUO, L., LUO, Q., ZHOU, K., YU, W., CHEN, Y., HUANG, C. & XIAO, Y. 2020. Wza gene knockout decreases *Acinetobacter baumannii* virulence and affects Wzy-dependent capsular polysaccharide synthesis. *Virulence,* 11**,** 1-13.

NIYONSABA, F. & OGAWA, H. 2005. Protective roles of the skin against infection: implication of naturally occurring human antimicrobial agents β-defensins, cathelicidin LL-37 and lysozyme. *Journal of Dermatological Science,* 40**,** 157-168.

NWUGO, C. C., GADDY, J. A., ZIMBLER, D. L. & ACTIS, L. A. 2011. Deciphering the iron response in *Acinetobacter baumannii*: a proteomics approach. *Journal of Proteomics,* 74**,** 44-58.

OBADIA, B., LACOUR, S., DOUBLET, P., BAUBICHON-CORTAY, H., COZZONE, A. J. & GRANGEASSE, C. 2007. Influence of tyrosine-kinase Wzc activity on colanic acid production in *Escherichia coli* K12 cells. *Journal of Molecular Biology,* 367**,** 42-53.

OPHIR, T. & GUTNICK, D. L. 1994. A role for exopolysaccharides in the protection of microorganisms from desiccation. *Applied and Environmental Microbiology,* 60**,** 740-745.

OVERBEEK, R., OLSON, R., PUSCH, G. D., OLSEN, G. J., DAVIS, J. J., DISZ, T., EDWARDS, R. A., GERDES, S., PARRELLO, B. & SHUKLA, M. 2013. The SEED and the Rapid Annotation of microbial genomes using Subsystems Technology (RAST). *Nucleic Acids Research,* 42**,** D206-D214.

PAKHARUKOVA, N., TUITTILA, M., PAAVILAINEN, S., MALMI, H., PARILOVA, O., TENEBERG, S., KNIGHT, S. D. & ZAVIALOV, A. V. 2018. Structural basis for *Acinetobacter baumannii* biofilm formation. *Proceedings of the National Academy of Sciences,* 115**,** 5558-5563.

PALMEN, R. & HELLINGWERF, K. J. 1997. Uptake and processing of DNA by *Acinetobacter calcoaceticus*–a review. *Gene,* 192**,** 179-190.

PANTOPHLET, R., SEVERIN, J. A., NEMEC, A., BRADE, L., DIJKSHOORN, L. & BRADE, H. 2002. Identification of *Acinetobacter* isolates from species belonging to the *Acinetobacter calcoaceticus-Acinetobacter baumannii* complex with monoclonal antibodies specific for O antigens of their lipopolysaccharides. *Clinical and Diagnostic Laboratory Immunology,* 9**,** 60-65.

PAPATHANAKOS, G., ANDRIANOPOULOS, I., PAPATHANASIOU, A., PRIAVALI, E., KOULENTI, D. & KOULOURAS, V. 2020. Colistin-resistant *Acinetobacter baumannii* bacteremia: A serious threat for critically ill patients. *Microorganisms,* 8**,** 287.

PARKER, D. & PRINCE, A. 2011. Innate immunity in the respiratory epithelium. *American Journal of Respiratory Cell and Molecular Biology,* 45**,** 189-201.

PARROW, N. L., FLEMING, R. E. & MINNICK, M. F. 2013. Sequestration and scavenging of iron in infection. *Infection and Immunity,* 81**,** 3503-3514.

PELEG, A. Y., BELL, J. M., HOFMEYR, A. & WIESE, P. 2006. Inter-country transfer of Gram-negative organisms carrying the VIM-4 and OXA-58 carbapenem-hydrolysing enzymes. *Journal of Antimicrobial Chemotherapy,* 57**,** 794-795.

PELEG, A. Y., DE BREIJ, A., ADAMS, M. D., CERQUEIRA, G. M., MOCALI, S., GALARDINI, M., NIBBERING, P. H., EARL, A. M., WARD, D. V. & PATERSON, D. L. 2012. The success of *Acinetobacter* species; genetic, metabolic and virulence attributes. *PLoS*

One, 7**,** e46984.

PELEG, A. Y., SEIFERT, H. & PATERSON, D. L. 2008. *Acinetobacter baumannii*: emergence of a successful pathogen. *Clinical Microbiology Reviews,* 21**,** 538-582.

PEREZ, F. & BONOMO, R. A. 2014. Vaccines for *Acinetobacter baumannii:* Thinking "out of the box". *Vaccine,* 32.

PIPERAKI, E.-T., TZOUVELEKIS, L., MIRIAGOU, V. & DAIKOS, G. 2019. Carbapenem-resistant *Acinetobacter baumannii:* in pursuit of an effective treatment. *Clinical Microbiology and Infection,* 25**,** 951-957.

PIRES, S. & PARKER, D. 2019. Innate immune responses to *Acinetobacter baumannii* in the airway. *Journal of Interferon & Cytokine Research,* 39.

POIREL, L. & NORDMANN, P. 2006. Carbapenem resistance in *Acinetobacter baumannii*: mechanisms and epidemiology. *Clinical Microbiology and Infection,* 12**,** 826-836.

POUR, N. K., DUSANE, D. H., DHAKEPHALKAR, P. K., ZAMIN, F. R., ZINJARDE, S. S. & CHOPADE, B. A. 2011. Biofilm formation by *Acinetobacter baumannii* strains isolated from urinary tract infection and urinary catheters. *FEMS Immunology & Medical Microbiology,* 62**,** 328-338.

POWERS, M. J., HERRERA, C. M., TUCKER, A. T., DAVIES, B. W. & TRENT, M. S. 2019. Isolation of lipid cell envelope components from *Acinetobacter baumannii*. *Acinetobacter baumannii.* Springer.

POWERS, M. J. & TRENT, M. S. 2018. Expanding the paradigm for the outer membrane: *Acinetobacter baumannii* in the absence of endotoxin. *Molecular Microbiology,* 107**,** 47-56.

PRESTON, A. & APICELLA, M. A. 1999. The genetics of capsule and lipooligosaccharide biosynthesis in *Haemophilus influenzae*. *Genetics of Bacterial Polysaccharides***,** 91.

PRESTON, A., MANDRELL, R. E., GIBSON, B. W. & APICELLA, M. A. 1996. The lipooligosaccharides of pathogenic Gram-negative bacteria. *Critical Reviews in Microbiology,* 22**,** 139-180.

PRUITT, K. D., TATUSOVA, T. & MAGLOTT, D. R. 2006. NCBI reference sequences (RefSeq): a curated non-redundant sequence database of genomes, transcripts and proteins. *Nucleic Acids Research,* 35**,** D61-D65.

QI, L., LI, H., ZHANG, C., LIANG, B., LI, J., WANG, L., DU, X., LIU, X., QIU, S. & SONG, H. 2016. Relationship between antibiotic resistance, biofilm formation, and biofilm-specific resistance in *Acinetobacter baumannii*. *Frontiers in Microbiology,* 7**,** 483.

QIU, H., KUOLEE, R., HARRIS, G. & CHEN, W. 2009. High susceptibility to respiratory *Acinetobacter baumannii* infection in A/J mice is associated with a delay in early pulmonary recruitment of neutrophils. *Microbes and Infection,* 11**,** 946-955.

QIU, H., KUOLEE, R., HARRIS, G., VAN ROOIJEN, N., PATEL, G. B. & CHEN, W. 2012. Role of macrophages in early host resistance to respiratory *Acinetobacter baumannii* infection. *PloS One,* 7**,** e40019.

QURESHI, Z. A., HITTLE, L. E., O'HARA, J. A., RIVERA, J. I., SYED, A., SHIELDS, R. K.,

PASCULLE, A. W., ERNST, R. K. & DOI, Y. 2015. Colistin-resistant *Acinetobacter baumannii*: beyond carbapenem resistance. *Clinical Infectious Diseases,* 60**,** 1295-1303.

RAETZ, C. R. & WHITFIELD, C. 2002. Lipopolysaccharide endotoxins. *Annual Review of Biochemistry,* 71**,** 635-700.

RAGLAND, S. A. & CRISS, A. K. 2017. From bacterial killing to immune modulation: Recent insights into the functions of lysozyme. *PLoS Pathogens,* 13**,** e1006512.

RAGLAND, S. A., SCHAUB, R. E., HACKETT, K. T., DILLARD, J. P. & CRISS, A. K. 2017. Two lytic transglycosylases in *Neisseria gonorrhoeae* impart resistance to killing by lysozyme and human neutrophils. *Cellular Microbiology,* 19.

RANJIT, D. K. & YOUNG, K. D. 2016. Colanic acid intermediates prevent de novo shape recovery of *Escherichia coli* spheroplasts, calling into question biological roles previously attributed to colanic acid. *Journal of Bacteriology,* 198**,** 1230-1240.

RATHINAVELU, S., ZAVROS, Y. & MERCHANT, J. L. 2003. *Acinetobacter lwoffii* infection and gastritis. *Microbes and Infection,* 5**,** 651-657.

RAVASI, P., LIMANSKY, A. S., RODRIGUEZ, R. E., VIALE, A. M. & MUSSI, M. A. 2011. ISAba825, a functional insertion sequence modulating genomic plasticity and *bla*OXA-58 expression in *Acinetobacter baumannii*. *Antimicrobial Agents and Chemotherapy,* 55**,** 917-920.

RAYMOND, C. K., POWNDER, T. A. & SEXSON, S. L. 1999. General method for plasmid construction using homologous recombination. *Biotechniques,* 26**,** 134-141.

RAYMOND, C. K., SIMS, E. H. & OLSON, M. V. 2002. Linker-mediated recombinational subcloning of large DNA fragments using yeast. *Genome Research,* 12**,** 190-197.

REESE, M. G. 2001. Application of a time-delay neural network to promoter annotation in the *Drosophila melanogaster* genome. *Computers & Chemistry,* 26**,** 51-56.

REGUEIRO, V., CAMPOS, M. A., PONS, J., ALBERTÍ, S. & BENGOECHEA, J. A. 2006. The uptake of a *Klebsiella pneumoniae* capsule polysaccharide mutant triggers an inflammatory response by human airway epithelial cells. *Microbiology,* 152**,** 555-566.

REPIZO, G. D., GAGNÉ, S., FOUCAULT-GRUNENWALD, M.-L., BORGES, V., CHARPENTIER, X., LIMANSKY, A. S., GOMES, J. P., VIALE, A. M. & SALCEDO, S. P. 2015. Differential role of the T6SS in *Acinetobacter baumannii* virulence. *PloS One,* 10**,** e0138265.

RIBERA, A., ROCA, I., RUIZ, J., GIBERT, I. & VILA, J. 2003. Partial characterization of a transposon containing the tetA determinant in a clinical isolate of *Acinetobacter baumannii*. *Journal of Antimicrobial Chemotherapy,* 52**,** 477-480.

RICHIE, D. L., WANG, L., CHAN, H., DE PASCALE, G., SIX, D. A., WEI, J.-R. & DEAN, C. R. 2018. A pathway-directed positive growth restoration assay to facilitate the discovery of lipid A and fatty acid biosynthesis inhibitors in *Acinetobacter baumannii*. *PLOS One,* 13**,** e0193851.

ROBBINS, J. B., SCHNEERSON, R., XIE, G., HANSON, L. Å. & MILLER, M. A. 2011. Capsular polysaccharide vaccine for Group B *Neisseria meningitidis, Escherichia coli* K1, and *Pasteurella haemolytica* A2. *Proceedings of the National Academy of Sciences,* 108**,** 17871-

17875.

ROBERSON, E. B. & FIRESTONE, M. K. 1992. Relationship between desiccation and exopolysaccharide production in a soil *Pseudomonas sp. Applied and Environmental Microbiology,* 58**,** 1284-1291.

ROBERTS, I. S. 1996. The biochemistry and genetics of capsular polysaccharide production in bacteria. *Annual Reviews in Microbiology,* 50**,** 285-315.

ROCA, I., MARTI, S., ESPINAL, P., MARTINEZ, P., GIBERT, I. & VILA, J. 2009. CraA, a major facilitator superfamily efflux pump associated with chloramphenicol resistance in *Acinetobacter baumannii*. *Antimicrobial Agents and Chemotherapy,* 53**,** 4013-4014.

RODRÍGUEZ-BAÑO, J., MARTI, S., SOTO, S., FERNÁNDEZ-CUENCA, F., CISNEROS, J., PACHÓN, J., PASCUAL, A., MARTÍNEZ-MARTÍNEZ, L., MCQUEARY, C. & ACTIS, L. 2008. Biofilm formation in *Acinetobacter baumannii*: associated features and clinical implications. *Clinical Microbiology and Infection,* 14**,** 276-278.

RONISH, L. A., LILLEHOJ, E., FIELDS, J. K., SUNDBERG, E. J. & PIEPENBRINK, K. H. 2019. The structure of PilA from *Acinetobacter baumannii* AB5075 suggests a mechanism for functional specialization in *Acinetobacter* type IV pili. *Journal of Biological Chemistry,* 294**,** 218-230.

ROSENBERG, M. 2017. Adhesion to hydrocarbons and microbial hydrophobicity—do the MATH. *FEMS Microbiology Letters,* 364**,** fnx069.

ROSENBERG, M., GUTNICK, D. & ROSENBERG, E. 1980. Adherence of bacteria to hydrocarbons: a simple method for measuring cell-surface hydrophobicity. *FEMS Microbiology Letters,* 9**,** 29-33.

ROUTSIAS, J. G., KARAGOUNIS, P., PARVULESKU, G., LEGAKIS, N. J. & TSAKRIS, A. 2010. In vitro bactericidal activity of human β-defensin 2 against nosocomial strains. *Peptides,* 31**,** 1654-1660.

RUMBO, C., GATO, E., LÓPEZ, M., DE ALEGRIA, C. R., FERNÁNDEZ-CUENCA, F., MARTÍNEZ-MARTÍNEZ, L., VILA, J., PACHÓN, J., CISNEROS, J. M. & RODRÍGUEZ-BAÑO, J. 2013. Contribution of efflux pumps, porins, and β-lactamases to multidrug resistance in clinical isolates of *Acinetobacter baumannii*. *Antimicrobial Agents and Chemotherapy,* 57**,** 5247-5257.

RUNNEGAR, N., SIDJABAT, H., GOH, H. S., NIMMO, G. R., SCHEMBRI, M. A. & PATERSON, D. L. 2010. Molecular epidemiology of multidrug-resistant *Acinetobacter baumannii* in a single institution over a 10-year period. *Journal of Clinical Microbiology,* 48**,** 4051-4056.

RUSSO, T. A., BEANAN, J. M., OLSON, R., MACDONALD, U., COX, A. D., MICHAEL, F. S., VINOGRADOV, E. V., SPELLBERG, B., LUKE-MARSHALL, N. R. & CAMPAGNARI, A. A. 2013. The K1 capsular polysaccharide from *Acinetobacter baumannii* is a potential therapeutic target via passive immunization. *Infection and Immunity,* 81**,** 915-922.

RUSSO, T. A., LUKE, N. R., BEANAN, J. M., OLSON, R., SAUBERAN, S. L., MACDONALD, U., SCHULTZ, L. W., UMLAND, T. C. & CAMPAGNARI, A. A. 2010. The K1 capsular polysaccharide of *Acinetobacter baumannii* strain 307-0294 is a major virulence factor. *Infection and Immunity,* 78**,** 3993-4000.

RYU, S. Y., BAEK, W.-K. & KIM, H. A. 2017. Association of biofilm production with colonization among clinical isolates of *Acinetobacter baumannii*. *The Korean Journal of Internal Medicine,* 32**,** 345-351.

SABRA, W., KIM, E.-J. & ZENG, A.-P. 2002. Physiological responses of *Pseudomonas aeruginosa* PAO1 to oxidative stress in controlled microaerobic and aerobic cultures. *Microbiology,* 148**,** 3195-3202.

SAITO, H., SAKAKIBARA, Y., SAKATA, A., KURASHIGE, R., MURAKAMI, D., KAGESHIMA, H., SAITO, A. & MIYAZAKI, Y. 2019. Antibacterial activity of lysozyme-chitosan oligosaccharide conjugates (LYZOX) against *Pseudomonas aeruginosa*, *Acinetobacter baumannii* and Methicillin-resistant *Staphylococcus aureus*. *Plos One,* 14**,** e0217504.

SAMBROOK, J. & RUSSELL, D. W. 2006. Agarose gel electrophoresis. *Cold Spring Harbor Protocols,* 2006**,** pdb. prot4020.

SANCHEZ-LARRAYOZ, A. F., ELHOSSEINY, N. M., CHEVRETTE, M. G., FU, Y., GIUNTA, P., SPALLANZANI, R. G., RAVI, K., PIER, G. B., LORY, S. & MAIRA-LITRÁN, T. 2017. Complexity of complement resistance factors expressed by *Acinetobacter baumannii* needed for survival in human serum. *The Journal of Immunology,* 199**,** 2354-2368.

SANCHEZ-ROMERO, J. M., DIAZ-OREJAS, R. & DE LORENZO, V. 1998. Resistance to tellurite as a selection marker for genetic manipulations of Pseudomonas strains. *Applied and environmental microbiology,* 64**,** 4040-4046.

SAND, M., STAHL, J., WACLAWSKA, I., ZIEGLER, C. & AVERHOFF, B. 2014. Identification of an osmo-dependent and an osmo-independent choline transporter in *Acinetobacter baylyi*: implications in osmostress protection and metabolic adaptation. *Environmental Microbiology,* 16**,** 1490-1502.

SARMA, J. V. & WARD, P. A. 2011. The complement system. *Cell and Tissue Research,* 343**,** 227-235.

SAROJ, S. D., CLEMMER, K. M., BONOMO, R. A. & RATHER, P. N. 2012. Novel mechanism for fluoroquinolone resistance in *Acinetobacter baumannii*. *Antimicrobial Agents and Chemotherapy,* 56**,** 4955-4957.

SCHMIDT, M. A., RILEY, L. W. & BENZ, I. 2003. Sweet new world: glycoproteins in bacterial pathogens. *Trends in Microbiology,* 11**,** 554-561.

SCHNEIDER, C. A., RASBAND, W. S. & ELICEIRI, K. W. 2012. NIH Image to ImageJ: 25 years of image analysis. *Nature Methods,* 9**,** 671.

SCHNEIDER, G., DOBRINDT, U., BRÜGGEMANN, H., NAGY, G., JANKE, B., BLUM-OEHLER, G., BUCHRIESER, C., GOTTSCHALK, G., EMÖDY, L. & HACKER, J. 2004. The pathogenicity island-associated K15 capsule determinant exhibits a novel genetic structure and correlates with virulence in uropathogenic *Escherichia coli* strain 536. *Infection and Immunity,* 72**,** 5993-6001.

SCHNIDER-KEEL, U., LEJBØLLE, K. B., BAEHLER, E., HAAS, D. & KEEL, C. 2001. The Sigma Factor AlgU (AlgT) Controls Exopolysaccharide Production and Tolerance towards Desiccation and Osmotic Stress in the Biocontrol Agent *Pseudomonas fluorescens* CHA0. *Applied and Environmental Microbiology,* 67**,** 5683-5693.

SCHOOLEY, R. T., BISWAS, B., GILL, J. J., HERNANDEZ-MORALES, A., LANCASTER, J., LESSOR, L., BARR, J. J., REED, S. L., ROHWER, F. & BENLER, S. 2017. Development and use of personalized bacteriophage-based therapeutic cocktails to treat a patient with a disseminated resistant *Acinetobacter baumannii* infection. *Antimicrobial Agents and Chemotherapy,* 61.

SCORPIO, A., CHABOT, D. J., DAY, W. A., O'BRIEN, D. K., VIETRI, N. J., ITOH, Y., MOHAMADZADEH, M. & FRIEDLANDER, A. M. 2007. Poly-γ-glutamate capsule-degrading enzyme treatment enhances phagocytosis and killing of encapsulated *Bacillus anthracis*. *Antimicrobial Agents and Chemotherapy,* 51**,** 215-222.

SCOTT, N. E., KINSELLA, R. L., EDWARDS, A. V., LARSEN, M. R., DUTTA, S. M., SABA, J., FOSTER, L. J. & FELDMAN, M. F. 2014. Diversity within the *O*-linked protein glycosylation systems of *Acinetobacter* species. *Molecular & Cellular Proteomics,* 13**,** 2354-2370.

SCOTT, P., DEYE, G., SRINIVASAN, A., MURRAY, C., MORAN, K., HULTEN, E., FISHBAIN, J., CRAFT, D., RIDDELL, S. & LINDLER, L. 2007. An outbreak of multidrug-resistant *Acinetobacter baumannii-calcoaceticus* complex infection in the US military health care system associated with military operations in Iraq. *Clinical Infectious Diseases,* 44**,** 1577-1584.

SEBENY, P. J., RIDDLE, M. S. & PETERSEN, K. 2008. *Acinetobacter baumannii* skin and soft-tissue infection associated with war trauma. *Clinical Infectious Diseases,* 47**,** 444-449.

SEGAL, A. W. 2005. How neutrophils kill microbes. *Annual Reviews in Immunology,* 23**,** 197-223.

SELASI, G. N., NICHOLAS, A., JEON, H., NA, S. H., KWON, H. I., KIM, Y. J., HEO, S. T., OH, M. H. & LEE, J. C. 2016. Differences in biofilm mass, expression of biofilm-associated genes, and resistance to desiccation between epidemic and sporadic clones of carbapenem-resistant *Acinetobacter baumannii* sequence type 191. *PloS One,* 11.

SHAH, S., SINGHAL, T. & NAIK, R. 2015. A 4-year prospective study to determine the incidence and microbial etiology of surgical site infections at a private tertiary care hospital in Mumbai, India. *American Journal of Infection Control,* 43**,** 59-62.

SHASHKOV, A. S., KENYON, J. J., ARBATSKY, N. P., SHNEIDER, M. M., POPOVA, A. V., KNIREL, Y. A. & HALL, R. M. 2018. Genetics of biosynthesis and structure of the K53 capsular polysaccharide of *Acinetobacter baumannii* D23 made up of a disaccharide K unit. *Microbiology,* 164**,** 1-4.

SHASHKOV, A. S., LIU, B., KENYON, J. J., POPOVA, A. V., SHNEIDER, M. M., SOF'YA, N. S., ARBATSKY, N. P., MIROSHNIKOV, K. A., WANG, L. & KNIREL, Y. A. 2017. Structures of the K35 and K15 capsular polysaccharides of *Acinetobacter baumannii* LUH5535 and LUH5554 containing amino and diamino uronic acids. *Carbohydrate Research,* 448**,** 28-34.

SHETE, V. B., GHADAGE, D. P., MULEY, V. A. & BHORE, A. V. 2010. Multi-drug resistant *Acinetobacter* ventilator-associated pneumonia. *Lung India,* 27**,** 217.

SHI, W.-F., JIANG, J.-P. & MI, Z.-H. 2005. Relationship between antimicrobial resistance and aminoglycoside-modifying enzyme gene expressions in *Acinetobacter baumannii*. *Chinese Medical Journal,* 118**,** 141-145.

SINGH, A., WYANT, T., ANAYA-BERGMAN, C., ADUSE-OPOKU, J., BRUNNER, J., LAINE, M. L., CURTIS, M. A. & LEWIS, J. P. 2011. The capsule of *Porphyromonas gingivalis* leads to a reduction in the host inflammatory response, evasion of phagocytosis, and increase in virulence. *Infection and Immunity,* 79**,** 4533-4542.

SINGH, J. K., ADAMS, F. G. & BROWN, M. H. 2018. Diversity and function of capsular polysaccharide in *Acinetobacter baumannii*. *Frontiers in Microbiology,* 9.

SKAAR, E. P. 2010. The battle for iron between bacterial pathogens and their vertebrate hosts. *PLoS Pathogens,* 6**,** e1000949.

SKERNIŠKYTĖ, J., KRASAUSKAS, R., PÉCHOUX, C., KULAKAUSKAS, S., ARMALYTĖ, J. & SUŽIEDĖLIENĖ, E. 2018. Surface-related features and virulence among *Acinetobacter baumannii* clinical isolates belonging to international clone I and II. *Frontiers in Microbiology,* 9**,** 3116.

SMANI, Y., DOMINGUEZ-HERRERA, J. & PACHÓN, J. 2013. Association of the outer membrane protein Omp33 with fitness and virulence of *Acinetobacter baumannii*. *The Journal of Infectious Diseases,* 208**,** 1561-1570.

SMITH, M. G., GIANOULIS, T. A., PUKATZKI, S., MEKALANOS, J. J., ORNSTON, L. N., GERSTEIN, M. & SNYDER, M. 2007. New insights into *Acinetobacter baumannii* pathogenesis revealed by high-density pyrosequencing and transposon mutagenesis. *Genes & Development,* 21**,** 601-614.

SOARES, N. C., CABRAL, M. P., GAYOSO, C., MALLO, S., RODRIGUEZ-VELO, P., FERNÁNDEZ-MOREIRA, E. & BOU, G. 2010. Associating growth-phase-related changes in the proteome of *Acinetobacter baumannii* with increased resistance to oxidative stress. *Journal of Proteome Research,* 9**,** 1951-1964.

SOON, R. L., LI, J., BOYCE, J. D., HARPER, M., ADLER, B., LARSON, I. & NATION, R. L. 2012. Cell surface hydrophobicity of colistin-susceptible vs resistant *Acinetobacter baumannii* determined by contact angles: methodological considerations and implications. *Journal of Applied Microbiology,* 113**,** 940-951.

SPELLBERG, B. & BONOMO, R. A. 2013. "Airborne assault": a new dimension in *Acinetobacter baumannii* transmission. *Critical Care Medicine,* 41.

SPSS 2007. SPSS version 16.0. *Chicago, IL: SPSS Incorporated.*

SRINIVASAN, V. B., VAIDYANATHAN, V. & RAJAMOHAN, G. 2015. AbuO, a TolC-like outer membrane protein of *Acinetobacter baumannii,* is involved in antimicrobial and oxidative stress resistance. *Antimicrobial Agents and Chemotherapy,* 59**,** 1236-1245.

SRINIVASAN, V. B., VENKATARAMAIAH, M., MONDAL, A., VAIDYANATHAN, V., GOVIL, T. & RAJAMOHAN, G. 2012. Functional characterization of a novel outer membrane porin KpnO, regulated by PhoBR two-component system in *Klebsiella pneumoniae* NTUH-K2044. *PLoS One,* 7.

STANDISH, A. J., SALIM, A. A., ZHANG, H., CAPON, R. J. & MORONA, R. 2012. Chemical inhibition of bacterial protein tyrosine phosphatase suppresses capsule production. *PloS One,* 7**,** e36312.

STOKES, R. W., NORRIS-JONES, R., BROOKS, D. E., BEVERIDGE, T. J., DOXSEE, D. &

THORSON, L. M. 2004. The glycan-rich outer layer of the cell wall of *Mycobacterium tuberculosis* acts as an antiphagocytic capsule limiting the association of the bacterium with macrophages. *Infection and Immunity,* 72**,** 5676-5686.

STRUVE, C. & KROGFELT, K. A. 2003. Role of capsule in *Klebsiella pneumoniae* virulence: lack of correlation between in vitro and in vivo studies. *FEMS Microbiology Letters,* 218**,** 149-154.

SUBRAMANIYAN, A., NAIR, S., JOSEPH, N. M. & KANUNGO, R. 2017. Profile of Multidrug Resistant *Acinetobacter baumannii* Infections among Hospitalized Patients. *Journal of Medical Science and Clinical Research,* 5**,** 23111-5.

SULLIVAN, M. J., PETTY, N. K. & BEATSON, S. A. 2011. Easyfig: a genome comparison visualizer. *Bioinformatics,* 27**,** 1009-1010.

SYCZ, G., DI VENANZIO, G., SARTORIO, M. G., NGUYEN-HUNG, L., SCOTT, N. E., BEATTY, W. L. & FELDMAN, M. F. 2021. Modern *Acinetobacter baumannii* clinical isolates replicate inside spacious vacuoles and egress from macrophages. *bioRxiv*.

TAHOUN, A., MASUTANI, H., EL-SHARKAWY, H., GILLESPIE, T., HONDA, R. P., KUWATA, K., INAGAKI, M., YABE, T., NOMURA, I. & SUZUKI, T. 2017. Capsular polysaccharide inhibits adhesion of *Bifidobacterium longum* 105-A to enterocyte-like Caco-2 cells and phagocytosis by macrophages. *Gut Pathogens,* 9.

TAKOI, H., FUJITA, K., HYODO, H., MATSUMOTO, M., OTANI, S., GORAI, M., MANO, Y., SAITO, Y., SEIKE, M. & FURUYA, N. 2019. *Acinetobacter baumannii* can be transferred from contaminated nitrile examination gloves to polypropylene plastic surfaces. *American Journal of Infection Control,* 47**,** 1171-1175.

TALBOT, U. M., PATON, A. W. & PATON, J. C. 1996. Uptake of *Streptococcus pneumoniae* by respiratory epithelial cells. *Infection and Immunity,* 64**,** 3772-3777.

TALYANSKY, Y., NIELSEN, T. B., YAN, J., CARLINO-MACDONALD, U., DI VENANZIO, G., CHAKRAVORTY, S., ULHAQ, A., FELDMAN, M. F., RUSSO, T. A. & VINOGRADOV, E. 2021. Capsule carbohydrate structure determines virulence in *Acinetobacter baumannii*. *PLoS Pathogens,* 17**,** e1009291.

TATAR, L. D., MAROLDA, C. L., POLISCHUK, A. N., VAN LEEUWEN, D. & VALVANO, M. A. 2007. An *Escherichia coli* undecaprenyl-pyrophosphate phosphatase implicated in undecaprenyl phosphate recycling. *Microbiology,* 153**,** 2518-2529.

TIPTON, K. A., CHIN, C.-Y., FAROKHYFAR, M., WEISS, D. S. & RATHER, P. N. 2018. Role of capsule in resistance to disinfectants, host antimicrobials and desiccation in *Acinetobacter baumannii*. *Antimicrobial Agents and Chemotherapy,* 62**,** e01188-18.

TIPTON, K. A., DIMITROVA, D. & RATHER, P. N. 2015. Phase-variable control of multiple phenotypes in *Acinetobacter baumannii* strain AB5075. *Journal of Bacteriology,* 197**,** 2593-2599.

TIPTON, K. A. & RATHER, P. N. 2017. An ompR-envZ two-component system ortholog regulates phase variation, osmotic tolerance, motility, and virulence in *Acinetobacter baumannii* strain AB5075. *Journal of Bacteriology,* 199**,** e00705-16.

TOMARAS, A. P., DORSEY, C. W., EDELMANN, R. E. & ACTIS, L. A. 2003. Attachment to

and biofilm formation on abiotic surfaces by *Acinetobacter baumannii*: involvement of a novel chaperone-usher pili assembly system. *Microbiology,* 149**,** 3473-3484.

TOMASCHEK, F., HIGGINS, P. G., STEFANIK, D., WISPLINGHOFF, H. & SEIFERT, H. 2016. Head-to-head comparison of two multi-locus sequence typing (MLST) schemes for characterization of *Acinetobacter baumannii* outbreak and sporadic isolates. *PLoS One,* 11**,** e0153014.

TRAUB, W. H. 1989. *Acinetobacter baumannii* serotyping for delineation of outbreaks of nosocomial cross-infection. *Journal of Clinical Microbiology,* 27**,** 2713-2716.

TRIPP, J. D., LILLEY, J. L., WOOD, W. N. & LEWIS, L. K. 2013. Enhancement of plasmid DNA transformation efficiencies in early stationary-phase yeast cell cultures. *Yeast,* 30**,** 191-200.

TROTTIER, V., SEGURA, P. G., NAMIAS, N., KING, D., PIZANO, L. R. & SCHULMAN, C. I. 2007. Outcomes of *Acinetobacter baumannii* infection in critically ill burned patients. *Journal of Burn Care & Research,* 28**,** 248-254.

TSUCHIYA, T., NAKAO, N., YAMAMOTO, S., HIRAI, Y., MIYAMOTO, K. & TSUJIBO, H. 2012. NK1. 1+ cells regulate neutrophil migration in mice with *Acinetobacter baumannii* pneumonia. *Microbiology and Immunology,* 56**,** 107-116.

TUCKER, A. T., NOWICKI, E. M., BOLL, J. M., KNAUF, G. A., BURDIS, N. C., TRENT, M. S. & DAVIES, B. W. 2014. Defining gene-phenotype relationships in *Acinetobacter baumannii* through one-step chromosomal gene inactivation. *MBio,* 5**,** e01313-14.

UCKAY, I., SAX, H., HARBARTH, S., BERNARD, L. & PITTET, D. 2008. Multi-resistant infections in repatriated patients after natural disasters: lessons learned from the 2004 tsunami for hospital infection control. *Journal of Hospital Infection,* 68**,** 1-8.

UMLAND, T. C., SCHULTZ, L. W., MACDONALD, U., BEANAN, J. M., OLSON, R. & RUSSO, T. A. 2012. In vivo-validated essential genes identified in *Acinetobacter baumannii* by using human ascites overlap poorly with essential genes detected on laboratory media. *MBio,* 3**,** e00113-12.

VALENZUELA, J. K., THOMAS, L., PARTRIDGE, S. R., VAN DER REIJDEN, T., DIJKSHOORN, L. & IREDELL, J. 2007. Horizontal gene transfer in a polyclonal outbreak of carbapenem-resistant *Acinetobacter baumannii*. *Journal of Clinical Microbiology,* 45**,** 453-460.

VALENZUELA, M., ALBAR, J. P., PARADELA, A. & TOLEDO, H. 2011. *Helicobacter pylori* Exhibits a Fur-Dependent Acid Tolerance Response. *Helicobacter,* 16**,** 189-199.

VAN FAASSEN, H., KUOLEE, R., HARRIS, G., ZHAO, X., CONLAN, J. W. & CHEN, W. 2007. Neutrophils play an important role in host resistance to respiratory infection with *Acinetobacter baumannii* in mice. *Infection and Immunity,* 75**,** 5597-5608.

VANDECRAEN, J., CHANDLER, M., AERTSEN, A. & VAN HOUDT, R. 2017. The impact of insertion sequences on bacterial genome plasticity and adaptability. *Critical Reviews in Microbiology,* 43**,** 709-730.

VERMEULEN, C., CROSS, A., BYRNE, W. & ZOLLINGER, W. 1988. Quantitative relationship between capsular content and killing of K1-encapsulated *Escherichia coli*. *Infection and Immunity,* 56**,** 2723-2730.

VIGNESH, K. S. & DEEPE JR, G. S. 2016. Immunological orchestration of zinc homeostasis: The battle between host mechanisms and pathogen defenses. *Archives of Biochemistry,* 611**,** 66-78.

VILA, J., MARCOS, A., MARCO, F., ABDALLA, S., VERGARA, Y., REIG, R., GOMEZ-LUS, R. & DE ANTA, T. J. 1993. In vitro antimicrobial production of beta-lactamases, aminoglycoside-modifying enzymes, and chloramphenicol acetyltransferase by and susceptibility of clinical isolates of *Acinetobacter baumannii*. *Antimicrobial Agents and Chemotherapy,* 37**,** 138-141.

VILACOBA, E., ALMUZARA, M., GULONE, L., TRAGLIA, G. M., FIGUEROA, S. A., SLY, G., FERNÁNDEZ, A., CENTRÓN, D. & RAMÍREZ, M. S. 2013. Emergence and spread of plasmid-borne tet (B):: ISCR2 in minocycline-resistant *Acinetobacter baumannii* isolates. *Antimicrobial Agents and Chemotherapy,* 57**,** 651-654.

VINOGRADOV, E., MACLEAN, L., XU, H. H. & CHEN, W. 2014. The structure of the polysaccharide isolated from *Acinetobacter baumannii* strain LAC-4. *Carbohydrate Research,* 390**,** 42-45.

VOGEL, C. F., GARCIA, J., WU, D., MITCHELL, D. C., ZHANG, Y., KADO, N. Y., WONG, P., TRUJILLO, D. A., LOLLIES, A. & BENNET, D. 2012. Activation of inflammatory responses in human U937 macrophages by particulate matter collected from dairy farms: an in vitro expression analysis of pro-inflammatory markers. *Environmental Health,* 11**,** 17.

VOLLMER, W. & HÖLTJE, J.-V. 2004. The architecture of the murein (peptidoglycan) in Gram-negative bacteria: vertical scaffold or horizontal layer (s)? *Journal of Bacteriology,* 186**,** 5978-5987.

WANG-LIN, S. X., OLSON, R., BEANAN, J. M., MACDONALD, U., BALTHASAR, J. P. & RUSSO, T. A. 2017. The capsular polysaccharide of *Acinetobacter baumannii* is an obstacle for therapeutic passive immunization strategies. *Infection and Immunity,* 85**,** e00591-17.

WANG, G., OLCZAK, A., FORSBERG, L. S. & MAIER, R. J. 2009. Oxidative stress-induced peptidoglycan deacetylase in *Helicobacter pylori*. *Journal of Biological Chemistry,* 284**,** 6790-6800.

WANG, H., WILKSCH, J. J., LITHGOW, T., STRUGNELL, R. A. & GEE, M. L. 2013. Nanomechanics measurements of live bacteria reveal a mechanism for bacterial cell protection: the polysaccharide capsule in *Klebsiella* is a responsive polymer hydrogel that adapts to osmotic stress. *Soft Matter,* 9**,** 7560-7567.

WANG, J., ZHOU, Z., HE, F., RUAN, Z., JIANG, Y., HUA, X. & YU, Y. 2018. The role of the type VI secretion system *vgrG* gene in the virulence and antimicrobial resistance of *Acinetobacter baumannii* ATCC 19606^{T}. *PloS One,* 13**,** e0192288.

WANG, X., COLE, C. G., DUPAI, C. D. & DAVIES, B. W. 2020. Protein aggregation is associated with *Acinetobacter baumannii* desiccation tolerance. *Microorganisms,* 8**,** 343.

WANG, X. & QUINN, P. J. 2010. Lipopolysaccharide: Biosynthetic pathway and structure modification. *Progress in Lipid Research,* 49**,** 97-107.

WEBER, B. S., HARDING, C. M. & FELDMAN, M. F. 2016. Pathogenic *Acinetobacter*: from the cell surface to infinity and beyond. *Journal of Bacteriology,* 198**,** 880-887.

WEBER, B. S., LY, P. M., IRWIN, J. N., PUKATZKI, S. & FELDMAN, M. F. 2015. A multidrug resistance plasmid contains the molecular switch for type VI secretion in *Acinetobacter baumannii*. *Proceedings of the National Academy of Sciences,* 112**,** 9442-9447.

WEBSTER, C., TOWNER, K. J. & HUMPHREYS, H. 2000. Survival of *Acinetobacter* on three clinically related inanimate surfaces. *Infection Control and Hospital Epidemiology,* 21**,** 246-246.

WENDT, C., DIETZE, B., DIETZ, E. & RÜDEN, H. 1997. Survival of *Acinetobacter baumannii* on dry surfaces. *Journal of Clinical Microbiology,* 35**,** 1394-1397.

WHITFIELD, C. 1995. Biosynthesis of lipopolysaccharide O antigens. *Trends in microbiology,* 3**,** 178-185.

WHITFIELD, C. 2006. Biosynthesis and assembly of capsular polysaccharides in *Escherichia coli Annual Reviews in Biochemistry,* 75**,** 39-68.

WHITFIELD, C. & PAIMENT, A. 2003. Biosynthesis and assembly of Group 1 capsular polysaccharides in *Escherichia coli* and related extracellular polysaccharides in other bacteria. *Carbohydrate Research,* 338**,** 2491-2502.

WHITMORE, S. E. & LAMONT, R. J. 2012. Tyrosine phosphorylation and bacterial virulence. *International Journal of Oral Science,* 4**,** 1-6.

WHO 2014. Antimicrobial resistance: global report on surveillance 2014.

WHO. 2017. *Global priority list of antibiotic-resistant bacteria to guide research, discovery, and development of new antibiotics* [Online]. World Health Organisation Available: http://www.who.int/medicines/publications/WHO-PPL-Short_Summary_25Feb-ET_NM_WHO.pdf [Accessed].

WIEGAND, I., HILPERT, K. & HANCOCK, R. E. 2008. Agar and broth dilution methods to determine the minimal inhibitory concentration (MIC) of antimicrobial substances. *Nature Protocols,* 3**,** 163.

WIELAND, K., CHHATWAL, P. & VONBERG, R.-P. 2018. Nosocomial outbreaks caused by *Acinetobacter baumannii* and *Pseudomonas aeruginosa*: Results of a systematic review. *American Journal of Infection Control,* 46**,** 643-648.

WIESNER, J. & VILCINSKAS, A. 2010. Antimicrobial peptides: the ancient arm of the human immune system. *Virulence,* 1**,** 440-464.

WILLENBORG, J., FULDE, M., DE GREEFF, A., ROHDE, M., SMITH, H. E., VALENTIN-WEIGAND, P. & GOETHE, R. 2011. Role of glucose and CcpA in capsule expression and virulence of *Streptococcus suis*. *Microbiology,* 157**,** 1823-1833.

WILLIS, L. M. & WHITFIELD, C. 2013. Chapter 17 - Capsule and lipopolysaccharide. *In:* DONNENBERG, M. S. (ed.) *Escherichia Coli (Second Edition).* Boston: Academic Press.

WILSON, B. R., BOGDAN, A. R., MIYAZAWA, M., HASHIMOTO, K. & TSUJI, Y. 2016. Siderophores in iron metabolism: from mechanism to therapy potential. *Trends in Molecular Medicine,* 22**,** 1077-1090.

WONG, D., NIELSEN, T. B., BONOMO, R. A., PANTAPALANGKOOR, P., LUNA, B. &

SPELLBERG, B. 2017. Clinical and pathophysiological overview of *Acinetobacter* infections: a century of challenges. *Clinical Microbiology Reviews,* 30**,** 409-447.

WOOD, C. R., OHNECK, E. J., EDELMANN, R. E. & ACTIS, L. A. 2018. A light-regulated type I pilus contributes to *Acinetobacter baumannii* biofilm, motility and virulence functions. *Infection and Immunity***,** IAI. 00442-18.

WOODWARD, L. & NAISMITH, J. H. 2016. Bacterial polysaccharide synthesis and export. *Current Opinion in Structural Biology,* 40**,** 81-88.

WU, C.-C., WANG, C.-K., CHEN, Y.-C., LIN, T.-H., JINN, T.-R. & LIN, C.-T. 2014. IscR regulation of capsular polysaccharide biosynthesis and iron-acquisition systems in *Klebsiella pneumoniae* CG43. *PloS One,* 9**,** e107812.

WU, M.-F., YANG, C.-Y., LIN, T.-L., WANG, J.-T., YANG, F.-L., WU, S.-H., HU, B.-S., CHOU, T.-Y., TSAI, M.-D. & LIN, C.-H. 2009. Humoral immunity against capsule polysaccharide protects the host from *magA*$^{+}$ *Klebsiella pneumoniae*-induced lethal disease by evading Toll-like receptor 4 signaling. *Infection and Immunity,* 77**,** 615-621.

WUGEDITSCH, T., PAIMENT, A., HOCKING, J., DRUMMELSMITH, J., FORRESTER, C. & WHITFIELD, C. 2001. Phosphorylation of Wzc, a tyrosine autokinase, is essential for assembly of group 1 capsular polysaccharides in *Escherichia coli*. *Journal of Biological Chemistry,* 276**,** 2361-2371.

WYRES, K. L., CAHILL, S. M., HOLT, K. E., HALL, R. M. & KENYON, J. J. 2020. Identification of *Acinetobacter baumannii* loci for capsular polysaccharide (KL) and lipooligosaccharide outer core (OCL) synthesis in genome assemblies using curated reference databases compatible with Kaptive. *Microbial Genomics,* 6.

XAYARATH, B. & YOTHER, J. 2007. Mutations blocking side chain assembly, polymerization, or transport of a Wzy-dependent *Streptococcus pneumoniae* capsule are lethal in the absence of suppressor mutations and can affect polymer transfer to the cell wall. *Journal of Bacteriology,* 189**,** 3369-3381.

YANG, D., CHEN, Q., SCHMIDT, A. P., ANDERSON, G. M., WANG, J. M., WOOTERS, J., OPPENHEIM, J. J. & CHERTOV, O. 2000. LL-37, the neutrophil granule–and epithelial cell–derived cathelicidin, utilizes formyl peptide receptor–like 1 (FPRL1) as a receptor to chemoattract human peripheral blood neutrophils, monocytes, and T cells. *The Journal of Experimental Medicine,* 192**,** 1069-1074.

YANG, F.-L., LOU, T.-C., KUO, S.-C., WU, W.-L., CHERN, J., LEE, Y.-T., CHEN, S.-T., ZOU, W., LIN, N.-T. & WU, S.-H. 2017. A medically relevant capsular polysaccharide in *Acinetobacter baumannii* is a potential vaccine candidate. *Vaccine,* 35**,** 1440-1447.

YOON, E.-J., CHABANE, Y. N., GOUSSARD, S., SNESRUD, E., COURVALIN, P., DÉ, E. & GRILLOT-COURVALIN, C. 2015. Contribution of resistance-nodulation-cell division efflux systems to antibiotic resistance and biofilm formation in *Acinetobacter baumannii*. *MBio,* 6**,** e00309-15.

YOTHER, J. 2011. Capsules of *Streptococcus pneumoniae* and other bacteria: paradigms for polysaccharide biosynthesis and regulation. *Annual Review of Microbiology,* 65**,** 563-581.

YOUNG, D. M., PARKE, D. & ORNSTON, L. N. 2005. Opportunities for genetic investigation afforded by *Acinetobacter baylyi*, a nutritionally versatile bacterial species that is highly

competent for natural transformation. *Annual Reviews in Microbiology,* 59**,** 519-551.

ZAHN, M., BHAMIDIMARRI, S. P., BASLÉ, A., WINTERHALTER, M. & VAN DEN BERG, B. 2016. Structural insights into outer membrane permeability of *Acinetobacter baumannii*. *Structure,* 24**,** 221-231.

ZEIDLER, S. & MÜLLER, V. 2019a. Coping with low water activities and osmotic stress in *Acinetobacter baumannii*: significance, current status and perspectives. *Environmental Microbiology,* 21**,** 2212-2230.

ZEIDLER, S. & MÜLLER, V. 2019b. The role of compatible solutes in desiccation resistance of *Acinetobacter baumannii*. *MicrobiologyOpen,* 8**,** e00740.

ZEIDLER, S. & MÜLLER, V. 2020. Unusual deprivation of compatible solutes in *Acinetobacter baumannii*. *Environmental Microbiology*.

ZENATI, K., TOUATI, A., BAKOUR, S., SAHLI, F. & ROLAIN, J. 2016. Characterization of NDM-1-and OXA-23-producing *Acinetobacter baumannii* isolates from inanimate surfaces in a hospital environment in Algeria. *Journal of Hospital Infection,* 92**,** 19-26.

ZHANG, W., AUROSREE, B., GOPALAKRISHNAN, B., BALADA-LLASAT, J.-M., PANCHOLI, V. & PANCHOLI, P. 2017. The role of LpxA/C/D and pmrA/B gene systems in colistin-resistant clinical strains of *Acinetobacter baumannii*. *Frontiers in Laboratory Medicine,* 1**,** 86-91.

ZHOU, K., TANG, X., WANG, L., GUO, Z., XIAO, S., WANG, Q. & ZHUO, C. 2018. An Emerging Clone (ST457) of *Acinetobacter baumannii* Clonal Complex 92 With Enhanced Virulence and Increasing Endemicity in South China. *Clinical Infectious Diseases,* 67**,** S179-S188.

ZIMBLER, D. L., PARK, T. M., ARIVETT, B. A., PENWELL, W. F., GREER, S. M., WOODRUFF, T. M., TIERNEY, D. L. & ACTIS, L. A. 2012. Stress response and virulence functions of the *Acinetobacter baumannii* NfuA Fe-S scaffold protein. *Journal of Bacteriology,* 194**,** 2884-2893.

ZIMBLER, D. L., PENWELL, W. F., GADDY, J. A., MENKE, S. M., TOMARAS, A. P., CONNERLY, P. L. & ACTIS, L. A. 2009. Iron acquisition functions expressed by the human pathogen *Acinetobacter baumannii*. *Biometals,* 22**,** 23-32.